



Wang, Yilin (2022) *Exploring novel mechanisms underlying synovial fibroblast-mediated pathogenesis in arthritis: role of ARNO and sialylation in stromal inflammation*. PhD thesis.

<https://theses.gla.ac.uk/83268/>

Copyright and moral rights for this work are retained by the author

A copy can be downloaded for personal non-commercial research or study, without prior permission or charge

This work cannot be reproduced or quoted extensively from without first obtaining permission in writing from the author

The content must not be changed in any way or sold commercially in any format or medium without the formal permission of the author

When referring to this work, full bibliographic details including the author, title, awarding institution and date of the thesis must be given

Enlighten: Theses

<https://theses.gla.ac.uk/>
research-enlighten@glasgow.ac.uk



University
of Glasgow

**Exploring Novel Mechanisms Underlying
Synovial Fibroblast-mediated
Pathogenesis in Arthritis: Role of ARNO
and Sialylation in Stromal Inflammation**

Yilin Wang
BM, MSc

A thesis submitted in fulfilment of the requirements
for the degree of Doctor of Philosophy

School of Infection and Immunity,
College of Medical, Veterinary & Life Sciences,
University of Glasgow.

November 2022

Abstract

Synovial fibroblasts (SFs) not only maintain articular homeostasis in a health state, but also play a key role in joint destruction in immune articular diseases, such as rheumatoid arthritis (RA). In RA, activated SFs undergo intrinsic alterations, adopting an aggressive phenotype that damages cartilage and bone. The dysregulated cell migratory property and hyper-inflammatory responses are hallmarks of activated SFs. However, deactivation of these cells is not currently possible. This study investigated two potential novel sites of invention, namely defining the ARNO and Sialic acid arms of the project. The central aim of this study was to understand the regulation of ARNO and sialic acid in SFs in a proinflammatory microenvironment and the function of ARNO and sialic acid in SF-dependent migration and inflammation.

On the one hand, ARNO (the ARF Nucleotide-Binding Site Opener) is a dominant activator of ARF (ADP-ribosylation factor) proteins that regulate cell adhesion, migration, and cytoskeleton reorganisation in many cell types. The elevated expression of ARNO in leukocyte-rich RA shows ARNO might be regulated in a pro-inflammatory milieu, indicating the potential role of ARNO in SF-dependent physiopathology. We demonstrated that IL-1 β upregulated ARNO expression and ARF6 activation in SFs, whilst SFs transfected with ARNO siRNA exhibited reduced motility and formation of focal adhesion. Surprisingly therefore, ARNO modulated the IL-1 β -induced inflammatory response in SFs and the inhibition of ARNO greatly reduced the production of cytokines, chemokines and other immunomodulators.

On the other hand, glycosylation is one of the most common protein modifications, and the glycoconjugates on plasma membranes are involved in a wide range of biological functions, including cell-cell interactions and inflammation. Alterations in glycosylation have been observed in chronic diseases, but how changes in the cell glycome affect SF physiopathology remains largely unknown. We combined transcriptomic and glycomics analysis to investigate glycosylation-dependent SF physiopathology. We demonstrated that the pro-inflammatory cytokine TNF α modulates SF cell surface glycosylation by inhibiting the expression of ST6Gal1 and subsequently reducing α 2-6 sialylation. In addition, SFs from arthritic mice exhibited reduced cell surface sialylation and

sialylation was associated with functional SF subsets. Removal of cell surface sialic acid with sialidase from *C. perfringens* provided evidence that loss of sialic acid transforms SF into a pathogenic phenotype with hyper-inflammatory response and enhanced migration property.

Overall, this work highlights the importance of ARNO and sialic acid in SF-mediated inflammation and pathogenic migration, bridging cell motility to inflammatory responses, and offering new perspective on targeting SF deactivation in arthritic joints.

Table of Contents

Abstract	ii
List of tables	vii
List of Figures	viii
Acknowledgement	x
Publications	xi
Author's Declaration	xii
Abbreviations	xiii
Chapter 1 General introduction	1
1.1 Rheumatoid arthritis	1
1.2 Physiopathology of the synovium	2
1.2.1 Normal synovium.....	2
1.2.2 Rheumatoid synovium.....	3
1.3 Synovial fibroblast	4
1.4 Rheumatoid arthritis synovial fibroblast (RASf)	5
1.4.1 RASfs adopt an aggressive phenotype	5
1.4.2 Interactions of RASf with immune cells	7
1.4.3 Functional subsets of RASf	8
1.4.4 Treatment of RA by targeting SFs	9
1.5 Collagen-induced arthritis (CIA) mouse model	10
1.6 ARNO-ARF6	11
1.6.1 ADP-ribosylation factor (ARF) family of guanine-nucleotide-binding (G) proteins and their regulators	11
1.6.1.1 ARF-GEFs	13
1.6.1.2 ARNO-ARF6 axis.....	14
1.7 Cell sialylation	16
1.7.1 Sialic acid biosynthesis and metabolism	17
1.7.2 Sialic-acid-recognising proteins	19
1.7.3 Sialic acid in human diseases	20
1.7.3.1 Cancer.....	20
1.7.3.2 Infection	21
1.7.3.3 Immunology	22
1.8 Thesis Aims	23
Chapter 2 Materials and methods	34
2.1 Mice	34
2.2 Collagen-induced arthritis (CIA) mouse model	34
2.3 Mouse SF isolation and culture	34
2.4 CD11b+ cell depletion	35
2.5 Mouse SF sorting	36
2.6 Histology	36
2.6.1 Joint paraffin blocks	36
2.6.2 Haematoxylin and Eosin (H&E) staining.....	36
2.7 Short interference RNA (siRNA) transfection	37
2.8 De-sialylation of SFs in vitro	37

2.9	Cell migration assay	37
2.10	Flow cytometry	38
2.11	ELISAs	39
2.12	Enzyme-linked lectin assays (ELLA)	39
2.13	MTS cell viability assay	39
2.14	Western blots	40
2.15	GTP pull down assay	41
2.16	Immunofluorescence staining	41
2.17	RNA isolation and RT-qPCR	42
2.18	RNA sequencing and data analysis	42
2.19	Mass spectrometric analysis of glycans	43
2.20	Statistical analysis	44
Chapter 3 Characterisation of arthritic SFs		49
3.1	Introduction	49
3.2	Results	50
3.2.1	Characteristics of arthritic SFs	50
3.2.2	SF responses to inflammatory cytokines	53
3.3	Discussion	54
Chapter 4 ARNO modulates SF migration and inflammation		71
4.1	Introduction	71
4.2	Results	72
4.2.1	IL-1 β upregulates ARNO expression and further activation of ARF6 in murine SFs.....	72
4.2.2	ARNO regulates SF motility and focal adhesion formation.....	73
4.2.3	ARNO regulates inflammatory SF response to IL-1 β stimulation.....	74
4.2.4	Effect of ARNO silencing on the SF transcriptomic profile.....	78
4.2.5	Role of ARNO in regulating the pathogenic response to IL-1 β	79
4.2.6	ARNO expression in SF subsets	81
4.3	Discussion	82
Chapter 5 Investigating the role of sialic acid in SF pathogenesis		121
5.1	Introduction	121
5.2	Results	122
5.2.1	Glycosylation pathways associated with SF pathogenesis.....	122
5.2.1.1	SF glycosylation transcriptomic profile	122
5.2.1.2	Altered sialylation in arthritic SFs.....	123
5.2.1.3	SF subsets are differentially sialylated	123
5.2.2	Loss of α 2-6 sialylation is associated with inflammatory SFs.....	124
5.2.2.1	TNF α suppresses St6gal1 expression and α 2-6 sialylation	124
5.2.2.2	Inhibition of St6gal1 induces cytokine production in SFs.....	126
5.2.2.3	Desialylation of SF enhances cell migration.	126
5.2.2.4	<i>In vitro</i> desialylation of SFs triggers rapid pro-inflammatory responses.....	127
5.3	Discussion	130
Chapter 6 General discussion		157
6.1	The leading role of SFs in the pathogenesis of arthritis.....	157
6.2	ARNO and sialic acid regulate SF migration	158

6.2.1	Inhibition of ARNO reduces the migration of SFs	158
6.2.2	Sialic acid modulates cell migration.....	159
6.3	ARNO and sialic acid regulate the inflammatory response of SFs.....	161
6.3.1	Inhibition of ARNO suppresses SF inflammation	161
6.3.2	Loss of sialic acid induces the production of pro-inflammatory mediators in SFs.....	162
6.4	ARNO and Sialylation: walk the same way?.....	165
Chapter 7	Reference.....	169

List of tables

Table 2-1 List of antibodies used for FACs sorting.	46
Table 2-2 List of antibodies used for western blot.	47
Table 2-3 Antibodies used for immunofluorescence studies.	48

List of Figures

Figure 1.1 Normal synovium (X200 magnification).	25
Figure 1.2 Haematoxylin and Eosin staining of joint tissue from patients with RA.	26
Figure 1.3 Synovial fibroblasts in normal and rheumatoid synovium.	27
Figure 1.4 Characteristics of SFs in RA.	28
Figure 1.5 Schematic of ARF GDP and GTP cycle.	29
Figure 1.6 Structure of glycoconjugates.	30
Figure 1.7 Structure of Neu5Ac and Neu5Gc in mammalian cells.	31
Figure 1.8 Biosynthesis of Neu5Ac.	32
Figure 1.9 Two main linkage configurations of sialic acid.	33
Figure 2.1 Schematic of cell migration assay.	45
Figure 3.1 Mesenchymal cells invade into arthritis joint cavity.	58
Figure 3.2 Profile of isolated synovial cells.	59
Figure 3.3 Functional enrichment and network analysis comparing naïve and arthritic SFs.	60
Figure 3.4 Functional enrichment of differential expressed genes in sorted CIA SFs compared to sorted naïve SFs.	61
Figure 3.5 Profile of isolated synovial cells.	63
Figure 3.6 Profile of isolated synovial cells.	65
Figure 3.7 Purity check of <i>in vitro</i> cultured SFs.	66
Figure 3.8 Purity check of <i>in vitro</i> cultured SFs.	67
Figure 3.9 <i>ex vivo</i> cultured SFs retain their inflammatory characteristics.	68
Figure 3.10 IL-1 β induces cytokine production in SFs.	69
Figure 3.11 IL-1 β induces cytokine production in SFs.	70
Figure 4.1 IL-1 β upregulates ARNO expression in SFs.	89
Figure 4.2 IL-1 β upregulates ARNO expression in SFs.	91
Figure 4.3 Inhibition of ARNO inactivates ARF6.	92
Figure 4.4 ARNO regulates SF migration.	93
Figure 4.5 Inhibition of ARNO does not disturb SF proliferation.	94
Figure 4.6 Inhibition of ARNO reduces SF adhesion.	95
Figure 4.7 Inhibition of ARNO reduces vinculin formation.	97
Figure 4.8 Inhibition of ARNO reduces vinculin formation.	98
Figure 4.9 Silencing ARNO expression reduces IL-1 β mediated cytokine production.	99
Figure 4.10 ARNO mediates the phosphorylation of STAT3 in SFs.	100
Figure 4.11 Silencing ARNO does not affect MAPK signaling phosphorylation. ...	102
Figure 4.12 Silencing ARNO does not affect MAPK signaling phosphorylation. ...	104
Figure 4.13 ARNO mediates the phosphorylation of AKT in SFs.	105
Figure 4.14 Inhibition of STAT3 phosphorylation by Cpd188 reduces cell migration and CCL2 production.	107
Figure 4.15 PI3K-AKT signaling pathway regulates cytokine production in SFs.	109
Figure 4.16 Transcriptome characteristics of ARNO-silenced SFs in response to IL- 1 β stimulation.	111
Figure 4.17 Transcriptome characteristics of ARNO-silenced SFs in response to IL- 1 β stimulation.	112
Figure 4.18 Transcriptome characteristics of ARNO-silenced SFs in response to IL- 1 β stimulation.	114
Figure 4.19 ARNO knockdown reshapes IL-1 β -mediated inflammatory response.	116

Figure 4.20 ARNO knockdown reduces IL-1 β -mediated inflammatory response in CIA SFs.	117
Figure 4.21 Gating strategy for SF subsets sorted from mouse joint synovial tissue.	118
Figure 4.22 ARNO expression varies with arthritis progression.	119
Figure 4.23 Expression of ARNO in synovial tissue of patients with rheumatoid arthritis.	120
Figure 5.1 Overview of potential glycan biosynthesis profile.	133
Figure 5.2 Synovial fibroblasts from arthritic mice exhibit a distinct glycomics transcriptomic profile.	134
Figure 5.3 N-linked sialylated glycans were reduced in expanded murine arthritic SFs.	135
Figure 5.4 α 2-6 sialylation is reduced in arthritic SFs.	136
Figure 5.5 Sialyltransferases are modulated in inflammatory SFs.	137
Figure 5.6 TNF α inhibits St6gal1 expression.	138
Figure 5.7 TNF α inhibits St6gal1 expression further downregulates α 2-6 sialylation in SFs.	140
Figure 5.8 TNF α reduces sialylated N-glycans in SFs.	141
Figure 5.9 Inhibition of St6gal1 enhances cytokine secretion.	142
Figure 5.10 Inhibition of St6gal1 enhances cytokine secretion.	143
Figure 5.11 <i>C. perfringens</i> sialidase cleaves α 2-6 and α 2-3 sialic acid from cell surface.	144
Figure 5.12 Heat inactivates sialidase.	145
Figure 5.13 Desialylation enhances SF migration.	146
Figure 5.14 Desialylation does not affect SF proliferation and metabolism.	147
Figure 5.15 Transcriptomic profile of desialylated SFs.	148
Figure 5.16 Transcriptomic profile of desialylated SFs.	149
Figure 5.17 Desialylation enhances the inflammatory response of SFs.	151
Figure 5.18 Comparison of the transcriptomic profile of desialylated and IL-1 β -stimulated naïve SFs.	152
Figure 5.19 Comparison of the transcriptomic profile of desialylated and IL-1 β -stimulated naïve SFs.	153
Figure 5.20 Comparison of the transcriptomic profile of desialylated and IL-1 β -stimulated naïve SFs.	154
Figure 5.21 Enzymatic removal of sialic acid modulates cell sialyltransferase expression and sialylation.	156
Figure 6.1 Illustration of Gal-3 binding to galactose in SFs.	167
Figure 6.2 Molecular mechanisms by which ARNO and sialic acid regulated SF migration and inflammation.	168

Acknowledgement

Over the past four years, I have been assisted and supported by many wonderful individuals. My sincere thanks go out to all of you for your contribution.

First and foremost, I would like to express my deepest and sincerest gratitude to my supervisors, Dr Miguel Pineda and Professor Maggie Harnett. Thanks for their invaluable guidance, inspiration, encouragement and support throughout my PhD study. Their enthusiasm and kindness have provided me with a great deal of encouragement. The care and support they provided enabled me to complete my lab work and thesis. I would like to extend my gratitude in particular to Miguel, who has spent so much time teaching me laboratory techniques. It is an honour for me to be able to study with you for my PhD. I appreciated the excellent supervision you provided me throughout the process. I am very fortunate.

I would like to express my sincere appreciation to all those who have helped me during my PhD studies. My thanks go out to Ms Diane Vaughan for providing me with excellent training in flow cytometry and cell sorting. I would like to thank Aneesah and Piaopiao for their assistance at the bench. I enjoyed working and being friends with you! Caglar, thank you so much for helping me with the R code. You are a genius when it comes to omics data analysis. Please accept my sincere gratitude for the ideas you have always shared with me, Yinbo.

I would like to express my sincere gratitude to the warm and welcoming people of Glasgow. I never felt like I was in a foreign country during my stay in the city. Besides, I would like to thank the China Scholarship Council for funding my living expenses and the University of Glasgow for waiving my tuition fees.

I would also like to thank my friends Mengyi, Xing, Zhaoyang, Jinyuan and Xiang for their personal support over the years. I would like to extend a special thanks to Zhaoyang for always being there for me over the past four years as well as for contributing excellent cooking skills. Last but not least, I would like to thank my family for their unconditional love and support. It would not have been possible for me to study in the UK and meet such wonderful people without your assistance.

Publications

Publications authored by the candidate on research relating to this thesis.

Wang, Y., Pan, P., Khan, A., Çil, Ç. & Pineda, M.A. 2022, "Synovial Fibroblast Sialylation Regulates Cell Migration and Activation of Inflammatory Pathways in Arthritogenesis", *Frontiers in immunology*, vol. 13, pp. 847581-847581. (Research paper)

Wang, Y., Çil, Ç., Harnett, M.M. & Pineda, M.A. 2021;2022;, "Cytohesin-2/ARNO: A Novel Bridge Between Cell Migration and Immunoregulation in Synovial Fibroblasts", *Frontiers in immunology*, vol. 12, pp. 809896-809896. (Research paper)

Wang, Y., Khan, A., Antonopoulos, A., Bouché, L., Buckley, C.D., Filer, A., Raza, K., Li, K., Tulusso, B., Gremese, E., Kurowska-Stolarska, M., Alivernini, S., Dell, A., Haslam, S.M. & Pineda, M.A. 2021, "Loss of α 2-6 sialylation promotes the transformation of synovial fibroblasts into a pro-inflammatory phenotype in arthritis", *Nature communications*, vol. 12, no. 1, pp. 2343-2343. (Research paper)

Author's Declaration

“I declare that, except where explicit reference is made to the contribution of others, that this dissertation is the result of my own work and has not been submitted for any other degree at the University of Glasgow or any other institution.”

Printed Name: YILIN WANG

Signature: _____

Abbreviations

AAL	Aleuria Aurantia Lectin
AIA	Adjuvant-induced arthritis
AKT	Protein kinase B
ARF6	ADP-ribosylation factor 6
ARNO	ARF nucleotide-binding site opener
Asn	Asparagine
B4galt	β -1,4-Galactosyltransferase genes
BSA	Bovine serum albumin
CCL2	Chemokine ligand 2
Cdc42	Cell division control protein 42 homolog
CDH11	Cadherin 11
CFA	Complete Freund's adjuvant
CIA	Collagen-induced arthritis
CMAS	CMP-Sialic acid synthetase
CMP-Neu5Ac	Cytosine 5'-monophosphate N-acetylneuraminic acid
CP	Clostridium perfringens sialidase
CXCL-	Chemokine (C-X-C motif) ligand
Cyth	Cytohesin
DMARDs	Disease-modifying antirheumatic drugs
Dnmt1	DNA Methyltransferase 1
DOCK	Dedicator of cytokinesis
ECM	Extracellular matrix
EGF	Epidermal growth factor
ELISA	Enzyme-linked immunosorbent assay
ELLA	Enzyme-linked lectin assay
EOC	Epithelial ovarian cancer
ERK	Extracellular signal-regulated kinases
ES	Excretory-secretory
FAK	Focal adhesion kinase
FAP	Fibroblast activating protein
FBS	Fetal bovine serum
Fuc	Fucose
Gal	Galactose
Gal-3	Galectin 3
GalNAc	N-acetylgalactosamine
GDP	Guanosine diphosphate
Glc	Glucose
GlcNAc	N-acetylglucosamine
GO	Gene Ontology
GPCRs	G-protein-coupled receptors
GTP	Guanosine triphosphate
H & E	Haematoxylin and eosin
HA	Hyaluronic acid

ICAM-1	Intercellular adhesion molecule 1
ID injection	Intradermal injection
Ig	Immunoglobulin
IL-	Interleukin
IP injection	Intraperitoneal injection
ITIM	Immunoreceptor tyrosine-based inhibitory motif
kDa	Kilo Daltons
KEGG	Kyoto Encyclopedia of Genes and Genomes
LFA-1	lymphocyte function- associated antigen 1
LPS	Lipopolysaccharide
MAA	Maackia amurensis lectin
Man	Mannose
MAPK	Mitogen-activated protein kinase
MFI	Mean fluorescence intensity
MMP	Matrix metalloproteinase
MS	Mass spectrometry
MTX	Methotrexate
Myd88	Myeloid differentiation primary response 88
NANP	N-Acetylneuraminic Acid Phosphatase
NANS	N-acetylneuraminic acid synthase
NF- κ B	Nuclear factor kappa B
Nfkbib	NF-kappa-B inhibitor beta
NGF	Nerve growth factor
NSAIDs	Non-steroidal Anti-Inflammatory Drugs
NT	Non-treated
OASF	Osteoarthritic synovial fibroblasts
OPG	Osteoprotegerin
PA	Phosphatidic acid
PBS	Phosphate buffered saline
PCA	Principal component analysis
PDGF	Platelet-derived growth factor
PDPN	Podoplanin
PDT	Photodynamic therapy
PH domain	Pleckstrin homology domain
PI3K	Phosphatidylinositide 3-kinase
PIP2	Phosphatidylinositol 4,5-bisphosphate or PtdIns(4,5)P2
PIP3	Phosphatidylinositol 3,4,5 trisphosphate
PIP5K	Phosphatidylinositol 4-Phosphate-5 kinase
PLD	Phospholipase D
PNA	Peanut agglutinin
PTP	Protein tyrosine phosphatase
qPCR	Quantitative polymerase chain reaction
RA	Rheumatoid arthritis
Rac1	Ras-related C3 botulinum toxin substrate 1
RANKL	Receptor activator of nuclear factor kappa-B ligand
RASF	Rheumatoid arthritis synovial fibroblast

RhoA	Ras homolog family member A
Rock	Rho-associated coiled-coil-containing protein kinase
Ser	Serine
SF	Synovial fibroblast
SHP-1	Src homology region 2 domain-containing phosphatase-1
SHP-2	Src homology region 2 domain-containing phosphatase-2
Siglecs	Sialic acid-binding immunoglobulin-type lectins
siRNA	Small interfering RNA
SNA	Sambuccus nigra agglutinin
St3gal1	ST3 Beta-Galactoside Alpha-2,3-Sialyltransferase 1
St3gal3	ST3 Beta-Galactoside Alpha-2,3-Sialyltransferase 3
St3gal4	ST3 Beta-Galactoside Alpha-2,3-Sialyltransferase 4
St3gal6	ST3 Beta-Galactoside Alpha-2,3-Sialyltransferase 6
St6gal1	ST6 Beta-Galactoside Alpha-2,6-Sialyltransferase 1
St6galNAc5	ST6 N-Acetylgalactosaminide Alpha-2,6-Sialyltransferase 5
STA	Serum-transfer arthritis
STAT	Signal transducer and activator of transcription
STM	Synovial tissue macrophage
STs	Sialyltransferases
TGF-β1	Transforming growth factor beta 1
Thr	Threonine
TLR	Toll like receptor
TNF	Tumor necrotic factor
TNFRSF11b	TNF Receptor Superfamily Member 11b
TNFSF11	TNF Superfamily Member 11
UDP-GlcNAc	Uridine 5'-diphosphate N-acetylglucosamine
V-ATPase	Vacuolar-type H ⁺ adenosine triphosphatase
VCAM-1	Vascular cell adhesion protein 1
VE	Vascular endothelial
VEGF	Vascular endothelial growth factor
VLA-4	Very late antigen-4

Chapter 1 General introduction

1.1 Rheumatoid arthritis

Rheumatoid arthritis (RA) is a chronic autoimmune disease characterized by synovitis along with synovial hyperplasia, progressive joint destruction and even deformity if the disease remains untreated. In developed countries, approximately 0.5-1.0% of adults suffer from RA, and women are 2-3 times more likely to have arthritis than men (Brennan-Olsen et al., 2017). Although the exact etiologic of RA has not been fully investigated, it is clear that genetic and environmental factors, such as sex, smoking and obesity, contribute to the development of RA. Approximately 60% of RA risk is attributed to genetic factors (MacGregor et al., 2000). Besides, the origin of RA is believed to have originated in the New World and has since spread to the rest of the world due to European expeditions during the 16th and 17th centuries (Rothschild and Woods, 1990, Rothschild et al., 1992). The geographical spread of RA may be influenced by environmental factors such as pathogens or dietary components that alter the microbiome. This rising new hypothesis that a link exists between RA and oral or intestinal microorganisms. RA is a chronic autoimmune disease, the molecular disorder may start years before the disease is diagnosed. The joint destruction of RA begins with stromal cell activation and joint vasculitis, followed by infiltration of immune cells into the synovial membrane and cartilage, lining synovial hyperplasia, pannus formation, progressive cartilage erosion and eventually bone destruction. Although new anti-inflammatory biological therapies have significantly improved the clinical outcome of patients with RA, there is still no cure and treatments are not always effective due to the molecular and cellular heterogeneity observed in RA patients (Turner and Filer, 2015). Thus, some patients still do not respond to modern drugs, reflecting an incomplete understanding of RA pathophysiology. Therapy is currently focused on relieving pain and slowing disease progression (Ishchenko and Lories, 2016). Painkillers and Non-steroidal Anti-Inflammatory Drugs (NSAIDs) are initially given to patients with RA to release symptoms and reduce joint inflammation, although these drugs are not able to stop disease progression. The next line of drugs includes disease-modifying antirheumatic drugs (DMARDs) and biological agents. DMARDs, such as Methotrexate (MTX), reduce joint inflammation and associated tissue destruction (Pincus et al., 2002) and are used in autoimmune

diseases and cancer. However, MTX is poorly tolerated in elderly groups, with about half of the patients stopping treatment due to side effects (Harrison et al., 2005). Treatment and outcome of RA patients have been dramatically improved by the application of modern Biologics. Biological agents are designed to target specific inflammatory cells, cellular interactions, and inflammatory cytokines responsible for driving tissue damage and local inflammation (Curtis and Singh, 2011). Several Biologics are already available for commercial use, such as TNF-antagonists etanercept, infliximab and adalimumab, B-cell depleting agent rituximab and IL-1 inhibitor anakinra. These Biologics are used for the treatment of RA which does not respond to typical DMARDs which, especially combined with MTX, exhibit sustained clinical effectiveness (Pincus et al., 2002, Kremer et al., 2003). Although biologics have improved disease outcomes for many RA patients, half of established RA patients still do not meet the criteria for clinical remission and the immunosuppressive effects of biologics inevitably increase the likelihood of infection. Therefore, a better understanding of the pathophysiology of RA and the discovery of novel mechanisms of action may provide new treatment options.

1.2 Physiopathology of the synovium

1.2.1 Normal synovium

The synovium is a highly specialised tissue crucial for joint function. It forms the joint cavity, nourishing chondrocytes and wrapping the joints filled with synovial fluid. The synovium is soft tissue which is anatomically and functionally divided into two main areas, the lining and sub-lining layers (Figure 1-1). The lining layer is mainly composed of two types of cells, while the sub-lining layer is relatively acellular and includes a small number of adipocytes, fibroblasts, blood vessels and resident immune cells (Smith et al., 2003). The synovium is the central site of inflammation for several musculoskeletal conditions, such as RA and psoriatic arthritis (PSA). In health, the lining layer of the synovium contains only two to three cells thickness, which produces synovial fluid for joint lubrication and nutrition. Perhaps unexpectedly, healthy synovium contains some levels of pro-inflammatory factors, such as cytokines like IL-1 β , TNF α or IL-17, but far less than the inflamed synovium in RA (Smith et al., 2003, Singh et al., 2004). Additionally, healthy synovium presents high levels of anti-inflammatory

cytokine production, such as IL-1 receptor antagonist (Smith, 2011), indicative of a homeostatic state ready to control inflammation and local immune responses. Moreover, the expression of tumour necrosis factor receptor superfamily member 11b (Tnfrsf11b) is abundant whereas tumour necrosis factor ligand superfamily member 11 (Tnfsf11) is rarely observed (Smith et al., 2003, Singh et al., 2004). Tnfsf11, also known as Receptor Activator of Nuclear Factor kappa-B Ligand (RANKL) is a regulator for osteoclast differentiation, and therefore, increased expression of Tnfrsf11 results in increased osteoclast production and bone disruption. Tnfrsf11b, also known as Osteoprotegerin (OPG), as a decoy receptor for Tnfsf11, which inhibits osteoclastogenesis and bone resorption (Simonet et al., 1997). The ratio of RANKL/OPG is a common marker for physiological bone regeneration, a balance between osteoclast and osteoblast activity. Overall, the greater expression of OPG than RANKL in health synovium is more beneficial to prevent joint damage.

1.2.2 Rheumatoid synovium.

During RA, the synovium undergoes a profound transformation, moving from a healthy homeostatic tissue to an enlarged pathogenic structure that supports local inflammation and tissue damage (Figure 1-2). During RA, the synovium becomes hyperplastic and invades the joint cavity, destroying the cartilage and leading to swelling, pain and deformity (Firestein, 2003). This hyperplasia occurs in both lining and sub-lining areas. The synovial lining layer is thickened, from 1-2 cell layers to over 10 cell layers. The expanded synovium leads to the formation of a pathological tissue called pannus that invades into adjacent cartilage (Figure 1-2). The pannus is mainly composed of SFs and osteoclasts (Huber et al., 2006). The structure of the sub-lining membrane undergoes dramatic changes in cell number and content which transforms from a relatively acellular to a hyperplastic and inflammatory infiltrative tissue due to the recruitment of immune cells, including T cells, B cells and macrophages (Takemura et al., 2001).

Lining layer hyperplasia is a hallmark of RA. Two cell types are resident in the lining synovium, the synovium fibroblast (SF) and the synovial tissue macrophage (STM). Recent Single-cell transcriptomic-based studies have demonstrated that both populations are highly heterogeneous, and both adopt an activated

phenotype, producing pro-inflammatory mediators which recruit immune cells to the joint cavity (Alivernini et al., 2020, Mizoguchi et al., 2018). Additionally, SF-STMs crosstalk contributes to the perpetuation of autocrine networks by producing cytokines such as IL-1 β , TNF α and GM-CSF (Bartok and Firestein, 2010). Besides, SFs are involved in arthritis progression as they contribute to the pannus formation and cartilage destruction by producing extracellular matrix-degrading enzymes (Bartok and Firestein, 2010) and activated SFs in the sub-lining synovium increase expression of vascular endothelial growth factor (VEGF). VEGF promotes angiogenesis, further facilitating the invasion of the synovium by immune cells (del Rey et al., 2009). These infiltrating cells interact with activated SFs and STMs promoting further release of pro-inflammatory cytokines, which ultimately maintain the persistence of inflammation in the affected joints.

1.3 Synovial fibroblast

Stromal synovial fibroblasts (SFs) are a key component of the synovial membrane, maintaining cartilage integrity and joint homeostasis (Figure 1-3A). As described above, they are found in both lining and sub-lining layers of the synovium. Like other mesenchymal cells, SFs contribute to the formation and maintenance of synovial extracellular matrix (ECM) by producing laminin, collagens and fibronectin, among other matrix components, and ECM-degrading enzymes, such as Matrix metalloproteinases (MMPs). SFs express cell adhesion proteins, such as integrins, ICAM, VCAM and selectins, which are involved in migration and interaction with other cells. SFs also express cadherin 11 (CDH11), whose engagement induces the production of pro-inflammatory cytokines (Chang et al., 2011a, Lee et al., 2007). Unlike fibroblasts found in other anatomical locations, SFs produce hyaluronic acid (HA), proteoglycan 4 and UDP-glucose 6-dehydrogenase (Schumacher et al., 1994, Jay et al., 2000), molecules that are designed to lubricate synovial joints and reduce motion friction (Smith et al., 2019). Although no definitive markers for SFs have been identified, markers such as podoplanin (PDPN), CD90 and vimentin are widely used in combination with other negative markers in immunohistochemistry and flow cytometry to identify SFs.

1.4 Rheumatoid arthritis synovial fibroblast (RASf)

1.4.1 RASfs adopt an aggressive phenotype

RA was initially described as an autoimmune disease, and therefore the initiation and perpetuation of disease were thought to be exclusively dependent on immune cells. However, recent studies highlighted the role of stromal cells in the persistence of joint inflammation, even though these are non-immune system cells (Firestein, 1996, Buckley et al., 2001). SFs are the most abundant stromal cells in synovium, and their inflammatory and tissue-damaging effects contribute to the pathogenesis of RA (Figure 1-3B) (Croft et al., 2019).

In RA, SFs change from a relatively quiescent state to an activated, aggressive state, becoming important immunoregulators (Figure 1-4). Activated SFs modulate joint immune responses by producing large amounts of cytokines and chemokines (Bartok and Firestein, 2010), which facilitate the recruitment of immune cells and maintain joint inflammation. In addition to being a major source of cytokines, SFs also serve as an important target for cytokine action which drives RASfs towards aggressive behaviour and promotes crosstalk between RASfs and other synovial cell types. Interestingly, SFs exhibit a different response compared to macrophages upon LPS stimulation. Macrophages reduce their inflammatory response during sustained stimulation, whereas SFs from RA patients maintain the ability to produce pro-inflammatory factors throughout the disease (Klein et al., 2017, Foster and Medzhitov, 2009, Klein et al., 2016). The intolerance to inflammatory stimuli further supports the idea that SFs sustain local inflammatory responses.

Besides, SFs facilitate synovium angiogenesis to maintain and promote joint inflammation. In RA, SFs produce a variety of angiogenic growth factors including cytokines, chemokines and vascular endothelial growth factor (VEGF) (Jackson et al., 1997, Dimberg, 2010). Angiogenesis increases the vascularization of the synovium which facilitates the recruitment of immune cells from the bloodstream into the synovium. Accumulation of leukocytes in the articular cavity is a hallmark characteristic of RA. Moreover, the accumulation of leukocytes in the synovial space reduces synovium oxygen concentration and

establishes hypoxic conditions. This hypoxic microenvironment further promotes angiogenesis (Jackson et al., 1997, Krock et al., 2011).

Activated SFs facilitate the influx of immune cells and joint angiogenesis which contribute to the perpetuation of joint inflammation and eventually result in structural damage. SFs disrupt the supporting structures of joints in RA through a variety of mechanisms (Noss and Brenner, 2008, Sabeh et al., 2010). One mechanism is the increase in the number of SFs, leading to synovial hyperplasia and consequent pannus formation. Pannus is an aggressive tissue whose growth leads to the destruction of cartilage and bone (Gravallese, 2002). Both the proliferation of SFs and the reduction in programmed cell death lead to synovial hyperplasia. On the one hand, exposure of SFs to platelet-derived growth factor (PDGF) and cytokines in the inflamed joints triggers SF proliferation (Lafyatis et al., 1989, Freundlich et al., 1986). On the other hand, SFs express multiple pro-survival factors to inhibit SF apoptosis (Bai et al., 2004, Meinecke et al., 2007). For example, RASFs highly express CD147 which resist TNF α -induced apoptosis (Zhai et al., 2016).

Elevated motility is another characteristic of RASF. Multiple signaling pathways and adhesion molecules are involved in SF migration in 2D and 3D environments. *In vivo* studies suggest that activated SFs in arthritic joints can travel from inflamed joints to unaffected joints through blood vessels to initiate cartilage destruction, perhaps indicating that SFs may play a role in transmitting inflammation between joints (Lefevre et al., 2009, Hillen et al., 2017). Although the fundamental mechanism of dissemination of arthritis to unaffected joints is not clear, long-distance migration of activated SF at least partly contributes to it. Adhesion molecules are required in this abnormal migration. Under inflamed conditions, SFs produce elevated adhesion molecules, which increased the attachment of SFs. The invasive behaviour of SFs requires the attachment of SFs to the matrix components of cartilage, synthesis of ECM-degrading enzymes and activate signaling pathways (Firestein, 2017, Tian et al., 2002), with multiple adhesion molecules required in this step. For instance, α 5 integrin-mediated activity is required for SF attachment to cartilage, and its expression is elevated in RA synovium. (Lowin et al., 2009). Corroborating this pathogenic role, the ability of SFs to attach and invade the cartilage tissue was reduced when integrin expression was inhibited (Peters et al., 2012).

Furthermore, inhibition of focal adhesion kinase (FAK), the downstream regulator of integrins, also blocks the invasion of cartilage by SFs (Shelef et al., 2014). Apart from FAK, the MAPK and PI3K pathways are also activated following integrin binding (Yee et al., 2008), playing a key role in SF-dependent cartilage and ECM degradation. In addition, the interactions between integrins and fibronectin-derived peptides induce the expression of MMPs (De Franceschi et al., 2015). For example, FAK binding to MAPK and PI3K regulates the expression of MMPs (Sawai et al., 2005, Kwiatkowska et al., 2011) which damages cartilage by degrading ECM. Elevated production of MMPs induced by pro-inflammatory cytokines, such as IL-1 β and TNF α , also enhances the production of RANKL. Besides, SFs express elevated myostatin in RA which accelerates RANKL mediated osteoclastogenesis (Dankbar et al., 2015).

1.4.2 Interactions of RASF with immune cells

The interaction of SFs with infiltrated immune cells contributes to joint inflammation and pathological changes. SFs and STMs show an intimate relationship as they are anatomically close to each other in the synovial membrane. Two populations of macrophages have been described, playing pro- and anti-inflammatory roles depending on their phenotypes. Like SFs, activated STMs produce TNF α and IL-1 β contributing to joint inflammation. Reflecting the SF-STM cross-talk, SFs produce fewer cytokines and MMPs in the absence of STMs (Bondeson et al., 2010). Interestingly, STM IFN- γ production and STM responsiveness to exogenous IFN- γ are inhibited when co-culture with SFs (Donlin et al., 2014). This inhibition may contribute to RA pathogenesis and cartilage erosion as IFN- γ inhibits osteoclast formation (Tang et al., 2018). Although studies have shown that local signals induce macrophage differentiation and specialization (Rosas et al., 2014, Okabe and Medzhitov, 2014), little is known about how SFs affect STM differentiation and phenotype.

The interactions between SFs and infiltrating immune cells contribute to structuring the immune response. Enhanced survival and inhibited apoptosis are observed in T cells when co-cultured with SFs (Scott et al., 1990, Salmon et al., 1997), which may contribute to the persistence of inflammation. Besides, the cell adhesion molecules expressed in SFs interact with ligands on T cells facilitating cell infiltration and retention in the synovium. For instance, VLA-4

(very late antigen-4) expressed by T cells interacts with VCAM-1 (vascular cell adhesion protein-1) expressed on SFs to enhance T cell adhesion (van Dinther-Janssen et al., 1991). VCAM-1 is greatly increased in RASF (Hardy et al., 2013), indicating increased interaction between T cells and SFs during arthritis.

Besides, apart from the effect on cell motility, the binding of VLA-1 (very late antigen 1) on T cells and ICAM-1 (intercellular adhesion molecule-1) also reduces the threshold of T cell activation (Brunmark and O'Rourke, 1997). B cells are also affected by SFs in a similar manner to T cells. RASFs enhance B cell survival by elevating the expression of B cell activation factor (BAFF), a proliferation-inducing ligand IL-6 (APRIL), VCAM1 and CXCL12 (Burger et al., 2001, Reparonschuijt et al., 2000, Bombardieri et al., 2011). The expression of APRIL and BAFF by SFs also promotes B cell differentiation and activation (Bombardieri et al., 2011), increasing the production of autoantibodies. The participation of SFs in B cell differentiation and survival further supports the idea that SFs enhance joint immune responses.

1.4.3 Functional subsets of RASF

The phenotypic and functional heterogeneity of SFs has recently started to be grasped, with several studies aiming to understand the molecular mechanisms underlying the functional specialisation of synovial fibroblasts. The functions of fibroblasts can vary on their specific anatomical sites (McGettrick et al., 2009). Likewise, recent studies revealed that the fibroblast compartment is often highly heterogeneous within a particular location, such as the joint synovium where several subsets have been identified (Mizoguchi et al., 2018, Croft et al., 2019). Within the synovium, lining and sub-lining SFs express different surface markers which are related to their different physiological functions. SFs localised in the lining layer express VCAM-1 whereas sub-lining SFs express CD90 and CD248 (Croft et al., 2016, Maia et al., 2010) of which the expression of CD248 was remarkably increased in inflamed synovium (Hardy et al., 2013, Maia et al., 2010). Besides, knocking out CD248 reduces the severity of arthritis, with less synovial hyperplasia, cartilage damage and less immune cell accumulation (Maia et al., 2010), suggesting the role of sub-lining SFs in bone and cartilage destruction. A single cell sequencing-based study classified SFs into three groups based on the expression of CD34 and CD90 (Mizoguchi et al., 2018), with CD34+ SFs being more involved in MMPs production and osteoclastogenesis whereas

CD34- SFs produced more cytokines upon stimulation. Distinct SF sub-populations also exhibit varied proliferative stages, adhesion capabilities and responses to stimulations, forming distinct microenvironments in the joint. Some studies have also shown that DNA Methylation signatures are quite diverse between SFs in hips and knees, which suggests different pathogenesis of RA in anatomical locations and may explain the variability in the response to drugs of patients with arthritis (Ai et al., 2016, Frank-Bertoncelj et al., 2017).

1.4.4 Treatment of RA by targeting SFs

Chronic inflammation in the joint is perpetuated by pro-inflammatory networks generated by immune cells, such as T cells, B cells and NK cells. These cells produce a large amount of cytokines and chemokines leading to swelling and cartilage damage. Current biological therapies target these immune cells, as well as the cytokines that they produce (Choy et al., 2013). Therapeutics for RA include B cell depletion, T cell blocking and cytokine antagonists, which have greatly improved the clinical outcomes in RA. These biological agents targeting the immune system decrease inflammation and joint damage and represent a great advance in RA management. In spite of this, these biologics still are not the best treatment for RA since they suppress immune responses to antigens in a non-specific manner, increasing the risk of pathogenic infections, particularly in light of the COVID-19 pandemic. Hence, new therapeutic approaches need to be developed that reduce the impact on host defences and targeting SFs emerges as a potential strategy under this concept.

Surface markers associated with distinct fibroblast subsets may represent an opportunity to target these cells. RASFs exhibit different expression levels of surface markers compared to healthy SFs, and this change in expression correlates with arthritis pathogenesis. Thereby, it could be possible to selectively target SFs based on their phenotype, like targeting surface receptors of SFs such as CDH11 and fibroblast activating protein (FAP). CDH11 deficient mice are resistant to inflammatory arthritis (Lee et al., 2007), and strategies to target CDH11 for RA are currently being evaluated. As adjuvant therapy for RA, the monoclonal antibody RG6125 against CDH11 passed the Phase I clinical trial but failed in Phase II clinical trial due to poor efficacy (Finch et al., 2019). Targeting FAP is of interest. The expression of FAP is a feature of activated SFs,

which play key pathogenic roles in synovial inflammation and joint destruction (Croft et al., 2019). Deletion of FAP+ SFs reduces both inflammation and bone erosion in the arthritis mouse model (Croft et al., 2019). However, systemic depletion of FAP+ stromal cells leads to cachexia and anaemia in mice (Roberts et al., 2013). Therefore, local depletion of FAP+ SFs may be used to improve clinical outcomes of RA. Dorst et al. (Dorst et al., 2020) have demonstrated the possibility of depleting local FAP+ SFs with photodynamic therapy (PDT). PDT is clinically used to treat abnormal cells located in areas of the body where a light source is accessible, such as skin, eyes and lungs. Although the experiments were carried out on RA synovial biopsies, they may open new clinical alternatives.

The SFs of patients with RA also exhibit abnormal expression of intracellular proteins and abnormal signal transduction. Targeting these proteins that contribute to the aggressive phenotype of RASFs, such as invasiveness and migration, may become a potential therapeutic strategy. For example, the protein tyrosine phosphatase (PTP) family, which contributes to the aggressive phenotype of RASFs, have been considered as RA therapy target (Doody et al., 2015, Stanford et al., 2016a, Stanford et al., 2016b). PTPs regulate phosphorylation of JAK/STAT and FAK, further modulating cellular responses such as cell migration and inflammatory response (Böhmer and Friedrich, 2014, Xu and Qu, 2008, Fang et al., 2015). Signaling pathways such as STATs and FAK are highly activated in RASFs. Thus, targeting intracellular proteins to modulate RASF signaling can offer a therapeutic approach, in addition to surface markers. The following sections will focus on an intracellular protein, ARNO, and a sugar molecule expressed on surface glycoconjugates, sialic acid, which we hypothesised may contribute to SF-mediated pathogenesis in RA.

1.5 Collagen-induced arthritis (CIA) mouse model

Although the pathophysiology of RA has been extensively studied, there is still a lack of knowledge regarding the underlying causes of RA. In view of this, together with limited patient samples and healthy controls, as well as the requirement for more effective therapeutics, studies are being conducted on animal models of arthritis, including testing new treatments and identifying proinflammatory mediators and markers of disease progression (Williams, 1998).

Multiple rodent arthritis models are available for research use, such as collagen-induced arthritis (CIA) model, adjuvant-induced arthritis (AIA) model and K/BxN serum-transfer arthritis (STA) model. All of these models involve multiple immune mediators, such as cytokines and chemokines, of which CIA and AIA models demonstrate other clinical characteristics, including proliferation of synovial tissue and destruction of cartilage and bone (Christensen et al., 2016, Carlson et al., 1985). Compared to CIA model, the symptoms of AIA model tend to be less severe and transient (Carlson et al., 1985).

CIA mouse model was first described in 1980 (Courtenay et al., 1980). Joint inflammation can be observed in mice during CIA in rodents when immunized with type II collagen. In this thesis, DBA/1 mice were used to conduct CIA models, as this model shares similar arthritis progression and exacerbations of relevance for this study, such as bone and cartilage erosion, pannus formation, synovial hyperplasia, leukocytes infiltration and loss of joint mobility (Trentham, 1982). Besides, RA and CIA share similar susceptibility associated with major histocompatibility (MHC) class II molecules (Park et al., 2016). Another important similarity between RA and CIA is the presence of pro-inflammatory modulators in the inflamed joints, including cytokines (IL-1 β , TNF α , IL-17) and MMPs (Marinova - Mutafchieva et al., 1997, Sandya et al., 2009). In this thesis, all arthritic SFs were obtained from CIA mice to study pathological changes compared with SFs obtained from naïve DBA/1 mice.

1.6 ARNO-ARF6

1.6.1 ADP-ribosylation factor (ARF) family of guanine-nucleotide-binding (G) proteins and their regulators

Regulation of cell adhesion and reorganization of actin cytoskeleton are necessary for cell motility. The ADP-ribosylation factor (ARF) family of small GTPases, which is a member of the Ras superfamily, is involved in multiple biological processes, such as membrane trafficking, cell spreading and cell cycle (Hassa et al., 2006). ARF proteins are highly conserved in evolution, present in the early evolution of eukaryotes and found in parasites, yeast, animals and humans (J J Murtagh et al., 1992). Like other GTP-binding proteins, ARFs cycle between the GTP-bound state (activated) and GDP-bound state (inactivated),

which is mediated by guanine nucleotide-exchange factors (GEFs) and GTPase-activating proteins (GAPs), respectively (Figure 1-5). ARFs are ubiquitously expressed in eukaryotic cells for membrane traffic and lipid modification (Kahn et al., 2006). Six subtypes of ARFs in eukaryotic cells were defined, Arf1-Arf6, which were classified into three classes based on the similarity of amino-acid sequencing (Kahn et al., 2006). Class I ARF proteins (Arf1, Arf2 and Arf3) are over 96% identical, localise at Golgi apparatus and play roles in vesicular trafficking (Kondo et al., 2012). Class II ARF proteins (Arf4 and Arf5) play roles in the trans-Golgi network (Sadakata et al., 2010). Arf6, which is the only member of class III, is uniquely localised at the inner side of the plasma membrane and is key for cytoskeleton organisation and membrane traffic (Sadakata et al., 2010, Peters et al., 1995).

Among the ARF isoforms, ARF1 and ARF6 are the two most characterized ARF proteins, regulating cell migration in a variety of cells (Cao et al., 2005, Santy and Casanova, 2001, Xu et al., 2017). ARF1 Promotes the formation of carrier vesicles by the assembly of coat protein complexes at the sites of vesicle formation (Stearns et al., 1990), whereas ARF6 control cell spreading and motility via regulation of protein adhesion complexes (Santy and Casanova, 2001, Casalou et al., 2016, Wurtzel et al., 2015). The role of ARFs in cancer cells has been well studied. Interestingly, ARFs are significantly associated with poor cancer prognosis (Gu et al., 2017) and elevated ARF6 enhances breast cancer invasiveness (Hashimoto et al., 2004, Morishige et al., 2008). Apart from that, ARF1 and ARF6 are also involved in a wide range of pathophysiological processes in the development of tumours, such as migration, apoptosis, cell cycle and signal transduction (Stearns et al., 1990, Cao et al., 2005, Kim et al., 2015, Luchsinger et al., 2018, Gu et al., 2017, Hashimoto et al., 2004, Wu and Kuo, 2012a, Brown et al., 2001).

The metastasis and invasion of cells require internalization and recycling of integrins (De Franceschi et al., 2015), and several ARFs are involved in controlling integrin trafficking. For example, Arf1 interacts with B1-integrin to regulate breast cancer cell migration (Norman et al., 1998) and proliferation (Boulay et al., 2011), and B1-integrin requires ARF6 for cell diffusion, as ARF6 inactivation inhibits the recycling of integrin to plasma membranes (Powelka et al., 2004). However, few studies have linked ARFs to SFs, even when increased

invasion and migration are fundamental features in both tumours and arthritis. As was explained before, in RA, SFs adopt an aggressive phenotype, exhibiting the characteristics of high proliferation and enhanced migration which are reminiscent of cancer cells. Besides, RASFs play leading roles in the formation of pannus (Xue et al., 1997). Pannus is described as the invasive granulation tissue covering the articular surface, and the formation of pannus is one of the factors for joint pain. The growth of pannus exacerbates joint inflammation, and it invades cartilage similarly to a local tumour migrating to new tissue.

1.6.1.1 ARF-GEFs

ARF-GEFs mediate the exchange of GDP for GTP to activate the biological actions of ARFs. There are 15 mammalian ARF GEFs in total, which were divided into six groups based on their sequencing similarities including Cytohesins, BIGs, BRAG, FBX, EFA6 and GBF (Sztul et al., 2019). ARF GEFs exhibit differential subcellular localisations which may affect the specificity of activation of ARFs by GEFs, such as BIGs localise to the nucleus, trans-Golgi network and endosomes that activate ARF1 and ARF3, whereas cytohesin 1 (CYTH1) localises at the plasma membrane and endosomes and activate ARF1 and ARF6.

All ARF GEFs contain a conserved catalytic Sec7 domain (Jackson and Casanova, 2000) whose role is to catalyse the activation of ARFs. The biological functions of different GEFs activating the same ARF are different, probably due to the divergent sequences outside the Sec7 domain. ARF-GEFs, such as cytohesins, BRAG and EFA6, contain a pleckstrin homology domain (PH domain) which interact with phospholipids facilitating membrane recruitment. Compared to the Sec7 domain, the PH domain is less conserved, and its function varies among families of ARF-GEFs. For instance, the PH domain plays leading roles in Cytohesin (including Cyth1, ARNO, Cyth3 and Cyth4) function, such as lipid binding (DiNitto et al., 2003) and autoinhibition of the Sec7 domain (DiNitto et al., 2007). Interestingly, GTP-bound ARF6 (activated state) recruits ARNO to the plasma membrane via PH domain binding, implementing a positive-feedback loop which further promotes ARF6 activation (Cohen et al., 2007).

1.6.1.2 ARNO-ARF6 axis

ARF nucleotide binding site opener (ARNO; also known as CYTH2), one out of four members of the cytohesin family, is a key member of ARF GEFs in charge of GTP binding of ARF1, ARF3 and ARF6, playing key roles in cell motility, adhesion and endocytic trafficking (Brown, 2001, Torii et al., 2010, Ito et al., 2018). Although GTP-bound ARF1 and ARF6 exhibit almost identical conformation (Pasqualato et al., 2001), the GDP-bound conformations are different, allowing them to interact with distinct ARF-GEFs, suggesting that GEFs determine the cellular functions of ARF isoforms (Ménétrety et al., 2000). For example, G protein-coupled receptors (GPCRs) are involved in ARNO-mediated biological effects, as increased ARNO expression enhances the internalization of these receptors (Claing et al., 2001, Macia et al., 2012). Likewise, β -arrestins, adaptor and scaffold proteins with multiple functions, transmit extracellular signals across the plasma membrane and β -arrestin binds with ARNO inducing ARF6 activation thereby enhancing receptor internalization. Additionally, activated β -arrestin interacts with ARF6-GDP to facilitate the ARNO-induced loading of GTP (Claing et al., 2001). While ARF1 has no effect on β -arrestin regulated receptor endocytosis (Claing et al., 2001), which may be due to that activated ARF1 localise at Golgi whereas GTP-bound ARF6 localise at the plasma membrane.

Although, the canonical pathway involves ARNO stimulating the exchange of GTP on ARF6; GTP-bound ARF6, in turn, is capable of recruiting ARNO to the plasma membrane via interaction with the PH domain of ARNO in the presence of phosphoinositides (Cohen et al., 2007). Unlike other cytohesin members, ARNO interacts with focal adhesin complex regulating actin remodelling (Frank et al., 1998), further regulating cell migration. For instance, ARNO regulates adipocyte migration via downstream activation of Arf6 through interaction with the focal adhesion adaptor protein Paxillin. Besides, ARF6 promotes cell migration in epithelial cells by facilitating adherent junction disassembly through its effect on endocytosis of adhesion molecules and by inducing peripheral actin rearrangements (Palacios et al., 2001). Although the upstream GEF of ARF6 is not described in this paper, this cannot rule out a role for ARNO in ARF6 activation. ARNO also acts on other downstream proteins to mediate cell migration. Santy and Casanova (Santy and Casanova, 2001) have shown that overexpression of ARNO also induces epithelial cell migration through the

downstream activation of phospholipase D and the Rho GTPase. This translocation behaviour requires the activation of PI3-Kinase upon the stimulation of epidermal growth factor (EGF), insulin or nerve growth factor (NGF) (Venkateswarlu et al., 1998a, Venkateswarlu et al., 1998b). During cellular migration, cytoskeleton remodelling is required to form protrusions, in which multiple signaling pathways are involved.

PI3K-AKT signaling pathway is an important pathway in the regulation of cellular biological effects, such as lipid transport, cell proliferation, inflammation, and cancer metastasis (Gentilini et al., 2007, Hankittichai et al., 2020, Liu et al., 2019). Inhibition of PI3K-AKT pathway results in weakened cell migration induced by cytokines, chemokines and growth factors (Park et al., 2020, Gentilini et al., 2007). PI3-kinase activation is required to translocate ARNO from cytosol to plasma membrane, which is evidenced by pharmacologically blocking PI3K stop the ARNO relocation (Cohen et al., 2007). The recruitment of ARNO to membranes is dependent on its PH domain, which recognizes phosphatidylinositol 4,5 bisphosphate (PIP₂) and phosphatidylinositol 3,4,5 trisphosphate (PIP₃) (Klarlund et al., 2000). PI3K generates PIP₃, this process allows the recruitment of PIP₃ effectors, such as AKT, GEFs and GAPs, to plasma membrane, hence by triggering PIP₃ binding to ARNO-PH domain, this interaction translocates ARNO to plasma membrane for further biological process (Venkateswarlu et al., 1998b). For example, ARNO is involved in PI3K-dependent angiogenic signaling regulating endothelial permeability by activating the AKT pathway (Mannell et al., 2012). Apart from PI3K-AKT signaling pathway, Tague et al. (Tague et al., 2004) has reported that the activation of extracellular signal-regulated kinase (ERK) signaling pathway is required for ARF6-regulated cancer cell invasion. This is the first report linking ARF6-regulated cell invasion with the ERK signaling pathway. In addition, it has been shown that the endothelium permeability is increased by IL-1 β and subsequent activation of MyD88-ARNO-ARF6 cascade (Zhu et al., 2012). In this study, inhibition of ARNO with siRNA increased the localization of VE-cadherin on the endothelial cell surface and blocked IL-1 β -induced endothelial permeability. This study pointed out that the MyD88-ARNO-ARF6 pathway disrupts endothelium stability via the destruction of vascular endothelial (VE)- cadherin cell surface localisation and subsequent tissue structure dissociation. Interestingly, SecinH3, a cytohesins inhibitor,

greatly reduced white blood cell exudation in an air-pouch mouse model (Zhu et al., 2012), revealing the role of cytohesins in inflammatory response, including ARNO. *In vivo*, endothelial cells form a barrier to control the movement of inflammatory cells out of blood vessels and into tissues which is important for mediating local inflammation responses (Poerber and Sessa, 2007), reminiscent of the role of SFs in joint structure.

1.7 Cell sialylation

Like intracellular proteins, plasma membrane-bound glycan chains also play leading roles in cellular responses. The importance of glycans in cellular responses was acknowledged later than other cell constituents, such as proteins, lipids and nucleic acids. It could have been mainly due to the later development of techniques to study basic glycobiology compared to proteins, as glycans are more challenging to identify, purify and quantify (Sharon and Lis, 1981). The emergence of glycobiology, which revolves around the cellular biology of glycans, has filled a gap in the scientific glycan study, although glycans are still far less prominent in the minds of many scientists, in addition to the limitations of experimental tools. Despite this, glycoscientists have relied on limited conditions confirmed the key roles of glycans in cellular function.

Glycans are ubiquitous in living organisms, playing key roles in regulating cellular functions such as signaling, cell-cell interaction and pathogen immunity. N- and O-linked complex sugar residues make up the majority of glycoproteins (Wilson, 2002). When binding to proteins, O-linked glycans attach to serine (Ser) or threonine (Thr) residues, which occur in both eukaryotes and prokaryotes, while N-linked glycans attach to asparagine (Asn) residues, which occur mainly in eukaryotes (Figure 1-6). The glycan moiety in human glycoproteins is made up of a variety of monosaccharides, including galactose (Gal), mannose (Man), fucose (Fuc), glucose (Glc), N-acetylglucosamine (GlcNAc), N-acetylgalactosamine (GalNAc) and sialic acids, and the process of assembling monosaccharides into glycans is dependent on enzymes such as glycosyltransferases and glycosidases. The involvement of different enzymes determines the diversity of monosaccharide structures which are the keys to the functional diversity of glycans. Glycosylation is a common mechanism in nature, occurring in both

prokaryotes and eukaryotes, whereas sialic acids are primarily found on eukaryotic cell surfaces.

Sialic acids, one class of glycans, are a family of nine carbon sugar acids, which are found on the outer cell surface of higher animals and some microorganisms (Figure 1-6) (Varki, 2008). Sialic acid is the only negatively charged monosaccharide, and along with its heterogeneity, it is known to be an important regulator of cell biology and migration. Over 50 different derivatives of sialic acid family members have been reported to occur in Nature (Schauer and Kamerling, 2018), with the two most commonly expressed members being N-acetylneuraminic acids (Neu5Ac) in human cells and N-Glycolylneuraminic acid (Neu5Gc) in non-human cells (Schauer and Kamerling, 1997). The conversion of Neu5Ac to Neu5Gc is catalysed by cytidine monophosphate N-acetylneuraminic acid hydroxylase (CMAH), an enzyme that is lacking in humans (Varki, 2010). The difference between Neu5Ac to Neu5Gc is a single oxygen atom at position 5 (Figure 1-7) and the mutation of gene CMAH in humans has become a hotspot to discuss the difference of sialic acid biology between human and non-human lineages.

In all cells and most secreted proteins of vertebrates, sialic acids are highly enriched and play key roles in cancer metastasis, embryogenesis, viral infection, and immune response (Schwarzkopf et al., 2002, Hauselmann and Borsig, 2014, Nguyen et al., 2021). Due to their localisation at the outermost end of glycan chains (Varki, 2007), sialic acids serve as binding sites for pathogens, lectins and enzymes (Lehmann et al., 2006). Apart from the function of sialic acids themselves, the interactions between sialic acids and sialic acid recognizing proteins, such as selectins and Siglecs, regulate a wider range of biological processes.

1.7.1 Sialic acid biosynthesis and metabolism

The synthesis of sialic acid is a complex process that varies between different forms of sialic acid, and even for the same form of sialic acid, the pathway of synthesis differs between bacteria and eukaryotes. Here is an example of the synthesis of Neu5Ac in eukaryotes (Figure 1-8). Neu5Ac is synthesized in the cytosol by three enzymes from uridine 5-diphosphate N-acetylglucosamine (UDP-

GlcNAc). The first two steps catalysed by GNE are UDP-GlcNAc converted to ManNAc (N-acetylmannosamine) followed by phosphorylation to ManNAc-6-P (ManNAc 6-phosphate). Then, ManNAc-6-P is converted to NeuAc-9p by NANS (Neu5Ac 9-phosphate synthase) with PEP (phosphoenolpyruvate). Next, Neu5Ac is produced by the dephosphorylation of Neu5Ac-9-P by NANP (N-Acetylneuraminic Acid Phosphatase) and transferred into nucleus. Neu5Ac in the nucleus is activated by CMAS (CMP-Sialic acid synthetase) to form CMP-Neu5Ac. CMP-Neu5Ac is then transferred into Golgi where sialyltransferases (STs) catalyse the transfer of CMP-Neu5Ac conjugate on the cell surface (Figure 1-8).

Sialic acid can be released by sialidases, such as endogenous neuraminidases (Neu1-4) or even neuraminidases produced by pathogens. Part of this released sialic acid will be pumped back to cytosol where it is either integrated into another cycle of glycosylation or it is cleaved by sialic acid aldolase (Verheijen et al., 1999). The released sialic acid can also be taken up by pathogens to mimic host cells, facilitating evasion of immune surveillance by pathogens (Stencel-Baerenwald et al., 2014). In addition to sialidases, which regulate the de-sialylation process, sialyltransferases are the enzymes responsible for adding sialic acid to cell glycoconjugates.

Sialyltransferases (STs) catalyse the transfer of sialic acid from donors to the terminal position of oligosaccharide, forming O-linked and N-linked glycoproteins and glycolipids (Harduin-Lepers et al., 2005). Three configurations are identified based on the forms of linkage of sialic acid to terminal galactose or N-acetylgalactosamine: α 2-3, α 2-6 and α 2-8. Compared to the α 2-8 linkage, α 2-3 and α 2-6 are much more common in all species (Figure 1-9). A total of 20 sialyltransferases have been found so far in humans. Among all the sialyltransferases, there are six α 2-3 sialyltransferases including St3gal I-VI, eight α 2-6 sialyltransferases including St6gal I-II and St6galNAc I-VI, and six α 2-8-sialyltransferase including St8sia I-VI. Reflecting its biological relevance, abnormal levels of sialylation have been linked to a wide range of diseases, including rheumatoid arthritis (Matsumoto et al., 2000), microbial infections (Bateman et al., 2010), and cancer (Recchi et al., 1998).

1.7.2 Sialic-acid-recognising proteins

A variety of biological functions are performed by sialic acid due to its unique physical and chemical properties. For example, their negative charge properties lead to anti-adhesive effects on erythrocytes, keeping the blood circulation free from unwanted cellular interactions (Varki, 2008). Besides, sialic acids serve as binding sites for various pathogens and proteins, such as Human Influenza viruses, sialic-acid-binding immunoglobulin-like lectins (Siglecs) and selectins (Schauer, 2000, Varki, 2007, Lehmann et al., 2006). In most of these interactions, these pathogens and proteins recognise specific forms of sialic acids present in glycan chains. Interactions with pathogens were described in 1.7.3.2.

The Siglecs and selectins bind to sialic acid and immunoglobulin domains. The vast majority of immune cells express Siglecs which inhibit the activation of immune cells and signaling pathways (Avril et al., 2006). There are two kinds of categories of Siglecs based on genome similarity and evolutionary conservation. One category includes sialoadhesin (Siglec-1), CD22 (Siglec-2), Siglec-4 (also known as myelin-associated glycoprotein, MAG), and Siglec-15. The second category includes CD33-related Siglecs. The biological effects resulting from the binding of Siglecs to sialic acid are influenced by the type of sialic acid bound to the Siglec. For example, CD22 is highly specific for α 2-6 linked sialic acid which is predominantly found on B cells (Kelm et al., 1994, Powell et al., 1995). α 2-6 sialic acid acts as a ligand of CD22 and B cell receptor signalling is inhibited in B cells lacking ST6Gal I (an α 2-6 sialic acid enzyme) that forms the CD22 ligand (Collins et al., 2006). Besides, CD22 recognises and binds α 2-6 sialic acid to regulate B cell adhesion (Powell et al., 1993) and liposomal containing high-affinity CD33 ligands that inhibit Ig-E mediated mast cell activation also prevent mice from anaphylaxis (Duan et al., 2019). In addition, most CD33-related Siglecs and CD22 contain one or more cytosolic immunoreceptor tyrosine-based inhibitory motifs (ITIMs) that function as inhibitory receptors (Ravetch and Lanier, 2000). Src family kinases phosphorylate the ITIMs when they bind to ligands, resulting in the recruitment of intercellular signaling inhibitory proteins, such as Src homology region 2 domain-containing phosphatase-1 (SHP-1), SHP-2 and suppressor of cytokine signalling 3 (SOCS3) (Crocker et al., 2007). It has been demonstrated that SOCS3 bind to the phosphorylated ITIMs of CD33 and

inhibit cell proliferation induced by pro-inflammatory cytokines (Orr et al., 2007). A defect in the tyrosine kinase Lyn of the SRC family greatly lowers the threshold for B cell activation by inhibiting the phosphorylation of CD22 and recruitment of SHP-1 (Cornall et al., 1998), suggesting that the development of exogenous specific Siglecs may be a potential therapeutic approach for certain autoimmune diseases.

Furthermore, sialic acids are required for the recognition and binding process of most ligands of the selectin family, which regulates the movement of leukocytes along the endothelium, and interactions among immune cells, tumour cells and platelets (McEver, 2002, Ivetic et al., 2019, Tyrrell et al., 1991, Rosen et al., 1985). Selectins, expressed in most immune cells, play a key role in many cellular interactions related to inflammatory processes, cell adhesion and homeostasis (McEver, 2015, Ley, 2003). Recruited immune cells from blood vessels to the injured tissue are observed in acute inflammation. The step of recruiting leukocytes rolling along blood vessels involves adhesive interactions between leukocytes and vascular endothelial cells (Robbins et al., 2010). The leading role of leukocyte (L)-selectin, platelet (P)-selectin, and endothelial (E)-selectin in adhesion and migration of immune cells has been clearly demonstrated in numerous studies (McEver, 2002, Ivetic et al., 2019, Tyrrell et al., 1991). For example, selectins deficient mice exhibit reduced leukocyte rolling and neutrophils extravasation and are eventually dead in mucocutaneous infections (Robinson et al., 1999). Besides, Carbohydrate structural analysis revealed that sialyl Lewis X antigen, which consists of sialic acid, fucose and LacNac, serves as a ligand of selectins regulating leukocytes rolling (Kawashima et al., 2005). Leukocyte adhesion defects are also evident in ST3Gal-IV null mice, characterised by their reduced P- and E- selectin ligand activity on neutrophils (Ellies et al., 2002, Sperandio et al., 2006).

1.7.3 Sialic acid in human diseases

1.7.3.1 Cancer

A common characteristic of cancer cells is an altered glycosylation signature, which has been observed in multiple cell lines associated with metastasis and immune escape (Sato et al., 2005, Kemmner et al., 1992, Schraen-Maschke and

Zanetta, 2003, Adams et al., 2018). These alternations facilitate tumour metastasis by impacting several cell adhesion molecules including integrins, selectins and Siglecs (Zhuo et al., 2008, Guerrero et al., 2020b, Macauley et al., 2014). Enhanced selectin ligands on the tumour surface facilitate tumour cells binding to leukocytes and platelets, thereby enhancing metastasis and promoting escape from immune surveillance. Interestingly, enhanced expression of selectin ligands is associated with increased expression of glycosyltransferases, including sialyltransferases and fucosyltransferases (Dagia et al., 2006). For example, α 2-3 sialyltransferases synthesized Sialyl-Lewis X antigen to act as ligand for E-selectin, facilitating cancer cell metastasis (Numahata et al., 2002).

Sialylation pathways are overexpressed in cancer cells and are promising targets for cancer therapy. The altered sialylation of tumour cells affects their interactions with other cells in ways that affect adhesion, migration, and metastasis (Hauselmann and Borsig, 2014, Rodrigues and Macauley, 2018, Zhang et al., 2018). Moreover, α 2-6 linked sialic acid plays critical roles in natural killer (NK) cell-mediated lysis of leukaemia cell (van Rinsum et al., 1986). Some studies have described that hyper-sialylation of tumour cells assists tumour cells in avoiding recognition by NK cells, thus escaping from immune surveillance (Rodrigues and Macauley, 2018). For example, over-expression of St3gal1 promotes mammary tumour development (Picco et al., 2010). Similarly, St6gal1 is upregulated in many types of cancer cells, such as ovarian, breast and liver tumours (Schultz et al., 2013, Dall'Olio and Chiricolo, 2001, Dall'Olio et al., 2004). Interestingly, in hepatocellular carcinoma cells, overexpression of St6gal1, on the one hand, enhances cell proliferation and migration and on the other hand, decreases cell apoptosis and reduces T cell proliferation, hence facilitating tumorigenicity and escape from immune surveillance (Wang et al., 2019), suggesting the dual role of α 2,6 sialic acid in cell motility and immunoregulation.

1.7.3.2 Infection

The pathogens adhering to the mucosa gain access to the host cells and begin to proliferate. Pathogenic infections are usually initiated by sugar recognition, where sialic acid plays a key role in the infection and survival of the pathogen. On the one hand, pathogens exploit sialic acid to survive. Pathogens, such as

bacteria and viruses, mimic the host by synthesizing or obtaining sialic acid from the host cells to escape from immune surveillance (Severi et al., 2007, Khatua et al., 2010). On the other hand, sialic acid facilitates pathogens to establish infection. For example, *Toxoplasma gondii* invades host cells by recognising and binding to sialic acid on the surface of host cells, and studies have shown that there is a direct correlation between the number of intracellular parasites and the amount of sialic acid on the host cell surface (Monteiro et al., 1998).

1.7.3.3 Immunology

Sialic acids acting as ligands for glycan-binding proteins from humans, viruses and bacteria, play roles in immune responses, such as T cell migration, apoptosis and recruitment (Nan et al., 2007, Wang et al., 2019). Sialic acids as the terminal structure of glycoprotein and their characteristics of negative charge suggest that they play roles in the interaction with cell adhesion molecules and cell matrix components (Buschiazzo and Alzari, 2008). Multiple studies have linked the presence of α 2-3 and α 2-6 sialic acids with cell adhesion, migration and interaction with ECM (Bassagañas et al., 2014, Hsu et al., 2005, Shaikh et al., 2008). The role of sialic acid in cell adhesion is varied among cell types. In cancer cells, α -2,6 sialic acid is required for cell adhesion to ECM (Bassagañas et al., 2014, Yu et al., 2013), whereas in myeloid cells, removal of sialic acid from integrins enhances cell binding to fibronectin (Semel et al., 2002).

Sialic acids may be involved in the biological function of immunomodulators as cytokines, chemokines, antibodies and hormones are glycosylated (Opdenakker et al., 1995, Zheng et al., 2011, Raju et al., 2001). Besides, the incomplete glycosylation of IgG with galactose and sialic acid observed in rheumatoid arthritis leads to immune dysfunction (Dekkers et al., 2018). Additionally, sialic acids bind to the Siglec family of cell adhesion molecules, regulating immune responses (Crocker et al., 2007). Sialoadhesin/Siglec-1, which is expressed on macrophages, binds to sialylated LPS on bacteria and enhances their phagocytosis by macrophages (Jones et al., 2003). Besides, lack of Siglec-1 reduces immune response by reducing macrophages and CD8 T cells (Kobsar et al., 2006).

The function of immune cells is also regulated by sialyltransferases. St6gal1 is involved in B cell development as lack of St6gal1 impairs the activation and differentiation of mature B cells into plasma cells (Wuensch et al., 2000). Likewise, St3gal1 is linked with CD8 T cell homeostasis, as there is a dramatic reduction of CD8 T cells in St3gal1-deficient mice (Priatel et al., 2000). Overexpression of St6gal1 decreases the expression of proinflammatory cytokines, such as TNF α and IFN- γ , but increases immunosuppressive cytokines TGF- β 1 and IL-10 in Hepatocellular carcinoma cells (Wang et al., 2019).

Furthermore, loss of sialic acid increases the sensitivity of cells to microenvironmental stimuli; for example, culturing monocyte-derived dendritic cells with Ac53FaxNeu5Ac, a sialic acid transferase inhibitor that blocks sialic acid expression, decreases the threshold for TLR activation, thereby inducing cytokine production (Bull et al., 2017). In contrast, suppression of neuraminidase activity reduces the production of IFN- γ in T cell (Nan et al., 2007) and proinflammatory cytokines by macrophages (Liang et al., 2006). These data suggest that the downregulation of sialic acid expression is related to the activation of immune responses.

1.8 Thesis Aims

It is now established that the elevated migratory and cytokine production capacity of SFs contributes to tissue and cartilage damage and hence, pathogenesis of RA. This has attracted more attention to the use of SFs as therapeutic targets to avoid side effects associated with general immunosuppression. Despite extensive research into the biology of fibroblasts, there are still many gaps in fulfilling the inflammatory and migratory mechanisms.

Based on this, ARNO, which is ubiquitously expressed in mammalian cells and is known for its role in cell motility, has the potential to be involved in the regulation of pathogenic responses. For example, ARNO-mediated pathways may also be involved in the control traffic of SFs and mediators to the synovial space. Besides, it is well established that glycosylation regulates cell-cell interactions and immunoregulation, and glycosylation is abnormal in chronic inflammatory conditions. Therefore, the specific aims of the thesis were:

- to investigate the transcriptome signatures associated with inflammatory CIA SFs.

- to identify cytokine(s) in the arthritic joint with the ability to modulate ARNO expression and to characterize the role of ARNO-regulated signaling pathways in naïve and arthritic SFs.

- to investigate the regulation of SF sialylation under proinflammatory cytokines in the inflamed joints and to determine the inflammatory activities regulated by altered SF sialylome.

By addressing these objectives, those aims to investigate the potentially intertwined function of ARNO and sialic acid in the process of SF migration and inflammation, as well as in the progression of arthritis.

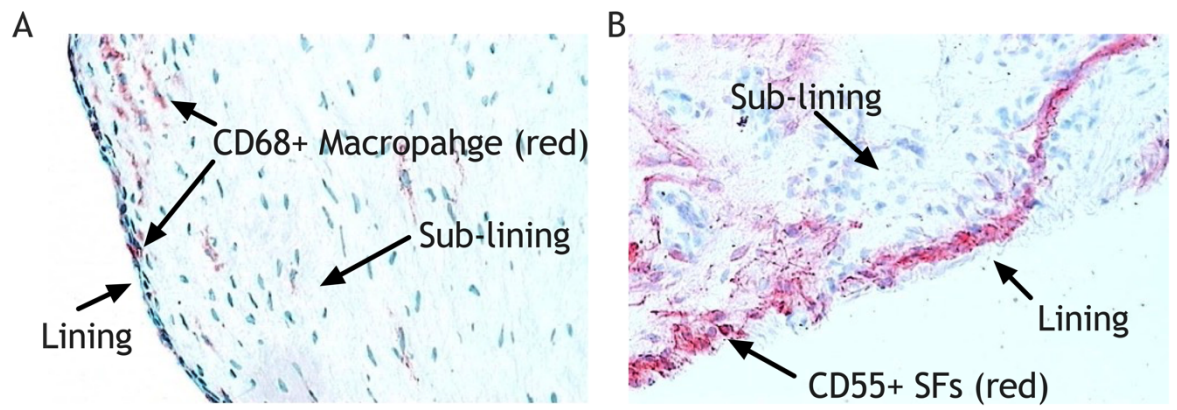


Figure 1-1 Normal synovium (X200 magnification).

Normal synovium stained for CD68+ macrophage (red, A) and CD55+ SFs (red, B).

Adapted from (Smith, 2011).

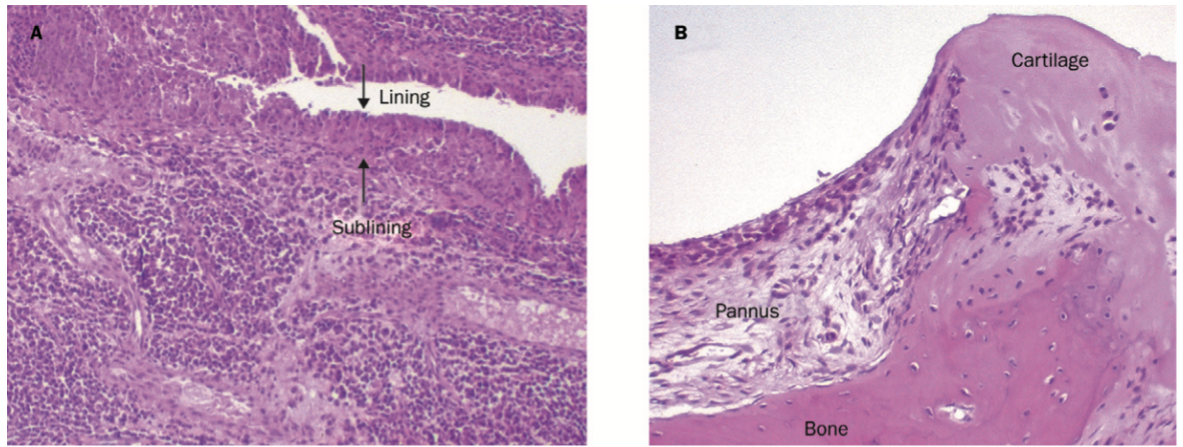


Figure 1-2 Haematoxylin and Eosin staining of joint tissue from patients with RA.

(A) Hyperplastic lining layer and inflammatory infiltrated sub-lining layer, indicated by arrows (X40 magnification). (B) Pannus tissue attaching to and invading adjacent bone and cartilage (X100 magnification).

Adapted from (Lee and Weinblatt, 2001).

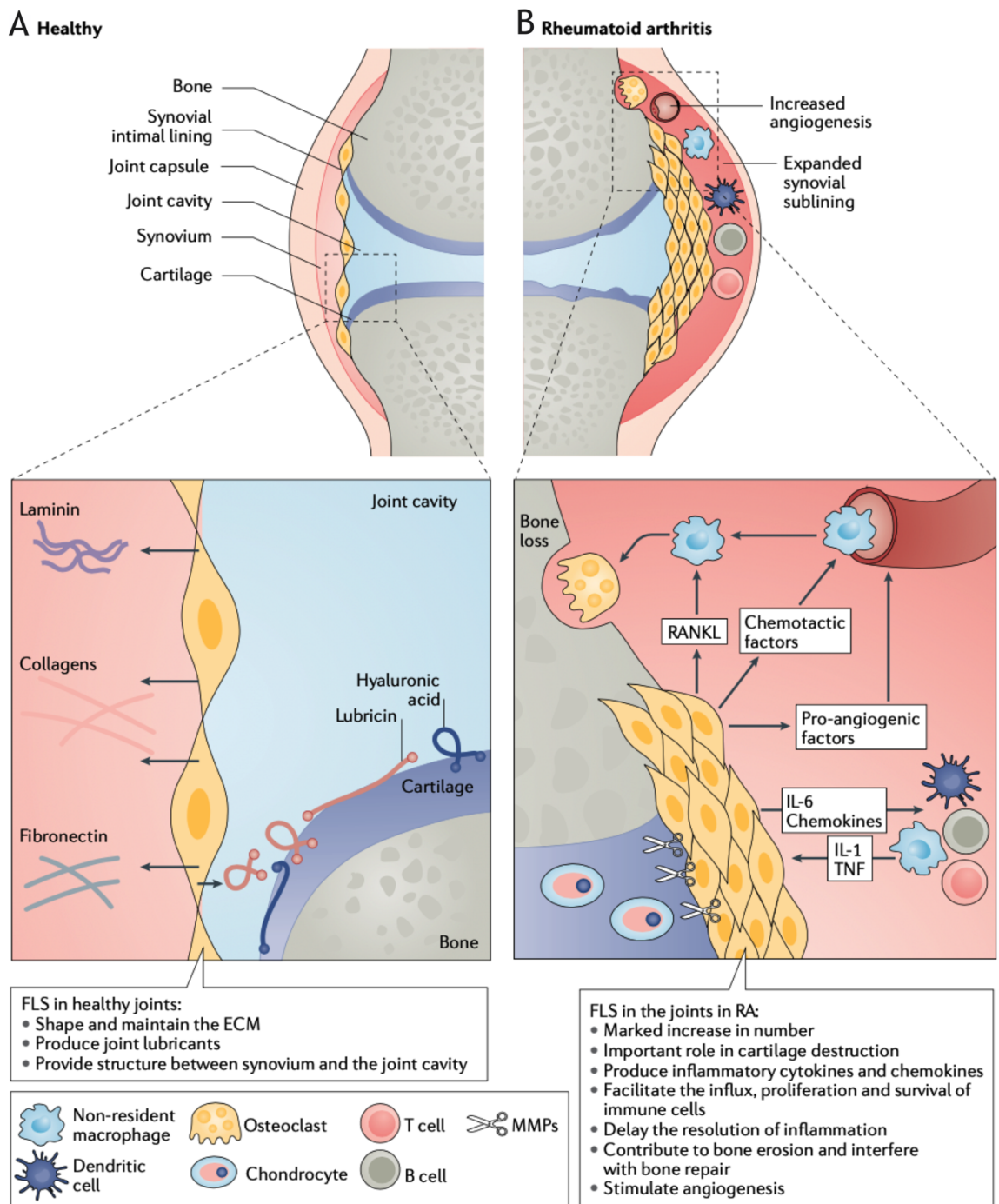


Figure 1-3 Synovial fibroblasts in normal and rheumatoid synovium.

(A) In healthy conditions, synovial fibroblasts (SFs) shape and maintain the extracellular matrix by producing laminin, collagens and fibronectin. SFs also lubricate synovial joints and provide structural support between synovium and joint cavity. (B) In RA, the number of SFs is greatly increased, which leads to the formation of pannus and the destruction of cartilage. Activated SFs produce pro-inflammatory and pro-angiogenic factors, which contribute to joint inflammation and angiogenesis. Activated SFs also produce RANKL, leading to cartilage and bone destruction. Adapted from (Nygaard and Firestein, 2020).



Figure 1-4 Characteristics of SFs in RA.

RASFs adopt an aggressive phenotype that distinguishes them from the SFs in healthy joints. The figure illustrates some of the major features of SFs in RA.

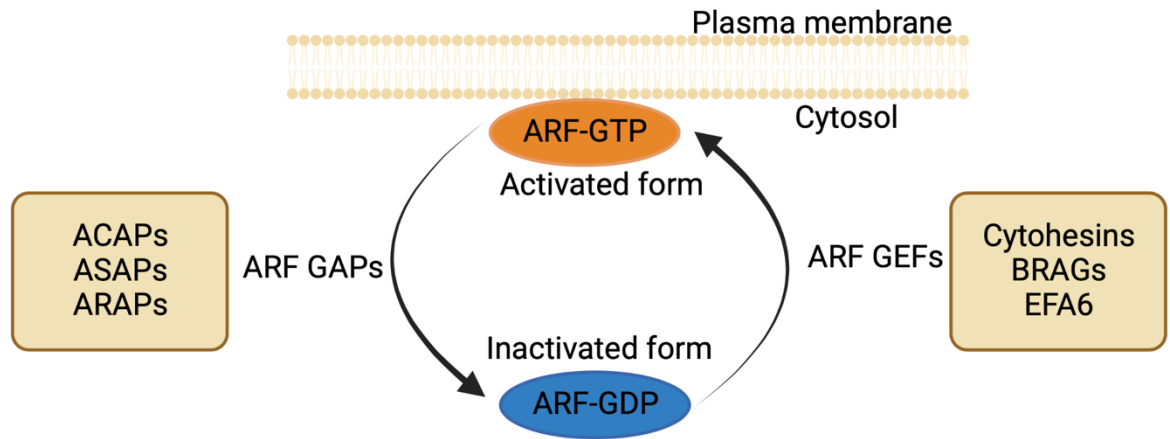


Figure 1-5 Schematic of ARF GDP and GTP cycle.

ARFs cycle between the GDP-bound (inactivated) and GTP-bound (activated) states depending on the activity of ARF GAPs and ARF GEFs respectively.

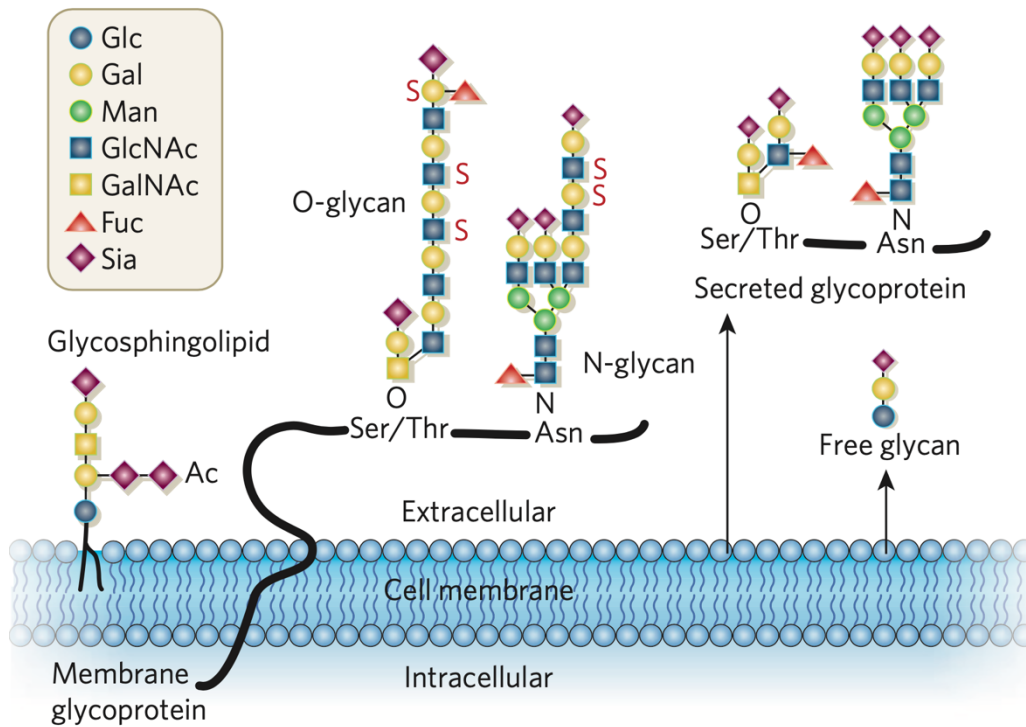


Figure 1-6 Structure of glycoconjugates.

Sialic acids localise at the terminal position of O-linked or N-linked glycans which attach to transmembrane proteins, glycosphingolipids, or secreted proteins. When binding to proteins, O-linked glycans attach to serine (Ser) or threonine (Thr) residues, whereas N-linked glycans attach to asparagine (Asn) residues. (Ac, O-acetyl ester; Fuc, fucose; Gal, galactose; GalNAc, N-acetylgalactosamine; Glc, glucose; GlcNAc, N-acetylglucosamine; Man, mannose; S, sulfate ester). Adapted from (Varki, 2007).

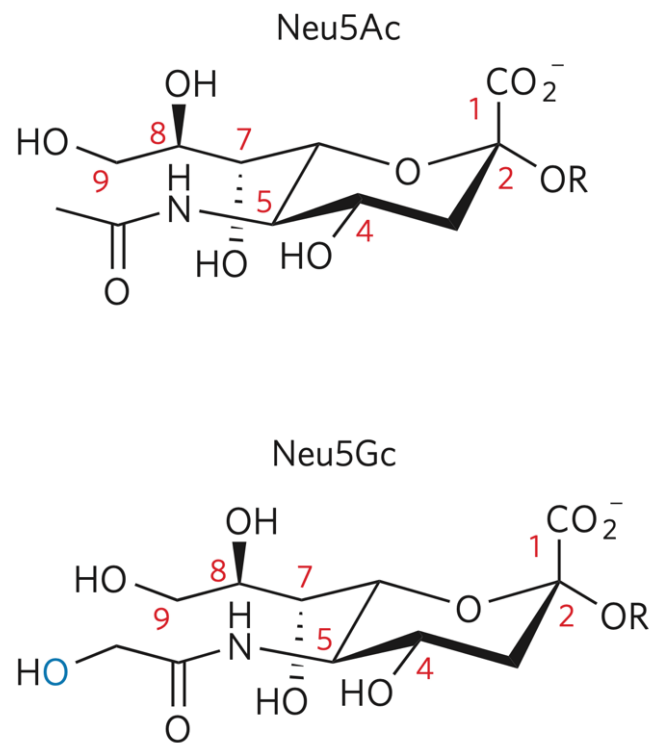


Figure 1-7 Structure of Neu5Ac and Neu5Gc in mammalian cells.

Two main structures of sialic acid have been found in mammalian cells, N-acetylneuraminic acid (Neu5Ac) and N-glycolylneuraminic acid (Neu5Gc). The difference between these two types of sialic acid is that Neu5Gc has an extra oxygen atom (blue).

Adapted from (Varki, 2007).

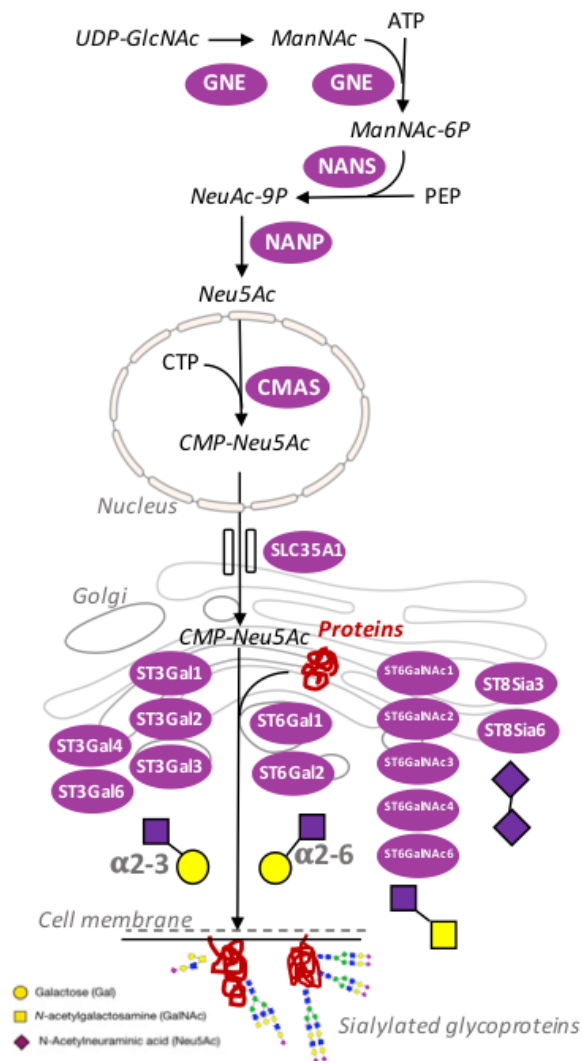


Figure 1-8 Biosynthesis of Neu5Ac.

Schematic diagram of the mammalian glycoprotein sialylation. Enzymes involved in the process include GNE, UDP-GlcNAc 2-epimerase/ ManNAc-6-kinase; NANS, Neu5Ac-9-P synthetase; NANP, Neu5Ac-9-P phosphatase; CMAS, CMP-Sialic acid synthetase; CMP-Neu5Ac transporter (SLC35A1), and sialyltransferases (ST).

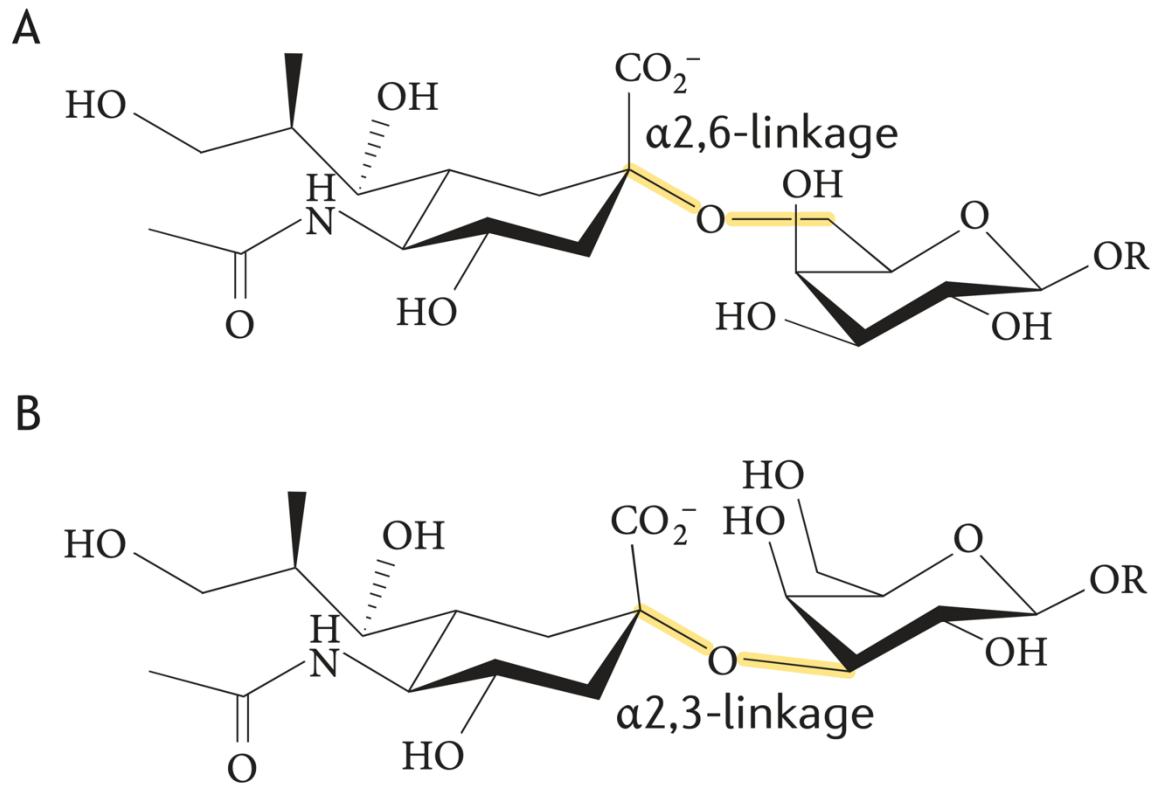


Figure 1-9 Two main linkage configurations of sialic acid.

Schematic of sialic acid attached to carbohydrate chains via α 2,6-linkage (A) or α 2,3-linkage (B).

Adapted from (Stencel-Baerenwald et al., 2014).

Chapter 2 Materials and methods

2.1 Mice

8-week-old male DBA/1 mice were purchased from Envigo (UK) and maintained in the Biological Services Unit of University of Glasgow according to the Home Office UK licences PIL IF5AC4409 and PPL P8C60C865 and the Ethics Review Boards (AWERB) of University of Glasgow.

2.2 Collagen-induced arthritis (CIA) mouse model

8 to 10-week-old male DBA/1 mice received 100 µg of 2 mg/ml Chicken or Bovine Type II collagen (MD Biosciences) emulsified with an equal amount of complete Freund's adjuvant (CFA) on day 0 via intradermally (ID) injection above the tail base. On day 21, mice received 200 µg of the same type of collagen as the first injection in PBS via intraperitoneal (IP) injection. Mice were monitored every two days for body weight, paw thickness and clinical scores. Clinical scores depend on pathological signs of joints and paws and range from 0-4 for each paw. Arthritis severity is scored as the following articular scale: 0 = no evidence of erythema or swelling, 1 = mild swelling and erythema of the ankle or tarsal joints, 2 = mild swelling and erythema of the ankle to the tarsal bone, 3 = moderate swelling and erythema of ankle to the metatarsal joints; 4 = erythema and severe swelling involving the ankle, foot, digits, or ankyloses (Brand et al., 2007). An overall score exceeding 10; or weight loss exceeding 20%; or paw thickness exceeding 4.5 mm; or more than three paws being inflamed was considered the endpoint of the model and the mouse was immediately euthanized.

2.3 Mouse SF isolation and culture

Isolation and culture of SFs were described as before (Armaka et al., 2009). Briefly, hind and front paws were harvested from mice, skin and soft tissue were removed, followed by washing 2 times in 70% ethanol and DMEM medium containing antibiotics (1% penicillin and streptavidin) before dissection. Paws were then transferred into fresh and sterile DMEM containing 10% FCS, 1% antibiotics, 1% nystatin, 1% glutamine and 1mg/ml type II collagenase (Sigma).

For FACS analysis samples, 1 mg/ml DNase I (Sigma) was added. Samples were incubated in a shaking incubator at 37°C for 80 min. After digestion, EDTA was added at a final concentration of 0.5 mM and samples were incubated at 37°C for 5 min. Following completion of the incubation time, samples were vortexed vigorously to release cells. Cells were then centrifuged, and the supernatant was discarded. For cell expansion, cells were resuspended in complete DMEM medium (10% FCS, 1% penicillin and streptavidin, 1% L-glutamine and 1% NEAA) and seeded in culture flasks. The culture medium was refreshed after 24 hours. Cells were fed twice a week and passaged when they reached 90% confluence using trypsin EDTA (ThermoFisher Scientific #25300054). Cells were used in passage 3 or 4. Cultured cell purity was assessed by flow cytometry before experiments, and CD11b⁺ cells were removed using magnetic bead technology (see section 2.4 below). For *in vitro* stimulation and inhibition of SFs, recombinant IL-1 β , IL-17 and TNF α (ImmunoTools) were used at 10 ng/ml. Cpd188 (Signa-Aldrich) was used to inhibit STAT3 activation for 30 min at 73 μ M. LY294002 (Signa-Aldrich #440204) and AKT inhibitor (Signa-Aldrich #124005) were used to inhibit PI3Ks and AKT activation following incubation for 24 hours at 20 μ M.

2.4 CD11b⁺ cell depletion

Contaminating CD11b⁺ cells in primary SF cultures were removed using Miltenyi Biotec bead technology. Cells were labelled with biotinylated anti-CD11b antibodies (Biolegend #101204) at 2 μ g/ml on ice for 15 mins diluted in PBS with labelling buffer (0.5% BSA and 2 mM EDTA) and washed twice to remove unbound antibodies by adding 3ml of labelling buffer. Cells (10^7 cells) were resuspended in 90 μ l labelling buffer and 10 μ l Anti-Biotin MicroBeads (MACS Miltenyi Biotec #130-090-485), mixed well and incubated for 15 minutes at 4°C. Cells were washed by adding 3 ml of labelling buffer and centrifuged at 300 g for 10 min. The supernatant was pipetted off completely. Cells were ready for separation by suspending in 500 μ l of labelling buffer. Magnetic separation columns were inserted into MACS® Separators which offer a strong magnet and rinsed with labelling buffer. The cell suspension was then added to columns, CD11b⁺ cells were magnetically adsorbed on the columns and the SFs were eluted. Purified SFs were collected by washing columns three times with labelling buffer. Cell

purity was validated by Flow cytometry analysis by expression of Podoplanin (PDPN) and absence of CD11b (Figure 3-7).

2.5 Mouse SF sorting

Cells from mouse synovium were obtained as in 2.3. Cells were then resuspended in red cell lysis buffer for 3 min at room temperature. The lysis was stopped by adding 20 ml cold PBS and samples were centrifuged at 1400 rpm for 5 min. Cells were then stained with Zombie Violet (Biolegend, #423113) or fixable viability dye eFluor 780 (eBioscience) at 1 µl/ml in PBS for 20 min on ice to exclude dead cells. Cells were then washed three times with FACS buffer (PBS with 0.5% FCS and 2mM EDTA), and Fc receptors were blocked using a CD16/CD32 specific antibody for 20 min on ice. Primary antibodies used were anti-CD31 (Invitrogen, #12-0311-81), anti-CD45 (Biolegend, #103106), anti-CD90.2 (Biolegend, #105316) and anti-PDPN (Biolegend, #156204). The antibodies used are listed in Table 2-1. Cells were incubated with primary antibodies diluted 1:200 in FACS buffer for 20 min on ice, then washed 3 times. Cell sorting was performed using FACS Aria III or FACS Aria IIU (All from BD, Figure 3-5A).

2.6 Histology

2.6.1 Joint paraffin blocks

Paws harvested from mice were fixed in 4% paraformaldehyde solution for 24 hours at room temperature. Bone decalcification, paraffin sectioning and H&E staining were completed at Histology Research Service, School of Veterinary Medicine, University of Glasgow.

2.6.2 Haematoxylin and Eosin (H&E) staining

For H&E staining, Paraffin sections/slides were heated in an oven at 60°C for at least 35 min to melt the wax. Sections were immersed in xylene to dewax and then in graded ethanol solutions (100%, 90% and 70%) to hydrate and then washed in running water to remove all reagents. Sections were then stained with Harris Haematoxylin for 2-3 min and washed under running water to remove excess dye. The staining background was reduced by dipping sections in 1% acid alcohol for a few seconds, quickly rinsing in running water, immersing in Scott's

Tap Water Substitute for 30 seconds and then quickly rinsing in running water. Counterstaining was then carried out by dipping sections in 70% ethanol 9-10 times and immersing in 1% Eosin for 2-3 min. Sections were then dehydrated by immersion in 90% ethanol for 1 min, 100% ethanol for 6 min and 100% xylene for 6 min. Sections were then mounted with DPX mountant and sealed with coverslips.

2.7 Short interference RNA (siRNA) transfection

ARNO siRNA (Qiagen, #SI00198632), St6gal1 siRNA (Qiagen, #SI01434699) or Allstars siRNA (negative control, Qiagen, #1027281) were transfected using HiPerFect Transfection reagent (Qiagen, #301705) according to the manufacturer's instructions. Briefly, siRNA was diluted in serum-free DMEM containing 1% L-Glutamine at a final concentration of 100 nM. HiPerFect Transfection reagent was added for 10-15 minutes at room temperature to form transfection complexes. The siRNA was added to cells in a dropwise manner to a final concentration of 10 nM. After 24 hours of incubation under growth conditions, the medium was refreshed, and incubation continued for 2 days to complete the first transfection. After the initial transfection, experiments were carried out or a second transfection was performed in the same way as indicated.

2.8 De-sialylation of SFs in vitro

Cells seeded in 6-well plates were washed three times with cold PBS and incubated for 1 hour under growth conditions with 100 mM/ml Neuraminidase from *Clostridium perfringens* (CP, Roche, #11585886001) diluted in sialidase buffer (PBS: RPMI 1640 = 1:1, pH=6.8) or sialidase buffer only (negative control, NT). Cells were then collected using Accutase™ cell dissociation reagent (ThermoFisher Scientific, #A1110501) for lectin staining or kept in culture for 3 hours in complete medium for RNA isolation.

2.9 Cell migration assay

SFs were seeded in 4-well u-dishes (ibidi, #80466) coated with fibronectin (R&D, # 1030-FN) or 12-well plates until confluency. Gaps were generated by removing

inserts (Figure 2-1) or scratching with P200 tips. The width of the cell-free area was measured when the gap was generated (T0) and 24 hours later under growth conditions (T24) using ImageJ software. The distance of cell migration is the difference between the widths of cell-free regions at two-time points.

2.10 Flow cytometry

For the cell purity check, anti-CD11b-FITC (Invitrogen, #11-0112-85) and anti-podoplanin-Alexa Flour 647 were used. Briefly, following trypsin treatment to detach cells, Fc receptors were blocked as described above, and cells were stained with antibodies (1:200) for 20 min on ice.

For proliferation studies, cells were labelled with 10 μ M proliferation dye eFlour 670 (eBiosciences, #65-0840-90) for 10 min on ice. Labelling was stopped by adding 4-5 volumes of complete culture medium for 5 min on ice. Some cells were then subjected to flow cytometry analysis (Day 0) and the rest of the cells were maintained in growth conditions at the indicated time prior to flow cytometry analysis.

For lectin staining, Peanut Agglutinin (PNA, #B-1075), Sambucus Nigra Lectin (SNA, #B-1305), Aleuria Aurantia Lectin (AAL, #B-1395), Maackia Amurensis Lectin II (MAA, # B-1265-1), all from vector laboratories were used at 2 μ g/ml. Non-specific binding to cells was blocked using carbon-free blocking buffer (vector laboratories, #SP-5040) for 20 min on ice before incubation with biotinylated lectins, diluted in PBS containing 5% carbon-free blocking buffer. Lectins were then detected with FITC-conjugated streptavidin (Biolegend, #405201) or Alexa Fluro 647-conjugated streptavidin (Biolegend, #2068269) or PE-conjugated Streptavidin Antibody (Biolegend, #410504) in PBS for 20 min on ice.

All samples were then diluted in DAPI (Sigma, #32670, dilution 1:1000) prior to analysis to differentiate between live and dead cells. Data were acquired using an LSR II flow cytometer (BD) and analysed using FlowJo version 10.8.0.

2.11 ELISAs

IL-6, CCL2 and MMP3 secretion were detected using ELISA kits (R&D, Duo set) following the instructions by the manufacturer. SFs were seeded in 96 well plates (Corning) at 10,000 cells per well in 150 μ l complete medium. For St6gal1 silencing experiments, supernatants were collected when the initial transfection was completed. Cell number was quantified using crystal violet (0.04 mg/ml, Sigma, #C0775). Briefly, cells were stained with 100 μ l of crystal violet for 30 min at room temperature, then washed at least three times to remove any residual dye, followed by adding 100 μ l of 1% SDS solution (Sigma, #05030) and incubation for 1 hour in a shaker. Absorbance was read at 595 nm using a Tecan Sunrise plate reader.

For ARNO mRNA silencing experiments, the initial transfection was performed in 12-well plates (Corning). Cells were then harvested, subjected to a second transfection in cell suspension prior to being seeded in 96-well plates. The supernatant was collected 24 hours after stimulation with 10 ng/ml IL-1 β .

2.12 Enzyme-linked lectin assays (ELLA)

SFs seeded in 96-well plates were washed three times with cold PBS. Cells were then fixed with Fixation buffer (Biolegend, #420801) for 20 min at room temperature in the dark. Fixed cells were washed (PBS containing 0.05% Tween20 (Sigma, #P1379)) and then incubated with carbon-free blocking buffer for 20 min to block nonspecific interactions. Cells were incubated with biotinylated lectins for 30 min in PBS containing 5% carbon-free blocking buffer. Lectin binding was detected with HRP-conjugated streptavidin (20 min) followed by washing three times with wash buffer. The visualisation reaction was induced with HRP substrate and plates were read at 405 nm using a Tecan Sunrise plate reader.

2.13 MTS cell viability assay

The viability of SFs treated with signal transduction inhibitors and *C. perfringens* sialidase was evaluated using tetrazolium dye MTS assay kit (Abcam, #ab197010). SFs were seeded in 96-well plates in 100 μ l culture medium per well until 90%

confluence reached. Following treatment, SFs were incubated with MTS solution (10 μ l MTS reagent in 100 μ l culture medium) for 4 hours under culture conditions. The absorbance was read at 490 nm using a Tecan Sunrise plate reader.

2.14 Western blots

Cells were harvested and lysed in RIPA buffer (Thermo Fisher Scientific, #89900) containing EASYpack protease inhibitor (Roche, #05892970001) and PhosSTOP tablet (Roche, #4906845001) and incubated for 30 min on a shaker at 4 °C. The lysed cells were then centrifuged at 15,000 x g for 15 minutes at 4 °C. Protein concentration was determined using the Pierce[®] BCA Protein Assay Kit (Thermo Scientific, #23225). Cell lysates were mixed with 10X reducing agent (Invitrogen, #NP0004) and 4X loading buffer (Invitrogen, # NP0007) and then kept at 70 °C for 10 min to denature the proteins. Proteins were separated by the NuPAGE Novex system (Invitrogen) using 4-12% Bis-Tris gels. Gels were run in NuPAGE[™] MOPS SDS Running Buffer (Invitrogen, #NP0001) at 150 V until the loading buffer reached the bottom of the gel. Proteins were transferred onto nitrocellulose membranes and the quality of transfer was assessed by incubating membranes with Ponceau red buffer. Membranes were then washed with TBS containing 0.1% Tween-20 (TBS-T) and blocked in 5% non-fat milk in TBS-T for 1 hour at room temperature. The membrane was then incubated with relevant primary antibodies, as shown in Table 2-2, diluted in 5% BSA in TBS-T overnight at 4 °C (1:5000 unless stated otherwise). The following antibodies were used: anti-Cytohesin2 (Santa Cruz Biotechnology, #sc-374640, 1:1000), anti-ARF6 (Cytoskeleton, #ARF-06, 1:500), anti-p44/42 MAPK (CST, #4695), anti-p44/42 MAPK phospho (CST, #9101), anti-GAPDH (CST, #2118), anti-P38 (CST, #9212), anti-P38 phospho (CST, #9211), anti-AKT (CST, #9272, 1:2000), anti-AKT phospho (CST, #9271, 1:2000), anti-STAT3 (CST, #9139) and anti-STAT3 phospho (CST, #9145). Membranes were washed three times with TBS-T before being incubated with anti-rabbit (CST, #7074P2) or anti-mouse (CST, #7076s) HRP-conjugated secondary antibodies for 1h at room temperature and washed three times in TBS-T. Membranes were incubated in Pierce[™] ECL Western blotting substrate (Thermo Scientific, #32106) and exposed to X-ray film. Protein bands were quantified using GelAnalyzer 2010a software with the relative integrated density values normalised to GAPDH or ERK1/2 expression values.

2.15 GTP pull down assay

ARF6-GTP was quantified using the Arf6 Pull-Down Activation Assay Biochem Kit (Cytoskeleton, #BK033-S) according to the manufacturer's instructions. Briefly, cells were lysed on ice in 200 μ l cell lysis buffer containing a protease inhibitor cocktail and centrifuged at 10,000 \times g for 1 min at 4 °C. An aliquot of 20 μ g lysate was saved for Western blot quantitation of total ARF6 expression. Then, 5 μ g GGA3- PBD beads were added to 125 μ g cell lysate to pull down ARFs-GTP and incubated at 4 °C on a rotator for 1 hour. The beads were washed three times with wash buffer to remove unbound protein. The beads with protein were then resuspended and boiled in Laemmli buffer (SigmaAldrich, #S3401) for analysis by Western blotting as described in 2.14.

2.16 Immunofluorescence staining

For cell staining, SFs (2000-5000) seeded on chamber slides were fixed in Fixation buffer for 10min at room temperature. Cells were washed three times with PBS and permeabilised with PBS 0.05% Triton X-100 for 10 min and blocked (PBS 1% BSA or 10% animal serum from the species in which the secondary antibody was raised) for 1 hour. Slides were washed three times in PBS-T before being incubated with primary antibody (Table 2-3) overnight at 4 °C. Slides were then washed three times in PBS-T and incubated with fluorochrome-conjugated secondary antibodies for 2 hours at room temperature.

For mouse joint sections (7 μ m thick) staining, samples were deparaffinized in Xylene and dehydrated using a gradient of ethanol solutions (100%, 90% and 70%). For antigen retrieval, samples were immersed in 10 mM sodium citrate buffer pH 6.0 at 98 °C for 30 min. Blocking and staining were performed the same as for cells. Slides were mounted with SlowFade™ Diamond Antifade Mountant with DAPI (ThermoFisher Scientific, #S36968) to stain nuclei and covered with glass coverslips and staining was visualized using an EVOS™ FL Auto 2 microscope.

For vimentin staining and data analysis, glass chamber slides (Thermo Scientific, #177402) were coated with 200 μ L of 1 μ g/ml fibronectin (R&D systems, #1030-FN) for 20 min at room temperature. Chamber slides were then washed with PBS. SFs were seeded in the slide and maintained under culture conditions for 4

hours. Any unattached cells are washed away followed by immunofluorescence staining and image taking as described above. Focal adhesion analysis was conducted using vinculin images according to the previous description (Horzum et al., 2014). A threshold area of $0.5 \mu\text{m}^2$ and circularity of 0-0.99 were used to analyse the images. A binarized image of the vinculin was measured, and several parameters were used, including the number of vinculin in each cell and the average length and area of each vinculin in each cell.

2.17 RNA isolation and RT-qPCR

RNA from SFs was isolated using either RNeasy Micro (Qiagen) or EZ-10 RNA Mini-Preps (Bio Basic) kits according to the manufacturer's instructions. Reverse transcription was performed using the High-Capacity cDNA Reverse Transcription Kit (Thermo Fisher Scientific) and RT-qPCR was performed using TaqMan™ Gene Expression Assay (ThermoFisher) or KiCqStart® SYBR® Green Primers (Sigma-Aldrich). The expression of actin in mice was used as endogenous control to normalise samples. Although the target protein, ARNO, might involve in actin cytoskeleton reorganisation, the cycle threshold values of actin did not deviate throughout the assays. Sybr green primers used were actin/NM_007393, Ccl9/NM_011338, Cxcl9/NM_008599, Cldn1/NM_016674, Cmas/NM_009908, Gne/NM_015828, Nans/ NM_053179, Slc35a1/NM_011895, St3gal1/NM_009177, St3gal3/NM_001161774, St3gal4/NM_009178, St3gal6/ NM_018784, St8sia6/NM_145838, St6gal1/NM_145933; St6galnac2/NM_009180, St6galnac4/NM_011373, St6galnac6/NM_001025311. Taqman mRNA primers were studied as follows: Actb/ Mm02619580_g1; Cyth2/ Mm00441008_m1; IL-6/ Mm00446190_m1; CCL2/ Mm00441242_m1; MMP3/ Mm00440295_m1; MMP13/ Mm00439491_m1; TNFRSF11b/ Mm00435454_m1; TNFSF11/Mm0041906_m1; St6gal1/Mm00486119_m1; St3gal3/ Mm00493353_m1; St3gal4 Mm00501503_m1, Myd88/ Mm00440338_m1; NFKBIB/ Mm01179097_m1; IL-1b/ Mm00434228_1 and human IL6/Hs00174131_m1, ST6GAL1/Hs00949382_m1, ST6GAL2/Hs00383641, HPRT/4333768T.

2.18 RNA sequencing and data analysis

Total RNA from both freshly isolated and cultured SFs was isolated. RNA integrity checks were performed using the Agilent 2100 Bioanalyzer System, with RNA

integrity number (RIN) value > 9 for all samples. Library preparation was done using RNA poly A selection at Glasgow Polyomics (Glasgow, UK). RNAseq reads were mapped to the mouse reference genome (GRCM38) using Hisat2 version 2.1.0. Featurecounts version 1.4.6 was used to quantify reads counts. Mouse ENSEMBL gene ID to gene symbol conversion was performed in BioTools (<https://www.biotoools.fr>). The differentially expressed (DE) genes were identified using DESeq2, and Principal component analysis (PCA) was performed using the R Bioconductor project DEBrowser (Kucukural et al., 2019). Genes passing a threshold of $P_{adj} < 0.01$ and $|\log_2\text{Foldchange}| > 1$ were considered as DE genes. Gene Ontology (GO) Biological Process enrichment and KEGG pathway enrichment were conducted with Metascape (Zhou et al., 2019) and PathfindR (Ulgen et al., 2019).

2.19 Mass spectrometric analysis of glycans

Ex vivo cultured SFs were washed at least three times with cold PBS before being scraped off from the tissue culture plate. Cell pellets were resuspended in cold ultrapure water prior to being homogenised and sonicated. Lipids were removed using methanol and chloroform, and precipitated proteins were then reduced and carboxymethylated using dithiothreitol and iodoacetic acid, followed by digestion with trypsin to generate glycopeptides. Glycopeptides were purified using a C18 cartridge (Oasis HLB Plus Waters) prior to N-glycosidase F (Roche) treatment to release intact N-glycans. Released N-glycans were permethylated and then purified using a C18 cartridge (Oasis HLB Plus Waters). The samples were sent to the Department of Life Sciences at Imperial College London to analyse the Mass-to-charge Ratio (m/z) of the permethylated glycans via Matrix-assisted laser desorption ionization-time of flight mass spectrometry (MALDI-TOF MS).

The bioinformatic GlycoWorkBench (GWB, version 1.1) (Ceroni et al., 2008) tool was used to annotate mass spectra with known glycan structures. For comparative studies, the relative expression of each sialylated glycan structure was evaluated by the ratio of sialylated versus non-sialylated twin structures for naïve and CIA SFs, and naïve and TNF treated (10 ng/ml, 48 hours) SFs.

2.20 Statistical analysis

All statistical analysis was performed with Prism 8 software (GraphPad). One-way analysis of variance (ANOVA) with Tukey's multiple comparison correction was used to test for comparing differences among multi-groups. For a data set with two groups, parametric data was analysed using Student's t-test and non-parametric data was analysed using the Mann-Whitney U test. * $p < 0.05$, ** $p < 0.01$, *** $p < 0.001$, **** $p < 0.0001$, ns = not significant.

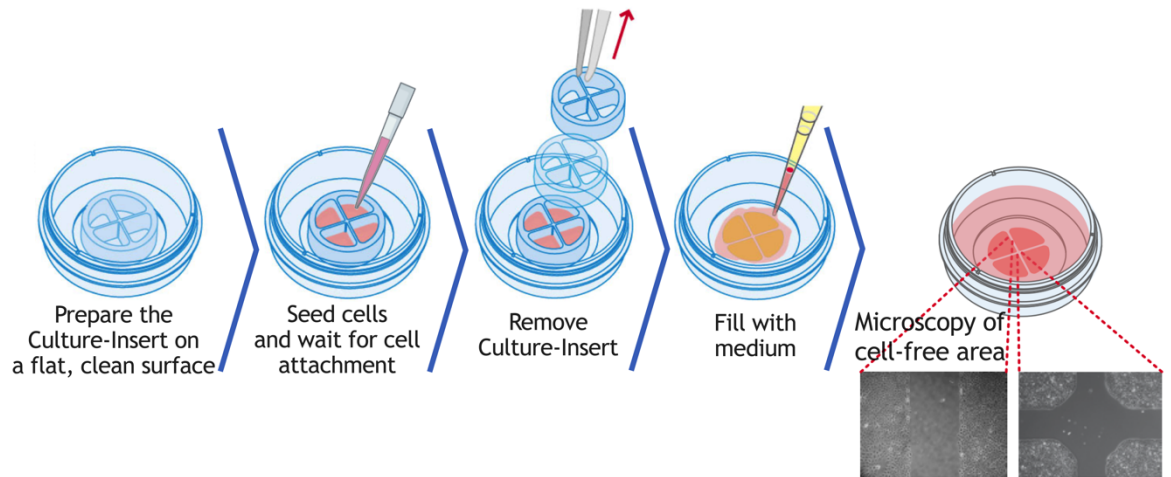


Figure 2-1 Schematic of cell migration assay.

Ibidi® 4 well μ -dishes were used to perform cell migration assays. SFs were seeded in the reservoirs and cultured until monolayer confluence reached. The silicone insert was then removed from μ -dish once four cell patches were generated. Cell migration was measured by calculating the gap of cell-free area at different time points.

Table 2-1 List of antibodies used for FACs sorting.

Antigen	Fluorophore	Clone	Supplier	Catalogue Number	Concentration used ($\mu\text{g/ml}$)
CD31	PE	390	Invitrogen	12-0311-81	2
CD45	PE	30-F11	Biolegend	103106	2
CD90.2	FITC	30-H12	Biolegend	105316	2
PDPN	Alexa Fluor 647	PMab-1	Biolegend	156204	2
CD16/CD32	N/A	93	Invitrogen	2083493	2
Viability dye	Zombie Violet	N/A	Biolegend	423113	1
Viability dye	eFluor 780	N/A	Invitrogen	65-0865-14	1

Table 2-2 List of antibodies used for western blot.

Antigen	Supplier	Catalogue Number	Dilution
ARNO	Santa Cruz	sc-374640	1:1000
ARF6	Cytoskeleton	ARF-06	1:500
GAPDH	Cell signaling	2118	1:5000
STAT3	Cell signaling	9139	1:5000
p-STAT3	Cell signaling	9145	1:5000
AKT	Cell signaling	9272	1:2000
p-AKT	Cell signaling	9271	1:2000
ERK	Cell signaling	4695	1:5000
p-ERK	Cell signaling	9101	1:5000
P38	Cell signaling	9211	1:5000
p-P38	Cell signaling	9212	1:5000

Table 2-3 Antibodies used for immunofluorescence studies.

Specificity	Supplier	REF/Cat No.	Dilution(v/v)
Vimentin	Sigma	V4630	1:200
Vinculin	Sigma	V9264	1:400
F-actin	Invitrogen	A31571	1:200

Chapter 3 Characterisation of arthritic SFs

3.1 Introduction

As explained in the general introduction, the synovium is a highly specialised tissue wrapping the joint and forming the joint cavity, composed of lining and sub-lining areas. In health, the lining layer contains two to three cell layers, which are predominantly composed by synovial fibroblasts (SFs) and macrophages (Smith, 2011). This part of synovium controls the molecular and cellular traffic between the synovium itself and the joint cavity. In RA, as a result of inflammation, the synovium undergoes abnormal hyperplasia, increasing in size to more than ten cell layers thick (Filer, 2013), as a result of SF activation and uncontrolled proliferation. Hyperplasia and abnormal migration of SFs can result in increased synovial permeability, and the destruction of synovial barrier may increase the infiltration of inflammatory cells and cytokines into the intra-articular space (the primary site of inflammation in RA), which in turn further promotes cell recruitment, increasing proliferation and disruption of barrier permeability. SFs are stromal cells that provide structural and nutritional support to the joint and also constitute a barrier that restricts the movement of inflammatory factors and infiltrating leukocytes into the articular cavity, maintaining joint development and homeostasis (Turner and Filer, 2015, Lefevre et al., 2009, Huber et al., 2006).

In addition to their well-described structural functions, SFs have been implicated in promoting joint inflammation and bone degeneration (Bartok and Firestein, 2010). Activated SFs produce proinflammatory cytokines, like IL-1 β , IL-17 and TNF α , to recruit immune cells infiltrating the joint. The recruited immune cells, such as T cells or neutrophils, also secrete proinflammatory cytokines that directly increase the proliferation of SFs, consolidating the synovial hyperplasia (Naylor et al., 2013), ultimately reinforcing the activation of SFs and compromising the SF-dependent barrier permeability. In addition to hyperproliferation, SFs also erode joints via secretion of matrix metalloproteinases (MMPs) and pannus formation (Bartok and Firestein, 2010). Overall, given the importance of SF-mediated pathology, these cells are a potential target for the development of novel anti-arthritic drugs.

In this thesis, the murine Collagen-Induced arthritis (CIA) model was chosen to investigate the characteristics of SFs and pathological pathways regulating SF migration and inflammation during arthritis. This animal model is well suited to the study of human RA as they share multiple pathological similarities (Holmdahl et al., 1989). As seen in RA, CIA mice exhibit bone and cartilage erosion, pannus formation, synovitis, swelling and loss of joint mobility (Trentham, 1982). Besides, CIA mice exhibit high expression of proinflammatory cytokines accumulating in arthritic joints, such as IL-1 β , IL-17 and TNF α (Marinova - Mutafchieva et al., 1997, Williams, 2004), and these cytokines play leading roles in driving clinical outcomes (Marinova - Mutafchieva et al., 1997, Williams et al., 1995, Williams et al., 1992, Thorbecke et al., 1992, Piguet et al., 1992, Joosten et al., 1996). The use of the CIA model is also convenient, as access to relevant clinical samples is very limited and as they are highly heterogenous, they would not provide the reproducible conditions required for the basic discovery science undertaken in this thesis. Importantly, tissue from the clinic has usually been exposed to immunosuppressive treatment, which could hide some of the cytokine-related effects of relevance to this study. In fact, experimental animal models are widely used for multiple purposes, including analysis of disease susceptibility, and disease progression markers and investigating more effective therapeutics (Williams, 1998), as we currently do not have an alternative *in vitro* model to study the complex immunological pathways associated with RA.

The aims of this chapter are to identify the transcriptome signatures associated with inflammatory CIA SFs, to compare their activation with that observed in the human disease, and to further understand the pathogenic transformation of SFs during arthritis, specifically by examining the response of *in vitro* expanded SFs to inflammatory factors.

3.2 Results

3.2.1 Characteristics of arthritic SFs

To investigate the characteristics of SFs in healthy and arthritic joints, paws and SFs from naïve mice and mice undergoing collagen-induced arthritis (CIA) were obtained. During the development of arthritis, mice showed sustained and severe swelling encompassing ankles, paws and digits (Figure 3-1A). Confirming

disease pathology, H&E staining (Figure 3-1B) showed that in CIA joints the synovium invaded the joint cavity and cartilage, whereas in naïve mouse joints the synovium wrapped around the joint cavity. The invasive behaviour of synovial tissue in CIA joints is mainly due to the hyperplasia of the lining synovia, leading to pannus formation and the subsequent destruction of cartilage (Xue et al., 1997).

Next, we investigated whether SFs play a role in disease pathogenesis in the CIA model by staining joints from naïve and CIA mice for expression of vimentin (Figure 3-1C, D), Vimentin is a marker for cells of mesenchymal origin of which elevated expression is also a predictive marker for bone damage (Syversen et al., 2010). Besides, SFs from RA generate vimentin fragments that can be used to differentiate such SFs from those associated with OA (Vasko et al., 2016). There are no specific markers to identify fibroblasts to date, but the expression of vimentin, in combination with the anatomical location, was used to localise SFs in tissue sections and also to confirm the stromal nature of cells grown *in vitro*. Vimentin-positive cells were indeed found to be more abundant in CIA mouse joints compared to naïve controls, and cell layers were thickened. Meanwhile, numerous fibroblasts accumulated in the cavity of CIA mouse joints, which is consistent with the published descriptions of arthritic joint pathology. This supports the idea that inflammatory SFs degrade and invade cartilage, playing a significant role in RA pathophysiology and symptoms (Bartok and Firestein, 2010, Bottini and Firestein, 2013, Mizoguchi et al., 2018). However, the precise underlying mechanisms of SF activation remain unclear.

To evaluate SF activation in CIA mice, transcriptomic studies were conducted in synovial cells isolated from naïve and CIA joints (n=3, clinical scores > 8). Endothelial cells and immune cells were identified and excluded by their expression of CD31 and CD45 respectively. SFs were identified and sorted by flow cytometry as low Zombie Violet stained (live cells) CD31-CD45-PDPN+ cells (Figure 3-2A-C). RNA was isolated for high-throughput transcriptome sequencing (RNA-seq) analysis. An aliquot of the sorted SFs was seeded in a chamber slide and their cell phenotype was identified by vimentin staining (Figure 3-2D). Principal Component Analysis (PCA) was used to confirm the distinction between the two mouse experimental groups based on transcriptional data (Figure 3-3A). All detected genes were plotted in a volcano plot and Differentially Expressed

(DE) genes were plotted in a heatmap (Figure 3-3B, C), with 290 upregulated genes and 87 downregulated genes [$p_{\text{adj}} < 0.01$ and $\log_2(\text{foldchange}) > 1$] in CIA compared to naïve SFs. To understand the relationship between transcriptome and functional changes, String Protein-Protein Interaction Network Functional Enrichment Analysis (Szklarczyk et al., 2019) was used to perform GO biological process pathway enrichment and this identified two main functional clusters for the upregulated DE genes: a) cell proliferation and b) immune responses and cell motility (Figure 3-3D). That enrichment reflected changes in cell proliferation, immune response and cell mobility were consistent with the pathophysiological phenotype of RASF. Corroborating this, the expression of pro-inflammatory factors that play a dominant role in arthritis, such as IL-1 β , CCL2, MMP3 and Tnfrsf11, were enriched. These results support the role of activated SFs in the perpetuation of chronic inflammation, and bone and cartilage erosion by proliferating and migrating to cartilage in an uncontrolled manner and hence validate the experimental model. Following this, KEGG (Figure 3-4A) and GO biological processes (Figure 3-4B) pathway enrichment was performed with the upregulated and downregulated DE genes recognised in Figure 3-3B. This showed that ‘cytokine signaling’ (IL-17, TNF and chemokines), ‘rheumatoid arthritis’, ‘Jak-STAT and NOD-like receptor signaling’ pathways were enriched in the upregulated DE genes in activated (CIA) SFs. On the other hand, downregulated genes were those more involved in cell adhesion and motility pathways, where focal adhesion, tight junction and cell adhesion molecules were enriched.

Although these results were performed on the total fibroblasts population, SFs are phenotypically and functionally heterogeneous (Croft et al., 2019, Croft et al., 2016, Mizoguchi et al., 2018), with the functional changes associated with the anatomical locations being the most obvious. Let alone comparing fibroblasts from skin and synovium, SFs from the lining and sub-lining layers of the synovium behave very differently (Mizoguchi et al., 2018). For example, hyperplasia of lining SFs tends to increase with time and inflammatory activity, and lining SFs are more sensitive to anti-TNF α treatment than sub-lining SFs (Izquierdo et al., 2011). To further investigate the characteristics of SFs from the lining layer and sub-lining layer, SFs from healthy and CIA mice were sorted as described in Figure 3-5 by flow cytometry. CD90 was used to discriminate SFs from the lining (CD90-) layer and sub-lining (CD90+) layer (Figure 3-5A). A higher number of

synovial cells were found in CIA joints compared to healthy joints (Figure 3-5B), with elevated expression of CD31 and CD45, reflecting an increased number of leukocytes and endothelial cells in the joints (Figure 3-5C).

Furthermore, the expression of PDPN was elevated in CIA SFs, both in lining SFs and in sub-lining SFs (Figure 3-6A), which correlates with the pathogenic phenotype of SFs (Croft et al., 2016). H&E and vimentin staining suggested that there was arthritic synovial hyperplasia and an increased number of SFs in the joint cavity (Figure 3-1B-D), however, the number of SFs recovered in arthritic mice by cell sorting, compared to naïve animals, was similar (Figure 3-6B). When the percentage of SFs in the lining and sub-lining synovium was calculated, this showed that the percentage of lining SFs increased in arthritis, while the proportion of sub-lining SFs decreased in arthritis (Figure 3-6C). This finding agrees with human pathology, where lining SFs are more proliferative than those found in the sub-lining areas (Bartok and Firestein, 2010). To investigate the immune response in SFs subsets, RNA was isolated from naïve and CIA lining and sub-lining SFs (CD90- and CD90+) and IL-6, CCL2 and MMP3 mRNA expression was examined (Figure 3-6D) since these inflammatory mediators play leading roles in joint inflammation and cartilage damage. The expression of these pro-inflammatory mediators was upregulated in CIA SFs compared to naïve SFs, confirming previous results (Croft et al., 2019).

3.2.2 SF responses to inflammatory cytokines

Having established the pathogenic change of SFs in the CIA model, we next investigated the characteristics of SFs in response to pro-inflammatory cytokines. To achieve that, SFs were cultured and expanded *ex vivo*, which allowed us to obtain enough SFs and check whether they were still responsive to cytokine stimulation. Murine SFs were isolated and expanded *in vitro*, and cultured SFs were harvested after three or four passages as previously described (Rosengren et al., 2007). Cell purity was checked prior to the experimental set up by flow cytometry, any CD11b+ contaminating cells were removed by magnetic bead technology (Figure 3-7). In addition, an extra cell purity check was performed by vimentin staining (Figure 3-8), as this ruled out the possibility of synovial macrophages being present in the cultures as contaminating cells, as they would be negative for vimentin staining.

To examine the phenotypic changes during *in vitro* culture, distinct subpopulations of SFs (lining and sub-lining SFs) from naïve and CIA mice were sorted by flow cytometry, followed by RT-qPCR to detect IL-6 and MMP3 expression in these freshly isolated SFs (Figure 3-9A) as well as in the SFs cultured for 20 days *in vitro* (Figure 3-9B). IL-6 and MMP3 were chosen as they are greatly upregulated in arthritis and are key factors of RA pathogenesis. When comparing gene expression in freshly isolated (Figure 3-9A) and *in vitro* cultured (Figure 3-9B) SFs, the expression of IL-6 and MMP3 was reduced in both naïve and CIA SFs. Especially for CIA CD90⁻ SFs, which tend to lose their aggressive phenotype and express relatively the same level of IL-6 and MMP3 as naïve SFs (Figure 3-9). This may be due to the alteration of cell-cell interactions, cell-matrix interactions, and microenvironment stimuli, such that these SFs exhibit lower pro-inflammatory properties.

To examine whether cultured SFs were responsive to cytokines and whether arthritic SFs retained their pro-inflammatory characteristics despite the partial loss of phenotype, SFs were stimulated with IL-1 β to create an inflammatory microenvironment. As expected, cytokine expression was upregulated in response to IL-1 β stimulation including IL-6, CCL2, MMPs and Tnfsf11 in both naïve SFs (Figure 3-10A) and SFs from mice undergoing experimental arthritis (Figure 3-10B). Besides, the increased cytokine production was consistent with the mRNA levels that SFs produce of IL-6, CCL2 and MMP3 upon IL-1 β stimulation (Figure 3-11A, B), and again SFs from CIA mice produce more cytokines than naïve SFs (Figure 3-11C). These data indicate that CIA SFs adopted a pathogenic phenotype *in vivo*, this aggressive phenotype was maintained *in vitro* and was revealed in response to inflammatory stimuli.

3.3 Discussion

This chapter aimed to describe the characteristics of SFs in naïve mice and mice undergoing experimental CIA, as well as the ability of *in vitro* cultured SFs to respond to inflammatory stimuli, like IL-1 β . In RA, inflammation exposes tissue and cells to a dysregulated cytokine network that leads to tissue damage (Naylor et al., 2013). As a result, activated SFs aggressively degrade and invade cartilage, playing an important role in RA pathophysiology and symptoms (Bartok and Firestein, 2010). Inhibition of SF activation would further reduce

proinflammatory cytokine production, osteoclastogenesis and leukocyte infiltration in the inflamed joints. Multiple factors contribute to the activation of SFs and strengthen destructive potential, including TNF α , IL-6 and IL-1 β , which are current therapeutic targets in RA (McInnes et al., 2016). However, which factors cause the early SF activation in RA, and whether early SF activation is the initial factor in inducing joint inflammation leading to joint destruction remains unclear. Here, RNAseq analysis reveals the transcriptome changes of activated SFs, revealing changes in three main physiological pathways: proliferation, immune responses and cell motility (Figure 3-3D). In addition, multiple cytokine-dependent signaling pathways were activated in CIA SFs compared to healthy cells. The persistent proinflammatory microenvironment contributes to the pathogenic phenotypes of SFs, but their aggressive features, like invading bone and cartilage and spreading between joints (Lefevre et al., 2009), suggests SFs, rather than immune cells, are a key target in the treatment of RA.

The CIA mouse model shares hallmarks with human RA, such as SFs being essential for the development of arthritis and chronically activated in the CIA model, keeping their pathogenic phenotype when cultured *ex vivo*. Although the CIA mouse model does not fully mimic human RA, the mouse model excludes environmental factors, and it is a suitable approach to detect pathological changes at the transcriptional level. Moreover, our results support that SFs sense the proinflammatory environment and respond by secreting multiple factors that stimulate inflammation and pathology. It is known that SFs respond to proinflammatory stimuli and that they return to a quiescent state when the inflammatory stimulus is removed (Alvaro-Gracia et al., 1990). This can explain why effector molecules released by arthritic SFs are decreased to basal levels under *in vitro* culture but can be rapidly restored by exposure to inflammatory cytokines milieu. Compared to naïve SFs, CIA SFs are hyperresponsive to IL-1 β , producing more cytokines and MMPs (Figure 3-11). The maintenance of this aggressive phenotype may be due to conservation of the genomic hypomethylation developed *in vivo* (Corbet et al., 2021, Karouzakis et al., 2009) resulting in a hyper-responsive phenotype in arthritis. DNA hypomethylation is an epigenetic change observed in multiple conditions, including cancer and autoimmune disease (Robertson, 2005). Studies have shown that such DNA

hypomethylation is associated with deficiency of Dnmt1 (DNA Methyltransferase 1) (Turek-Plewa and Jagodziński, 2005, Szyf, 2001). It has been shown that RASFs express less Dnmt1 *in vivo* and upon cytokine stimulation *in vitro* compared to osteoarthritic synovial fibroblasts (OASFs) derived from noninflammatory or low-grade inflammation arthritis (Karouzakis et al., 2009). The same trend was observed in CIA SFs compared to naïve SFs (Corbet et al., 2021). Intriguingly, the proinflammatory cytokines, such as IL-6 and IL-1 β , which are produced by RASFs further induce and maintain the genomic hypomethylation (Karouzakis et al., 2009). This hypomethylating milieu may further contribute to the epigenetic modification of SFs, ultimately rewiring them to an irreversibly aggressive phenotype.

In RA, activated endothelial cells express adhesion molecules and chemokines which recruit monocytes and leukocytes into the joint tissue (Szekanecz and Koch, 2000). Increased permeability of endothelial cells leads to migration of leukocyte into the synovium from the blood, hence worsening joint swelling (Kulka et al., 1955), confirmed by the cell sorting results showing the increase of immune cells and endothelial cells in the synovial membrane of arthritic joints (Figure 3-5C). The enrichment of endothelial cells may be due to a dysregulation of both proliferation and apoptosis. Certainly, the angiogenic response requires a high proliferation of endothelial cells, which on the one hand facilitates the migration of circulating leukocytes into the inflamed joint, and on the other hand, provides oxygen and nutrients to the increased number of cells in the joint (Paleolog, 2002).

Analysis of the ratio of sub-lining and lining SFs from naïve and CIA joints revealed that lining CD90⁺ SFs are the ones leading the synovium hyperplasia in the experimental model. This is reminiscent of that proposed for human RA, where lining SFs proliferate and invade the bone and cartilage. In addition, the elevated expression of PDPN observed in CIA SFs is consistent with the higher expression of PDPN in RASFs compared to normal SFs (Croft et al., 2016). Although arthritic SFs have been shown to be hyperproliferative, the number of cells recovered upon FACs sorting did not show significant quantitative differences between naïve and CIA SFs, this may be due to inadequate synovial digestion during cell collection, as collection of SFs relies on collagenase digestion of the synovium, and as the thickened arthritic synovium shares the

same digest conditions (speed, time and temperature) as naïve synovium, this may be less efficient for the CIA joints. Besides, this may be related to the CIA synovium being more resistant to collagenase digestion, since vimentin staining suggests that SFs are expanded in CIA joints. Furthermore, arthritic sub-lining SFs were shown to retain their pathological characteristics when cultured *ex vivo*, which is consistent with previous findings that they play a crucial role in the immune effector function (Croft et al., 2019).

The data reported in this chapter compared transcriptomic changes in naïve SFs and CIA SFs, emphasizing the pathogenic role of SFs in joint inflammation. Besides, they show that SFs cultured *in vitro* respond to pro-inflammatory cytokine (IL-1 β) stimulation and that (epigenetically rewired) CIA SFs maintain their hyper-inflammatory features when cultured *in vitro*. In addition to inflammation, RASFs are also characterised by enhanced migratory capacity, these two characteristics constitute the pathogenic phenotype of SFs in arthritis. Therefore, the aim of the following two chapters will be to explore the mechanisms or signalling pathways that regulate the migration and inflammation of SFs. Unlike *in situ* SFs, SFs cultured *in vitro* are deprived of contact with other cell types, three-dimensional living space and microenvironmental stimuli, especially those from inflammatory arthritis. Moreover, the phenotype and biological properties of SFs may change with repeated passages during *in vitro* culture (Zimmermann et al., 2000, Neumann et al., 2010). Nevertheless, although, SFs cultured *in vitro* are not completely mimicking *in vivo* physiology, they offer an initial approach to start mechanistic studies as a large number of cells are required. Besides, *in vitro* culture mixes cells from multiple mice and cell culture allows control of the physicochemical environment, which avoid differences due to variation between individual animals. Furthermore, using expanded SFs has a huge impact on research animal welfare, minimising the number of animals used in research. Thus, the *ex vivo* cultured SFs were chosen to investigate the role of the ARNO-ARF6 axis and sialic acid in pathophysiological mechanisms in mice undergoing CIA in the following chapters.

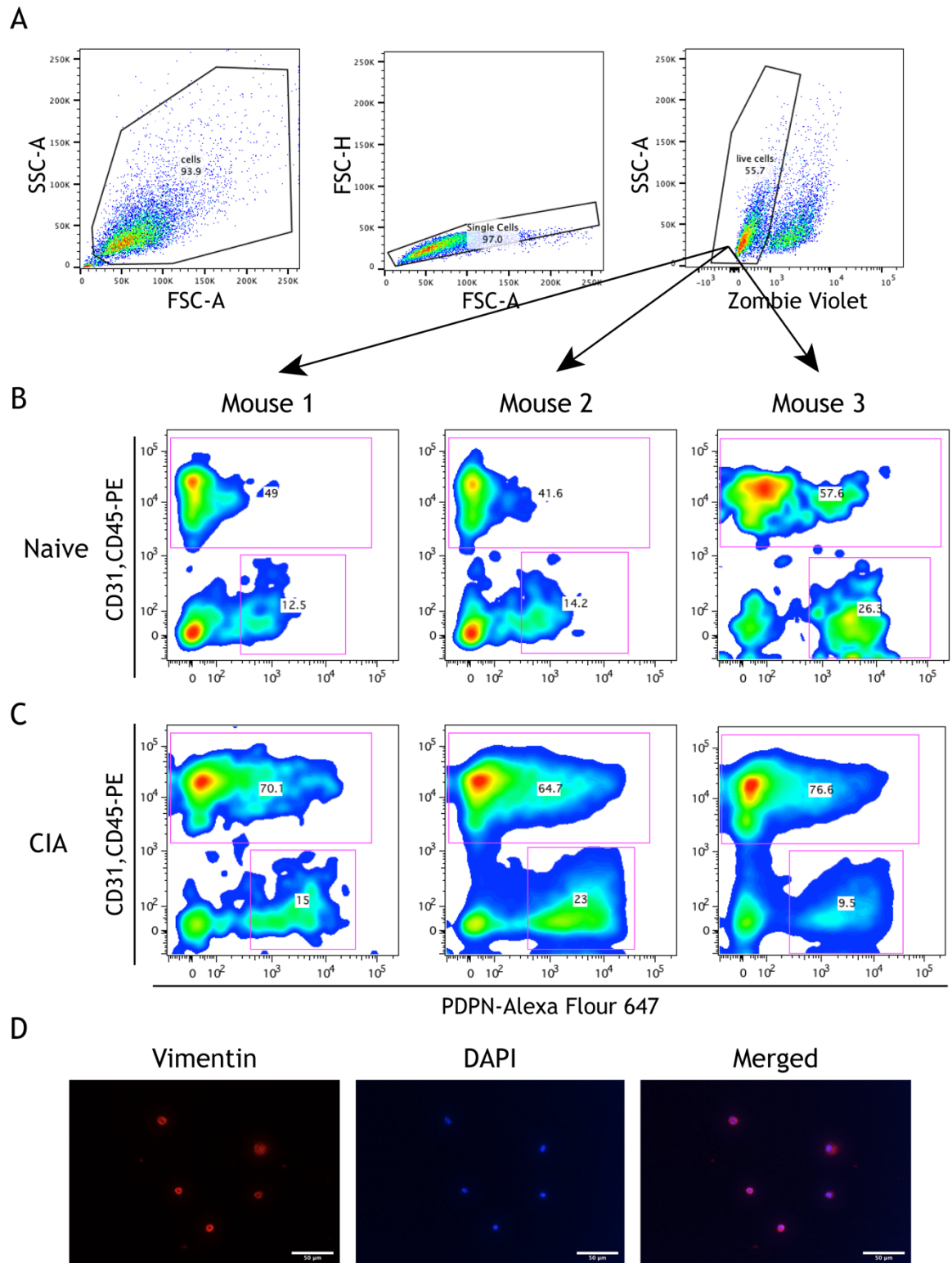


Figure 3-2 Profile of isolated synovial cells.

Cells were extracted from the paws of naïve and CIA mice. (A) Gating strategy of cell sorting is illustrated in dot plots. (B-C) Live synovial fibroblasts (Zombie Violet^{low}, PDPN⁺, CD31- and CD45-) from 3 naïve mice (B) and 3 CIA (score at 9, 10 and 11 respectively) mice (C) were sorted by flow cytometry. (D) An aliquot of sorted cells was seeded in a chamber slide and subsequently stained with vimentin (red) and DAPI (blue). Scale bar: 50 μ m. Images were obtained using an EVOSTM FL Auto 2 microscope. Data are representative of one experiment.

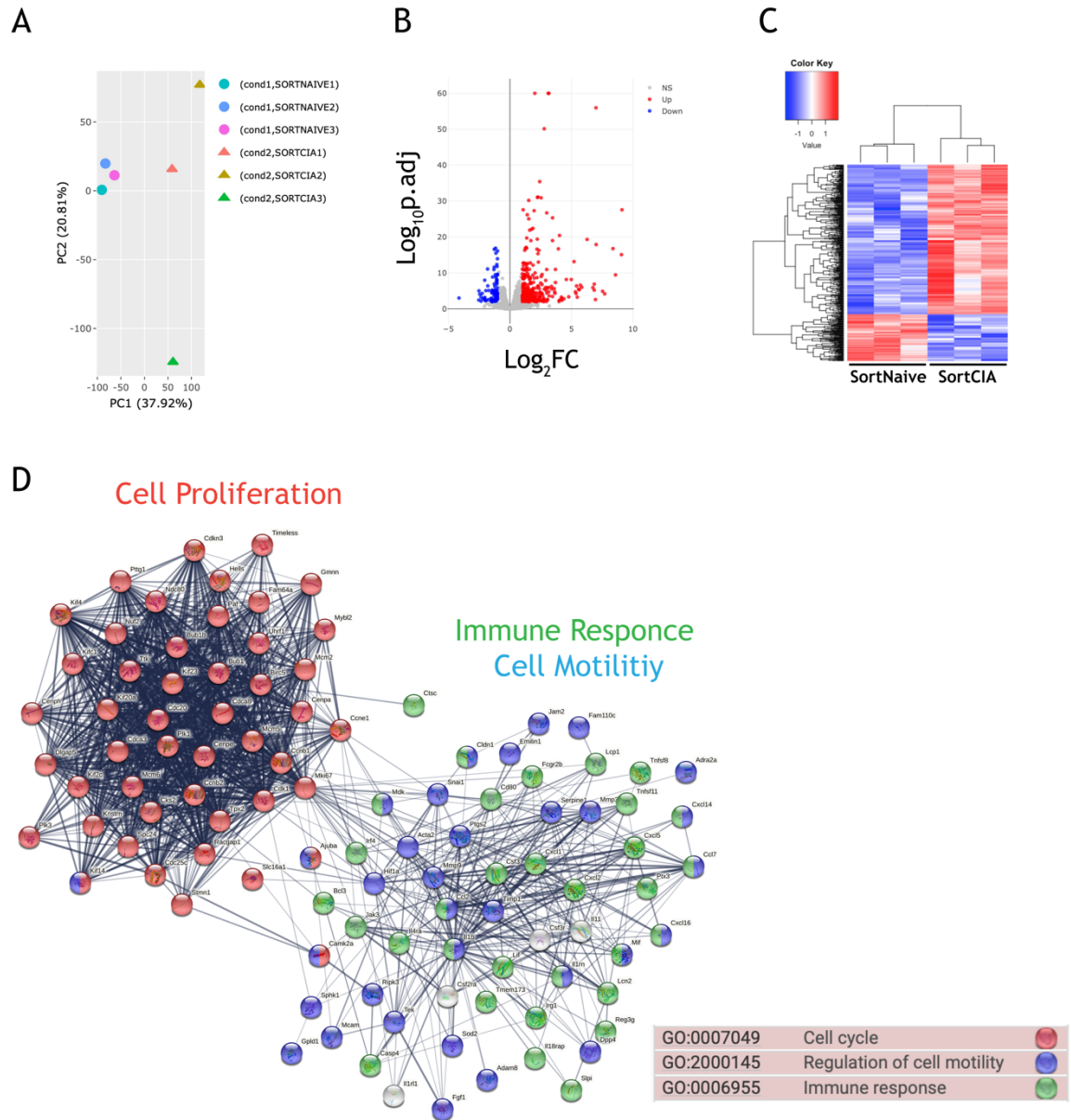


Figure 3-3 Functional enrichment and network analysis comparing naïve and arthritic SFs. RNA was extracted from fresh isolated SFs from naïve and CIA mice as shown in **Figure 3-2 A-C** and subjected to bulk RNAseq (75 bp paired-end, 30 M reads). (A) Principal component analysis (PCA) is shown that circles represent naïve SFs and triangles represent CIA SFs (cond: condition). (B) All detected genes were plotted in a volcano plot, genes that pass the threshold of $\text{padj} < 0.01$ and $|\log_2\text{Foldchange}| > 1$ were considered as differentially expressed genes. In CIA SFs, upregulated genes are coloured in red and downregulated genes are coloured in blue. (C) Heatmap shows the differentially expressed genes detected in (B). (D) GO (Gene Ontology) biological process pathway enrichment was performed on differentially expressed genes in (B) using the String protein-protein interaction network (<https://string-db.org>). Differentially expressed genes were clustered into two groups based on pathway enrichment. The colour of nodes distinguishes the pathways: red: cell proliferation; purple: regulation of cell movement; green: immune response.

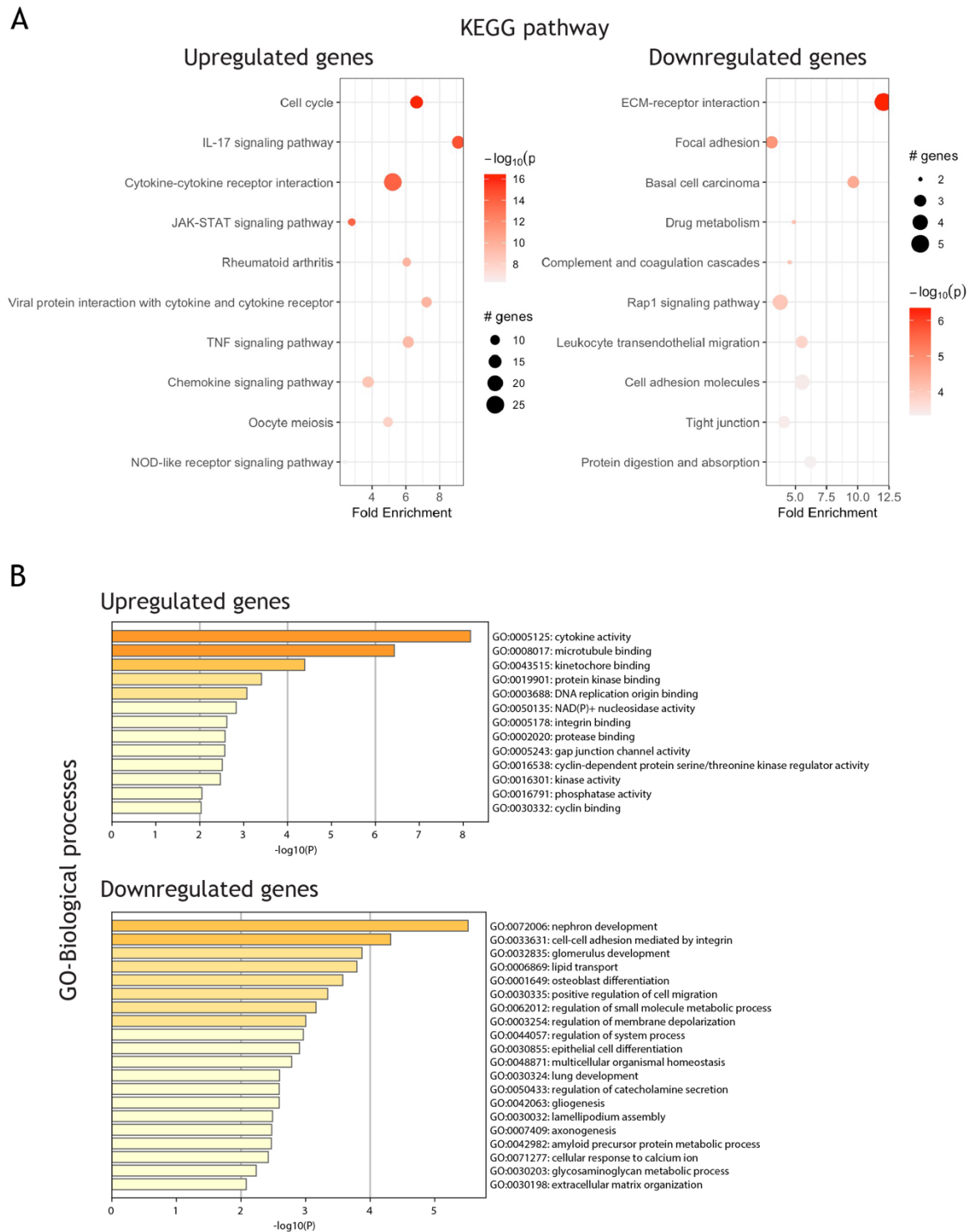


Figure 3-4 Functional enrichment of differential expressed genes in sorted CIA SFs compared to sorted naïve SFs.

Differentially expressed genes identified in **Figure 3-3B** were for pathway enrichment analysis of the KEGG pathway (A) and GO biological process (B). KEGG pathways were plotted in bubble charts using the PathfindR package, with fold change on the X-axis and $-\log_{10}$ p-value on the coloured scale. The size of the bubble is proportional to the number of differentially expressed genes. GO-biological process pathways were plotted in bar charts using Metascape (<https://metascape.org>).

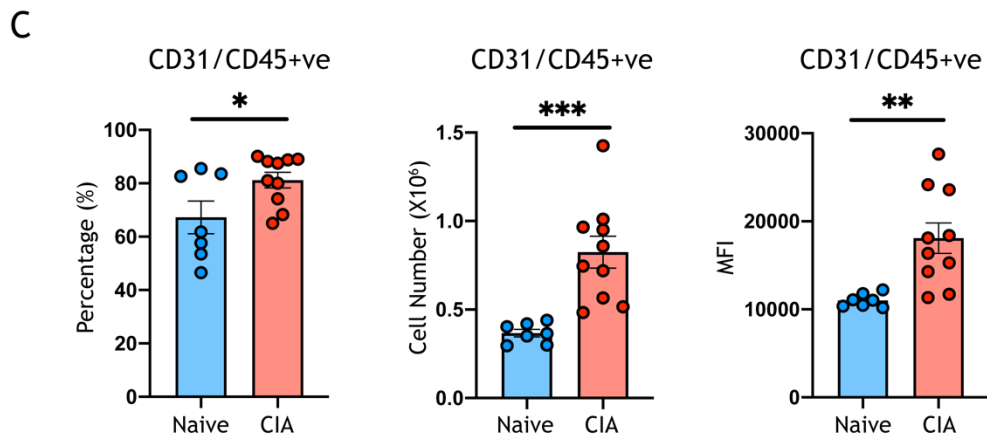
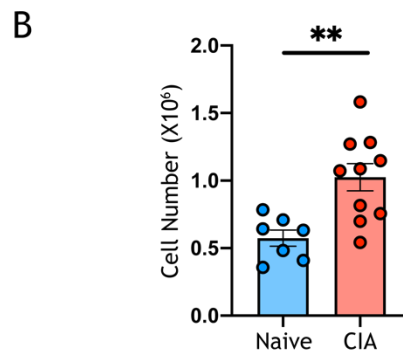
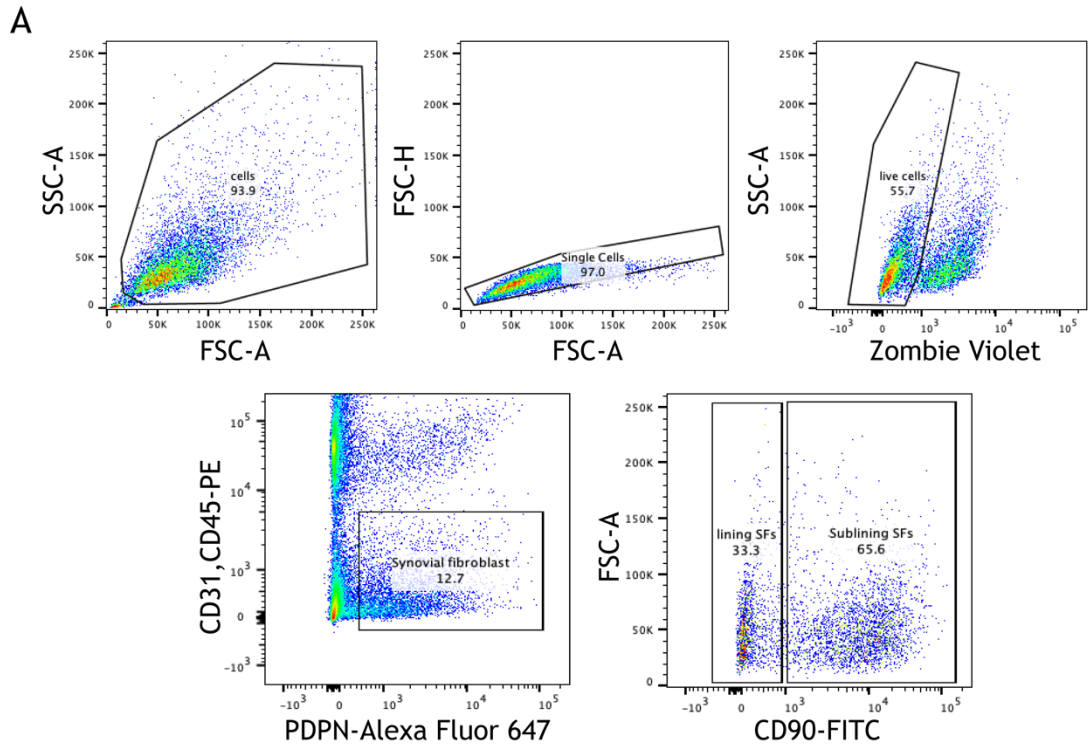
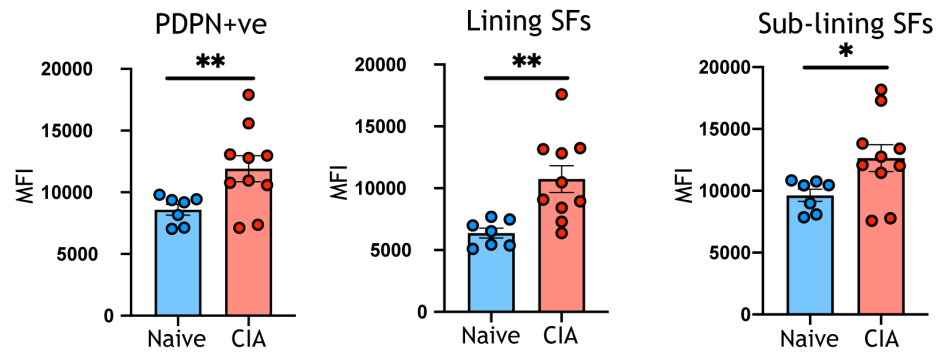


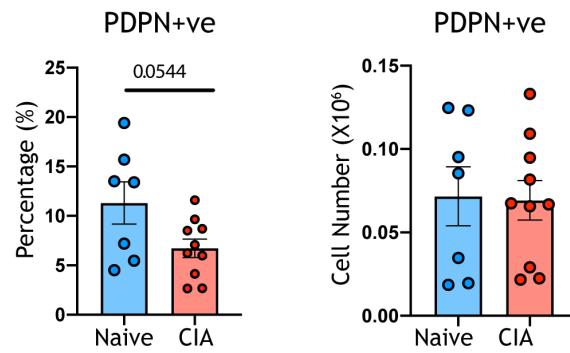
Figure 3-5 Profile of isolated synovial cells.

(A) Gating strategy of freshly isolated SFs subsets (CD90⁻ and CD90⁺) from mouse paws. SFs with lower CD90 expression were identified as lining SFs, while SFs with higher CD90 expression were identified as sub-lining SFs. (B) The total number of cells isolated from paws of naïve and CIA mice. (C) Percentage (left), number (middle) and mean fluorescence intensity (MFI, right) of CD31 and CD45 positive cells. In B and C, each dot represents an individual mouse, data are pooled from 2 independent experiments and presented as mean \pm SEM. Naïve n=7, CIA n=10. *p<0.05, **p<0.01, ***p<0.001 by the Mann-Whitney test.

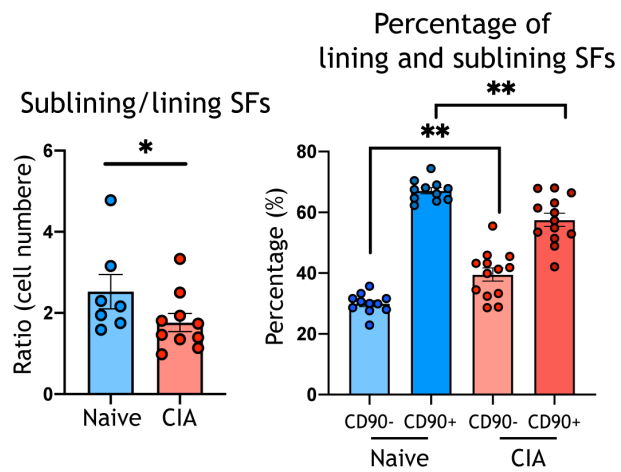
A



B



C



D

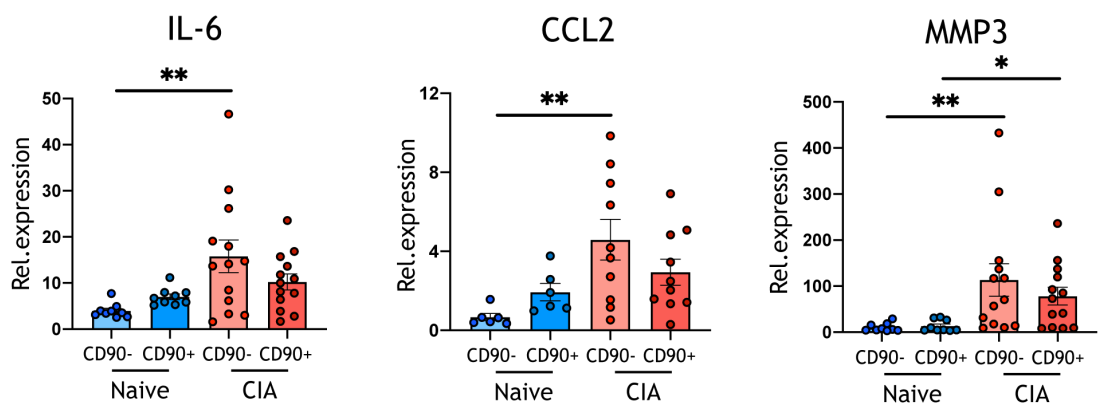


Figure 3-6 Profile of isolated synovial cells.

Synovial fibroblasts were isolated from naïve and arthritic mouse joints as in **Figure 3-5A**. (A) The MFI of PDPN in all identified SFs (left), lining SFs (CD90-, middle) and sub-lining SFs (CD90+, right). (B) Percentage (left) and number (right) of PDPN-positive cells isolated from mouse joints post to collagen digestion. (C) Ratio (left) and percentage (right) of sub-ling (CD90+) SFs and lining (CD90-) SFs. (D) RNA isolated from subsets of naïve and CIA SFs was subjected to RT-qPCR to quantify the expression of IL-6, CCL2 and MMP3. Each dot represents an individual mouse, data are pooled from 2 independent experiments and presented as mean \pm SEM. Naïve $n \geq 7$, CIA $n \geq 11$. * $p < 0.05$, ** $p < 0.01$ by the Mann-Whitney test.

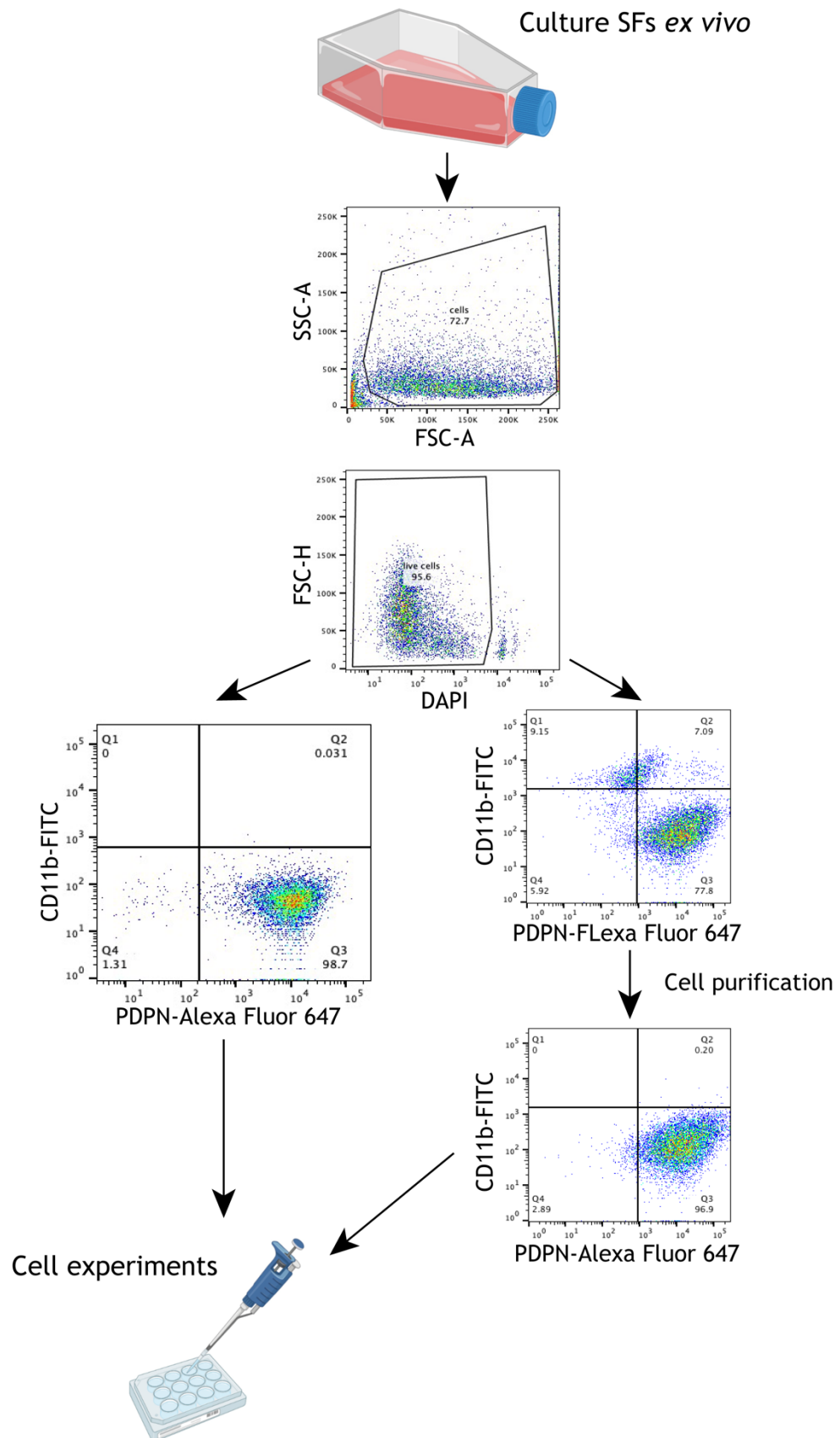


Figure 3-7 Purity check of *in vitro* cultured SFs.

Ex vivo cultured SFs were trypsinized and expression of CD11b and PDPN were checked by flow cytometry. Any contaminating CD11b+ cells were removed using the MACS cell separation column prior to the experimental setup.

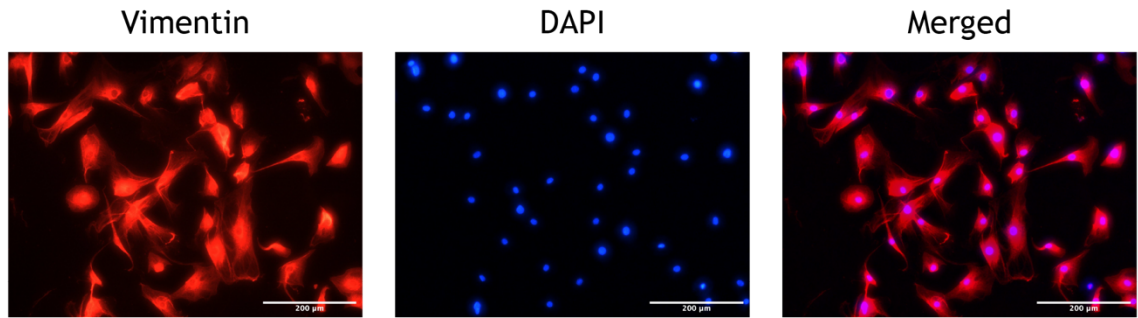


Figure 3-8 Purity check of *in vitro* cultured SFs.

Ex vivo cultured SFs were stained for vimentin expression, visualised using Alexa Fluor 647 (red) and counterstaining with DAPI (blue). Scale bar, 200 µm. Images were obtained using an EVOS™ FL Auto 2 microscope.

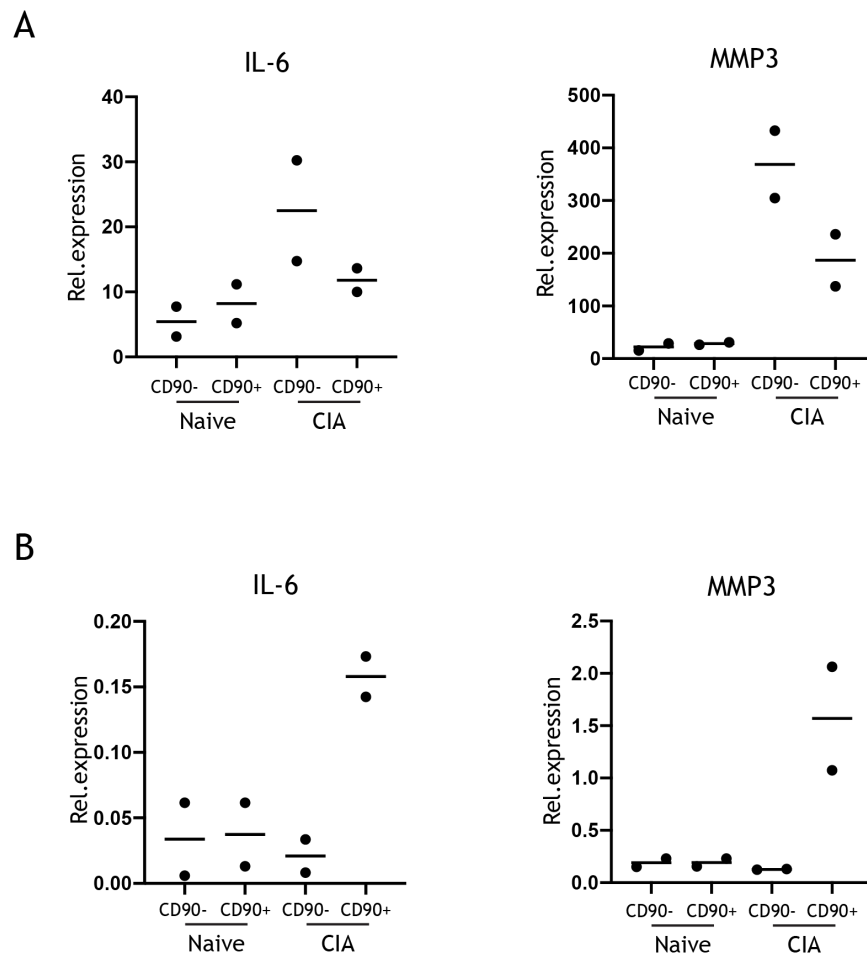
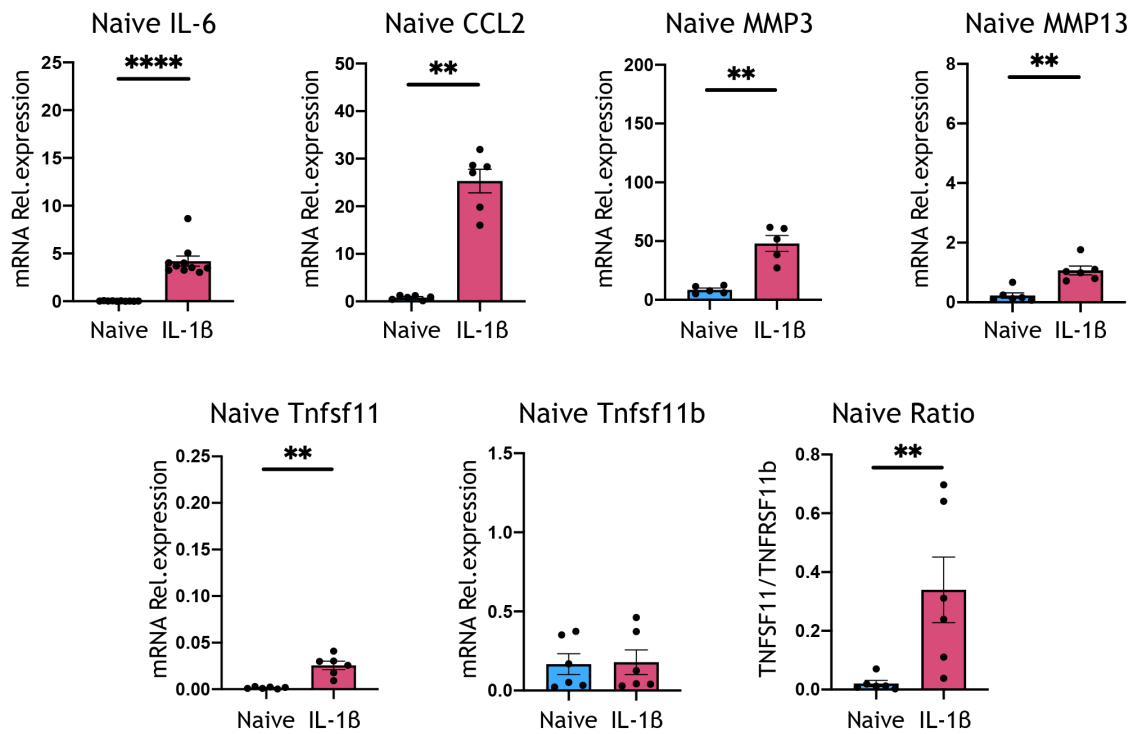


Figure 3-9 ex vivo cultured SFs retain their inflammatory characteristics.

Freshly isolated lining (CD90⁻) and sub-lining (CD90⁺) SFs were subjected to RNA extraction (A) or cultured *in vitro* for 20 days under growth condition (B) prior to RNA extraction. Relative expression of IL-6 and MMP3 were checked using RT-qPCR. Each dot represents an individual mouse (n=2), data are representative of 1 experiment.

A



B

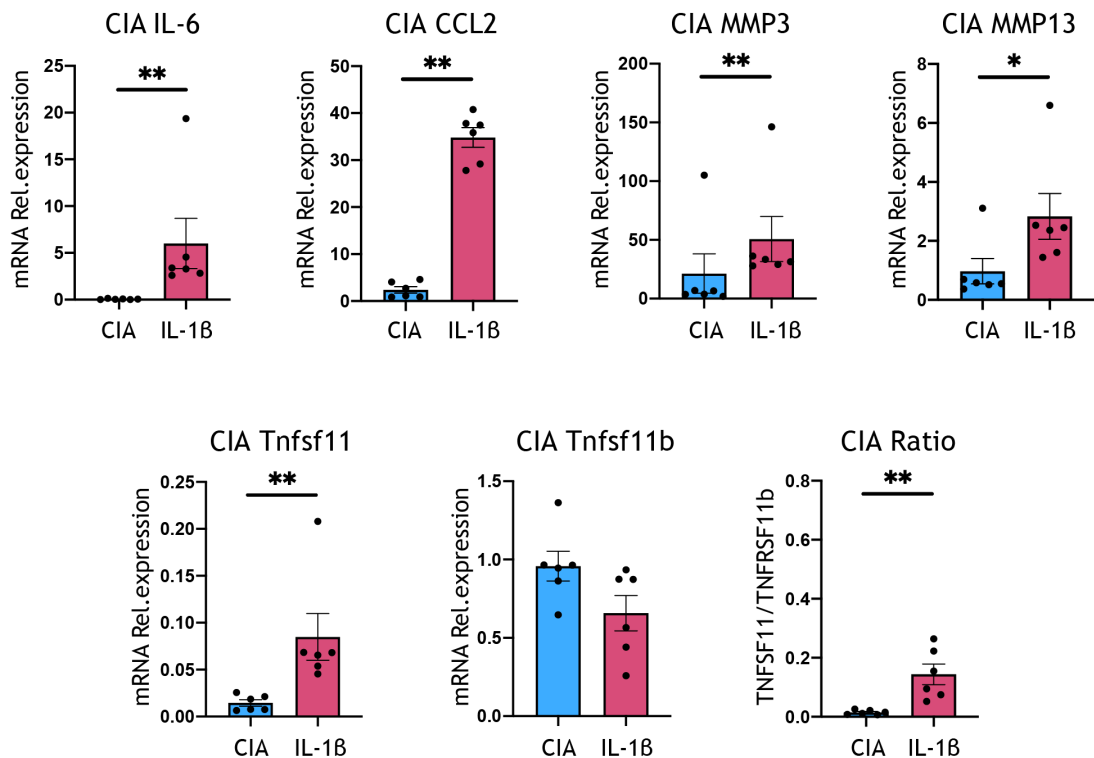
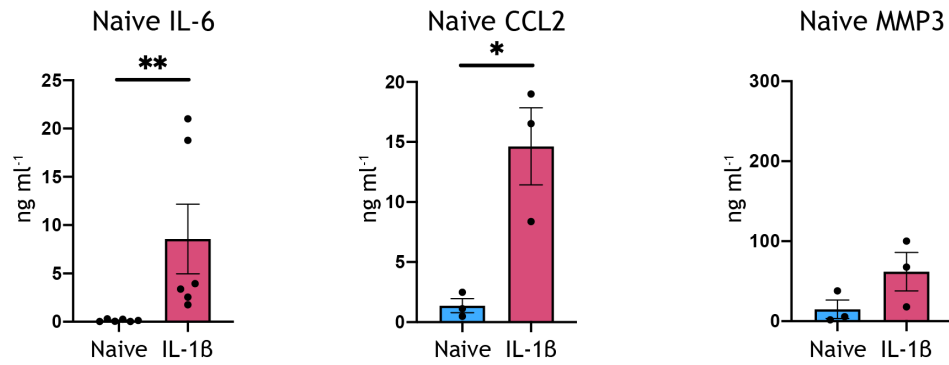


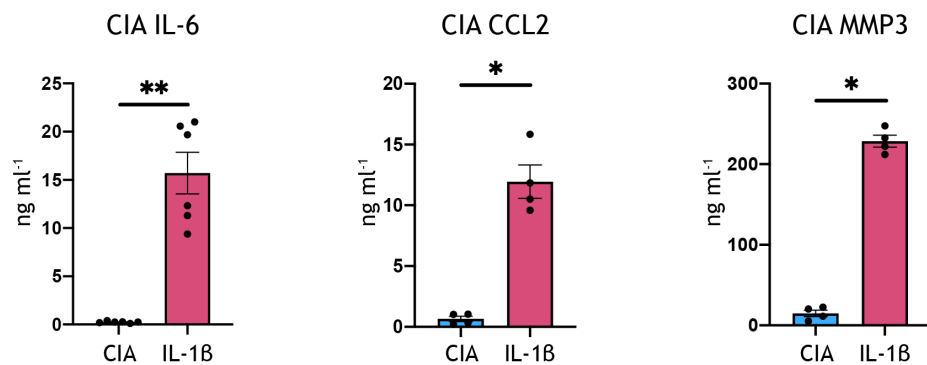
Figure 3-10 IL-1 β induces cytokine production in SFs.

SFs extracted from naïve (A) and arthritic (B) mice were cultured and expanded *ex vivo*. Cells were stimulated with 10 ng/ml IL-1 β for 6 hours prior to RNA extraction. Relative expression of IL-6, CCL2, MMP3, MMP13, Tnfsf11 and Tnfsf11b were assessed via RT-qPCR. Each dot represents one independent experiment analysed in technical triplicate, and error bars represent SEM (n \geq 6), *p<0.05, **p<0.01, ****p<0.0001 by the Mann-Whitney test.

A



B



C

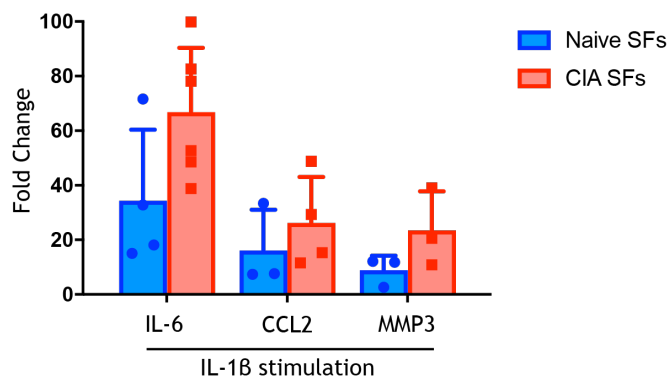


Figure 3-11 IL-1 β induces cytokine production in SFs.

SFs extracted from naïve (A) and arthritic (B) mice were cultured and expanded *ex vivo*. Cells were stimulated with 10ng/ml IL-1 β for 24 hours prior to collecting supernatant. The levels of IL-6, CCL2 and MMP3 in the supernatant were assessed by ELISA. (C) The bar chart shows the fold change of IL-6, CCL2 and MMP3 secretion following IL-1 β stimulation. Each dot represents one independent experiment analysed in technical triplicate, and error bars represent SEM (n \geq 3), *p<0.05, **p<0.01 by the Mann-Whitney test.

Chapter 4 ARNO modulates SF migration and inflammation

4.1 Introduction

Cell adhesion molecules and cytoskeletal changes determine the specificity of cell-cell and cell-ECM interactions (Gumbiner, 1996). Maintaining the stability of such interactions is important for the preservation of tissue structure (Gumbiner, 1996). Clear examples are the processes of wound healing or tumour metastasis, when cells become highly motile, they dissociate from neighbouring cells to crawl away. The enhanced cell movement requires changes in the expression of adhesion molecules and reorganization of actin cytoskeleton. The pathogenicity of SF is also related to changes in their adhesion and migration capacity. Here, the pathological migration of SF is the result of aberrant upregulation of adhesion molecules, like Cadherin-11 (CDH11) and integrins, and dysregulated expression of matrix-degrading enzymes, like the Matrix Metalloproteinases (MMPs) (Chang et al., 2011b, Clark et al., 2003). Although, several cell-signaling proteins are involved in the process of cell invasion and migration, such as Ras-related GTPases, focal adhesion kinases and mitogen-activated protein kinase (MAPK) family proteins (Hernández-Alcoceba et al., 2000, Mostafavi-Pour et al., 2003, Klemke et al., 1997), the mechanisms underpinning SF migration and invasiveness remain unclear.

In terms of cell communication, ARFs are known to regulate actin cytoskeleton and endosome membrane trafficking and have attracted considerable attention in recent years. ARFs modulate the interaction of cell adhesion molecules with the extracellular matrix as well as intracellular vesicle trafficking, and thus they have been proposed as potential targets for intervening in cell responses. ARNO, or Cytohesin-2, is one of the ARF activators with therapeutic potential. This molecule has been shown to promote cell migration and cellular adhesion molecule re-localization in many cell types (Lee et al., 2014, Mannell et al., 2012, Torii et al., 2010). For example, the ARNO-ARF6 axis regulates actin remodelling (Li et al., 2007, Frank et al., 1998), β 1 integrin recycling (Oh and Santy, 2012) and the formation of focal adhesion adapter protein (Torii et al., 2010). Recently, IL-1 β has been linked to the activation of the ARNO-ARF6 pathway in mediating vascular permeability (Zhu et al., 2012). In endothelial

cells, IL-1 β induces immune cell activation through an IL-1 β receptor-MyD88-IKK-NF κ B pathway, whilst disrupting VE-cadherin cell surface localisation via a Myd88-ARNO-ARF6 pathway. Moreover, decreased vascular permeability in the joints and reduced inflammatory symptoms were observed in CIA mice treated with the cytohesin inhibitor SecinH3 (Zhu et al., 2012), supporting a potential function of cytohesins in mediating inflammatory responses.

Hence, we hypothesised that inflammatory cytokines activate ARNO-ARF-dependent pathways which in turn, can promote the migration and inflammatory phenotype of SFs. Specifically, the aims of this chapter are to determine whether i) ARNO was expressed in SFs, and ii) whether inflammatory cytokines regulate ARNO expression to affect SF-dependent pathology.

4.2 Results

4.2.1 IL-1 β upregulates ARNO expression and further activation of ARF6 in murine SFs

To examine the expression of ARNO in SFs and to test the hypothesis of ARNO being regulated in inflammatory conditions, murine SFs were cultured and stimulated *in vitro* with pro-inflammatory cytokines which are enriched in inflamed joints during RA. IL-1 β , TNF α and IL-17 were chosen as they have been reported to be involved in the development of arthritis in animal models (Pineda et al., 2012, Rzepecka et al., 2015) and in human (Dennis et al., 2014, Huber et al., 2006). The expression of IL-6 mRNA was upregulated in response to treatment with the three cytokines (Figure 4-1A), whereas ARNO mRNA was only upregulated by IL-1 β in SFs isolated from naïve mice (Figure 4-1B, C) and SFs from mice undergoing experimental arthritis (Figure 4-1D). TNF α downregulated ARNO expression in naïve SFs and IL-17 has no effect on ARNO expression (Figure 4-1B-D), results that were consistent with previous observations in endothelial cells where IL-1 β increases ARNO expression (Zhu et al., 2012).

Once it was established that ARNO was expressed in SFs, and its expression was increased upon IL-1 β stimulation, we decided to conduct some experiments to examine its functional role. ARNO expression was knocked down using small interfering RNA (siRNA). An Allstars siRNA with no homology to any known mammalian gene was transfected as a negative control. A variety of methods are

available to obtain gene-silenced cells, including CRISPR, siRNA, and gene knockout mice. The siRNA technique was chosen due to its quicker and simpler workflow compared to CRISPR and the development of gene knockout mice. ARNO siRNA efficiently reduced ARNO mRNA (by $78.3\% \pm 0.08$, Figure 4-2A) and protein (by $79.1\% \pm 0.22$, Figure 4-2B) levels compared with Allstars control siRNA. Next, we evaluated the ARNO-ARF6 pathway, classically described as an intracellular vesicle transport regulator, but also linked to cell motility (Mannell et al., 2012, Santy and Casanova, 2001, Torii et al., 2010, Heun et al., 2020) and vascular permeability in immune dysregulated disease (Zhu et al., 2012, Davis et al., 2014, Mannell et al., 2012). To assess the ability of ARNO to activate ARF6 in SFs, ARF6-GTP (activated state) was examined in ARNO-silenced SFs by a GTP pull-down assay. As shown in Figure 4-3, ARF6 was activated in control SFs treated with IL-1 β (increased ARF6-GTP), but such activation was blocked when ARNO was knocked-down, indicating that ARNO is required to induce ARF6 activation in response to IL-1 β and confirming the functional presence of the IL-1 β -ARNO-ARF6 axis in SFs.

4.2.2 ARNO regulates SF motility and focal adhesion formation

As increased motility and cytoskeleton rearrangements are known hallmarks of SFs in inflammatory arthritis and the role of ARNO in modulating cellular migration has been previously demonstrated in other cell types (Torii et al., 2010). Thus, we next assessed the physiological functions of ARNO in the migration of SFs. Cells from naive mice were treated with IL-1 β in control and ARNO siRNA knocked-down SFs, and then subjected to wound healing assays (Figure 4-4). Although IL-1 β did not enhance SFs migration (Figure 4-4A), ARNO knockdown significantly reduced SFs motility (Figure 4-4B), which is consistent with the function of ARNO described in other cell types. To rule out that the observed results were a consequence of changes in cell proliferation rather than migration, cell proliferation and cell apoptosis of ARNO knocked-down and Allstars control-treated SFs were evaluated over a five-day period. Inhibition of ARNO had no significant effect on SF proliferation (evaluated by FACs) or cell death (evaluated with DAPI staining) (Figure 4-5). DAPI is a fluorescence dye which strongly binds to DNA and was selected as a marker to assess cell death as DAPI only passes through intact cellular membranes inefficiently, so dead cells bind more DAPI than live cells.

Surprisingly, when performing cell migration experiments, we found that ARNO knocked-down SFs were detached from plates even after very gentle washes, while control SFs adhered firmly to the plates (Figure 4-6). The interaction of adhesion molecules with extracellular matrix (ECM) is required for cell attachment to plates and the initiation of migration. ARNO knock-down SFs were detached from plates, probably reflecting that ARNO does not only regulate migration, but also regulates cell-ECM adhesion. Furthermore, cell surface receptors interacting with ECM also regulate multiple biological processes, including cell migration, adhesion, proliferation and apoptosis (Hastings et al., 2019). Hence, we hypothesised that ARNO regulates the expression of cell adhesion molecules assembled on ECM to modulate cell migration and adhesion, and experiments to evaluate pathways involved in cell-ECM interaction were subsequently conducted in ARNO knocked-down SFs.

Specifically, the expression of focal adhesion (FA) and vinculin was evaluated. FA is a multiprotein complex, acting as a scaffold which links F-actin and ECM-bound integrins (Figure 4-7A), playing key roles in cytoskeleton remodelling and cell movement (Oria et al., 2017). Vinculin is a key component in focal adhesion complexes that anchors F-actin to cell membrane. Vinculin expression was determined in SFs treated with IL-1 β and ARNO siRNA by immunofluorescence staining. Consistent with cell migration, no significant difference in vinculin expression was observed between naïve and IL-1 β treated SFs (Figure 4-7B, C). However, ARNO knockdown significantly reduced the number and structure (area and length) of vinculin on ECM (Figure 4-8), showing that ARNO is necessary for focal adhesion formation in SFs.

4.2.3 ARNO regulates inflammatory SF response to IL-1 β stimulation.

Upregulated cell-ECM adhesion and proinflammatory stimuli are both factors driving the destruction of articular cartilage. RASFs exhibit significantly higher invasion than OASFs (Lefevre et al., 2009), suggesting that the pathological migration might be related to a pro-inflammatory environment.

In addition, the cytokine IL-1 β is one of the pathogenic factors driving immune cell infiltration to the joint cavity and SF activation at the early stages of RA and

CIA (Kay and Calabrese, 2004). Although ARNO is not typically described as an inflammatory mediator, CIA mice treated with SecinH3 (inhibitor of cytohesins, including ARNO) exhibited significantly reduced acute inflammation (Zhu et al., 2012). Although the authors of this study concluded that the effect was due to changes in the endothelial barrier permeability, our results indicate that a direct effect on SFs via ARNO inhibition is also possible. Hence, we hypothesised that ARNO is required for cytokine secretion upon IL-1 β stimulation, via a pathway that could potentially integrate pathological invasiveness and inflammatory responses in arthritic SFs.

To test this hypothesis, SFs from naïve and CIA mice cultured *in vitro* were treated with either control or ARNO siRNA and subsequently stimulated with IL-1 β . Silencing ARNO expression significantly inhibited IL-1 β induced IL-6 and CCL2 secretion in naïve SFs (Figure 4-9A). Reduced MMP3 was also observed, although it did not reach statistical significance. Intriguingly, the reduction of IL-6, CCL2 and MMP3 in CIA SFs was stronger than in naïve SFs (Figure 4-9B), this may be due to the fact that CIA SFs were chronically activated and adopted an aggressive phenotype in a pro-inflammatory microenvironment *in vivo* and this phenotype maintained during *in vitro* culture, evidenced by the secretion of more inflammatory factors (Figure 3-11). Thus, ARNO knockdown induced greater anti-inflammatory effects in CIA SFs compared to naïve SFs, with IL-6, CCL2 and MMP3 reduced by 9.8, 2.1 and 1.6-fold in naïve SF but 13.1, 2.6 and 3.4-fold in CIA SF, respectively. Overall, we observed that silencing of ARNO inhibited IL-1 β mediated cytokine production and cell migration, suggesting that ARNO may sit at the intersection of inflammation and matrix invasiveness in SFs.

Next, the potential signalling pathways regulated by ARNO were investigated to gain more mechanistic understanding. Activated JAK/STAT3, MAPKs, and PI3K/AKT pathways play critical roles in initiating IL-6-mediated proinflammatory responses. Firstly, the STAT3 signaling pathway in relation to ARNO signalling was investigated. STAT3 mediates chronic inflammation and joint damage in RA (Mori et al., 2011, Ogura et al., 2008). Proinflammatory cytokines elevated in RA activate STAT3 signaling pathway, which further induces IL-6 expression (Mori et al., 2011). Results showed that silencing ARNO inhibits STAT3 phosphorylation upon IL-1 β stimulation in both naïve and CIA SFs with no significant inhibitory effect on total STAT3 (Figure 4-10A, B).

Then, the P38 and ERK MAPK pathways were also evaluated, as IL-1 β directly activate MAPKs to regulate the production of pro-inflammatory cytokines and play essential roles in RA pathogenesis (Deon et al., 2001). Although ARNO silencing inhibits IL-1 β -induced proinflammatory cytokine production (Figure 4-9), inhibition of ARNO has no effect on P38 and ERK MAPK activation in either naïve (Figure 4-11) or CIA (Figure 4-12) SFs. Although the JNK MAPK pathway was not examined in this thesis, it is likely that these MAPK kinases do not play a role in ARNO-mediated inflammation. The role of ARNO in AKT phosphorylation was also checked, as AKT signaling pathway maintains metabolic processes in joint tissue, participates in the development of osteoarthritis (Litherland et al., 2008), and also regulates cell migration and adhesion in multi-type of cells (Chin and Toker, 2009, Zheng et al., 2000, Gentilini et al., 2007, Higuchi et al., 2013). Inhibition of ARNO expression completely blocked AKT activation in both naïve (Figure 4-13A) and CIA SFs (Figure 4-13B), as phospho-AKT/total AKT was lower than basal levels (unstimulated control).

To validate our signalling data, the function of IL-1 β -ARNO-STAT3 and IL-1 β -ARNO-AKT axis in SFs was further explored using inhibitors selective for these pathways. Cpd188 was used to pharmacologically inhibit STAT3 signalling pathway, whilst LY294002 and AKT inhibitor were used to inhibit PI3K-AKT signalling pathway. Cpd188 effectively inhibits IL-1 β -induced STAT3 activation (Figure 4-14A) without affecting SF proliferation (Figure 4-14B). Besides, Cpd188 treatment reduced SF migration (Figure 4-14C), which is consistent with the cell migration results following ARNO knockdown. Moreover, inhibiting STAT3 signaling pathway with Cpd188 did not affect SF metabolism as indicated by the MTS viability/proliferation assay (Figure 4-14D). These results were similar to those of ARNO knockdown. Finally, the effect of blocking STAT3 on cytokine production upon IL-1 β stimulation was checked (Figure 4-14E). Whilst this showed that CCL2 secretion was reduced in Cpd188 treated SFs stimulated with IL-1 β , the production of IL-6 and MMP3 remained unchanged. Inhibition of STAT3 phosphorylation with Cpd188 did not reproduce the cytokine inhibition observed in the ARNO knockdown experiment (Figure 4-9), suggesting other ARNO-dependent signaling pathways might be involved in the production of these inflammatory mediators. PI3K/AKT signaling promotes the production of pro-inflammatory cytokines through the NF- κ B activation (Koorella et al., 2014).

PI3K/AKT signaling also play a key role in cell migration as inhibition of PI3K/AKT signalling inhibits membrane protrusion and thus cell migration (Kwiatkowska et al., 2011). Cell migration requires elevated dynamic remodelling of cytoskeleton and B1-integrin acting as a transmembrane adhering protein to connect the cytoskeleton with ECM and recycling during these processes relies on the phosphorylation of AKT (Li et al., 2005). Meanwhile, ARNO-dependent activation of ARF6 promotes B1-integrin distribution (Oh and Santy, 2010). Therefore, we hypothesised that ARNO regulates SF migration and cytokine production via ARNO-AKT axis.

To investigate the biological role of PI3K/AKT signaling pathway in SFs, two inhibitors were used i) LY294002, a potent inhibitor of PI3Ks (Maira et al., 2009) and ii) AKT inhibitor. The effect of LY294002 and AKT inhibitor on AKT phosphorylation at serine 473 was tested by western blot analysis. Based on the results of the AKT signaling pathway shown in Figure 4-13, other phosphorylation sites were not included. Like most kinase inhibitors, LY294002 was designed to compete with ATP and AKT inhibitor is a competitive phosphatidylinositol ether analogue (Toledo et al., 1999). Unexpectedly, LY294002 and AKT inhibitor did not block AKT phosphorylation (Figure 4-15A), but rather greatly inhibited total AKT expression resulting in a greater proportion of the available enzyme being phosphorylated (Figure 4-15B). Although the AKT inhibitor used in this thesis is less well characterised, it is known that LY294002 inactivates AKT by inhibiting PIP3 production. Thus, these unexpected results prompted us to investigate other biological functions regulated by PI3K/AKT signaling. PI3K/AKT signaling has been linked to cell proliferation, survival, migration and cytokine production (Xue and Hemmings, 2013, Park et al., 2020, Zegeye et al., 2018). The effect of LY294002 and AKT inhibitor on SF proliferation was checked by cell proliferation dye and showed that such inhibitor treatment does not affect cell proliferation (Figure 4-15C). SFs did appear to migrate slower under treatment with these inhibitors, but this did not reach statistical significance (Figure 4-15D). Consistent with previous studies, LY294002 blocked IL-6 and MMP3 production (Figure 4-15E) without affecting cell viability (Figure 4-15F), whereas interestingly, the AKT inhibitor had no effect on cytokine secretion upon IL-1 β stimulation (Figure 4-15E). LY294002 is not specific for PI3-kinase, as it also can repress calcium signalling (Tolloczko et al., 2004) and NF- κ B activation (Kim et

al., 2005). Thus, we cannot rule out the effect of other signaling effects on its actions on cytokine production by SFs. Interestingly, LY294002 enhanced AKT phosphorylation was also observed in gemcitabine-resistant pancreatic cancer cell line PK59 (Wang et al., 2017). Gemcitabine is the main drug currently used in the clinical treatment of pancreatic cancer. This further exploration of the role of ARNO-mediated AKT signaling on SFs is required.

4.2.4 Effect of ARNO silencing on the SF transcriptomic profile.

Our previous results revealed that ARNO plays a regulatory role in the IL-1 β -mediated pathological responses of SFs. Therefore, to fully define the ARNO-mediated signaling pathways and the role of ARNO in SFs during inflammation, we decided to conduct RNA-Seq experiments in ARNO siRNA treated SFs. Thus, RNA was isolated from naïve, IL-1 β stimulated and ARNO knockdown and IL-1 β stimulated SFs for subsequent bulk RNA-Seq analysis. PCA confirmed the distinct transcriptome profiles among the three groups (Figure 4-16A). Significant expressed genes [$|\log_2(\text{foldchange})| > 2$, $\text{padj} < 0.01$] among three groups were plotted in heatmap (Figure 4-16B). Although inhibition of ARNO attenuates the IL-1 β -induced proinflammatory modulators production, blocking ARNO does not simply return SFs to the unstimulated naïve phenotype. To investigate the biological role of ARNO in response to IL-1 β , we used K-means clustering, an unsupervised machine learning algorithm, to screen for genes that were upregulated by IL-1 β but suppressed by ARNO silencing. In total, 122 genes were found and were further subjected to String Protein-Protein Interaction Functional Enrichment (<https://string-db.org/>), of which 58 genes were functionally connected (Figure 4-16C). Analysis of these functionally connected genes showed significant enrichment of immune response and cell migration pathways (Figure 4-16C). Furthermore, corresponding KEGG pathway enrichment was performed showing that ‘JAK-STAT signaling (IL-23a, Csf2rb, Lif, Tslp, Csf3 and IL-6)’, ‘PI3K-AKT signaling (Lamb3, Itga2, Fgf2, Ngf, Fgf23, Ereg, IL-6 and Csf3)’ and ‘cytokine-cytokine receptor interaction (Tnfsf11, IL-1a, Ccl11, Cxcl2, Cxcl3, Ccl22, Cxcr3, Tnfrsf9, IL1rl1, IL-1 β , IL-33)’ pathways were enriched, reflecting the role of ARNO in cytokine production and their signaling pathways. Subsequently, genes that were upregulated by IL-1 β and also enhanced by ARNO silencing were also identified using K-means cluster, showing 94 genes, 34 of which were functionally connected upon String analysis (Figure 4-16D).

Chemokine signaling pathway was enriched in this group, which included the genes CCR3, CCL3, CCL4, CCL12, CXCL9 and CXCL13, but no cytokines were present.

These results further suggested that ARNO regulates IL-1 β -driven inflammatory responses. To investigate the regulatory function of ARNO in more detail, we performed a complementary analysis in the same dataset, directly comparing IL-1 β -stimulated SFs with those treated with IL-1 β and ARNO siRNA. PCA was performed (Figure 4-17A) and DE genes were plotted in a volcano plot (Figure 4-17B) with 384 upregulated and 434 downregulated genes pass the threshold of $p_{adj} < 0.01$ and $|\log_2\text{foldchange}| > 1$. To understand the pathway regulation as a consequence of the transcriptomic changes, up- and down- regulated genes were processed by KEGG pathway enrichment (Figure 4-17C) and this showed the JAK-STAT and focal adhesion pathways were enriched in the downregulated genes. By contrast, RAS and MAPK signaling pathways were enriched within both the up- and down- regulated gene groups, indicating their potential roles in mediating the release of inflammatory cytokines.

GO pathways were also significantly enriched in the list of DE genes (Figure 4-18), showing as top regulated pathways 'inflammatory response', 'metal ion homeostasis', 'regulation of secretion' and 'chemotaxis' in upregulated genes and 'chemotaxis', 'vasculature development', 'inflammatory response' and 'regulation of cell adhesion' in downregulated genes. These findings highlight the role of ARNO in immune responses and cell motility and also suggest the potential role of ARNO in angiogenesis.

4.2.5 Role of ARNO in regulating the pathogenic response to IL-1 β

Having confirmed that ARNO was involved in IL-1 β mediated SF inflammatory responses, including cytokine and chemokine production, we aimed to validate this finding by RT-qPCR. Three upregulated (MMP13, CLDN1 and Cxcl9) and 4 downregulated (IL-6, CCL9, Tnfsf11 and Tnfrsf11b) representative genes from the differentially expressed gene list were chosen (Figure 4-19A). IL-6, Cxcl9, CCL9 and MMPs were selected for their pro-inflammatory and matrix remodelling roles. Although MMP3 is not on the list of DE genes, it was chosen because it is a

key marker for disease activity and it plays key roles in joint destruction in RA (Lerner et al., 2018). CLDN1 was chosen as it regulates cell adhesion (Ewert et al., 2010). Tnfsf11 and Tnfrsf11b were selected based on their role in regulating bone damage. Tnfsf11 (RANKL) is an SF-produced regulator for osteoclast differentiation, increased expression of Tnfrsf11 results in increased osteoclast production and bone disruption (Kwan Tat et al., 2009). Tnfrsf11b (OPG) as a decoy receptor for Tnfsf11, which inhibit osteoclastogenesis and bone resorption (Simonet et al., 1997), and the ratio of Tnfsf11/Tnfrsf11b was used to evaluate osteoclastogenesis.

Gene expression was evaluated by RT-qPCR using an independent set of samples rather than those used for RNAseq, and SFs from naïve mice were transfected with ARNO or control siRNA followed with IL-1 β stimulation as before. Expression of CLDN1, CXCL9 and MMP13 were upregulated and MMP3 was unaffected in IL-1 β stimulated ARNO-silenced SFs (Figure 4-19B), which was consistent with what was observed in the RNASeq experiment. Expression of IL-6 and CCL9 was downregulated (Figure 4-19C), although there was no significant change in the expression of Tnfsf11 and Tnfrsf11b (Figure 4-19D) in ARNO knocked-down SFs upon IL-1 β stimulation.

To investigate the role of ARNO in regulating the pathogenic response to IL-1 β in cells expanded from an inflammatory environment, we repeated the RT-qPCR experiments with CIA SFs, which are chronically activated and adopt a pathogenic phenotype *in vivo*. Intriguingly, IL-1 β induced more ARNO expression in SFs from CIA (174%, Figure 4-20A) than naïve (139%, Figure 4-2A) mice. Inhibition of ARNO by siRNA was similar in naïve SFs ($78.3\% \pm 0.08$, Figure 4-2A) and CIA ($85.9\% \pm 0.05$ reduction, Figure 4-20A). Notably, inhibition of ARNO expression reduced Tnfsf11 expression upon IL-1 β stimulation, whereas the level of Tnfrsf11b tended to be upregulated whereas the mRNA levels of MMP3 and MMP13 were decreased in IL-1 β stimulated ARNO knockdown CIA SFs (Figure 4-20C). The regulation of MMPs and Tnfsf11/Tnfrsf11b axis in SFs has been shown to be dependent on the inflammatory milieu. Differential regulation of MMPs and Tnfrsf11 in naïve and CIA SFs by ARNO silencing implies that ARNO plays a distinct role in an inflammatory microenvironment.

4.2.6 ARNO expression in SF subsets

Our results demonstrated the role of ARNO in SF inflammatory responses in an *in vitro* setting. To evaluate the role of ARNO in more physiological conditions, we evaluated ARNO expression in individual SF subsets isolated from mouse synovial tissue. The recent discovery of SF subsets has led to new insights into the biological roles of fibroblasts in RA. The single-cell transcriptional analysis predicts their pathological behaviours, showing that functionally distinct SFs associated with specific tissue locations contribute differently to the pathogenesis of arthritis. Thereby, we investigated the expression of ARNO in lining (CD90-) and sub-lining (CD90+) SFs in the murine model. SFs were isolated from naïve and CIA mice and sorted into lining SFs (CD45-CD31-PDPN+CD90-) and sub-lining SFs (CD45-CD31-PDPN+CD90+) by flow cytometry (Figure 4-21A). Sorted SFs were then reloaded on flow cytometer to check the performance of sorting and purification of cells (Figure 4-21B). Surprisingly, no difference in ARNO expression was observed between CD90- and CD90+ SFs and ARNO was less expressed in CIA SFs than in naïve SFs, although the difference did not reach statistical significance (Figure 4-22A).

Next, we examined if there was a link between ARNO expression and clinical symptoms. We checked the expression of ARNO in inflamed versus 'healthy' (no signs of swollen and redness) paws of one mouse. CD90+ SFs (sub-lining SFs) produced more pro-inflammatory factors before the onset of symptoms such as erythema, but CD90- SFs (lining SFs) take the leading role in pro-inflammatory cytokines production, like IL-6, CCL2 and MMP3, after the onset of symptoms (Figure 4-22B-D). In contrast to the expression of inflammatory cytokines, expression of ARNO was decreased in the lining SFs after the onset of symptoms (E), indicating that fluctuations in ARNO expression were associated with disease progression. Besides, the arthritis mouse model cannot recapitulate the complexity of Figure 4-22 human arthritis and we have only compared the expression of ARNO in lining and sub-lining SFs. In fact, heterogeneity has been reported in the expression of SF surface markers as well as in SF functions (Mizoguchi et al., 2018, Zhang et al., 2019, Croft et al., 2016), and different SF subsets have been proposed based on the heterogeneity. Nevertheless, to investigate the expression of ARNO in human SF subsets, ARNO expression was examined in publicly available single-cell RNAseq and bulk RNAseq data

generated by Zhang et al. (Zhang et al., 2019). In this work, SFs from human RA synovial tissue were sorted by flow cytometer gating on CD45-PDPN⁺, then classified into four subsets based on the expression of CD34 (CD34⁺ sub-lining fibroblasts), HLA (HLA⁺ sub-lining fibroblasts), DKK3 (DKK3⁺ sub-lining fibroblasts) and CD55 (CD55 lining fibroblasts). The first observation was that ARNO (Cyth2) is also expressed in human SFs (Figure 4-23A). Then, ARNO expression was compared among subsets, showing that ARNO was most highly expressed in CD34⁺ sub-lining fibroblast (Figure 4-23B). Additionally, the expression of ARNO was checked in a bulk RNAseq dataset of leukocyte-rich RA, leukocyte-poor RA and OA fibroblasts that ARNO was significantly higher expressed in fibroblasts of leukocyte-rich RA patients, whereas this difference was not observed in B cell, T cell or monocyte (Figure 4-23C).

Furthermore, Mizoguchi's study reported that CD34⁺ SFs were characterised by enhanced invasion and migration, and high production of IL-6, CCL2 and CXCL12 in response to TNF α stimulation (Mizoguchi et al., 2018). In Zhang's study, leukocyte-rich RA was associated with significantly higher Krenn inflammation scores, which correlate with strong synovial leukocyte infiltration and increased abundance of IL-1 β ⁺ monocytes. These data support a regulatory role for ARNO in the synovial inflammatory microenvironment, as well as the differential expression of ARNO in distinct SF subsets during RA pathogenesis.

4.3 Discussion

The pathophysiology underlying SF activation and subsequent tissue damage are not yet fully understood, and thus the discovery of the mechanisms underpinning SF inflammation and invasion is therefore required in order to develop new treatments and therapeutic approaches that target these pathogenic cells. In this chapter, the impact of ARNO on inflammation and motility was investigated as a potential immunoregulatory mechanism in SFs. Results showed that inhibition of ARNO reduced cytokine production and cell migration in SFs. This is the first description of a role for ARNO in the context of synovial fibroblast biology, specifically defining it not only as a regulator of cytoskeleton reorganization and migration but also as a modulator of local inflammatory responses. The functions of ARNO were evidenced by the dysregulation of multiple biological effects upon mRNA silencing, such as inhibition of AKT and

JAK-STAT signaling pathways, dysregulated vinculin arrangement, reduced adhesion and migration, and reduced secretion of proinflammatory cytokines.

ARNO is primarily known as a regulator of cell migration, cell adhesion and actin cytoskeleton reorganisation (Salem et al., 2015, Santy and Casanova, 2001, Torii et al., 2010), although a few recent studies have linked the ARNO-ARF6 axis with the regulation of cell inflammation, in line with our findings. For example, ARF6 deficient macrophages produce less IL-1 β in ovalbumin (OVA)-induced allergic asthma mice model and pharmacological inhibition of ARF6-GEFs suppresses allergic inflammation in an allergic asthma mouse model (Lee et al., 2021). Similarly, ARNO knocked-down mice reduced antigen-specific IL-15 production and eosinophilic inflammation, hence reducing experimental allergic rhinitis (London et al., 2021). Besides, ARNO regulates epithelial cell inflammation by regulating NF- κ B and MAPK activation (Luong et al., 2018) and ARF6 was shown to be required for TLR9-dependent and TLR4-dependent NF- κ B activation (Van Acker et al., 2014, Wu and Kuo, 2012a, Wu and Kuo, 2012b). Although studies are gradually unravelling the role of ARNO-ARF6 axis in the regulation of inflammation, these findings are rare when compared to their roles in cell motility and regulation of actin cytoskeleton. Our results, therefore, provide new insight into the function of ARNO, indicating that it plays a role in integrating SF migration and SF inflammation.

Cell motility requires reorganization of the actin cytoskeleton to drive the extension of the plasma membrane. In fact, defects in actin cytoskeleton-regulating proteins are increasingly implicated in immunodeficiency and autoimmune diseases, supporting the linkage between cytoskeleton dynamics and immune response. For example, DOCK2 is a mediator of cytoskeletal reorganization and deficient mice (DOCK2 $^{-/-}$) show a defective migration of T and B lymphocytes in response to chemokines (Fukui et al., 2001). In addition, endothelial cytotoxicity upon TNF α action requires vimentin remodelling via RhoA/Rock and Raf-1/CK2 pathways (Yang et al., 2017). Moreover, vimentin regulates fibroblast proliferation and TGF- β 1 expression during wound healing, with fibroblasts with silenced vimentin expression exhibiting reduced TGF- β 1 and decreased proliferation (Cheng et al., 2016). These data raise an interesting hypothesis that the IL-1 β -ARNO-ARF6 axis induces focal adhesion formation and cytoskeleton reorganisation in SFs, processes which are necessary for SFs to

sense changes in the intra-articular microenvironment and respond by regulating signalling pathways and cytokine production. This hypothesis is in line with the results described in this chapter, suggesting that ARNO connects two hallmarks of RASFs: inflammation and migration.

Our results showed that ARNO deficiency impairs SF vinculin formation on ECM (Figure 4-8A, B) and cell migration (Figure 4-4B), but ARNO-dependent cell adhesion and migration seem to be independent of IL-1 β stimulation, as IL-1 β stimulation neither affected vinculin formation (Figure 4-7B, C) nor cell migration (Figure 4-4A). Although many studies support IL-1 β inducing cell migration and focal adhesion kinase activation (Mitchell et al., 2007, Yang et al., 2010, Mon et al., 2017), the results do not support that IL-1 β enhances SF migration and vinculin formation on extracellular matrix, at least in this *in vitro* culture manner. This may be due to the fact that IL-1 β -mediated cell migration is concentration-dependent, and further experiments based on concentration gradients may provide a better experimental setting. Migration assays were performed using a well-designed removable chamber without damaging cells, in contrast to traditional scratch assays. Regarding the cell migration conditions, 24 hours was selected as the experimental condition, simply because the pre-designed cell-free area is limited, and this cell-free area would not be fully occupied within 24 hours. However, the pre-designed distances and time may not be sufficient to observe differences in cell migration upon IL-1 β stimulation. Moreover, the migration assay used was not able to investigate cell chemotaxis, as the same stimulus was delivered to adjacent cells, either untreated or IL-1 β stimulated. Furthermore, the possibility of irregular movement of cells *in situ* cannot be ruled out and thus, live imaging would help to resolve this. As to focal adhesion, unlike ARNO, IL-1 β may regulate focal adhesion proteins in a phosphorylation-dependent manner as, for example, IL-1 β induces talin phosphorylation in human fibroblast (Qwarnström et al., 1991) and Paxillin phosphorylation is required for cell spreading, which is regulated via ERK signaling pathway (Ishibe et al., 2004). Similar findings also appear to apply to vinculin, since a higher level of vinculin phosphorylation was observed in epithelial cells with intact cell-cell junctions (Bays et al., 2014).

Apart from the effects on cell migration, we found that silencing ARNO also decreased the production of IL-6 and CCL2 in response to IL-1 β in naïve and CIA

SFs. Interestingly, the reduction in cytokine production upon ARNO silencing was stronger in CIA SFs compared with naïve cells. This might be a consequence of the arthritic microenvironment, in which cells adopt a proinflammatory phenotype that is maintained *in vivo* and *ex vivo* (Corbet et al., 2021, Frank-Bertoncelj et al., 2017). In line with this, CIA SFs exhibit hyperinflammatory responses that produce higher levels of pro-inflammatory cytokines upon IL-1 β stimulation compared to naïve SFs (Figure 4-9). This varied performance of ARNO in two activation stages of SFs suggests that the function of ARNO may be dependent on the precise composition of the inflammatory microenvironment. In addition to differences in cytokine production, inhibition of ARNO reduced the expression of MMP3 and MMP13 only in CIA SFs, but not in naïve SFs. Likewise, inhibiting ARNO reduced the ratio of Tnfsf11/Tnfrsf11b in CIA SFs not in naïve SFs, as CIA SFs exhibit a bone-damaging phenotype, suggesting that ARNO may induce bone and cartilage damage in specific human disease phenotypes. This idea is supported by experiments performed on an ovalbumin-induced rhinitis mouse model, where ARNO^{-/-} mice did not exhibit any apparent defects, but the expression of IL-5 was significantly reduced in ARNO^{-/-} rhinitis mice (London et al., 2021). Collectively, these data suggest that ARNO senses the microenvironment prior to mediating the inflammatory response and adjusts its responses to changes in the environment.

In terms of ARNO regulating pathogenic SF migration, ARNO could regulate this aspect of cell biology by activating Rho GTPases and lipid modification enzymes as, for example, Rac1 is a potential downstream regulator of ARNO for SF motility. Thus, ARNO colocalises with DOCK180/Elmo to promote the activation of Rac1 (Santy et al., 2005), which regulates membrane ruffling and development of lamellipodia (Santy and Casanova, 2001, Santy et al., 2005). In addition, activated Rac1 promotes epithelial cell migration via PI3K signaling, where integrins are required for Rac1-induced cell migration and invasiveness (Keely et al., 1997). Certainly, ARNO is required for integrin recycling (Salem et al., 2015, Dunphy et al., 2006, Oh and Santy, 2012), and cell migration is negatively affected by disrupting integrin recycling (Goldfinger et al., 2003, Tayeb et al., 2005, Powelka et al., 2004), evidencing a potential ARNO-Rac1-integrin recycling axis in SF migration. Besides, the ARNO-ARF6 axis activates lipid modification enzymes PIP5k and PLD, where PLD generates phosphatidic

acid (PA) by hydrolysing phosphatidylcholine and both PA and PIP5k induce the production of PIP2 (Honda, 1999). Elevated PIP2 induces actin polymerization, plasma membrane remodelling and cell migration (Brown et al., 2001), offering a potential (alternative/additional) link between ARNO-ARF6-PLD/PIP5Ks pathways and SF migration. Besides, activated ARF6 promotes autophagy by initiating the formation of autophagosomes via PLD and PIP2 production (Moreau et al., 2012). Activated autophagy induces joint destruction in RA by promoting osteoclastogenesis, as evidenced by pharmacological inactivation of autophagy preventing osteoclast differentiation (Lin et al., 2013). This is consistent with our results that ARNO inhibition reduces the expression of RANKL and the ratio of RANKL/OPG in SFs from CIA SFs, as RANKL induce autophagy and osteogenesis, suggesting that ARNO regulates cartilage destruction by activating autophagy in an ARNO-ARF6-PIP2/PLD axis.

It has been reported that in endothelial cells, the regulation of ARNO by IL-1 β stimulation is associated with increased vascular barrier permeability (Zhu et al., 2012). Interestingly, therefore, IL-1 β , but not IL-17 and TNF α upregulated ARNO expression in SFs. As with the vascular endothelial barrier, synovial fibroblasts and macrophages form a cellular barrier wrapping around the joint cavity (Culemann et al., 2019). Thus, IL-1 β may regulate the localisation of adhesion molecules on the surface of SFs, thereby disrupting the integrity of the synovial lining membrane, or barrier, leading to the infiltration of immune cells into the joint cavity and the initiation of immune responses. Notably, SecinH3 reduced acute inflammation in an air-pouch model, and joint damage in CIA model (Zhu et al., 2012), but this cannot rule out the role of other cytohesins in inflammatory responses. Thus to investigate the regulation of cytohesins upon cytokine stimulation, their expression was evaluated in an online RNAseq dataset which was generated by Slowikowski et al. (Slowikowski et al., 2019). Intriguingly, Cyth3 was down-regulated upon TNF α and IL-17 treatment. As Cyth3 and ARNO act in opposite ways in terms of cell adhesion and migration (Oh and Santy, 2010), it may be worthwhile to explore the role of Cyth3 in cellular inflammation.

To explore the molecular mechanisms of how ARNO-mediates pathological responses, STAT3 and PI3K/AKT signaling pathways were pharmacologically blocked with Cpd188, and LY294002 and the AKT inhibitor, respectively as both

pathways regulate cell migration and inflammatory responses (Zegeye et al., 2018, Ellis et al., 2010, Gentilini et al., 2007, Tian et al., 2013, Mori et al., 2011). Inhibition of STAT3 by Cpd188 reduced SF migration and CCL2 secretion (Figure 4-14C, E) whereas inhibiting PI3K by LY294002 greatly blocked IL-6 and MMP3 production upon IL-1 β stimulation (Figure 4-15E) and weakened cell migration, although the latter results did not achieve statistical significance (Figure 4-15D). However, the AKT inhibitor had no effect on either migration or cytokine release. Thus, SFs treated with Cpd188 and LY294002 partially replicate the biological role of ARNO (as evidenced by when it was silenced), suggesting that the common action of pathways or perhaps other pathway regulators are required for ARNO-modulated biological effects. Besides, for future exploration, it may be necessary to optimize the concentration for all of the inhibitors. For example, despite the recommendation of 73 μ m of Cpd188 to inhibit IL-6-induced STAT3 Tyr705 phosphorylation, this concentration may interfere with several signal transduction pathways. Additional experiments are required to demonstrate that other signaling pathways are not impaired.

Rho GTPases, such as RhoA and Rac1, are promising downstream effectors of ARNO that are upstream regulators of STAT3 and PI3K/AKT signaling pathways. For example, the RHOA/Rac1-STAT3 and RHOA/Rac1-PI3K/AKT axes are known for regulating the actin cytoskeleton and cell migration (Del Re et al., 2008, Lv et al., 2015). Moreover, these Rho GTPases activate NF- κ B to induce cytokine and MMPs production (Santy et al., 2005, Simon et al., 2000, Kheradmand et al., 1998, Williams et al., 2008, Fessler et al., 2006). Given their pathological consequences, the crosstalk amongst different signaling pathways regulated by ARNO under specific inflammatory conditions should be investigated in the future. It is important to emphasize that LY209002 and AKT inhibitor did not inhibit AKT phosphorylation levels but rather reduced total AKT, contrary to what was observed with ARNO silencing. To evaluate the blocking effect of LY209002 and AKT inhibition, the downstream proteins of the PI3K/AKT axis should be examined. Besides, further experiments blocking AKT phosphorylation are needed to investigate the regulation of AKT phosphorylation on the pathophysiology of SFs.

Collectively, in this chapter, we highlight the dual role of ARNO in regulating SF motility and inflammatory responses. Specifically, ARNO is required for SF

migration by impacting the formation of focal adhesions, and for modulating IL-1 β -induced inflammatory responses. Yet, further work is still required to fully understand the mechanisms of ARNO-mediated inflammatory response by SFs, but this work represents an important step forward. Although these data should be investigated in human RA, the role of ARNO in arthritis may open new avenues for SF therapeutic intervention without systemic immunosuppression, since inhibition of ARNO reduces inflammatory response, cell adhesion and cell-matrix interactions in SFs.

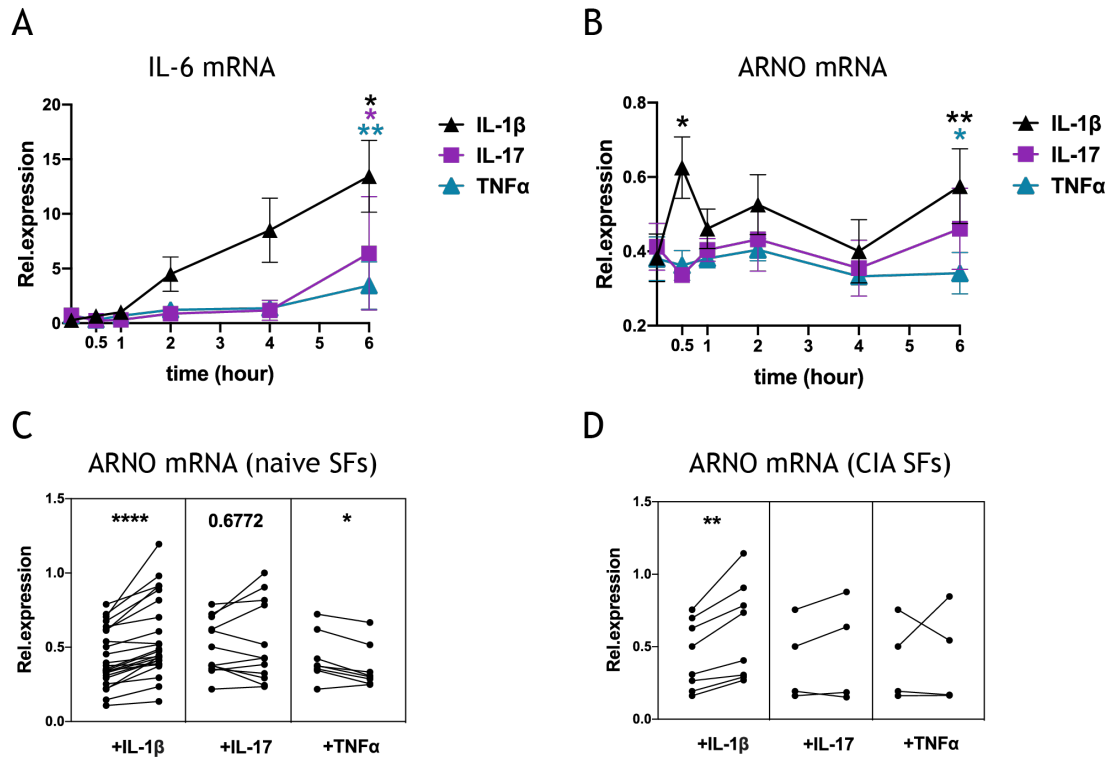
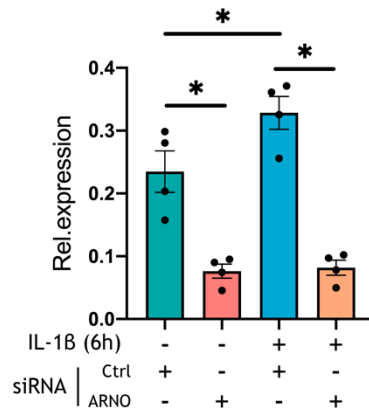


Figure 4-1 IL-1 β upregulates ARNO expression in SFs.

SFs were extracted from naive mice and expanded *ex vivo*. (A-B) Cells were treated with IL-1 β , IL-17, TNF α (all at 10ng/ml) or DMEM (as control) for 0.5h, 1h, 2h, 4h and 6h, RNA was extracted, and the expression of IL-6 (A) and ARNO (B) was analysed by RT-qPCR. Data are present as mean \pm SEM from at least three independent experiments analysed in technical triplicate. * p <0.05, ** p <0.01 by the Mann-Whitney test. (C-D) SFs extracted from naïve and CIA mice were expanded *ex vivo*. Cells were treated with IL-1 β , IL-17, TNF α (all at 10ng/ml) or DMEM (as control) for 6h, RNA was extracted and the expression of ARNO in naïve SFs (C) and CIA SFs (D) were analysed by RT-qPCR. Data are presented as changes in expression for individual experiment compared to control, with each dot representing one independent experiment analysed in technical triplicate. * p <0.05, ** p <0.01, **** p <0.0001 by Wilcoxon's matched-paired signed rank test.

A



B

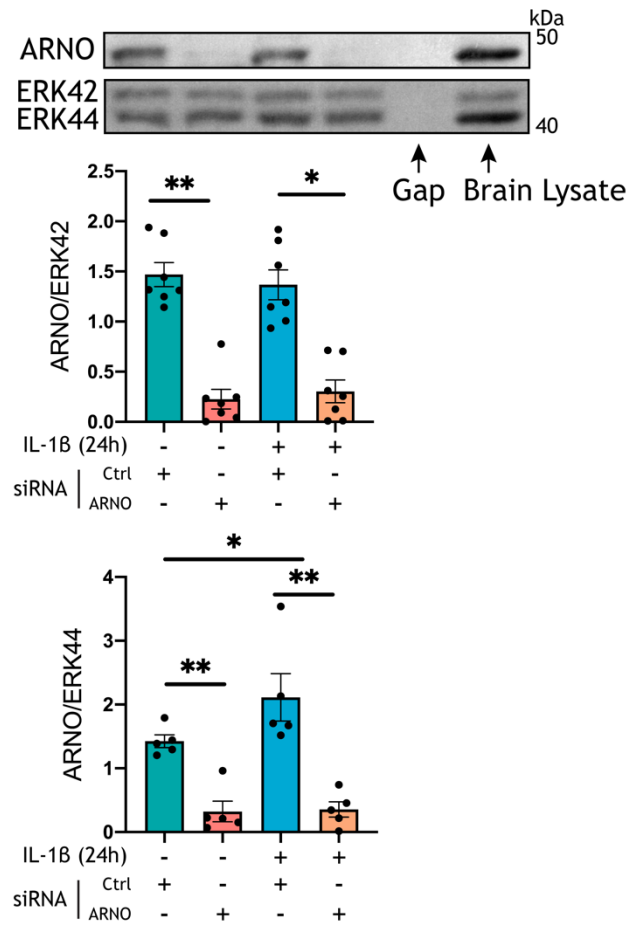


Figure 4-2 IL-1 β upregulates ARNO expression in SFs.

SFs extracted from naive mice were expanded *ex vivo*. Cells were transfected with either ARNO or Allstars (control) siRNA, followed by stimulation with recombinant IL-1 β (10 ng/ml) as indicated. (A) RNA was extracted from SFs after 6 hours of IL-1 β stimulation, and the expression of ARNO was evaluated by RT-qPCR. Each dot represents one independent experiment analysed in technical triplicate. Error bars represent SEM (n=4). $p^* < 0.05$ by the Mann-Whitney test. (B) SFs were transfected and stimulated as in (A), and proteins were extracted after 24 hours of IL-1 β stimulation. ARNO protein was detected by western blot, total Erk1/2 was used as loading control and whole brain lysate was loaded as a positive control as ARNO is abundantly expressed in brain tissue. Image shows one representative experiment. Bar chart shows the quantification of band intensity for ARNO normalised to ERK44 and ERK42, respectively. Each dot represents one independent experiment, and error bars represent SEM (n \geq 5). $p^* < 0.05$, $**p < 0.01$ by the Mann-Whitney test.

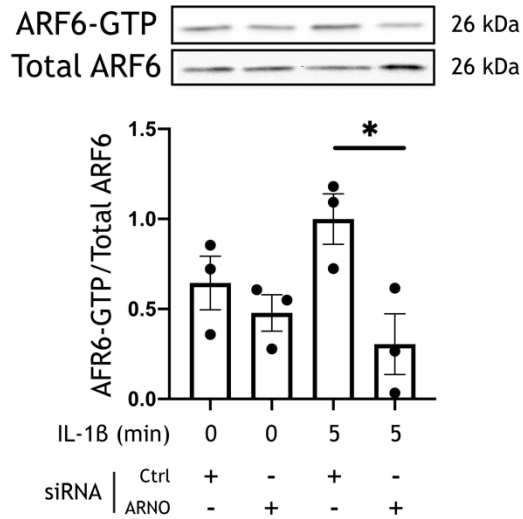


Figure 4-3 Inhibition of ARNO inactivates ARF6.

SFs were extracted from naïve mice and expanded *ex vivo*. Cells were transfected with either ARNO or Allstars (control) siRNA, followed by stimulation with recombinant IL-1 β (10 ng/ml, 5 minutes) as indicated. Total protein was thereafter harvested and assayed by ARF-GTP pull-down assay and immunoblotting with anti-ARF6 antibody. GDP and GTP γ S were loaded as negative and positive controls, respectively (data not shown). Bar chart shows the relative activation of ARF6 (ARF6-GTP/total ARF6). Each dot represents one independent experiment and error bars represent SEM. * $p < 0.05$, by the Mann-Whitney test.

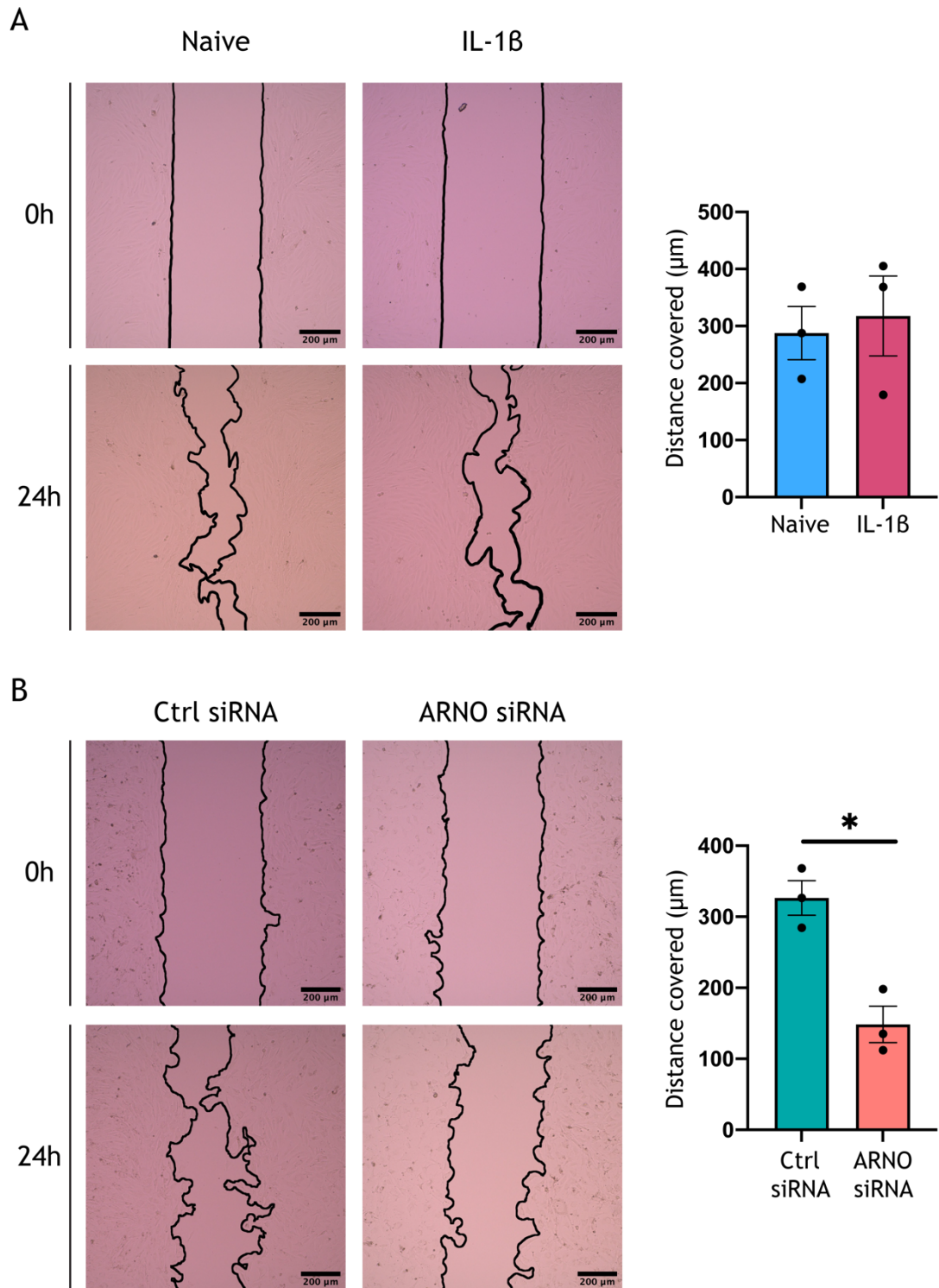


Figure 4-4 ARNO regulates SF migration.

SFs were extracted from naïve mice and expanded *ex vivo*. Cells were seeded in bovine fibronectin-coated migration chambers and grown until monolayer confluence. Cells were treated with 10ng/ml IL-1 β (A) or transfected with either ARNO or Allstars (control) siRNA (B). Migration assay was performed once the inserts were removed and ended after 24 hours of incubation. Images show one representative experiment. Superimposed black lines delineate the cell-free area. Bar charts show the mean of cell migration distance \pm SEM from three independent experiments. * $p < 0.05$, by the Mann-Whitney test. Scale bar: 200 μm .

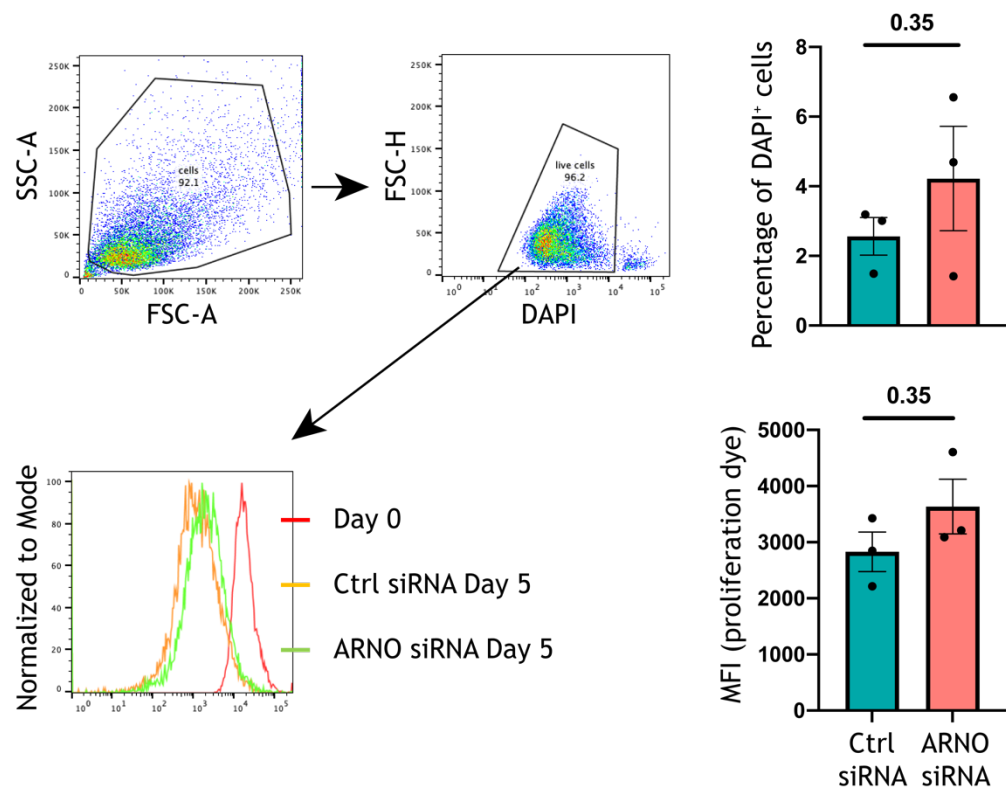


Figure 4-5 Inhibition of ARNO does not disturb SF proliferation.

SFs cultured *ex vivo* were labelled with proliferation dye eFlour 670, cells were either analysed by flow cytometry (day 0) or transfected with siRNAs (ARNO or Allstars) and continued in culture for 5 days (Day 5). The percentage of dead cells (higher DAPI staining) was evaluated by flow cytometry. Mean fluorescence intensity (MFI) was evaluated in live cells (lower DAPI staining) by flow cytometer. Histogram shows one representative experiment, with fluorescence intensity displayed on the X-axis, and relative percentage of cell populations displayed on Y-axis (Normalised to mode). Bar chart shows the percentage of DAPI+ cells and MFI of proliferation dye from three independent experiments, error bars represent SEM. Statistical significance was determined using the Mann-Whitney test.

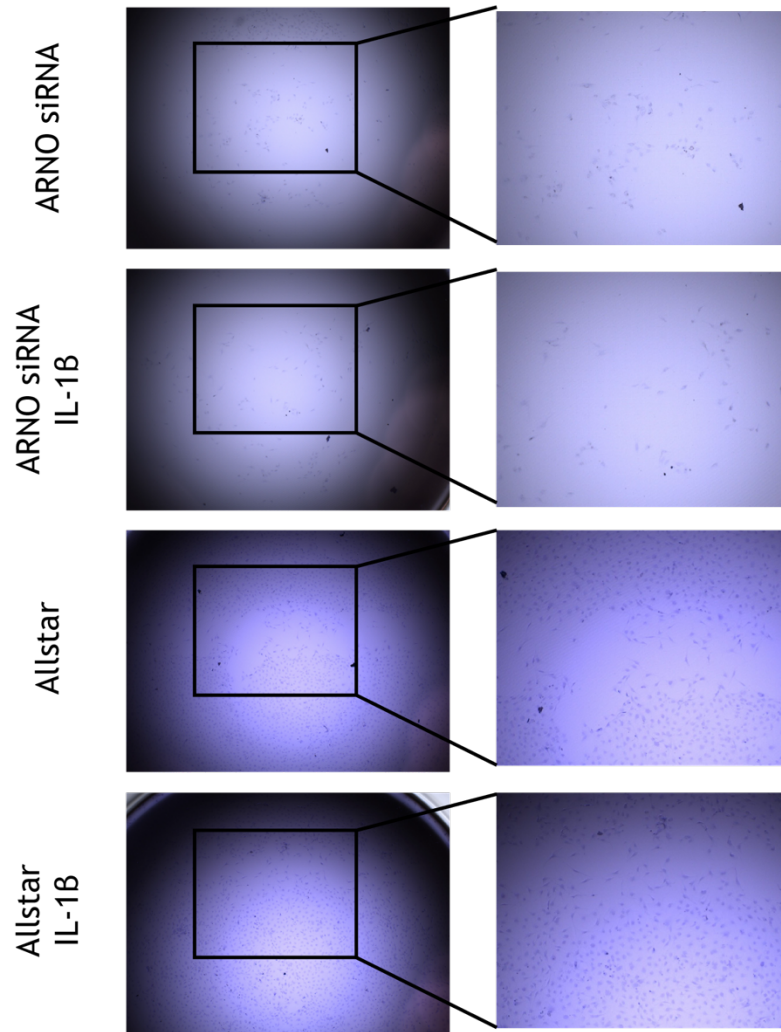
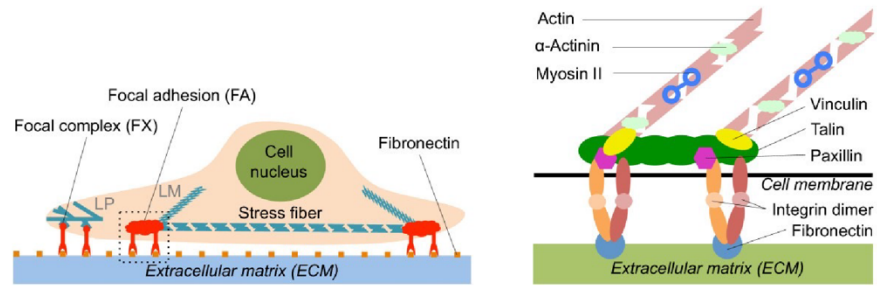


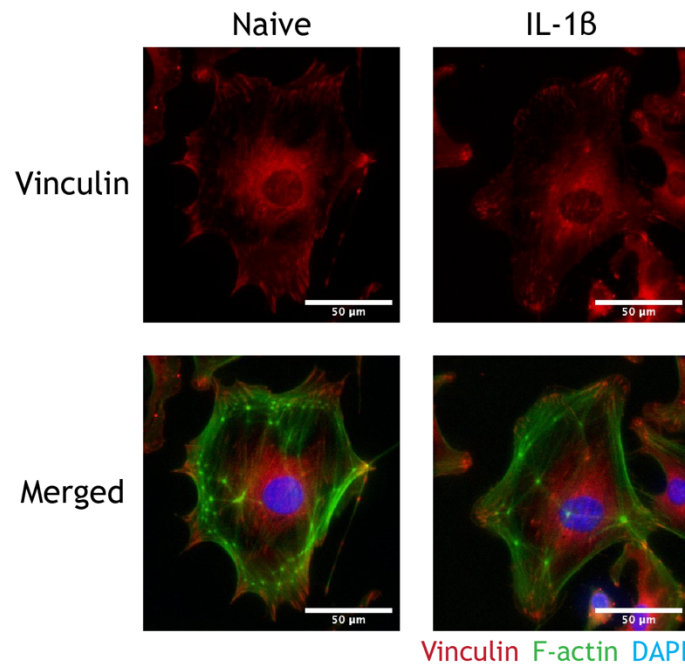
Figure 4-6 Inhibition of ARNO reduces SF adhesion.

SFs from naïve mice were extracted and expanded *ex vivo*. Cells (10^4) were seed in 96-well plates until confluence was reached, then transfected with either ARNO siRNA or Allstars (control) and then stimulated with IL-1 β (10ng/ml) for 24 hours as indicated. A straight line was scratched through the monolayer of cells using a 10 μ l pipette tip and incubation was continued for another 24 hours. Cells were then fixed with 4% formaldehyde and subsequently stained with 0.04% crystal violet. Data are from one independent experiment. Images were obtained using an EVOS XL Core microscope at x10 magnificant.

A



B



C

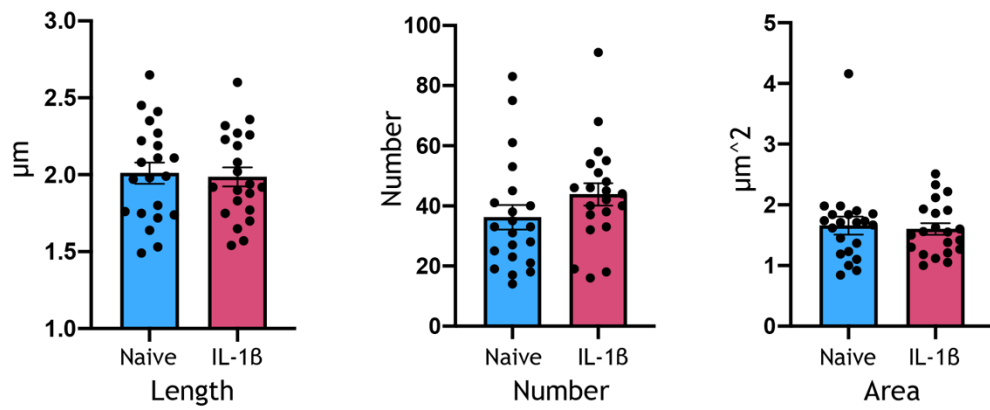


Figure 4-7 Inhibition of ARNO reduces vinculin formation.

(A) Scheme summarizing the components of focal adhesion and enlarged view of focal adhesion structure and main molecular components, figures are adapted from Hoffmann and Schwarz, 2013 (Hoffmann and Schwarz, 2013). Focal adhesion clustered with integrin which binds to ECM such as fibronectin. This basic mechanical connection is reinforced by proteins such as vinculin, paxillin or α -actinin. (B) SFs were extracted from naïve mice and expanded *ex vivo*. Cells were stimulated with 10ng/ml IL-1 β for 24 hours and seeded in a fibronectin-coated glass slide under the culture condition for 4 hours. Cells were then fixed, and immunofluorescence staining was carried out. Images presented reveal focal adhesion stained for F-actin (green), vinculin (red) and nucleus (blue). Scale bar: 50 μ m. (C) Bar charts were shown the mean of number, length and area of vinculin analysed in (B) with image J, each dot represents one single cell and data are from one independent experiment.

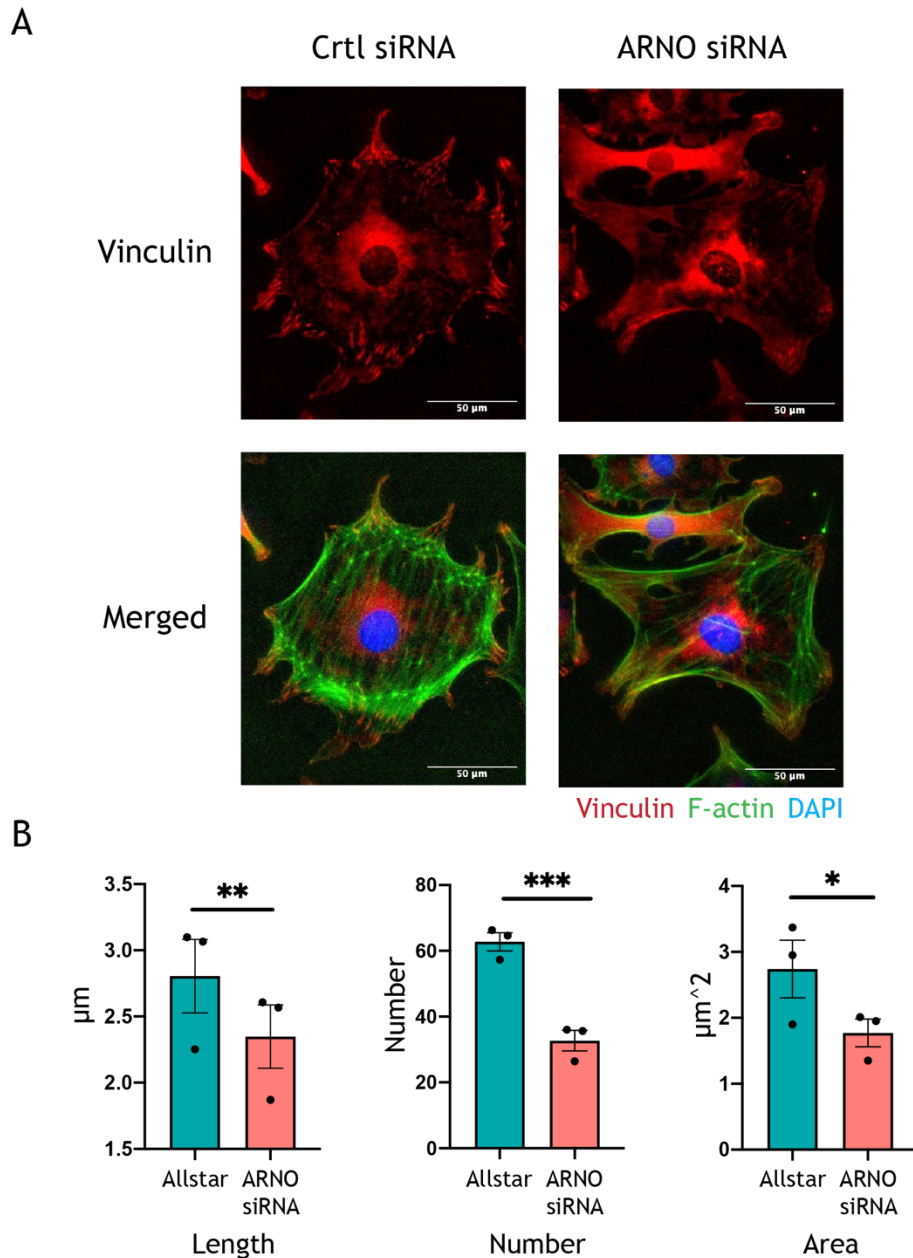


Figure 4-8 Inhibition of ARNO reduces vinculin formation.

(A) SFs were extracted from naïve mice and expanded *ex vivo*. Cells were transfected with either ARNO or Allstars (control) siRNA and seeded in a fibronectin-coated glass slide under the culture condition for 4 hours. Cells were then fixed, and immunofluorescence staining was carried out. Images presented reveal focal adhesion stained for F-actin (green), vinculin (red) and nucleus (blue). Scale bar: 50 μ m. (B) Bar charts were shown the mean number, length and area of vinculin analysed in (A) with image J, each dot represents one independent experiment with a minimum of 20 cells being analysed in each experiment. Error bars represent SEM (n=3). *p<0.05, **p<0.01, ***p<0.001 by the Mann-Whitney test.

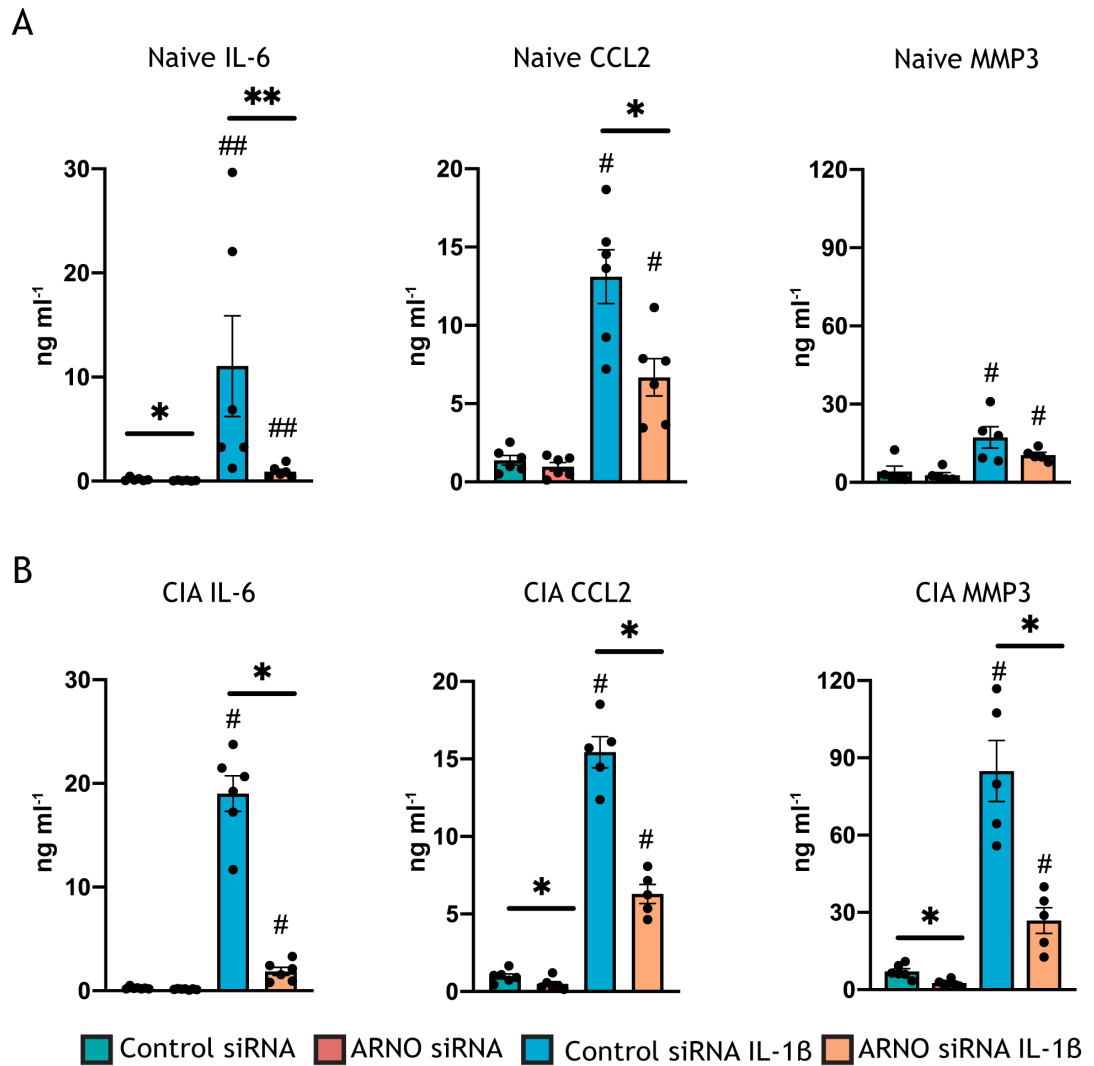
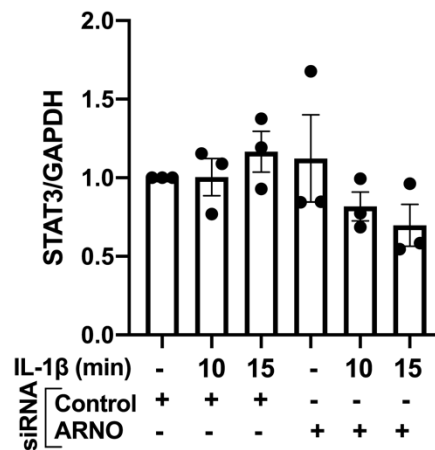
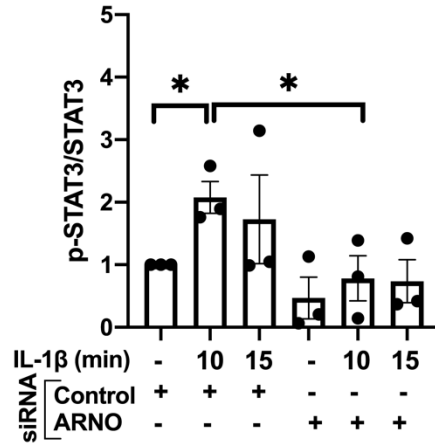
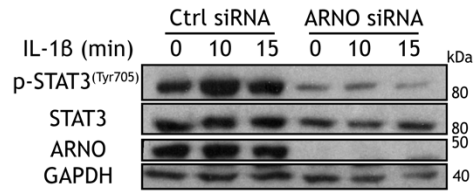


Figure 4-9 Silencing ARNO expression reduces IL-1 β mediated cytokine production.

SFs extracted from naïve (A) or CIA (B) mice were expanded *ex vivo*. Cells were transfected with ARNO or Allstars (control) siRNA, followed by 24 hours stimulation of IL-1 β (10ng/ml) as indicated. Supernatants were collected and the levels of IL-6, CCL2 and MMP3 in the supernatant were quantified by ELISA. Each dot represents one independent experiment analysed in technical triplicate; error bars represent SEM (n \geq 5). *p<0.05, **p<0.01 versus respective siRNA control; #p<0.05, ##p<0.01 versus unstimulated control, by the Mann-Whitney test.

A Naive SFs



B CIA SFs

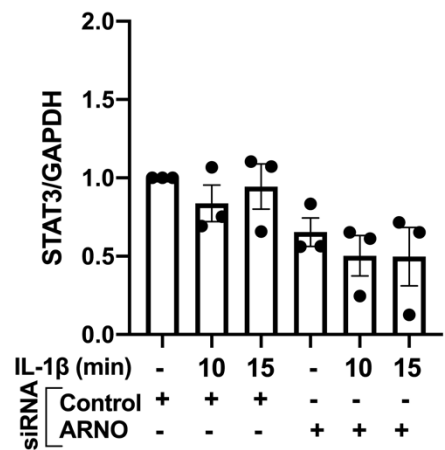
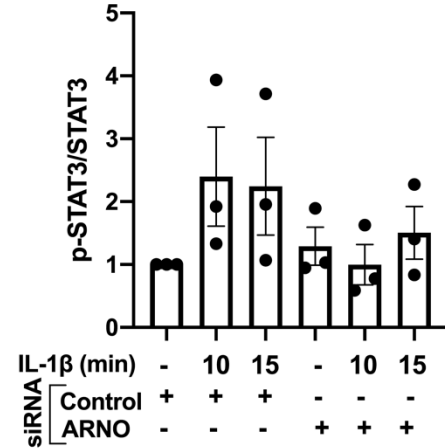
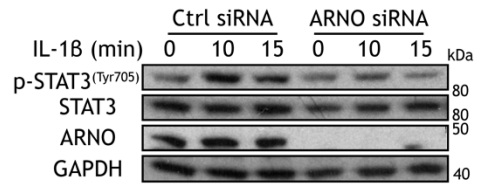
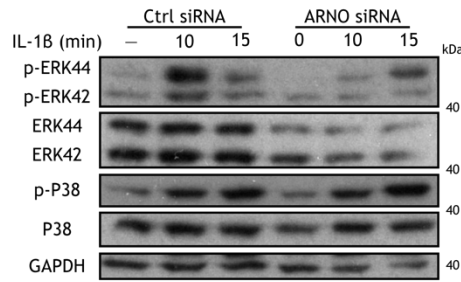


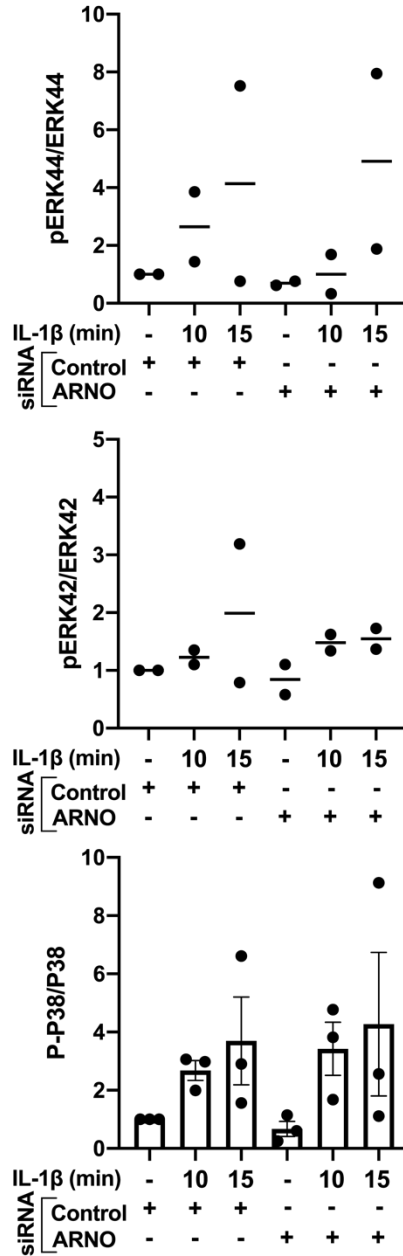
Figure 4-10 ARNO mediates the phosphorylation of STAT3 in SFs.

SFs from naïve (A) and CIA (B) mice were extracted and expanded *ex vivo*. Representative western blots of SFs treated with control and ARNO siRNA followed by IL-1 β (10ng/ml) treatment at indicated times. Anti-pSTAT3^{Tyr705}, STAT3, ARNO and GAPDH antibodies were used. Relative quantification of phosphorylated STAT3 in SFs was calculated as pSTAT3/STAT3/GAPDH band intensity. Changes in total protein expression were calculated as STAT3/GAPDH band intensity. Each dot represents one independent experiment, and error bars represent SEM (n=3). *p < 0.05 by the Mann-Whitney test.

A Naive SFs



B phospho/total



C total/GAPDH

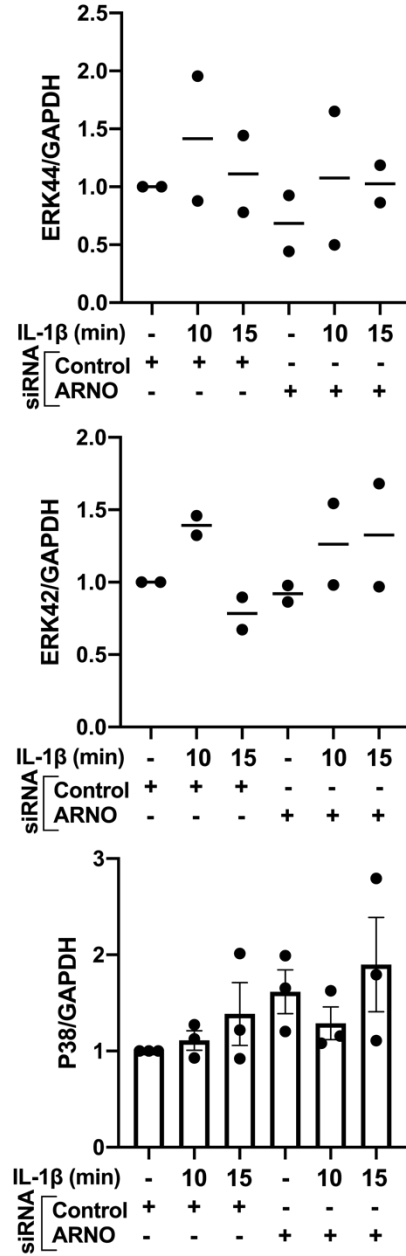
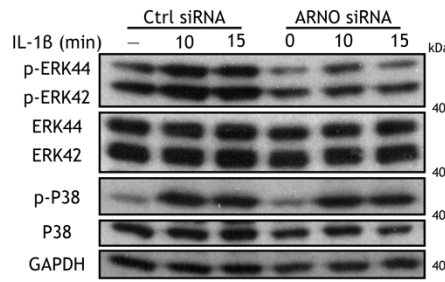


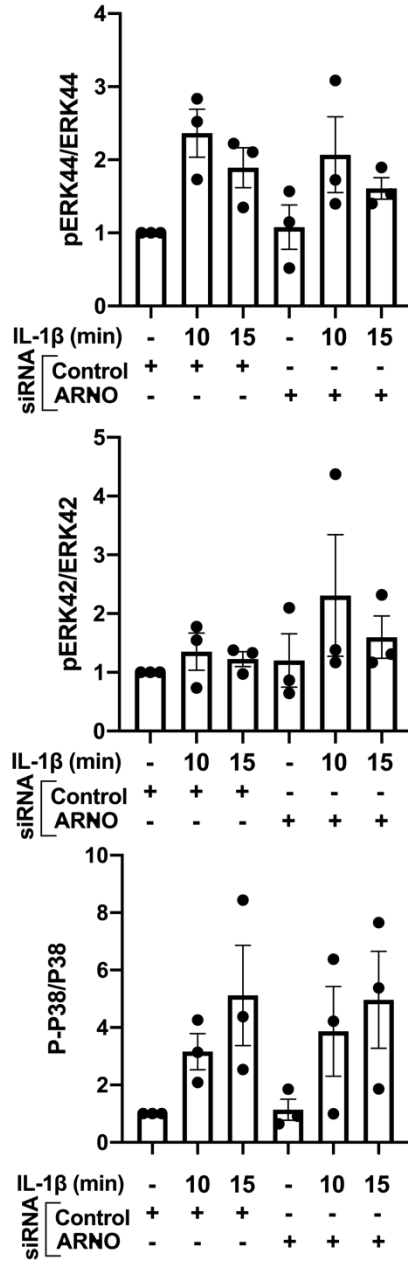
Figure 4-11 Silencing ARNO does not affect MAPK signaling phosphorylation.

SFs from naïve mice were extracted and expand *ex vivo*. Representative western blots of SFs treated with control and ARNO siRNA followed by 10ng/ml IL-1 β treatment at indicated times. Anti-pERK1/2, ERK1/2, p-P38, P38 and GAPDH antibodies were used. (B) Relative quantification of phosphorylated ERK1/2 and P38 in naive SFs, calculated as pERK44/ERK44/GAPDH, pERK42/ERK42/GAPDH and p-P38/P38/GAPDH band intensity. (C) Changes in total protein expression were calculated as ERK44/GAPDH, ERK42/GAPDH and P38/GAPDH band intensity. Each dot represents one independent experiment, and error bars represent SEM (n \geq 2).

A CIA SFs



B phospho/total



C total/GAPDH

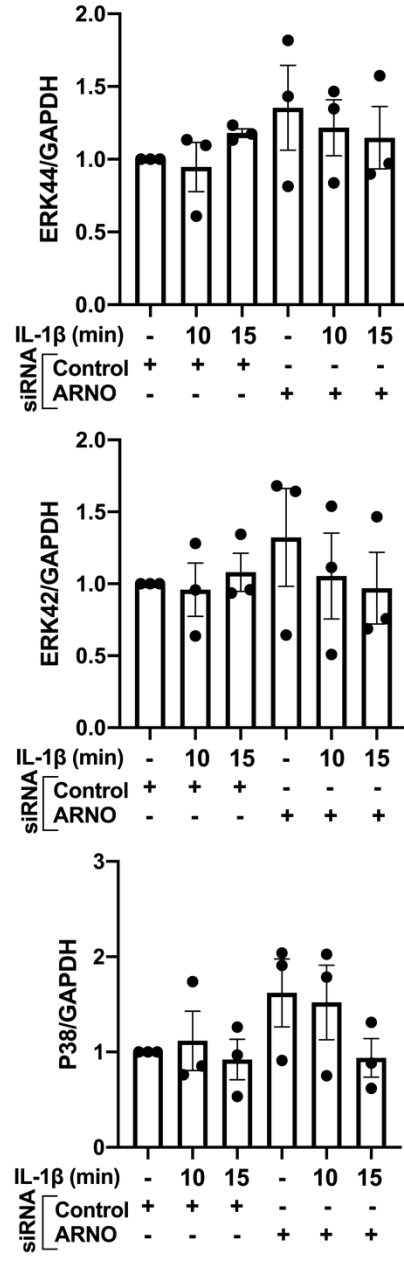


Figure 4-12 Silencing ARNO does not affect MAPK signaling phosphorylation.

SFs from CIA mice were extracted and expanded *ex vivo*. Representative western blots of CIA SFs treated with control and ARNO siRNA followed by 10ng/ml IL-1 β treatment at indicated times. Anti-pERK1/2, ERK1/2, p-P38, P38 and GAPDH antibodies were used. (B) Relative quantification of phosphorylated ERK1/2 and P38 in CIA SFs, calculated as pERK44/ERK44/GAPDH, pERK42/ERK42/GAPDH and pP38/P38/GAPDH band intensity. (C) Changes in total protein expression were calculated as ERK44/GAPDH, ERK42/GAPDH and P38/GAPDH band intensity. Each dot represents one independent experiment, and error bars represent SEM (n=3).

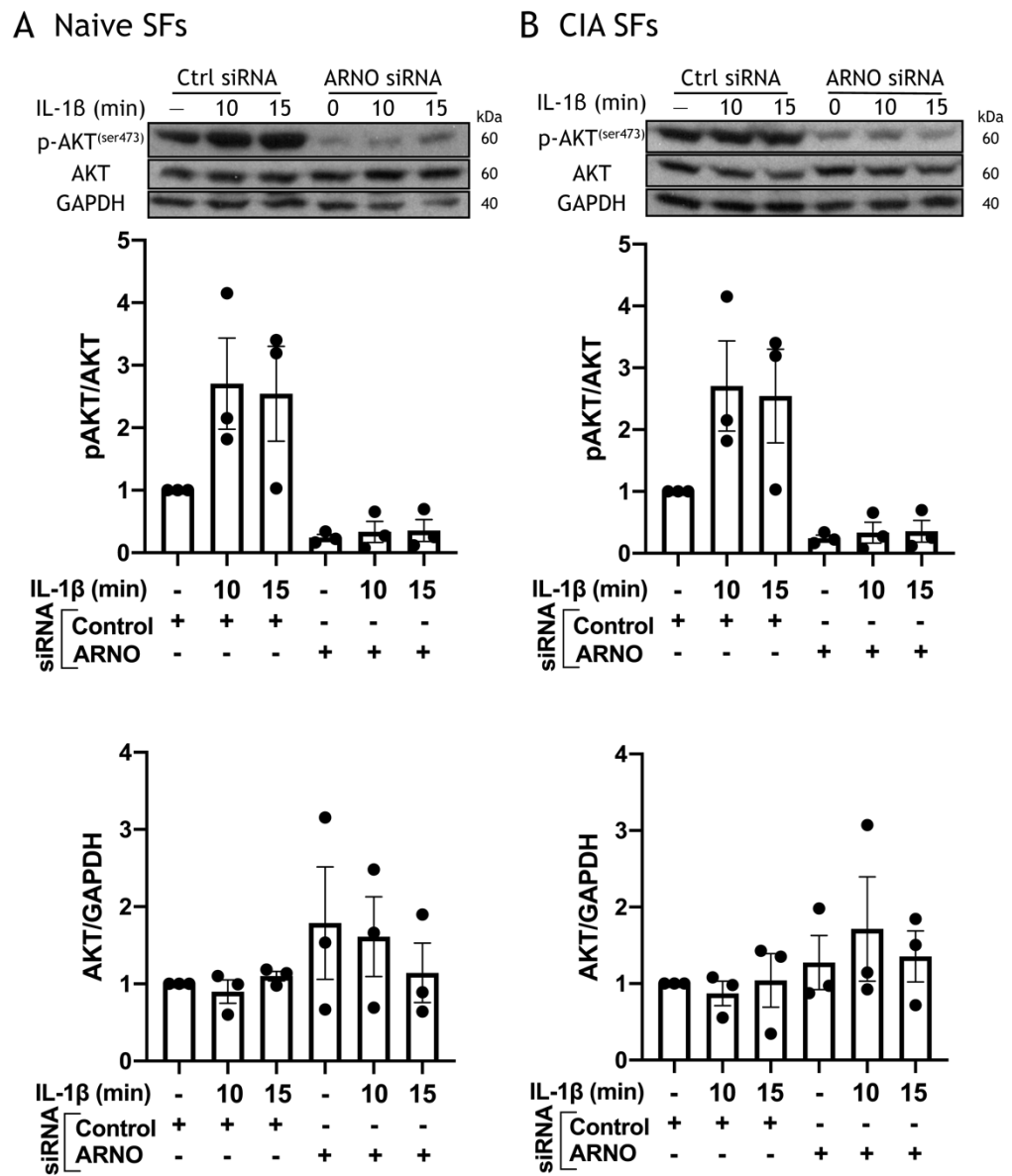


Figure 4-13 ARNO mediates the phosphorylation of AKT in SFs.

SFs from naïve (A) and CIA (B) mice were extracted and expanded *ex vivo*. Representative western blots of SFs treated with control and ARNO siRNA followed by IL-1 β (10ng/ml) treatment at indicated times. Anti- p-AKT^{ser473}, AKT and GAPDH antibodies were used. Relative quantification of phosphorylated AKT in SFs was calculated as p-AKT/AKT/GAPDH band intensity. Changes in total protein expression were calculated as AKT/GAPDH band intensity. Each dot represents one independent experiment, and error bars represent SEM (n=3).

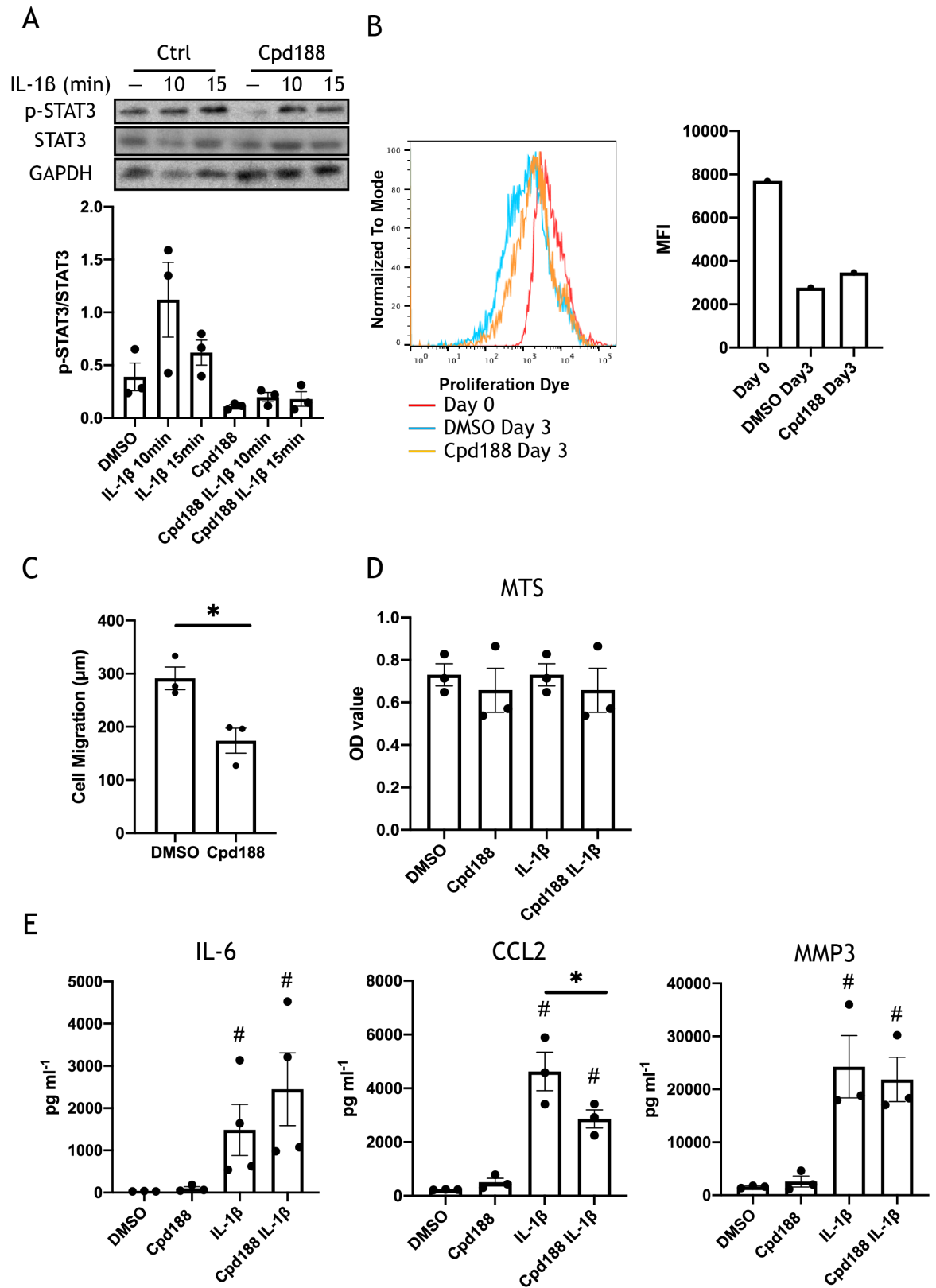


Figure 4-14 Inhibition of STAT3 phosphorylation by Cpd188 reduces cell migration and CCL2 production.

SFs from naïve mice were extracted and expanded *ex vivo*. (A) Representative western blots and quantification of STAT3 phosphorylation in control (DMSO) and Cpd188 (STAT3 inhibitor, 73 μ M) treated SFs followed by 10 ng/ml IL-1 β stimulation at indicated times, calculated as p-STAT3/STAT3/GAPDH band intensity (n=3). (B) SFs were labelled with proliferation dye eFlour 670, followed by flow cytometry analysis (Day0) or treated with Cpd188 and kept in culture for 3 days (Day 3). Bar chart shows the mean fluorescence intensity of proliferation dye on day 0 and day 3 (n=1). (C) SFs were seeded in the migration chamber until monolayer confluence was reached. Distance of SF migration was measured after treated with Cpd188 for 24 hours, error bars represent SEM (n=3); *p < 0.05 by the Mann-Whitney test. (D) Cell viability and metabolism after Cpd188 treatment were checked using MTS cell proliferation kit (n=3). (E) Control or Cpd188-treated SFs were stimulated with IL-1 β for 24 hours, supernatants were collected to quantify the levels of IL-6, CCL2 and MMP3 by ELISA. #p<0.05 versus unstimulated control, by the Mann-Whitney test. In all cases, one dot represents one individual experiment, analysed in technical triplicate for MTS and ELISA assays.

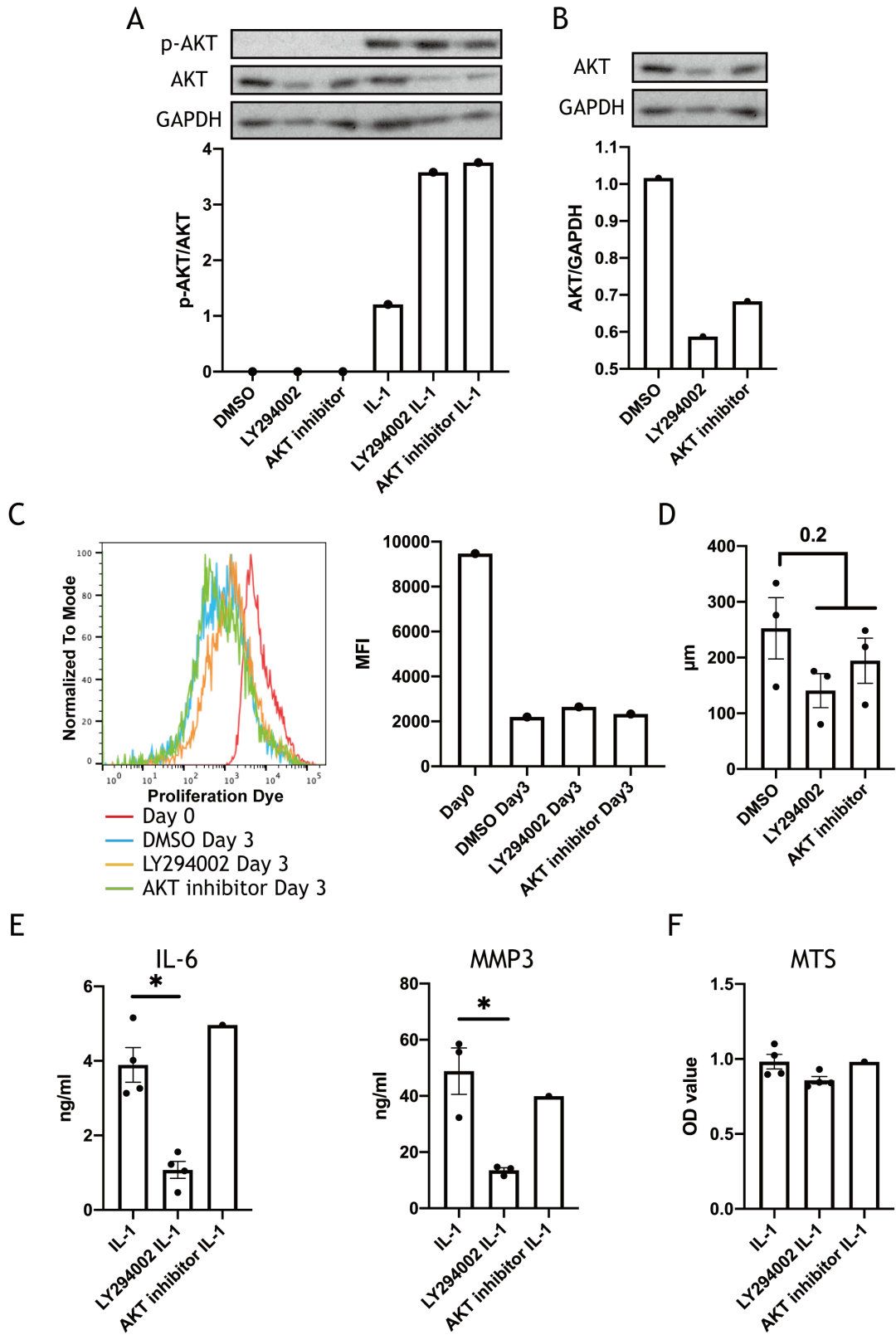
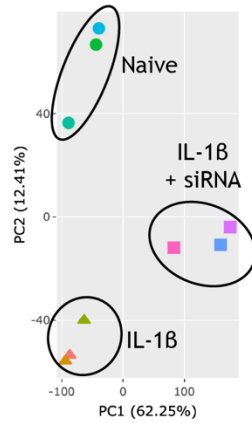


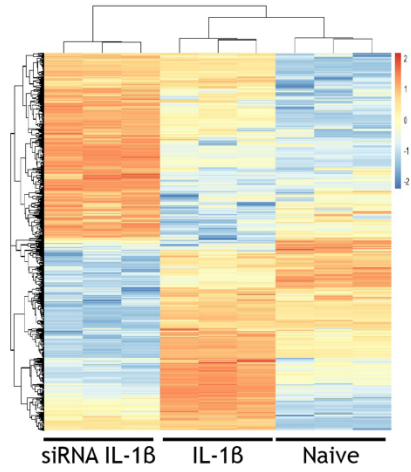
Figure 4-15 PI3K-AKT signaling pathway regulates cytokine production in SFs.

SFs from naïve mice were extracted and expand *ex vivo*. (A) Representative western blots and quantification of AKT phosphorylation in control (DMSO), Ly294002 (PI3K inhibitor, 20 μ M) and AKT inhibitor (20 μ M) treated SFs followed by 10 ng/ml IL-1 β stimulation for 15 minutes, calculated as p-AKT/AKT/GAPDH band intensity (n=1). (B) Representative western blots and quantification of total AKT in control (DMSO), Ly294002 (PI3K inhibitor, 20 μ M) and AKT inhibitor (20 μ M) treated SFs, calculated as AKT/GAPDH band intensity (n=1). (C) Flow cytometry analysis of the mean fluorescence intensity of proliferating dye in SFs cultured 3 days after treatment with Ly294002 or AKT inhibitors (n=1). (D) SFs were seeded in the migration chamber until monolayer confluence was reached. Distance of SF migration was measured 24 hours after treated with Ly294002 or AKT inhibitor, error bars represent SEM (n=3). Statistical analysis was carried out by the Mann-Whitney test. (E) Control or inhibitors-treated SFs were stimulated with IL-1 β for 24 hours, supernatants were collected to analyse IL-6 and MMP3 secretion by ELISA. *p<0.05 by the Mann-Whitney test. (F) Cell viability and metabolism after Ly294002 and AKT inhibitor treatment were checked using MTS cell proliferation kit. In all cases, one dot represents one individual experiment, analysed in technical triplicate for MTS and ELISA assays.

A

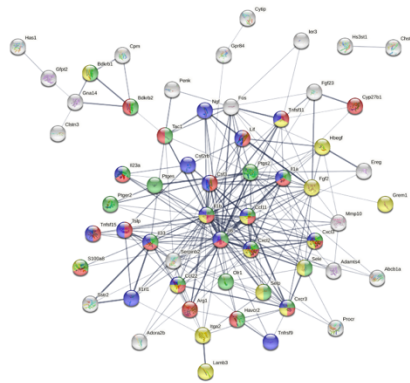


B



C

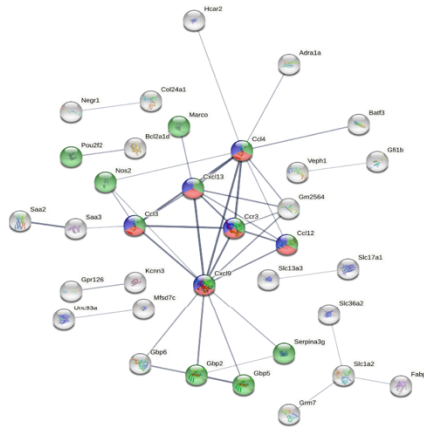
Up-regulated by IL-1B and suppressed by ARNO silencing



- KEGG: mmu04060
Cytokine-cytokine receptor interaction
- GO:0006955
Immune response
- GO:0006954
Inflammatory response
- GO:0016477
Cell migration

D

Up-regulated by IL-1B and enhanced by ARNO silencing



- KEGG: mmu04060
Cytokine-cytokine receptor interaction
- KEGG: mmu04062
Chemokine signaling pathway
- GO:0006955
Immune response

Figure 4-16 Transcriptome characteristics of ARNO-silenced SFs in response to IL-1 β stimulation.

RNA was isolated from naïve, IL-1 β treated and IL-1 β treated ARNO knockdown SFs and subject to bulk RNAseq. (A) Principal component analysis (PCA) for three groups. (B) Heatmap of differentially expressed genes among three experimental groups. Genes that passed a threshold of $p_{adj} < 0.01$ and $|\log_2\text{foldChange}| > 2$ were considered differentially expressed. (C) Differentially expressed genes that were upregulated by IL-1 β and suppressed by ARNO silencing in (B) were subjected to STRING protein-protein interaction network (<https://string-db.org>). (D) Differentially expressed genes that were upregulated by IL-1 β and enhanced by ARNO silencing in (B) were subjected to STRING protein-protein interaction network (<https://string-db.org>).

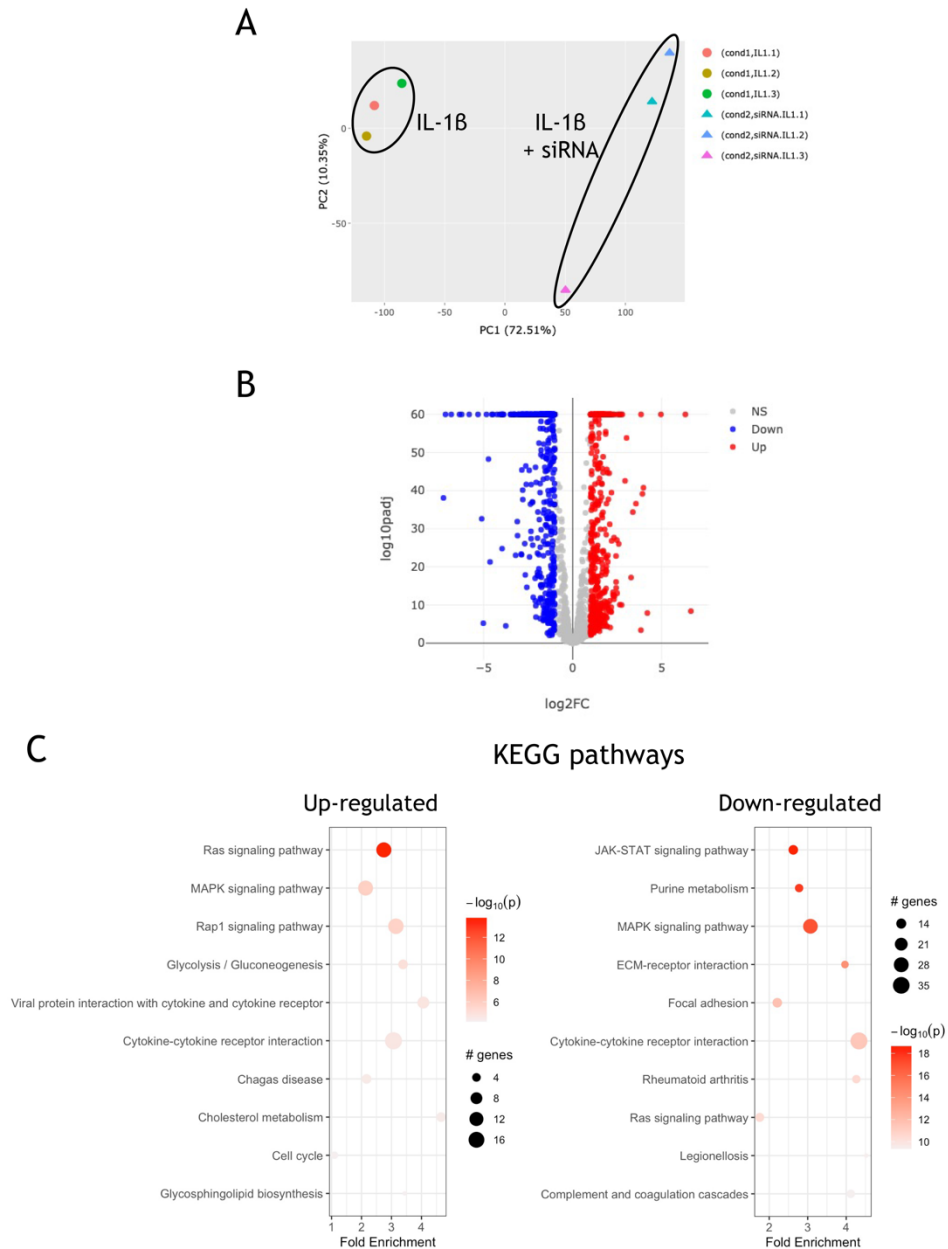
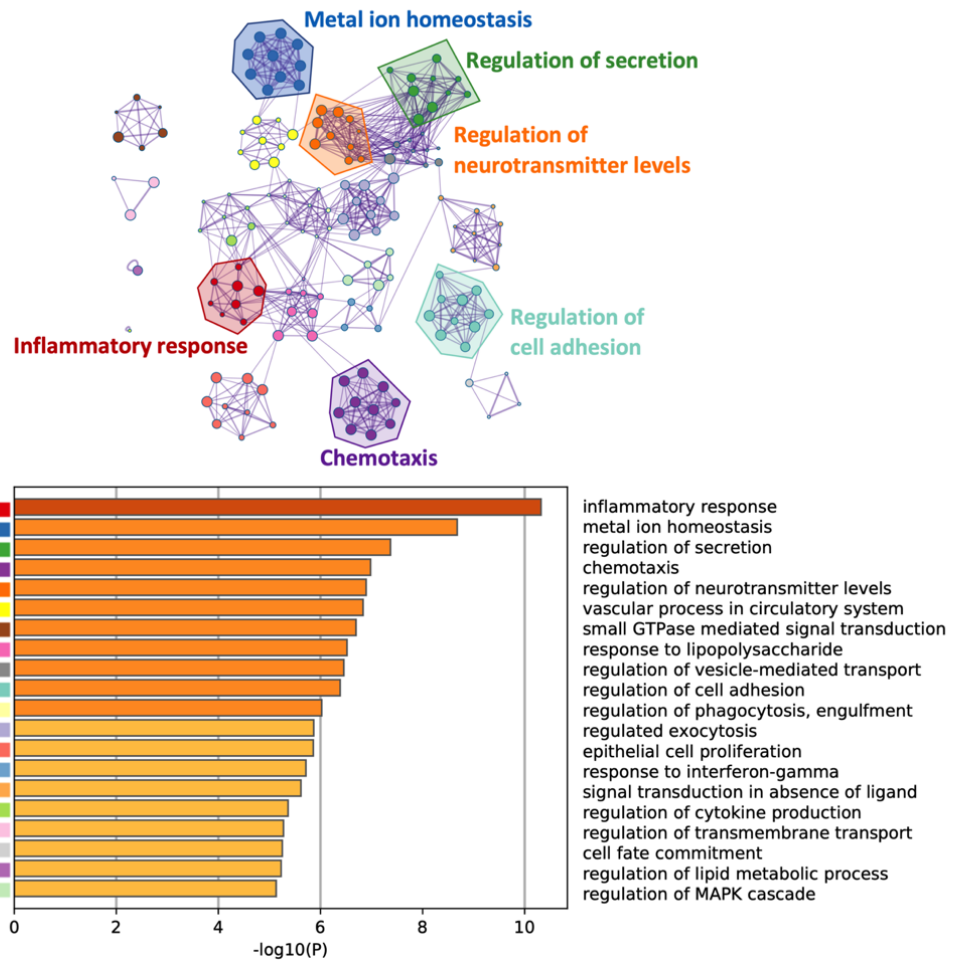


Figure 4-17 Transcriptome characteristics of ARNO-silenced SFs in response to IL-1 β stimulation.

RNAseq of IL-1 β treated and IL-1 β treated ARNO knockdown SFs in **Figure 4-16A**. (A) Principal component analysis. (B) All detected genes were plotted as a volcano plot. Genes that passed a threshold of $\text{padj} < 0.01$ and $|\log_2\text{foldChange}| > 1$ were considered as differentially expressed. Colour code, red: upregulated, blue: downregulated, in IL-1 β treated ARNO knockdown SFs. (C) DE genes identified in (B) were used to conduct KEGG pathway enrichment analysis. KEGG pathways were represented in bubble charts which were plotted according to fold enrichment on the x-axis and $-\log_{10}$ p-value on the coloured scale. The size is proportional to the number of differentially expressed genes.

A



B

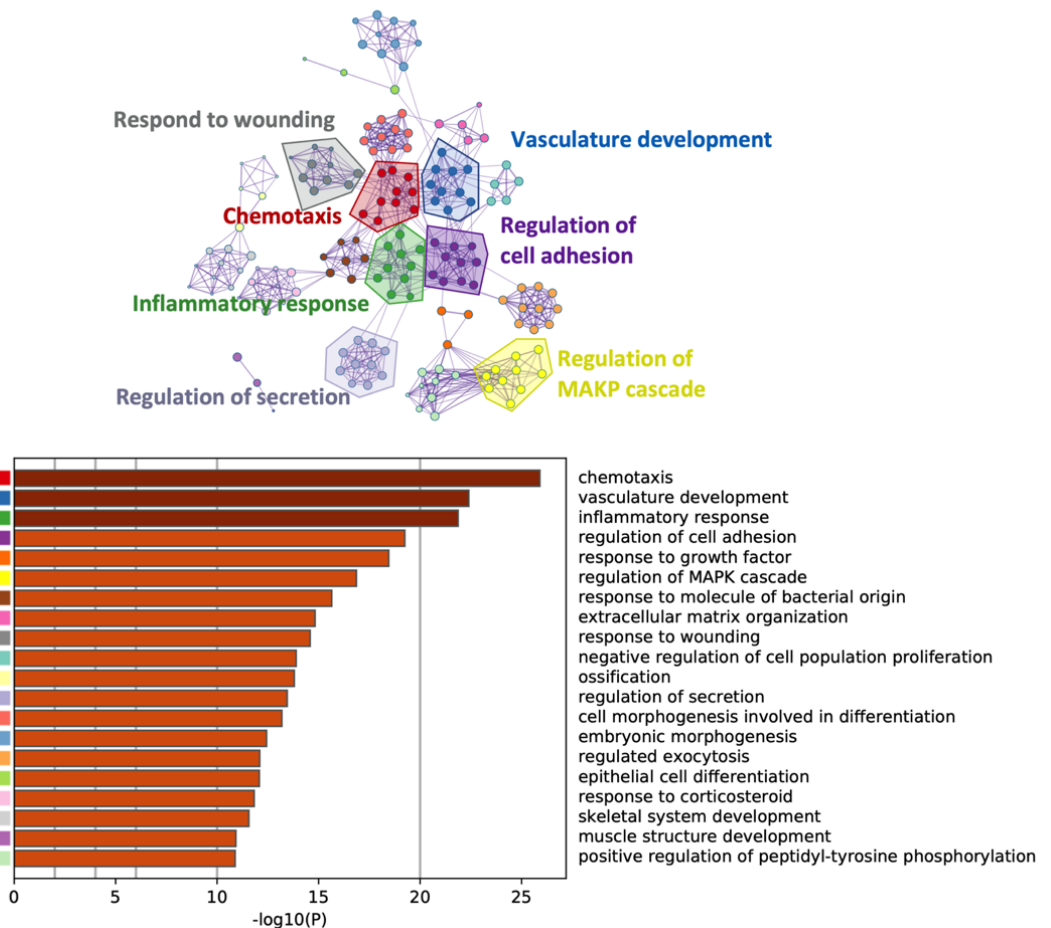


Figure 4-18 Transcriptome characteristics of ARNO-silenced SFs in response to IL-1 β stimulation.

The differentially expressed genes identified in **Figure 4-17B** were used to conduct GO-biological process pathway enrichment analysis. Metascape enrichment network diagrams illustrate the GO biological process pathways that were significantly enriched for upregulated (A) and down-regulated (B) genes.

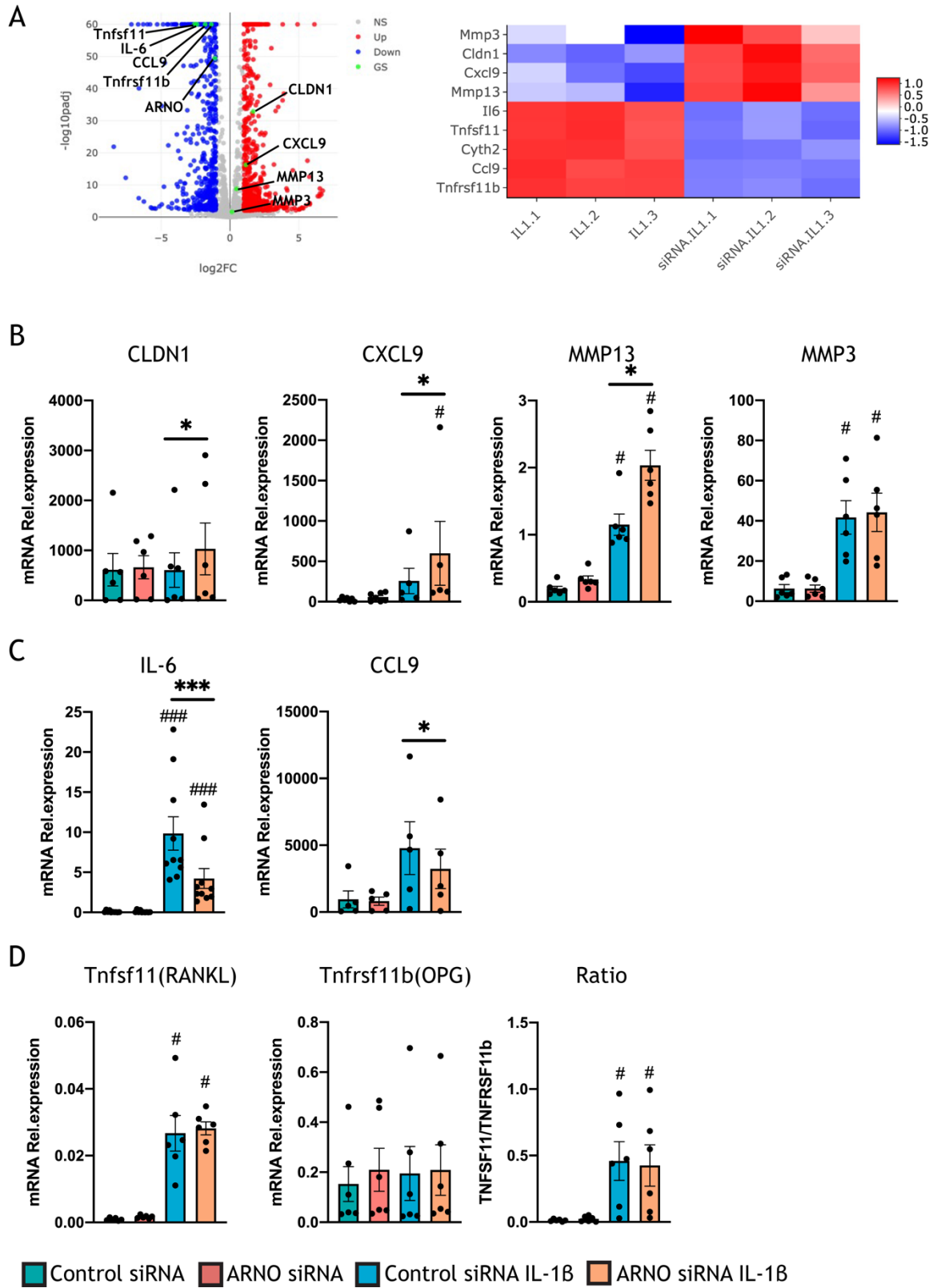


Figure 4-19 ARNO knockdown reshapes IL-1 β -mediated inflammatory response.

(A) Gene expression detected in **Figure 4-17B** for ARNO (Cyt2), CLDN1, CXCL9, MMP13, MMP3, IL-6, CCL9, Tnfsf11 and Tnfrsf11b. (B-D) RNA was isolated from control (Allstars) or ARNO siRNA transfected naïve SFs stimulated with IL-1 β as indicated. Relative mRNA expression of genes shown in (A) was evaluated by RT-qPCR. (B) CLDN1, CXCL9, MMP13 and MMP3. (C) IL-6 and CCL9. (D) Tnfsf11, Tnfrsf11b and ratio of Tnfsf11 and Tnfrsf11b. For (B–D), each dot represents one independent experiment, error bars represent SEM (n \geq 5), *p < 0.05, ***p < 0.001 versus respective siRNA control, #p < 0.05, ###p < 0.001 versus unstimulated control, by the Mann-Whitney test.

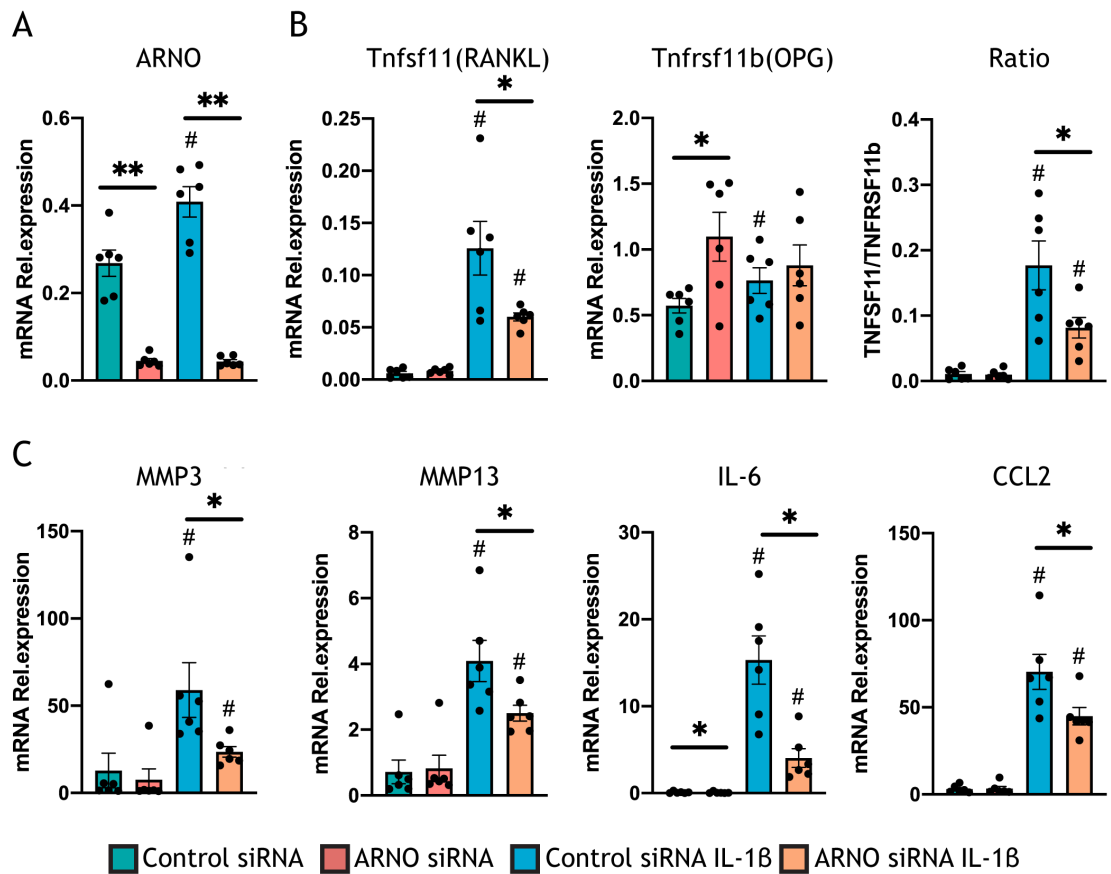


Figure 4-20 ARNO knockdown reduces IL-1 β -mediated inflammatory response in CIA SFs.

SFs were extracted from arthritic mice and expanded *ex vivo*. RNA was isolated from unstimulated and IL-1 β -stimulated SFs upon ARNO or Allstars siRNA transfection. Relative mRNA expression of genes was evaluated by RT-qPCR. (A) ARNO. (B) Tnfsf11, Tnfrsf11b and ratio of Tnfsf11 and Tnfrsf11b. (C) MMP3, MMP13, IL-6 and CCL2. Each dot represents one independent experiment, error bars represent SEM (n=6), *p < 0.05, **p < 0.01 versus respective siRNA control, #p < 0.05 versus unstimulated control, by the Mann-Whitney test.

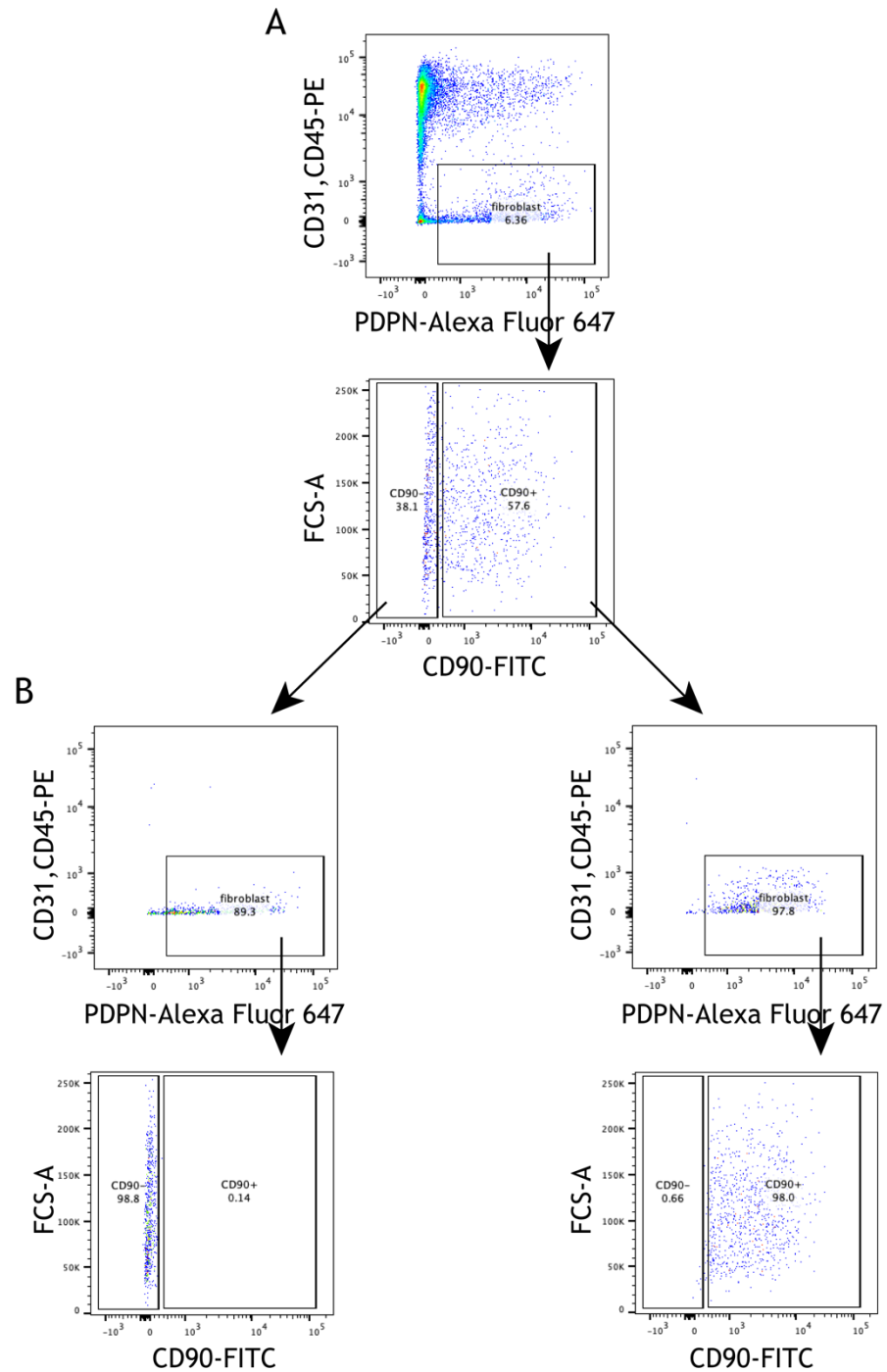


Figure 4-21 Gating strategy for SF subsets sorted from mouse joint synovial tissue.

Cells were isolated from joints of naïve mice and mice undergoing Collagen-Induced Arthritis. SFs were sorted by FACS gating on low viability dye, CD31⁻, CD45⁻ and PDPN⁺. Subsets of SFs were discriminated by the expression of CD90. (A) The sorting strategy is shown in the dot plots. (B) The purity of sorted SF subsets was examined by flow cytometry.

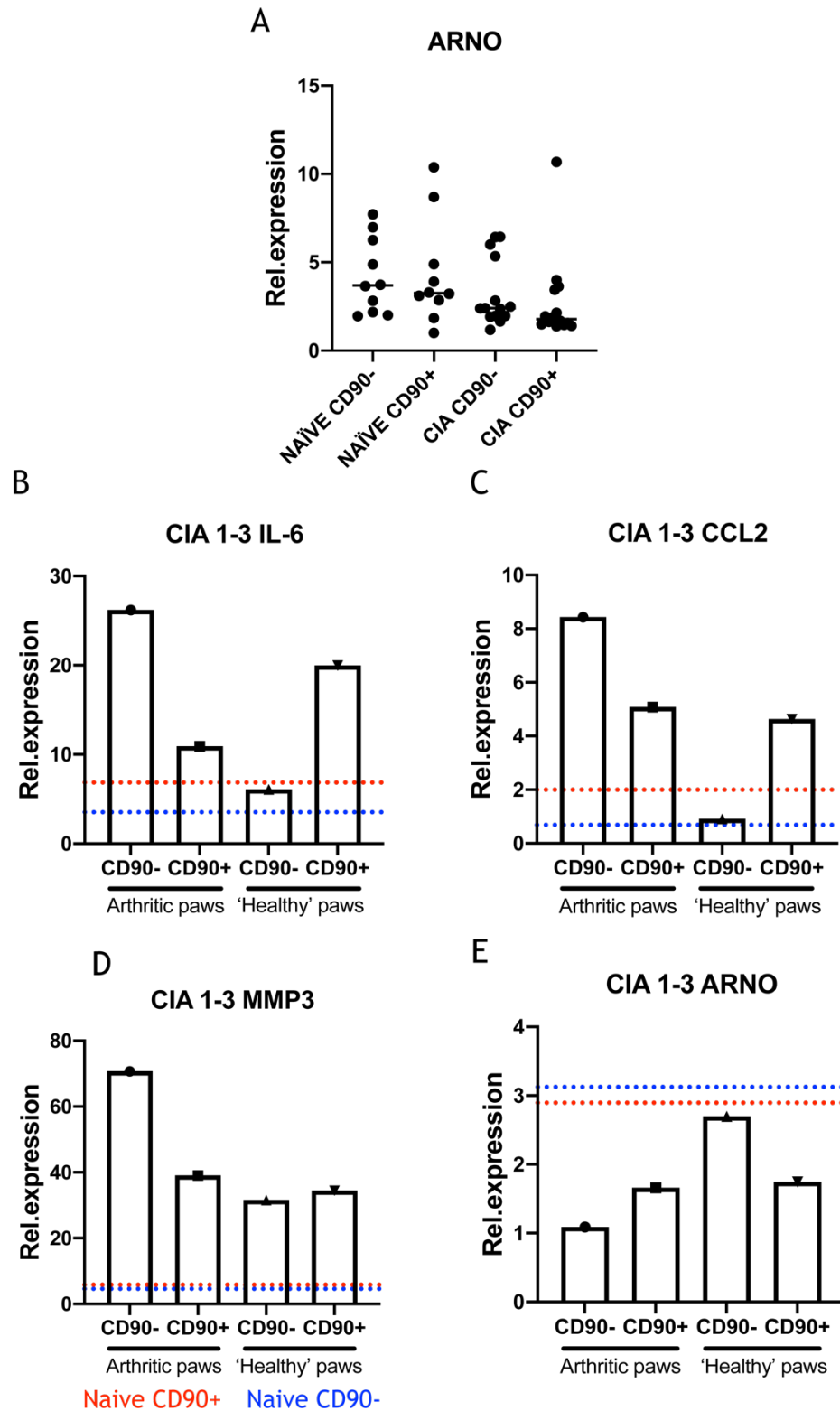


Figure 4-22 ARNO expression varies with arthritis progression.

(A) Relative expression of ARNO in SF subsets obtained in **Figure 4-21A** was quantified by RT-qPCR, each dot represents an individual mouse ($n \geq 10$). (B-E) SF subsets were sorted from the inflamed and 'healthy' (no signs of swollen and redness) paws of one CIA mouse. Relative expression of IL-6 (B), CCL2 (C), MMP3 (D) and ARNO (E) mRNA was quantified by RT-qPCR. The red dashed line represents the average expression of this gene in naive CD90+ SFs and the blue dashed line represents the average expression in naive CD90-SFs.

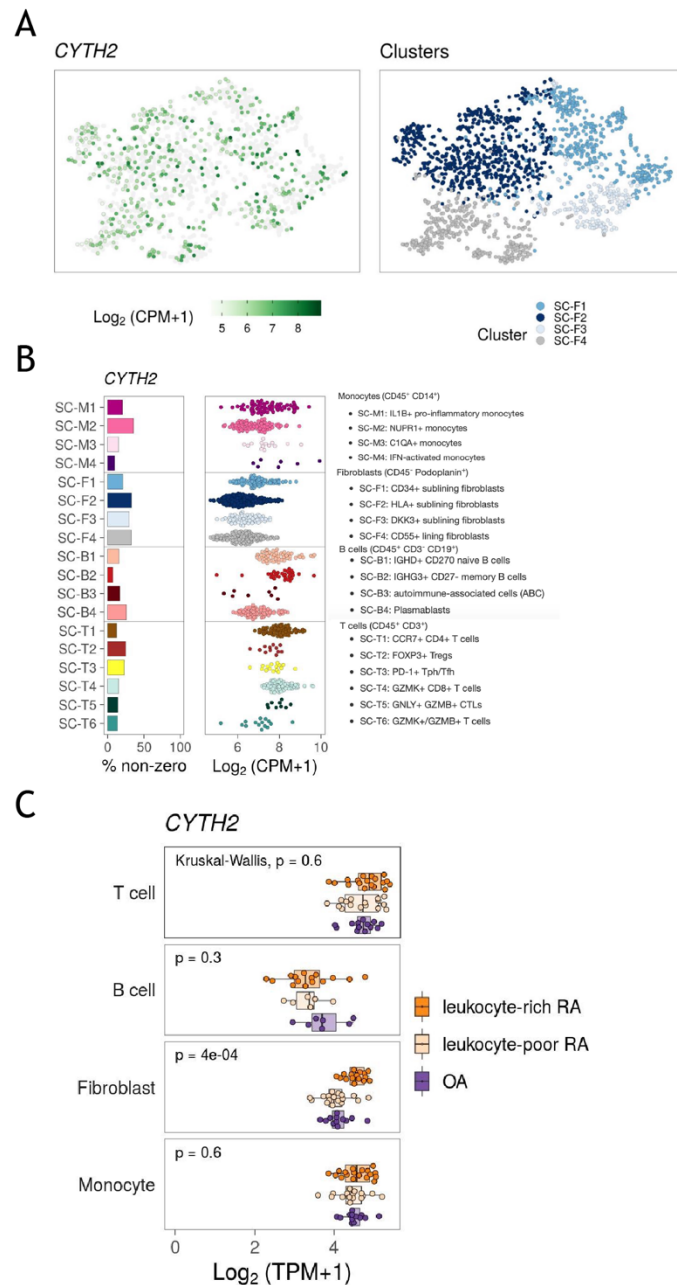


Figure 4-23 Expression of ARNO in synovial tissue of patients with rheumatoid arthritis.

(A) ARNO (Cyth2) expression profile in human synovial fibroblasts from single-cell RNAseq analysis. (B) Single-cell RNAseq analysis of ARNO (Cyth2) expression in subsets of monocyte, synovial fibroblast, B cell and T cell. (C) Comparative expression of ARNO (Cyth2) by bulk RNAseq in T cells, B cells, fibroblasts and monocytes in leukocyte-rich RA, leukocyte-poor RA and OA. Data were generated by Zhang F et al. (Zhang et al., 2019) to examine the inflammatory cell states in joint synovial tissues of rheumatoid arthritis.

Figures were downloaded from <https://immunogenomics.io/ampra/>.

Chapter 5 Investigating the role of sialic acid in SF pathogenesis

5.1 Introduction

In the previous chapter, the role of intracellular ARNO on the inflammatory response and motility of SFs was discussed; this chapter focuses on a type of molecules present on the cell surface, sialic acids, glycans that are also implicated in the regulation of inflammatory responses and cell motility. Glycosylation is a complex post-translational modification present in all eukaryotic cells, with a large number of biosynthetic enzymes involved in this process (Boyer, 2006). Glycosylation has been divided into several specific groups based on the type of glycosidic bond, including N-linked, O-linked and C-linked, with N-linked being a common type of glycosylation. Glycosylation increases the diversity of proteome by modifying the protein backbone in multiple aspects, including glycan composition, or glycan length and glycosidic linkage, to generate different glycoforms of the same protein. As an example of N-glycan glycosylation, multiple steps are involved in the glycan biosynthesis pathways, such as mannosylation, fucosylation, glycan branching and sialylation (Figure 5-1). Previous results from our group indicated that sialic acid was a key modification in the glycome of arthritic SFs. This chapter will therefore concentrate on the regulation and role of sialic acid in SFs.

Sialic acids are a family of nine carbon sugar acids, which are found at the ends of oligosaccharide chains attached to lipids and proteins of higher animals and some micro-organisms (Varki, 2008, Nakahashi et al., 2007). The biological significance of Sialic acid is well-documented, and dysregulation of cell sialylation is often associated with diseases. Sialic acid is attached to complex glycans in the endoplasmic reticulum and Golgi by sialyltransferases, which catalyse the reaction of transferring sialic acid residues from the CMP-activated sugar donor to a variety of receptor molecules (Chen and Varki, 2010). Sialyltransferases can recognise specific sugar substrates by adding sialic acid to O-linked or N-linked glycoproteins. Based on the type of linkage formed and the nature of sugar acceptor, eukaryotic sialyltransferases are classified into three groups: i) six β -galactoside α 2-3- sialyltransferases (ST3Gal I-VI), ii) two β -

galactoside α 2-6- sialyltransferases (ST6Gal I-II) and iii) six α 2-8- sialyltransferases (ST8Sia I-VI) (Li and Chen, 2012).

Tumour cells display an altered glycosylation profile. For example, the concentration of sialic acid in human serum was significantly increased in people with malignant tumours (Paszowska et al., 1998) and glycosylation regulates metastasis (Laubli and Borsig, 2019, Rodrigues et al., 2018). Glycosylation also regulates immune responses with, for example, desialylation promoting dendritic cell phagocytosis and production of pro-inflammatory cytokines (Cabral et al., 2013). Moreover, loss of sialic acids increases microvascular permeability by disrupting the endothelial cell-cell junctions (Deng et al., 2017, Betteridge et al., 2017). Besides, other biological processes, such as cell-matrix interaction, adhesion and protein targeting, are also affected by altered sialylation (Li and Chen, 2012, Betteridge et al., 2017).

However, little is known about the function of sialic acid on arthritic SFs. Sialic acids are ubiquitously distributed at the end of the carbohydrate chain of the outer cell surface, including synovial fibroblast. Interestingly, a recent study showed that TNF α induced ST6Gal-I proteolysis in endothelial cells and impaired endothelial cells tight junction function and monocyte-endothelial cell adhesion (Deng et al., 2017). The impaired cellular activity appears to be a consequence of unmasking galactose residues upon cytokine stimulation. Thus, as cytokines accumulate in the joint cavity in RA, they may regulate sialyltransferase expression in SFs, a potential novel mechanism contributing to the increased infiltration of cells and inflammatory factors following disruption of the synovial barrier integrity. Thereby, we hypothesised that sialic acid protects SFs from transforming into a pathogenic phenotype and changes in homeostatic sialylation may lead to local inflammatory responses.

5.2 Results

5.2.1 Glycosylation pathways associated with SF pathogenesis

5.2.1.1 SF glycosylation transcriptomic profile

To investigate the glycosylation signature of arthritic SFs, the expression of glycosylation genes from the UniProt knowledgebase (KW-0325) was analyzed in

RNAseq data of freshly isolated naïve and CIA SFs. Multiple glycosylation genes were differentially expressed in arthritic SFs (Figure 5-2A). Then, the expression of genes involved in sialylation was examined and plotted in volcano plot and heatmap. Among all these genes, St6gal1 and St8sia2 were reduced in arthritic SFs (Figure 5-2B). Interestingly, studies have shown that TNF α downregulates St6gal1 expression in endothelial cells and macrophages (Deng et al., 2017, Holdbrooks et al., 2020), indicating that α 2-6 sialic acid may be regulated in the inflammatory milieu.

5.2.1.2 Altered sialylation in arthritic SFs

To further investigate the modification of sialylated glycans in arthritic SFs, mass spectrometry (MS) based glycomic analysis was used to identify the N-glycan profiles of murine naïve (Figure 5-3A) and CIA (Figure 5-3B) SFs cultured *ex vivo*. This revealed that 15 sialylated structures were reduced in CIA SFs (Figure 5-3C). There are two dominant forms of sialic acid in fibroblasts, α 2-6-linkage (Figure 1-9A) and α 2-3-linkage (Figure 1-9B) and because this is relevant for their biological function and receptor binding, the ratio of α 2-3 and α 2-6 sialic acid linkages in SF glycoconjugates was studied by SNA and MAA II staining, which are specific lectins for α 2-6 and α 2-3 sialic acid respectively. The results showed that the binding of SNA was reduced (Figure 5-4A), whereas the binding of MAA II (Figure 5-4B) remains unchanged in CIA SFs compared with naïve SFs, indicating a reduction of α 2-6 sialic acid in arthritic SFs. This reduction may be due to the decreased expression of the α 2-6 sialyltransferases, St6gal1. PNA staining was chosen as control for sialic acid binding, as the presence of sialylated N-glycans inhibits PNA binding. Elevated PNA binding in Figure 5-4C also reflects the decrease of sialic acid in CIA SFs.

5.2.1.3 SF subsets are differentially sialylated

As described above, SFs are heterogeneous cells with a variety of anatomical and functional characteristics. SFs in specific areas of the synovium exhibit distinct characteristics, which contribute differently to the pathogenesis of arthritis (Croft et al., 2019, Mizoguchi et al., 2018). For example, SFs localised in the lining layer (CD90-) produce more MMPs which involve in bone and cartilage degradation, whereas SFs in the sub-lining layer (CD90+) are more proliferative,

migratory and produce more proinflammatory cytokines (Mizoguchi et al., 2018). Identifying the expression and regulation of sialic acid in subsets of SFs may therefore provide better insight into the mechanisms of SF-mediated pathogenesis in arthritis. Thus, the relative expression of α 2,3 and α 2-6 sialyltransferases was evaluated in the lining and sub-lining SFs from naïve and CIA mice (Figure 5-5). SFs were isolated and sorted as described in Chapter 3 (Figure 3-5A) and Chapter 4 (Figure 4-21). Briefly, SFs were identified as CD31-CD45-PDPN⁺ and based on the expression of CD90, SFs were sorted into lining SFs (CD90⁻) and sub-lining SFs (CD90⁺) by flow cytometry. Relative expression of sialyltransferases were evaluated by RT-qPCR.

In healthy synovium, sub-lining SFs exhibit higher expression of St6gal1, St3gal1 and St3gal2 compared with lining SFs, but the expression of St6galNac5, St3gal3, St3gal4 and St3gal6 were relatively similar, data which collectively suggest that the sub-lining synovium may have higher level of sialic acid compared to the lining synovium (Figure 5-5). In the arthritic synovium, differential expression of sialyltransferases was also observed between lining and sub-lining SFs, such as higher expression of St6GalNac5, St3gal1, St3gal2 and St3gal4 in sub-lining SFs compared with lining SFs (Figure 5-5). When compared to naïve SFs, St6gal1 was significantly reduced in CD90⁺ SFs (Figure 5-5A), and St6galNac5 was reduced in CD90⁻ arthritic SFs though not reaching statistical significance (Figure 5-5B). However, the expression of St3gals remained unchanged or upregulated, such as St3gal4 (Figure 5-5C-G), consistent with the SNA/MAA binding data showing that α 2-6 sialic acid was reduced in CIA SFs rather than α 2-3 sialic acid (Figure 5-4A, B). The lower expression of St6gal1 in arthritic sub-lining SFs may be associated with a higher inflammatory response in sub-lining synovium, as cells in sub-lining synovium produce more proinflammatory cytokines (Mizoguchi et al., 2018), suggesting a potential link between reduced α 2-6 sialic acid and inflammatory response.

5.2.2 Loss of α 2-6 sialylation is associated with inflammatory SFs

5.2.2.1 TNF α suppresses St6gal1 expression and α 2-6 sialylation

As mentioned above, arthritic SFs exhibit reduced α 2-6 sialylation which may be related to their high inflammatory responses. To investigate the mechanism of

reduced sialylation in arthritic SFs, we extracted SFs from mouse joints and cultured them *in vitro* to perform the following experiments. Sialylation of glycoproteins can be divided into two parts as shown in Figure 1-8, namely i) the synthesis of CMP-Neu5Ac and metabolic pathways, and ii) the transfer of sialic acid to complex glycans. A decrease in either of these may result in hyposialylated glycomes. To determine the mechanisms regulating cellular sialylation, we evaluated the expression of enzymes involved in these two steps including 5 genes in CMP-Neu5Ac synthesis (Cmas, Gne, Nanp, Slc35a1) and 10 sialyltransferases (St6gal1, St3gal1, St3gal3, St3gal3, St3gal6, St6galNac2, St6galNac4, St6galNac6, St3galNac3 and St8sia6) in responding to pro-inflammatory cytokines by qPCR using Sybr green probes. IL-1 β , IL-17 and TNF α were chosen as they play dominant roles in the pathogenesis of RA. To confirm that SFs were activated by these cytokines, IL-6 expression, which is upregulated in response to IL-1 β , IL-17 and TNF α , was selected as a positive control for cell activation (Figure 5-6A-C). The expression of Cmas, Gne, Nanp, Slc35a1 was not affected by any cytokine stimulation (Figure 5-6A-C). Indeed, these four genes were not differentially regulated in CIA SFs compared to naïve SFs, suggesting that hyposialylation in CIA SFs maybe not regulated by CMP-Neu5Ac synthesis. By contrast, IL-1 β upregulated St6gal1 in naïve SFs and St3gal4 in CIA SFs (Figure 5-6A), stimulating around a two-fold increase. Whilst IL-17 had no significant effect on these enzymes (Figure 5-6B), notably, TNF α greatly decreased St6gal1 expression in both naïve and CIA SFs (Figure 5-6C). These results were corroborated by dose dependent TNF α treatment (Figure 5-7A) and additional qPCR using TaqMan™ probes (Figure 5-7B). Based on the observed downregulation of St6gal1 mRNA in SFs upon TNF α stimulation, lectin binding was assessed by ELLA assay and further validated by flow cytometry analysis of SNA binding that TNF α downregulates α 2,6 sialic acid expression (Figure 5-7C, D). Finally, N-glycans from naïve and TNF α treated SFs were isolated and then subjected to MS-based glycan structure analysis which identified 15 sialylated N-glycans in naïve (Figure 5-8A) and TNF α treated (Figure 5-8B) SFs. In total, 12 sialylated N-glycans exhibited reduced sialylation in response to TNF α stimulation (Figure 5-8C), further supporting that TNF α reduces the sialylation of SFs.

5.2.2.2 Inhibition of St6gal1 induces cytokine production in SFs

SFs adopt a proinflammatory phenotype in RA, becoming the main providers of pro-inflammatory cytokines in the inflamed joint. Previous studies have demonstrated that desialylation triggers inflammatory responses in multiple cell types (Stamatos et al., 2004, Pappu and Shrikant, 2004, Cabral et al., 2013, Matsumoto et al., 2000). We have observed that arthritic SFs are desialylated *in vivo* and that the pro-inflammatory cytokine TNF α reduces SF sialylation *in vitro*. We, therefore, decided to manipulate cell sialylation *in vitro* to determine whether the loss of sialic acid is sufficient to initiate inflammatory responses. Specifically, siRNA was used to inhibit the expression of St6gal1, since this enzyme was downregulated in CIA SFs compared to naïve SFs (Figure 5-2B) and it is the only one responsible for modulating murine α 2-6 sialylated N-glycans, since St6Gal2 is not expressed in murine SFs. siRNA silencing of the expression of St6gal1 was confirmed by RT-qPCR (Figure 5-9A) and this inhibition of St6gal1 function reduced SNA binding to SFs (Figure 5-9B), confirming that loss of St6gal1 leads to a decrease of α 2-6 sialic acid. Assessment of cytokine production showed that SFs produce more IL-6 and CCL2 when St6gal1 was silenced and the secretion of MMP3 also elevated, although this did not reach statistical significance (Figure 5-10A). Notably, silencing ST6gal1 did not affect cell proliferation (Figure 5-10B).

5.2.2.3 Desialylation of SF enhances cell migration.

The increased production of pro-inflammatory cytokines in response to St6Gal1 silencing suggested that loss of α 2-6 sialic acid is sufficient to induce inflammatory pathways. To directly test whether the loss of sialic acid per se is a pathogenic change, we used *Clostridium perfringens* sialidase (CP) to remove sialic acid from cell surface without interfering with cell metabolism. CP is an enzyme that cleaves terminal sialic acid residues. Applied to SFs, CP treatment reduced both α 2-3 and α 2-6 sialic acids as demonstrated by the reduction in binding of MAA and SNA (Figure 5-11A, B). Additionally, CP mediated desialylation was confirmed by the increased PNA binding and unaffected AAL binding (Figure 5-11B) as PNA binds uncapped galactose (and the presence of sialic acid inhibits binding), whereas AAL binds to fucose which is not affected by CP treatment and acts therefore as a technical control. To ensure that sialidase

was free of LPS contamination as it was extracted from bacteria, sialidase was heat inactivated (85°C, 40 minutes), as verified by lectin binding using the ELLA assay (Figure 5-12A). Furthermore, treatment with inactivated CP did not recapitulate the induction of IL-6 and MMP3 expression, whereas heating had no impact on LPS-induced cytokine expression (Figure 5-12B), supporting the idea that the enhanced inflammatory response was induced by the loss of sialic acid.

Many studies have linked sialic acid with cancer cell metastasis and cell migration (Bull et al., 2013, Passaniti and Hart, 1988), which is reminiscent of the enhanced migratory and invasive properties of RASFs. Therefore, we hypothesised that the loss of sialic acid observed in arthritic SFs may modulate their cell migration. To test this hypothesis, cells seeded in migration chambers were CP-treated before performing the migration assay and this showed that migration was significantly enhanced in SFs deprived of sialic acid (Figure 5-13). Importantly, the loss of sialic acid has no effect on cell proliferation (Figure 5-14A) or cellular metabolism (Figure 5-14B).

5.2.2.4 *In vitro* desialylation of SFs triggers rapid pro-inflammatory responses

Having confirmed that exogenous hydrolysis of sialic acid promotes SFs migration as well as that inhibition of St6gal1 expression induces pro-inflammatory cytokine production, our next objective was to investigate whether there are other pathological effects regulated by loss of sialic acid. We, therefore, chose RNA sequencing to analyse the cellular transcriptome changes of SFs after loss of sialic acid. RNA was isolated from control and CP-treated SFs, then subjected to bulk-RNAseq analysis. PCA confirms the two groups exhibit distinct transcriptome profiles (Figure 5-15A), and the differentially expressed genes [$|\log_2(\text{DE fold change})| > 1$, $\text{padj} < 0.01$] are displayed in volcano plots (Figure 5-15B) showing 446 upregulated and 101 downregulated genes in CP-treated SFs compared with control SFs (SFs from naïve mice treated with sialidase dilution buffer). The DE genes were then investigated by KEGG pathway enrichment analysis (Figure 5-16). Strikingly, the pathways enriched with the upregulated genes were all about inflammatory responses, such as the TNF signaling, Rheumatoid arthritis and IL-17 signaling pathways (Figure 5-16A). These results

were consistent with the *St6gal1* silencing experiments and collectively, these data support the idea that SF desialylation triggers inflammation.

To further corroborate these results, 9 upregulated genes involved in arthritic pathogenesis were selected from RNAseq data (Figure 5-17A) and their gene expression in SFs was assessed by RT-qPCR in a set of independent experiments replicating CP-induced desialylation. The selected genes include the pro-inflammatory cytokines (IL-6, CCL2 and IL-1 β), matrix metalloproteinases (MMP3, MMP9 and MMP13), NF- κ B signaling pathway mediators (Myd88 and Nfkbib) and *Tnfsf11*, as it is involved in bone damage. *Tnfrsf11b* was selected as the *Tnfsf11*/*Tnfrsf11b* system regulates bone modelling and remodelling, although differences observed by RNASeq did not achieve statistical significance. In line with RNAseq data, cytokines (Figure 5-17B), MMPs (Figure 5-17C), Myd88 and Nfknib (Figure 5-17D) were upregulated, confirming that loss of sialic acid enhances cellular inflammation and matrix degradation. Likewise, the ratio of *Tnfsf11* and *Tnfrsf11b* was upregulated (Figure 5-17E), suggesting that desialylated SFs promote osteoclast formation.

Taken together, the results presented in this chapter so far suggest that loss of sialic acid transforms SFs into a pathogenic phenotype similar to that of arthritic cells, displaying enhanced migration and production of immunomodulatory factors. The upregulation of cytokines, chemokines and other immunomodulatory factors, as well as activated MyD88 signalling, are reminiscent of IL-1 β stimulation. The role of IL-1 β in the progression of RA has been well studied (Adachi et al., 2013, Pasi et al., 2015). To better illustrate the pathogenic effects triggered by hyposialylation, we compared the transcriptome changes in SFs following desialylation with those upon IL-1 β stimulation. Specifically, transcriptomic changes were compared between two data sets in naïve SFs: IL-1 β versus naïve (untreated) and CP versus non-treated control (sialidase buffer treated). There were 269 upregulated genes and 159 downregulated genes in IL-1 β treated SFs, whereas 446 upregulated genes and 101 downregulated genes in CP treated SFs (Figure 5-18A). In total 21.3% overlapping genes of which 17.2% were upregulated and 3.5% were downregulated (Figure 5-18B).

To study the roles of both the common and unique genes in the two data sets, genes were subjected to Metascape signaling analysis and protein-protein interaction analysis. Cytokines (such as IL-6, CCL2), chemokines (like Cxcl1, Cxcl5), MMPs (MMP3, MMP9) and CAMs (Vcam1, Icam1) were included in the common genes (Figure 5-19B) and displayed enrichment of the TNF signaling pathway, cytokine-cytokine receptor interaction and NF- κ B signaling pathways (Figure 5-19C). Apart from the common genes which exhibit an inflammatory signature, there were 380 unique genes only regulated in CP vs NT data set. Among these unique DE genes, inflammatory pathways, like TNF signaling pathway, cytokines-cytokine receptor interaction, NF- κ B signaling pathway were again enriched (Figure 5-20D). However, these inflammatory pathways were not enriched in the genes unique to IL-1 β stimulation (Figure 5-20B), suggesting that sialidase treatment induces more inflammation-related genes compared to IL-1 β treatment.

Of note, St6gal1 was significantly downregulated, whereas St3gal3 was significantly upregulated upon desialylation (Figure 5-21A) and the regulated genes were validated by RT-qPCR (Figure 5-21B). As St6gal1 catalyses the addition of α 2,6-linked sialic acids and St3gal3 catalyses the addition of α 2,3-linked sialic acids to terminal glycans, the decrease in St6gal1 and the increase in St3gal3 may indicate a slow recovery of α 2,6 sialylation and a fast recovery of α 2-3 sialylation.

To confirm that sialyltransferases expression affects sialic acid reconstitution, SFs were cultured 24 hours after CP treatment and lectin binding (SNA, MAA-II, AAL and PNA) were examined by flow cytometry. The results of lectin binding experiments showed a reduced α 2,6 sialylation rebuilding upon CP-treatment, as evidenced by decreased SNA-binding and increased PNA binding (Figure 5-21C). whereas α 2-3 sialylation was quickly recovered as MAA-II binding was the same as control (Figure 5-21C). These data suggest that the regulation of sialyltransferases induced by exogenous desialylation may create positive feedback *in vivo* to consolidate sialic acid-mediated inflammatory networks.

5.3 Discussion

Sialylation is involved in multiple biological processes, including cell motility, inflammation and signaling (Cabral et al., 2013, Hanasaki et al., 1995, Hanasaki et al., 1994, Wang et al., 2019). In this chapter, reduced α 2-6 sialylation was observed in SFs from arthritic mice compared with naïve mice. The regulation of sialyltransferases under proinflammatory microenvironment was investigated, showing that TNF α downregulates St6gal1 expression in SFs. Furthermore, we report that SFs undertake a pathogenic phenotype upon removal of surface sialic acid, inducing signaling pathways that highly overlap with those induced upon IL-1 β stimulation. However, sialic acid removal triggers more inflammatory genes and genes related to cell migration than IL-1 β stimulation. In any case, although many studies have revealed that altered sialylation is associated with cell invasiveness and immune response (Laubli and Borsig, 2019, Hanasaki et al., 1995, Wang et al., 2019, Pally et al., 2021), this is the first-time that sialic acid is linked with fibroblast biology, using both transcriptomics and MS based glycomics.

Sialic acids are widely distributed and abundant on the surface of mammalian cells. Reflecting their important role in cell and tissue homeostasis, aberrant glycosylation is a common feature and biomarker of cancer. In fact, SFs have been shown to exhibit tumour-like characteristics in patients with RA, where they exhibit destructive and aggressive features reminiscent of those observed in localised tumours (Liu et al., 2018). Particular changes in glycan biosynthesis have been described in cancer, specifically, downregulation of α 2-3 STs inhibit pancreatic ductal adenocarcinoma migration (Guerrero et al., 2020a), while inhibition of St6gal1 enhances breast cancer invasiveness (Pally et al., 2021), suggesting desialylation enhances cell migration due to the loss of α 2-6, not α 2-3, linked sialic acid. Besides, St6gal1 expression correlates with prostate cancer cell proliferation (Wei et al., 2016), but neither knockdown of St6gal1, nor sialidase treatment affected SF proliferation, suggesting that ST6gal1 regulation of cell proliferation may be restricted to specific cell types.

Apart from cell motility, desialylation triggered SF inflammatory responses, as reflected by their increased expression of cytokines, MMPs and chemokines, suggesting that sialylation participates in maintaining tissue homeostasis and

regulating inflammatory pathways in the joint cavity. In line with this, desialylated monocytes exhibit activated ERK1/2 MAPK signaling and associated increases in the production of proinflammatory mediators, such as IL-6, IL-1 β and MMP3 (Stamatos et al., 2004). Likewise, multiple signaling pathways were enriched when surface sialic acids of SFs were enzymatically removed (Figure 5-16A). Identification of the role of these enriched pathways may further contribute to the understanding of the molecular mechanisms used by sialic acid to modulate SF-dependent inflammatory responses.

Invasion and spread of SFs play a critical role in the development of polyarticular involvement and bone-damaging arthritis. Multiple pathways are involved in the development of elevated cellular local invasion and long-distance migration, but the specific proteins affected by desialylation have not been explored in this thesis. Changes in cell migration following desialylation are likely to be related to cell adhesion molecules, as α 2-6 linked sialic acid is expressed by adhesion molecules, such as ICAM-1 and VCAM-1, that are up-regulated by inflammatory cytokines (Hanasaki et al., 1994). Indeed, the RNAseq data show that enzymatic removal of sialic acid upregulates ICAM-1 and VCAM-1 expression (Figure 5-19B), findings that coincide with the increased migratory potential of SFs treated with sialidase (Figure 5-13B).

Intriguingly, the downregulation of ST6gal1 mRNA was restricted to the CD90+ sub-lining SFs, suggesting that sialic acid might play distinct roles among SF subsets. The microenvironment can be one factor affecting this as CD34- SFs, one phenotype of sub-lining SFs, are responsible for mediating inflammation (Croft et al., 2019), findings consistent with sialic acid downregulation being due to local increases in TNF α . Further sialic acid studies on the subsets of sub-lining SFs may therefore give better insight into linking ST6gal1 expression with SF biology. In addition, understanding the regulation of STs and sialic acid *in vivo* may help to understand the mechanisms underpinning initiation and progression of RA. Apart from the proinflammatory cytokines, such as TNF α , endogenous sialidase is another factor to consider. Other reports have shown that the activity of endogenous sialidases is elevated in activated immune cells, which trigger signaling pathways related to cell apoptosis and differentiation (Gee et al., 2003, Cross and Wright, 1991, Landolfi et al., 2004). Moreover,

environmental factors may contribute to the hyposialylation of SFs. For example, smoking reduces St6gal1 expression and α 2-6 sialylation leading to the increase of IL-6 secretion in bronchial epithelial cells (Krick et al., 2021), coinciding with the effect of desialylation observed in SFs (Figure 5-17). In fact, smoking is a risk factor for rheumatoid arthritis as smokers are at greater risk of developing rheumatoid arthritis, and one possible mechanism by which smoking causes RA is the formation of anti-citrullinated protein antibodies (ACPA) (Hedström et al., 2018). Strikingly, in humans and mouse models of arthritis, RA-associated IgG antibodies (including APAC) exhibited reduced sialylation, and artificially sialylation of APAC not only reduced arthritogenicity but also slowed arthritis progression in CIA mouse model (Ohmi et al., 2016). Altered sialylation might be a mechanism by which smoking triggers RA.

By contrast to autoimmune diseases, some cancers are associated with an insufficient immune response and their subsequent escape from immune surveillance. Interestingly, therefore, increased ST6gal1 is typically correlated with high tumour grades, metastasis, and poor prognosis in patients (Wei et al., 2016, Recchi et al., 1998). This may be explained by increased sialylation, which could reduce inflammatory activities, like cytokine release and leukocyte recruitment. Perhaps reflecting this, loss of sialic acid is a pathogenic phenotype in RA, perhaps showing two sides of the same coin in controlling inflammation. Potentially, sialylation status may be able to be used as a disease diagnosis. For example, a study about epithelial ovarian cancer (EOC), whose initiation and progression are associated with chronic inflammation, showed an increased ratio of α 2-3-linked to α 2-6-linked sialic acid in early and late stage EOC patients compared to age-matched health controls (Dedova et al., 2019). Establishing an α -2,3/ α -2,6-linked sialic acid ratio system may thus help in the early diagnosis of EOC and may also be applicable to the diagnosis of arthritis at early stage.

Overall, the results demonstrated that sialic acid regulates inflammatory responses and cell motility of SFs, with loss of sialic acid triggering SF migration and proinflammatory cytokine secretion. Nevertheless, the mechanisms mediating hypo-sialylation in sub-lining SFs and the underlying mechanisms of the signalling by which desialylation mediates the inflammatory response in SFs remain unclear. However, it is promising from a therapeutic context that the sialic acid linkage of N-glycans of SFs plays key roles in the pathogenesis of RA.

A

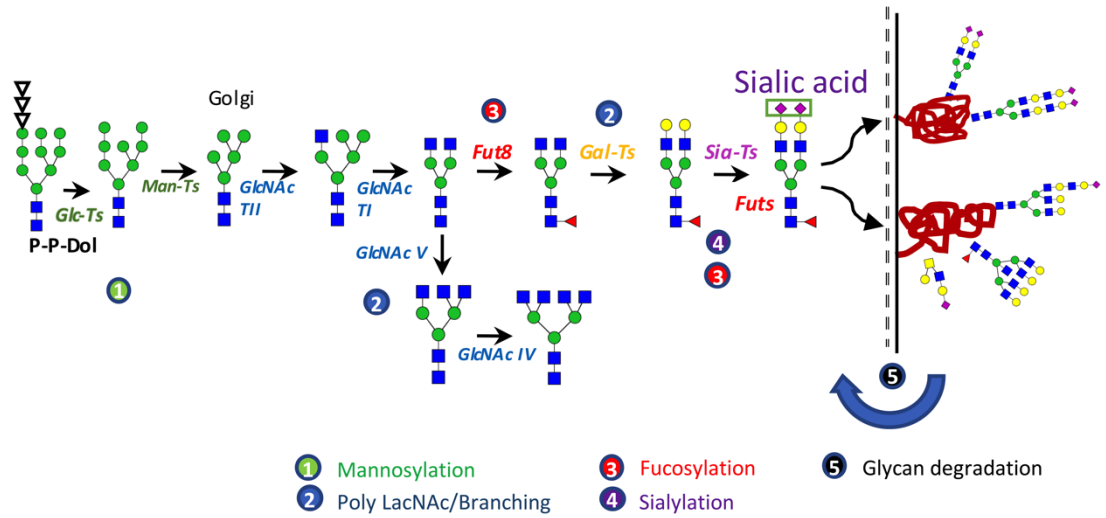


Figure 5-1 Overview of potential glycan biosynthesis profile.

Diagram of N-glycan biosynthesis pathways. (1) Mannosylation. (2) Poly LacNAc/Branching. (3) Fucosylation. (4) Sialylation. (5) Glycan degradation.

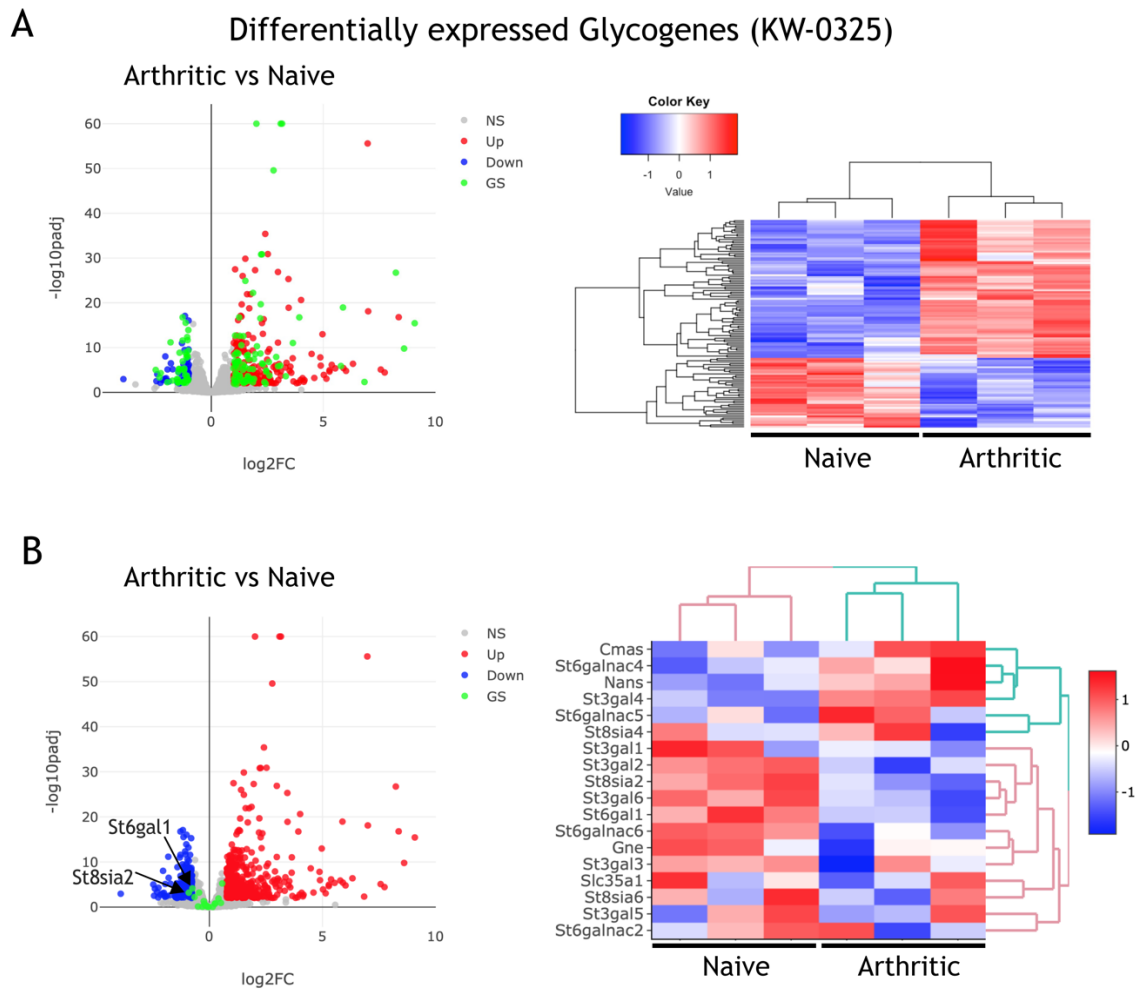


Figure 5-2 Synovial fibroblasts from arthritic mice exhibit a distinct glycogenes transcriptomic profile.

As shown in **Figure 3-2A-C**, RNA was isolated from fresh isolated SFs of 3 naïve and 3 CIA mice (score at 9, 10 and 11 respectively) and subjected to RNAseq analysis. Genes that passed a threshold of $\text{padj} < 0.01$ and $|\log_2(\text{foldChange})| > 1$ were considered as differentially expressed. Colour code, red: upregulated, blue: downregulated, in arthritic SFs. (A) All detected genes were plotted in a volcano plot, with differentially expressed glycoprotein genes (Uniprot KW-0325) highlighted in green. Differentially expressed glycoprotein genes (green) were plotted in a heatmap. (B) The distribution of sialyltransferases was highlighted in the volcano plot in green. The arrows pointed to two significantly differentially expressed genes, *St6gal1* and *St8sia2*. The expression of all sialyltransferases was plotted in a heatmap.

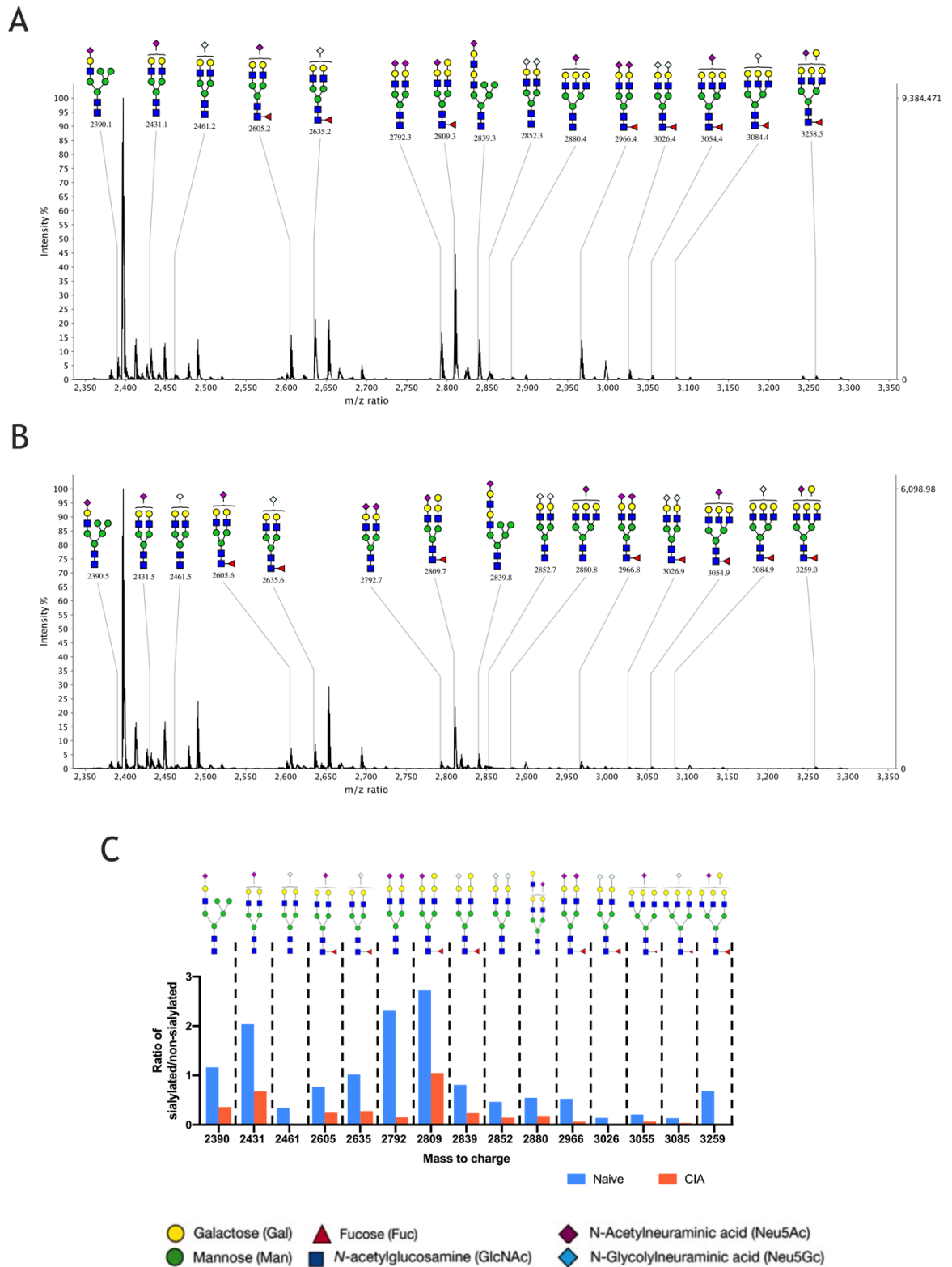


Figure 5-3 N-linked sialylated glycans were reduced in expanded murine arthritic SFs.

MALDI-TOF MS spectra of permethylated sialic acid N-glycans from naïve SFs (A) and arthritic SFs (B) cultured and expanded *in vitro*. (C) Histograms of relative signal intensity of different N-glycan with sialic acid from naïve SFs and arthritic SFs. Data are representative of 1 experiment.

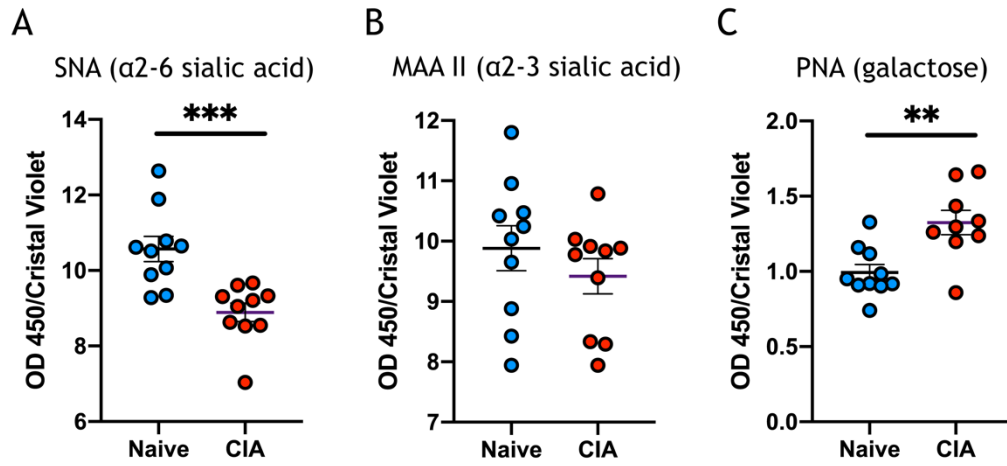


Figure 5-4 α2-6 sialylation is reduced in arthritic SFs.

SFs extracted from naïve and CIA mice were cultured and expanded *ex vivo*. (A) SNA, (B) MAA II and (C) PNA lectins were used to evaluate the presence of α2-6 sialic acid, α2-3 sialic acid and galactose respectively using enzyme-linked lectin assay (ELLA), data are from 10 biological replicates from 3 independent experiments. Lectins staining was normalised with cell number, ** $p < 0.01$, *** $p < 0.001$ by the Mann-Whitney test.

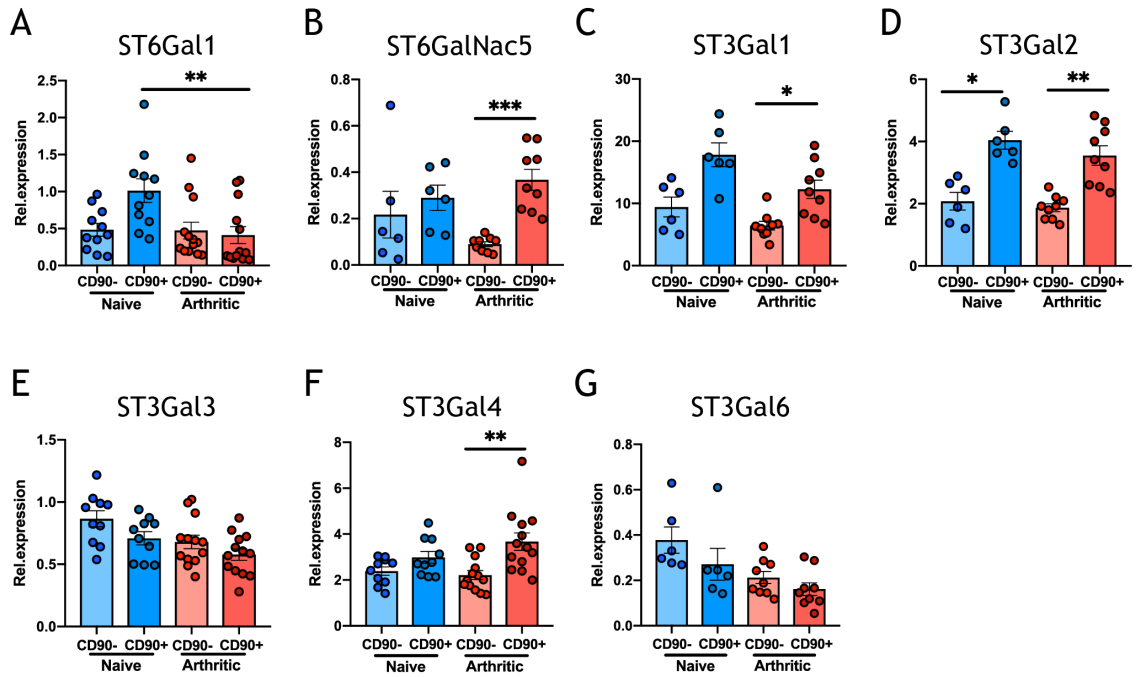


Figure 5-5 Sialyltransferases are modulated in inflammatory SFs.

Synovial fibroblasts from naive and CIA mice were isolated as shown in **Figure 3-5A**. Relative expression of (A) St6gal1, (B) St6GalNac5, (C) St3gal1, (D) St3gal2, (E) St3gal3, (F) St3gal4 and (G) St3gal6 in SF subsets were quantified by RT-qPCR. Data are represented as mean \pm SEM ($n \geq 10$); each dot represents SFs from one individual mouse. * $p < 0.05$, ** $p < 0.01$, *** $p < 0.001$ by Kruskal-Wallis test.

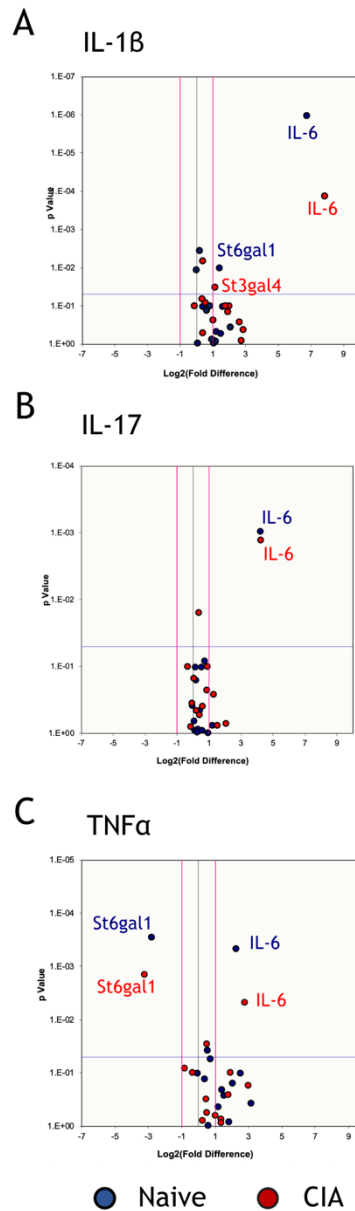
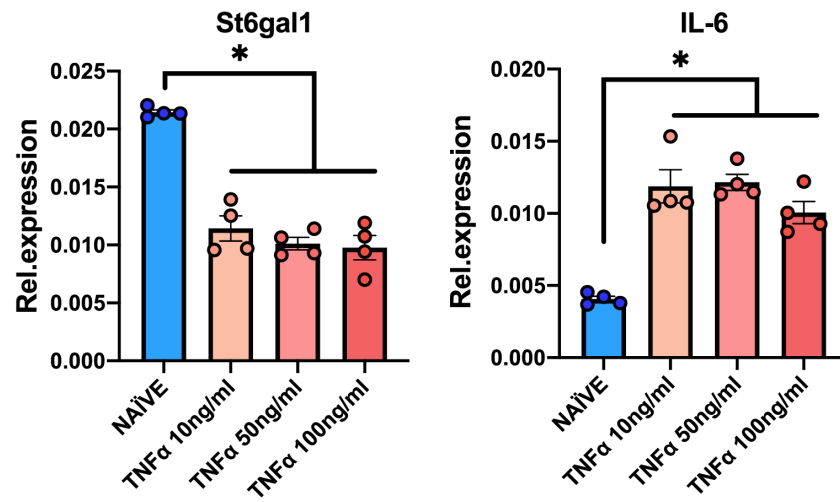


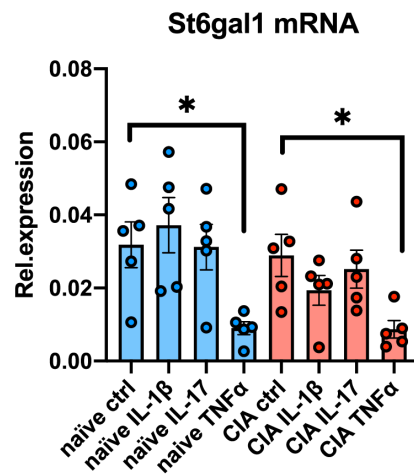
Figure 5-6 TNF α inhibits St6gal1 expression.

Synovial fibroblasts extracted from naïve and CIA mice were expanded *in vitro*. Cells were stimulated with IL-1 β (A), IL-17 (B) and TNF α (C) (10 ng/ml) for 6 hours and RNA was extracted. The expression of enzymes involved in the biosynthesis and transportation of sialic acid was evaluated by RT-qPCR using Sybr green probes. IL-6 was included as positive control for cytokine stimulation. Volcano plots show the log2foldchange (x-axis) in each gene expression between the samples versus its p-value (y-axis). The pink lines indicate two foldchange in gene expression and the blue line indicates the p=0.05 threshold for assessing statistical significance by t-test. Data are representative of three independent experiments. Color code: naïve SFs in blue, CIA SFs in red.

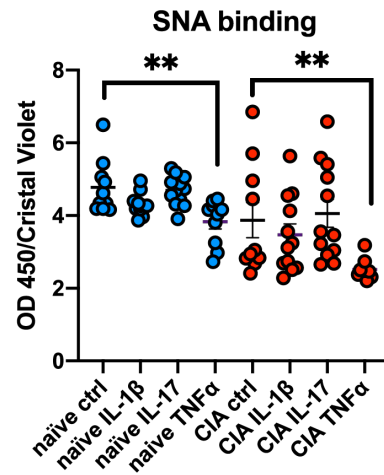
A



B



C



D

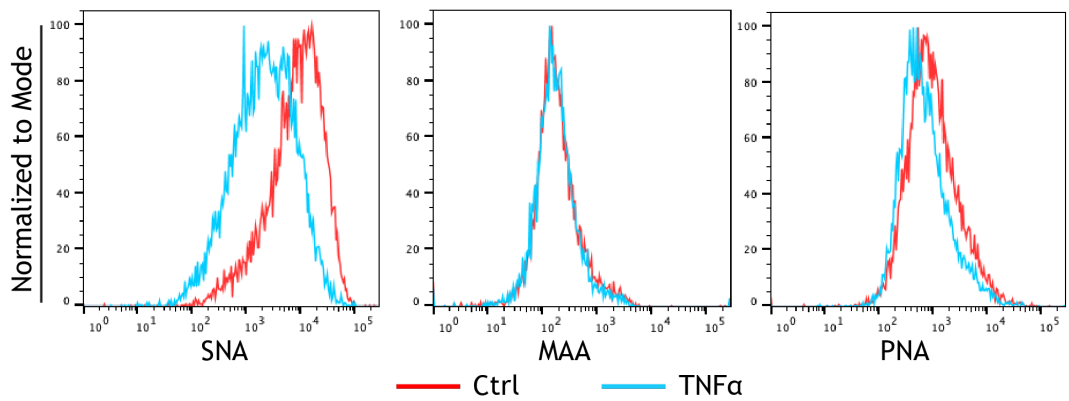


Figure 5-7 TNF α inhibits St6gal1 expression further downregulates α 2-6 sialylation in SFs.

SFs were extracted from naïve mice and expanded *in vitro*. (A) The mRNA levels of St6Gal1 and IL-6 in naïve SFs treated with increased concentration of TNF α for 6 hours were evaluated by RT-qPCR. Each dot represents one independent experiment, data were presented as mean \pm SEM (n=4). *p<0.05 by the Mann-Whitney test. (B) The mRNA levels of St6gal1 in naïve and CIA SFs following 10 ng/ml IL-1 β , IL-17 and TNF α stimulation for 6 hours were evaluated by RT-qPCR. Each dot represents one independent experiment, data are presented as mean \pm SEM (n \geq 3). *p<0.05 by the Mann-Whitney test. (C) SNA binding was calculated by ELLA assay to evaluate the presence of α 2-6 sialic acid in naïve and CIA SFs treated with 10ng/ml IL-1 β , IL-17 and TNF α for 48 hours. Data were from 3 (naïve) and 2 (CIA) independent experiments. **p<0.01 by the Mann-Whitney test. (D) Naïve SFs were treated with TNF α for 48 hours, then subjected to flow cytometry to detect the expression of SNA, MAA and PNA, data are representative of 1 experiment.

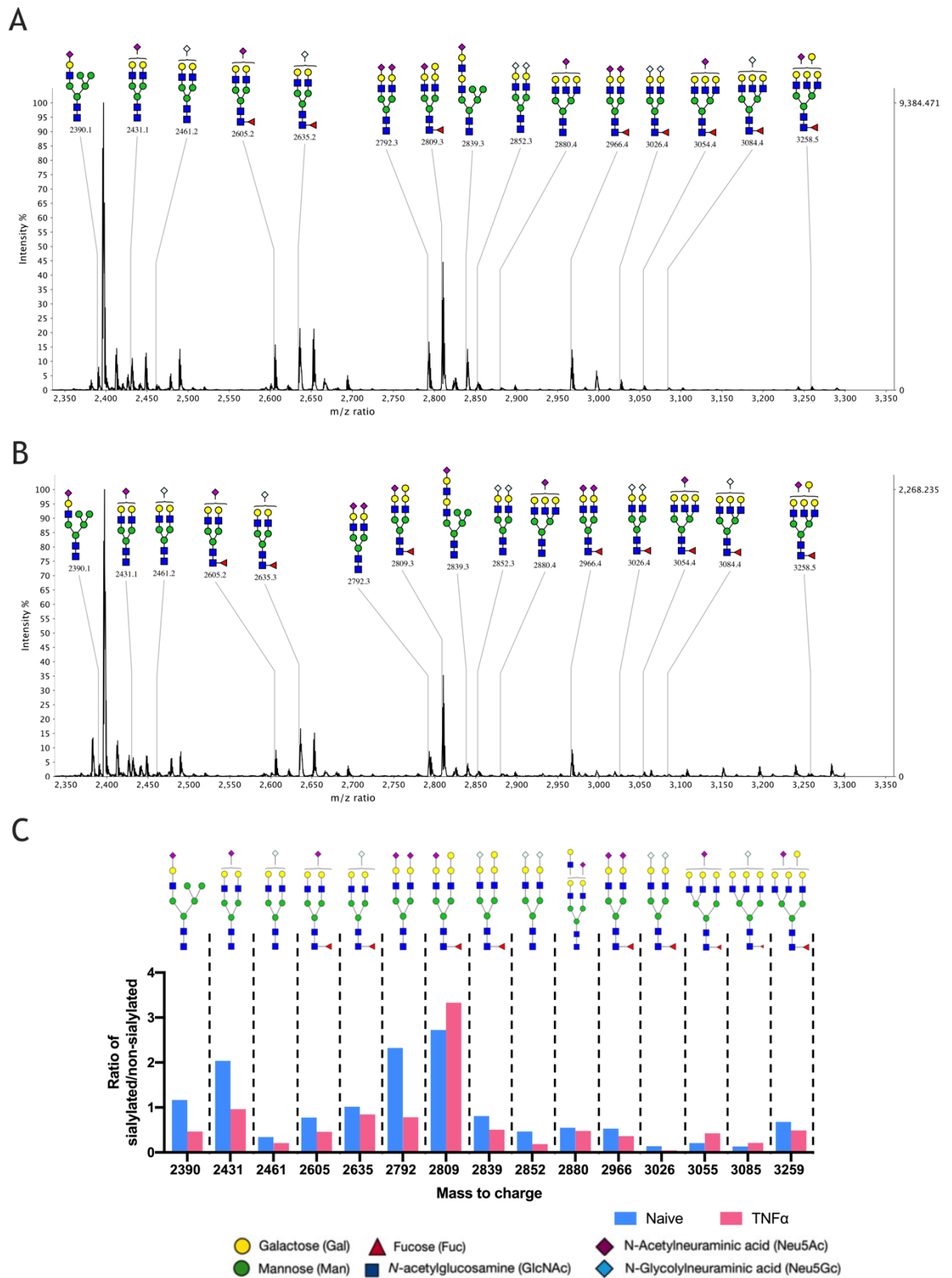


Figure 5-8 TNF α reduces sialylated N-glycans in SFs.

MALDI-TOF MS spectra of permethylated sialic acid N-glycans from naive SFs (A) and naive SFs treated with 10 ng/ml TNF α for 48 hours (B). (C) The relative signal intensity of sialylated N-glycans, calculated as twin structures of sialylated/non-sialylated ($n=1$). Color code: naive in blue, TNF α treated in pink. Data are representative of 1 experiment.

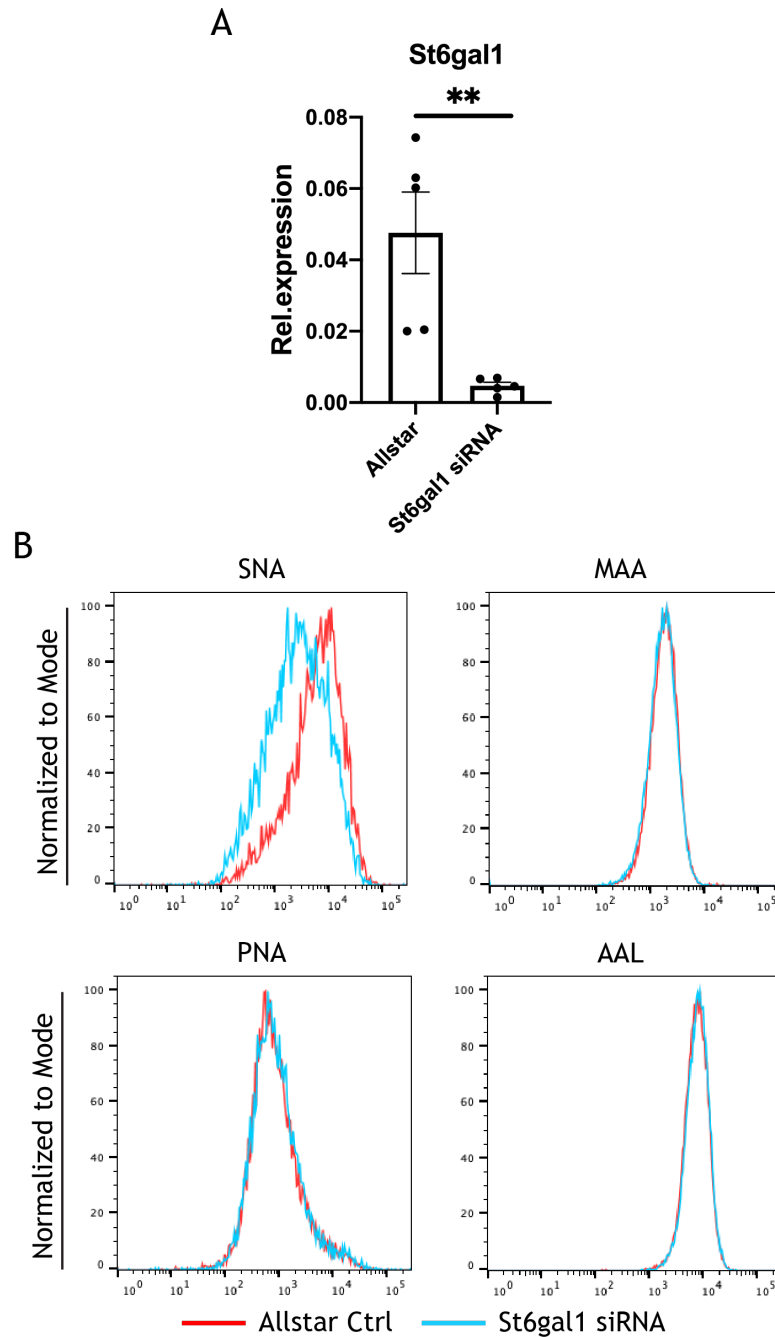
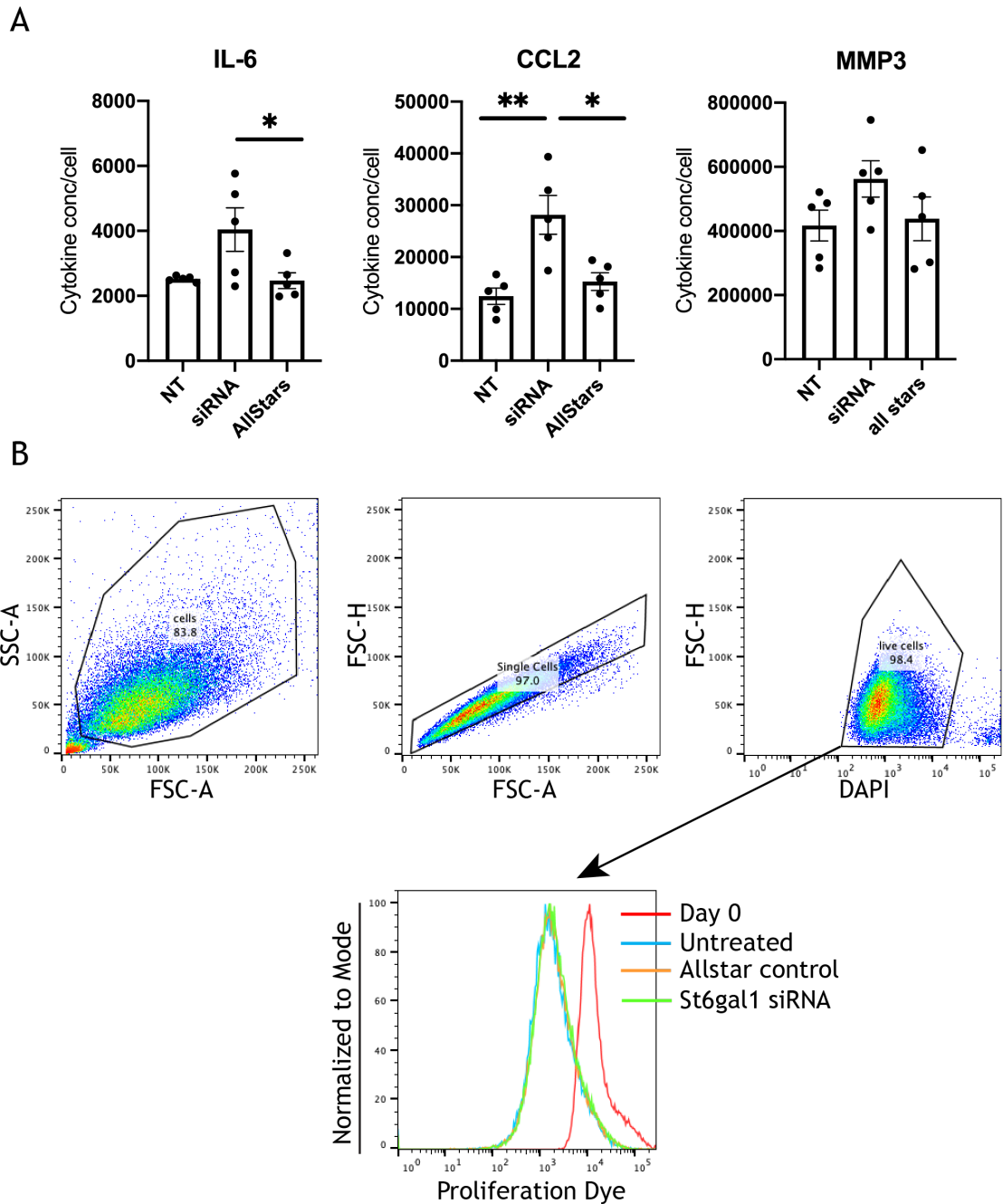


Figure 5-9 Inhibition of St6gal1 enhances cytokine secretion.

SFs were extracted from naïve mice and expanded *in vitro*. Cells were transfected with either St6gal1 or control (Allstars) siRNA. (A) RNA was extracted and the relative expression of St6gal1 was evaluated by RT-qPCR. Each dot represents one independent experiment, data are shown as mean \pm SEM (n=5). **p<0.01 by the Mann-Whitney test. (B) The presence of sialic acids on control and St6gal1 siRNA treated naïve SFs was examined by flow cytometry for the binding of SNA, MAA, PNA and AAL lectins, data are representative of 1 experiment.



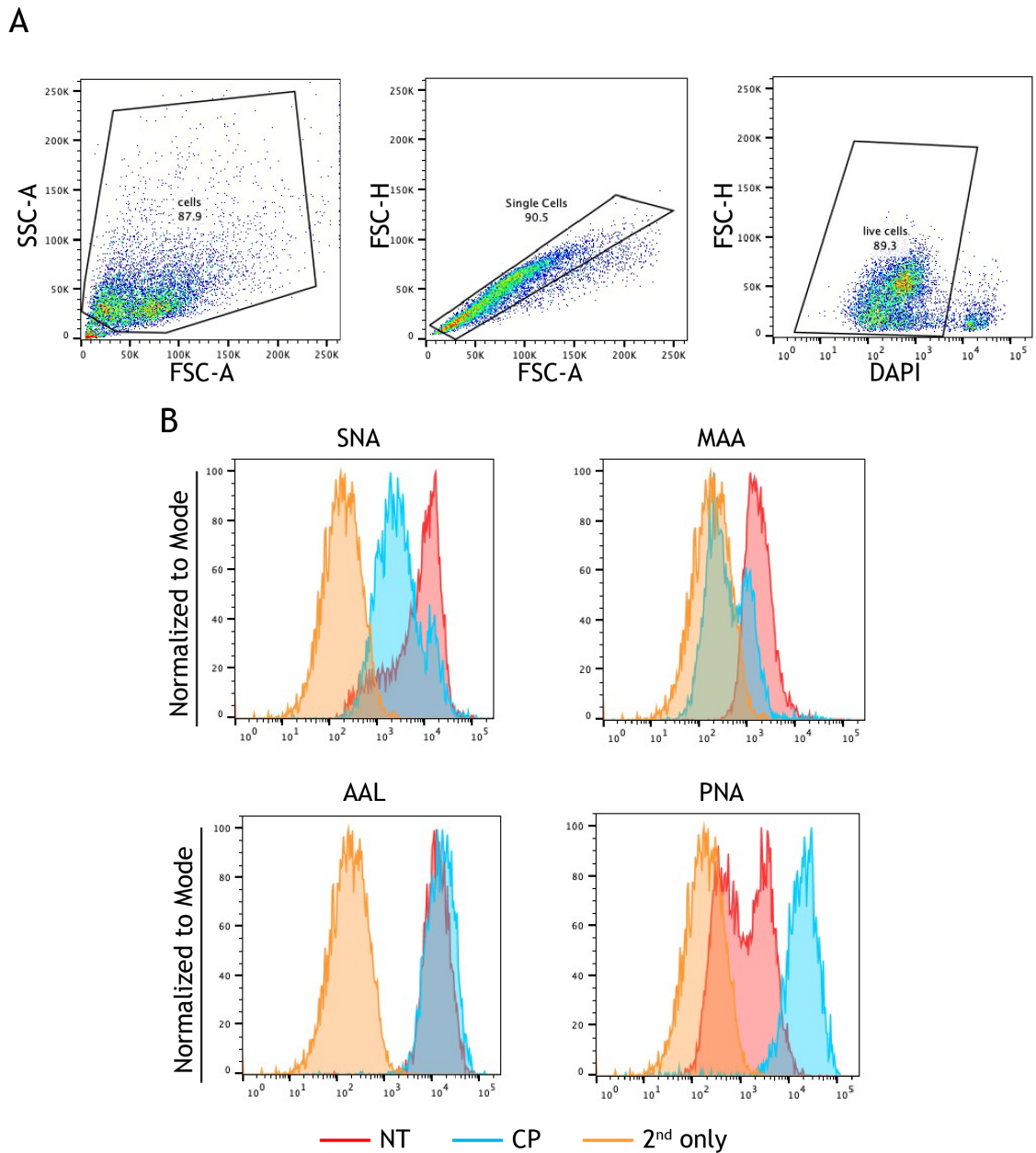


Figure 5-11 C. perfringens sialidase cleaves α 2-6 and α 2-3 sialic acid from cell surface.

SFs extracted from naïve mice were cultured and expanded *in vitro*. Cells were treated with 0.1 U/ml of *C. perfringens* sialidase (CP) for 1 hour to remove sialic acid from the cell surface. Control cells were treated with sialidase buffer for the same time. Control and sialidase-treated cells were stained with biotinylated lectins (SNA, MAA, PNA and AAL), followed by incubating with streptavidin Alexa Flour-647 prior to being analysed by flow cytometry (A), lectins binding was visualized by the histogram (B). Data are representative of 1 experiment.

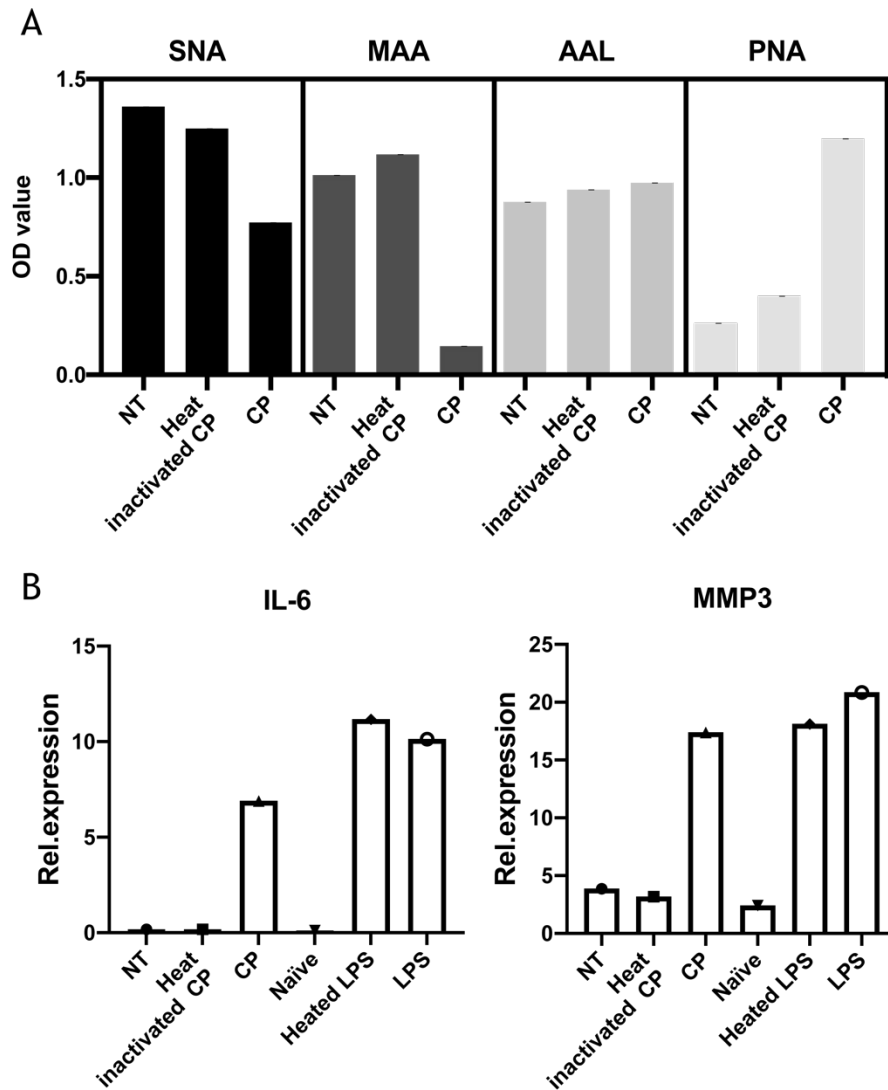


Figure 5-12 Heat inactivates sialidase.

(A) SNA, MAA, PNA and AAL binding on control, heat-inactivated CP (sialidase from *Clostridium perfringens*) (85 °C for 40min), and CP treated naïve SFs by ELLA assay. (B) Relative expression of IL-6 and MMP3 in naïve SFs treated with heat-inactivated CP, CP, heated LPS and LPS was assessed by RT-qPCR. Data are representative of 1 experiment.

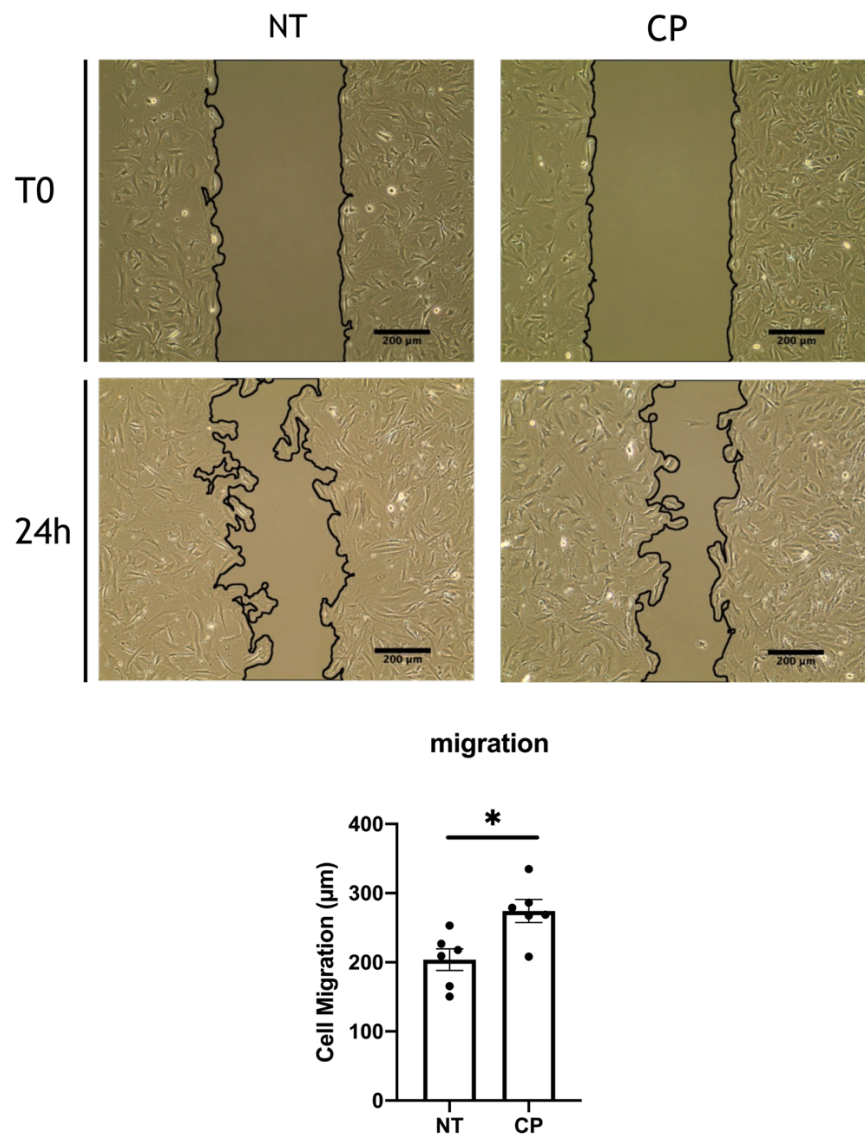


Figure 5-13 Desialylation enhances SF migration.

SFs were seeded in migration chambers and grown until monolayer confluence. Cells were then treated with *C. perfringens* (CP), and inserts were removed to conduct migration assays. The images represent one representative experiment, superimposed black lines define the cell-free area, scale bar: 200 μm. (B) Bar chart shows the mean of cell migration distance \pm SEM (n=5), each dot represents a biological replicate. *p < 0.05 by the Mann-Whitney test.

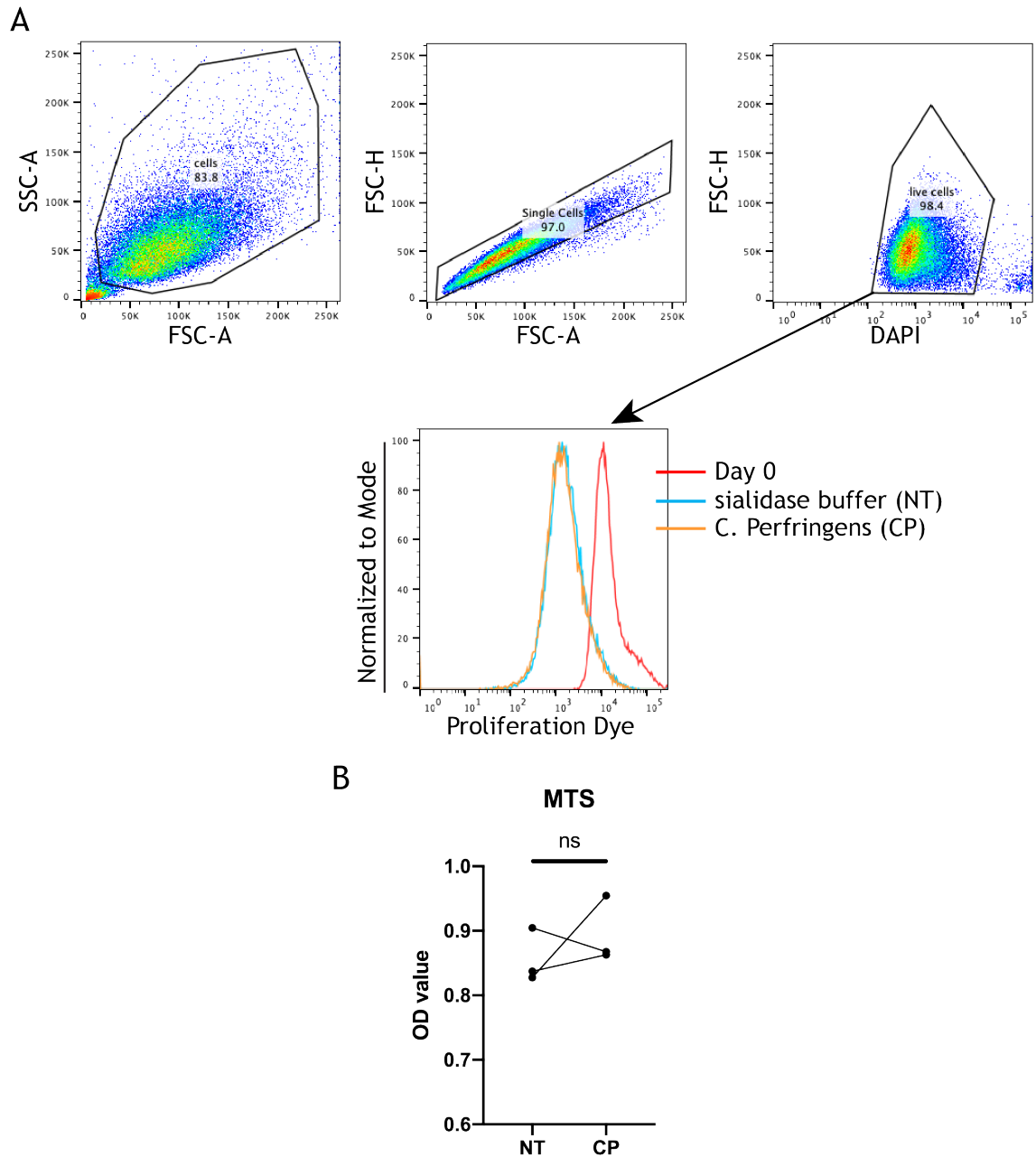


Figure 5-14 Desialylation does not affect SF proliferation and metabolism.

(A) SFs were stained with proliferation dye eFluor 670 and analysed by flow cytometry (Day0) or treated with 0.1 U/ml of *C. perfringens* sialidase for 1 hour and maintained in culture for 5 days (Day5), Data are representative of 1 experiment. (B) naïve SFs were seeded in 96-well plates, cultured to 90% confluence and then treated with 0.1 U/ml of *C. perfringens* for 1 hour, followed by MTS assays to check cell viability and metabolome activity. Data are representative of 3 independent experiments. ns: non-significant, by the Mann-Whitney test.

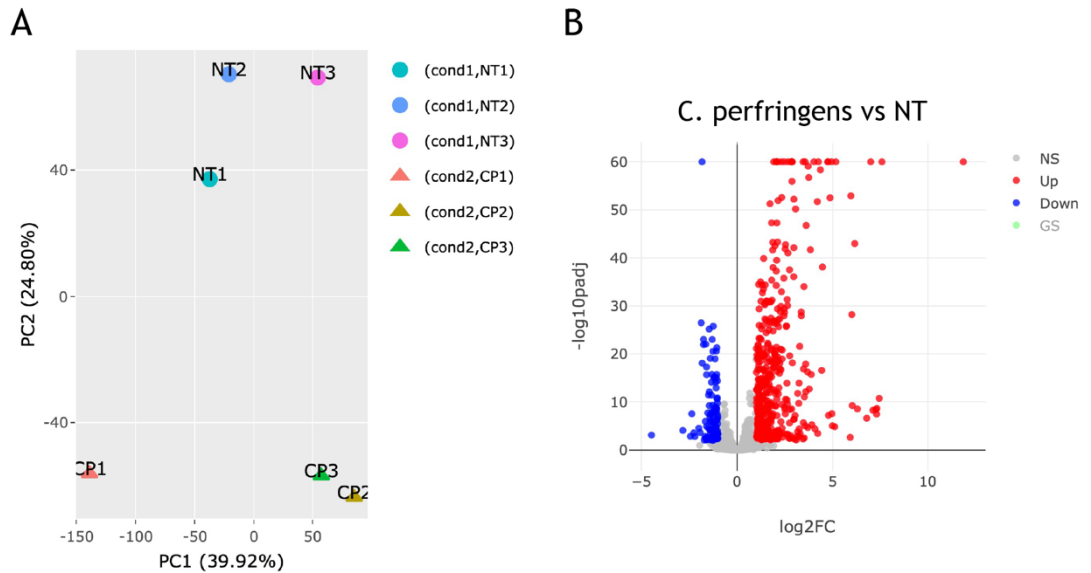


Figure 5-15 Transcriptomic profile of desialylated SFs.

SFs extracted from naïve mice were cultured and expanded *in vitro*. RNA was isolated from control (NT) and *C. perfringens* sialidase treated (CP) SFs and subjected to bulk RNA-seq (n=3). (A) Principal component analysis (PCA). (B) Volcano blot of all detected genes. Differentially expressed genes are defined as $\text{padj} < 0.01$ and $|\log_2 \text{FoldChange}| > 1$. Colour code, red: upregulated, blue: downregulated, in CP treatment.

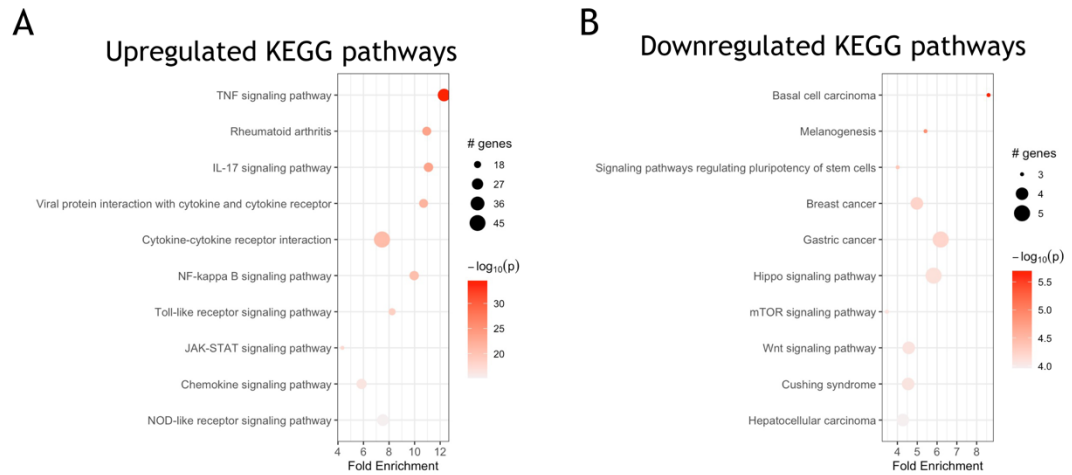


Figure 5-16 Transcriptomic profile of desialylated SFs.

Differentially expressed genes detected in **Figure 5-15B** were used to perform KEGG pathway enrichment using the PathfindR package. Enriched pathways for upregulated genes (A) and downregulated genes (B) were plotted in bubble chart with fold enrichment on the x-axis and $-\log_{10}$ p-value on the coloured scale. The size of bubble is proportional to the number of Differentially expressed genes in the given pathway.

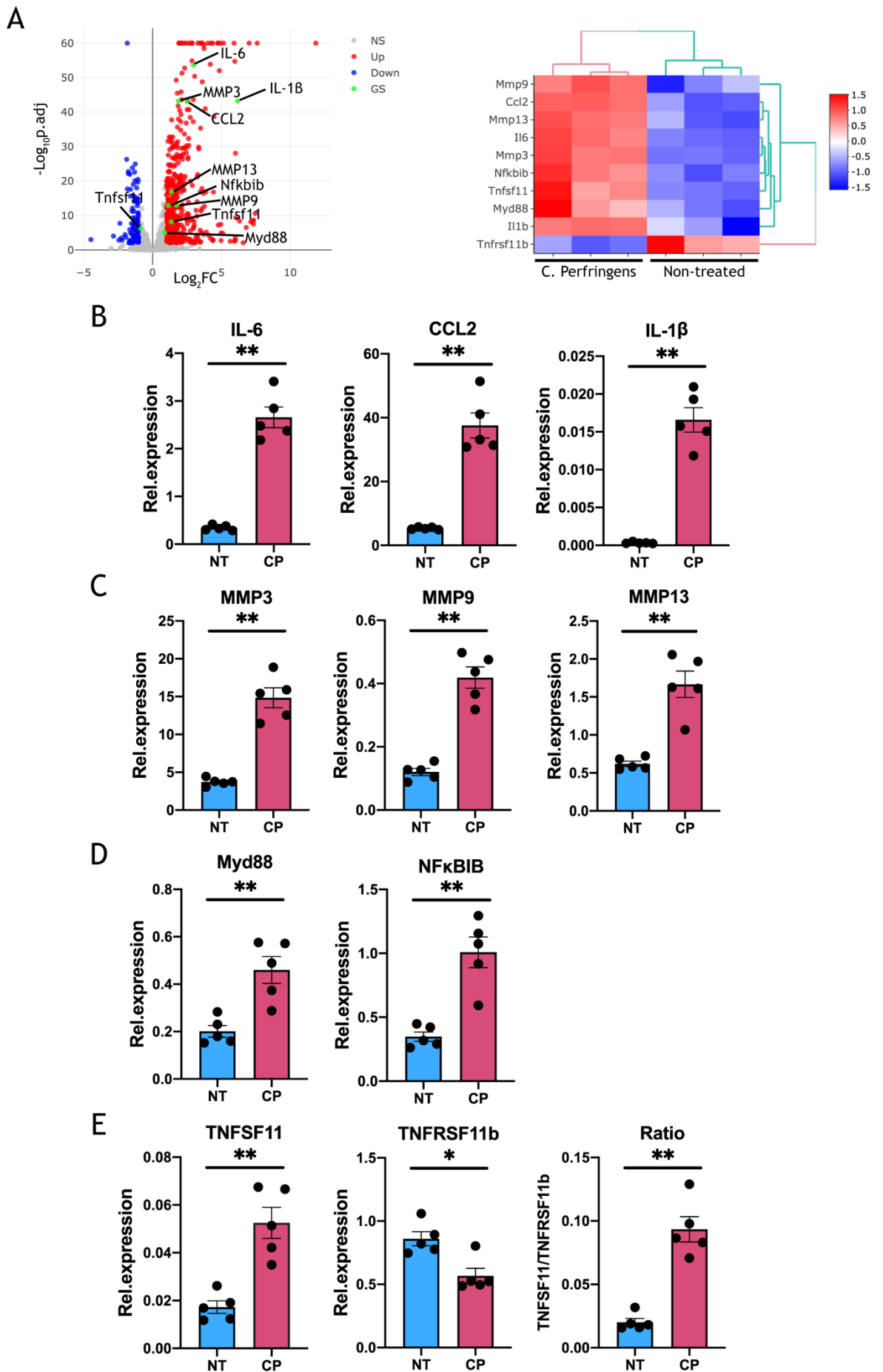


Figure 5-17 Desialylation enhances the inflammatory response of SFs.

(A) Gene expression detected in **Figure 5-15B** for IL-6, CCL2, MMP3, MMP9, MMP13, Tnfsf11, Tfrsf11b, IL-1 β , Myd88 and NF κ B1B. (B) RNA was isolated from control and *C. perfringens* sialidase treated naïve SFs. The relative expression of genes in (A) was evaluated by RT-qPCR. (B) IL-6, CCL2 and IL-1 β . (C) MMP3, MMP9 and MMP13. (D) Myd88 and Nfkb1b. (E) Tnfsf11 and Tfrsf11. For B-E, each dot represents one independent experiment, error bars represent SEM (n=5), *p<0.05, **p<0.01 by the Mann-Whitney test.

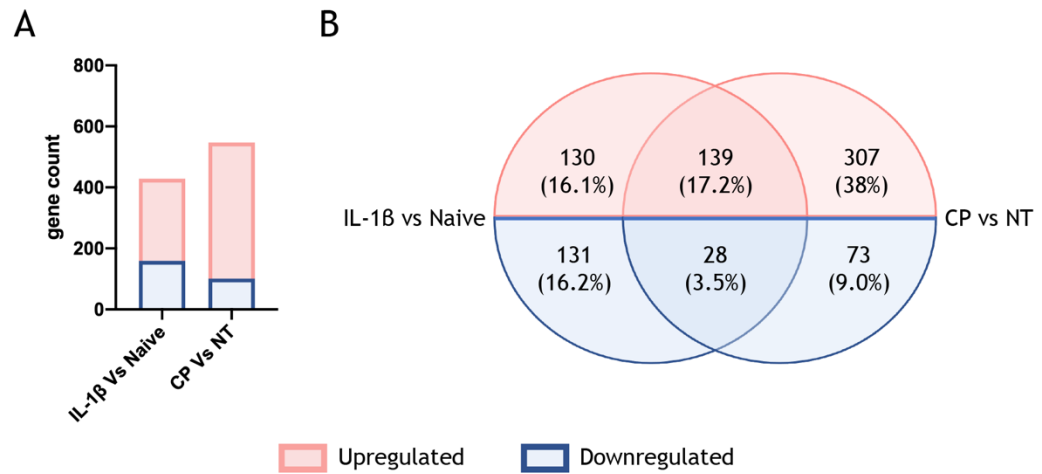


Figure 5-18 Comparison of the transcriptomic profile of desialylated and IL-1 β -stimulated naïve SFs.

Bulk-RNAseq was performed to identify differentially expressed genes ($p_{adj} < 00.1$ and $|\log_2\text{foldchange}| > 1$) in i) naïve and IL-1 β stimulated SFs, and ii) non-treated (NT) and C. perfringens-treated (CP) naïve SFs. (A) Bar chart shows the upregulated and downregulated gene numbers in IL-1 β vs naïve and CP vs NT comparisons. (B) Venn shows the number of common and unique up- and down-regulated differentially expressed genes identified in IL-1 β vs naïve and CP vs NT comparisons. Color code: upregulated in pink; downregulated in blue.

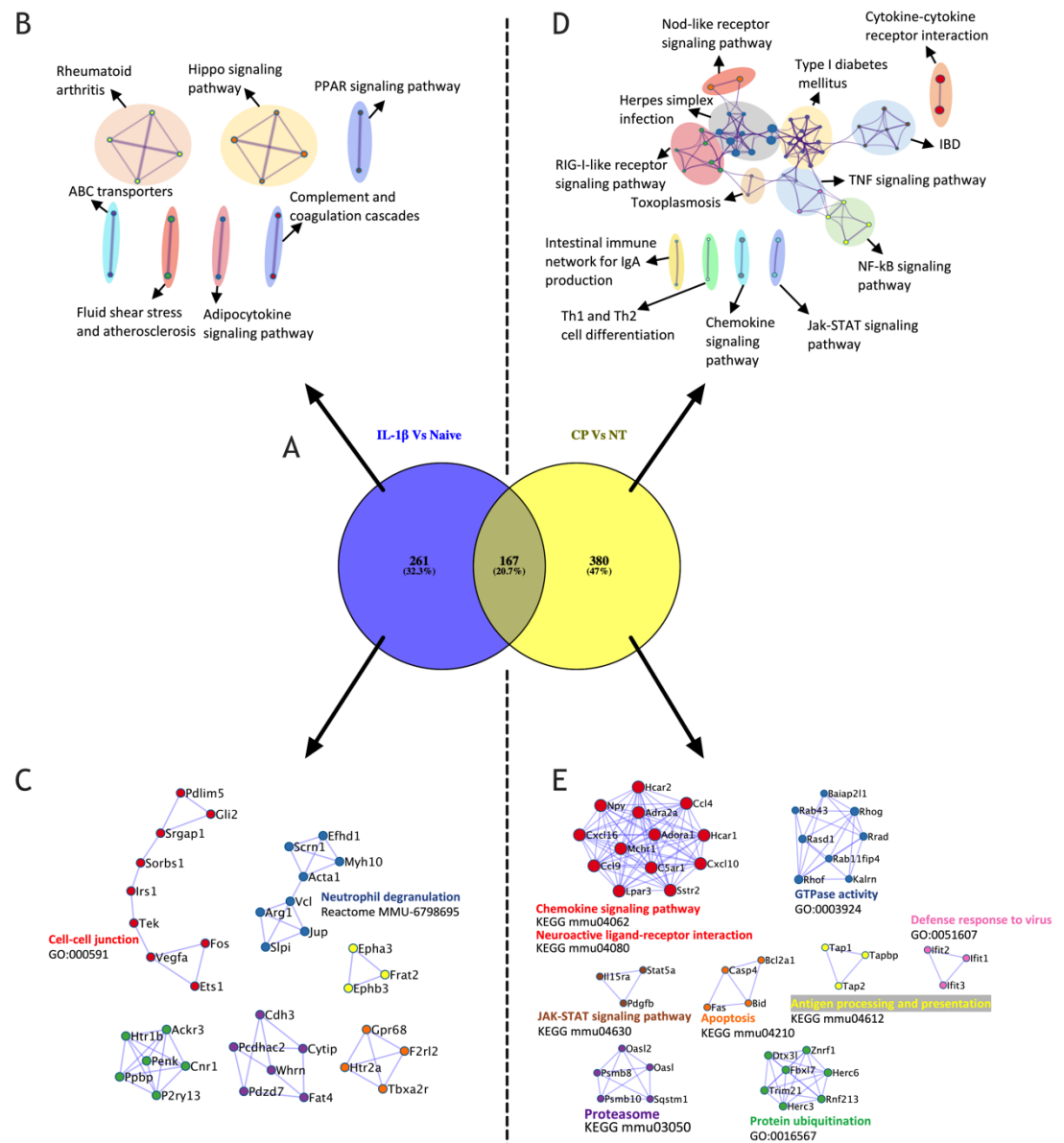
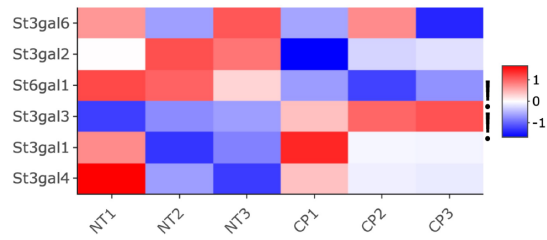


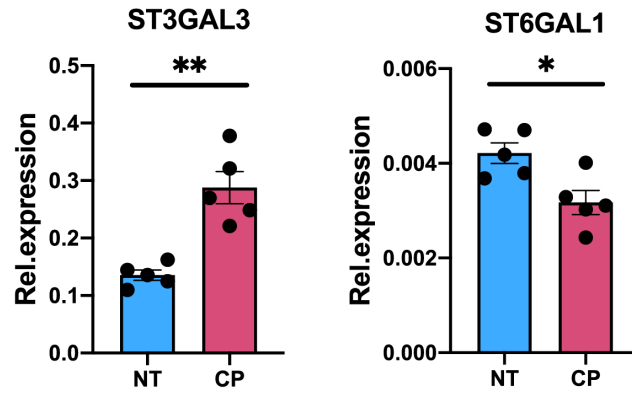
Figure 5-20 Comparison of the transcriptomic profile of desialylated and IL-1 β -stimulated naïve SFs.

(A) Venn shows the number of common and unique differentially expressed genes identified in IL-1 β vs naïve and CP vs NT comparisons. Unique genes in IL-1 β vs naïve data were used to perform KEGG pathway enrichment (B) and protein-protein interaction analysis in Metascape (C). Unique genes in CP vs NT data were used to perform KEGG pathway enrichment (D) and protein-protein interaction analysis in Metascape (E).

A



B



C 24h after CP treatment

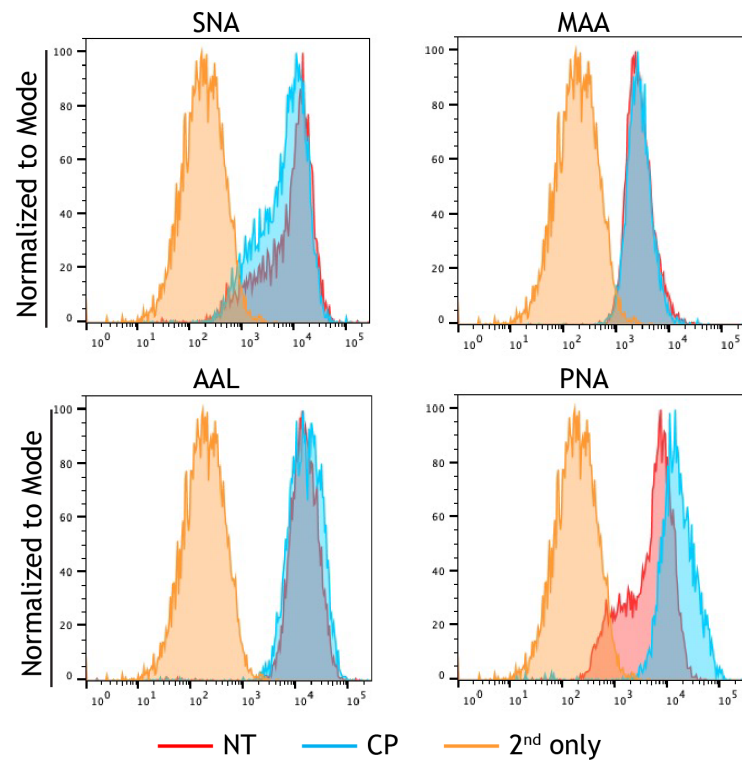


Figure 5-21 Enzymatic removal of sialic acid modulates cell sialyltransferase expression and sialylation.

(A) Heatmap of sialyltransferase expression detected in **Figure 5-15B**. Genes pass the threshold of $p_{adj} < 0.01$ and $|\log_2\text{foldchange}| > 1$ were labelled with !. (B) RNA was isolated from untreated (NT) and *C. perfringens* (CP) treated naïve SFs. Relative mRNA expression of differentially expressed genes in (A) was evaluated by RT-qPCR. Each dot represents one independent experiment, error bars represent SEM (n=5), * $p < 0.05$, ** $p < 0.01$ by the Mann-Whitney test. (C) Naïve SFs were treated with CP for 1 hour and then kept in culture for 24 hours. Cells were then collected and the presence of sialic acid on the cell surface was examined by flow cytometry for the binding of lectins (SNA, MAA, AAL and PNA).

Chapter 6 General discussion

6.1 The leading role of SFs in the pathogenesis of arthritis

Pannus formation is a hallmark of Rheumatoid arthritis (RA), which leads to pain, swelling and joint deformity. The histopathological feature of the synovial pannus is a hyperplastic synovial membrane primarily composed of synovial fibroblasts. Synovial fibroblasts (SFs) play a key role in perpetuating joint inflammation in RA via their migration and production of abundant cytokines. We refer to these aggressive SFs as activated SFs. Activated SFs exhibit pathological changes including the overexpression of immunoregulators, such as cytokines, chemokines, and MMPs, and altered expression of cell adhesion molecules. In terms of functionality, activated SFs serve on the one hand as the primary stromal cells to build up joint synovium, while, on the other hand, act as immune cells in the production of immunomodulators. In terms of response, Bottini and Firestein describe SFs as ‘passive responders’ and imprinted aggressors’ (Bottini and Firestein, 2013), as they accept stimuli from proinflammatory microenvironment, and epigenetically adopt a pro-inflammatory phenotype.

RA is the most common chronic autoimmune disease which affects about 1% of the worldwide population (Linos et al., 1980). Patients with RA are typically treated with immunosuppressive medications. However, such therapies can result in serious side effects, such as infection, and only half of the patients respond to them effectively (Ferro et al., 2017). Although the exact cause of RA is unknown, there are genetic and environmental factors that contribute to its development. Current translational medicine is focused on identifying novel therapeutic targets which suppress local inflammation without suppressing the ability of systemic immunity to clear pathogens. SFs contribute to the pathogenesis of RA in multiple aspects. The most prominent features include the release of inflammatory factors, cell recruitment, extracellular matrix degradation, and immune cell activation (Bottini and Firestein, 2013), as well as the ‘tumour-like’ features that allow SFs metastasis to healthy joints *in vivo* leading to polyarticular involvement (Lefevre et al., 2009).

The possibility of targeting SFs in RA has been discussed in recent years, driven by the advance in our understanding of the SF-dependent inflammation (Filer, 2013). Although it is not possible to inactivate SFs yet, blocking their biological effects, such as cytokines, chemokines and signaling pathways, is possible. This possibility has generated interest in cell adhesion and inflammation modulators which are expressed in SFs and could consequently improve outcomes of RA. Molecules located on the plasma membrane may be promising, as they act as scaffolds for the cytoskeleton, regulate cell deformation, and transmit and receive chemical and mechanical signals which may act as a bridge between cell adhesion and inflammation. In this thesis, two molecules related to intracellular and extracellular post-translational modifications were identified and investigated; ARNO, an intracellular protein located at the inner side of the plasma membrane, and sialic acid, which decorates glycoproteins on the outer cell membrane. Interestingly, both molecules, located at opposite sides of the cell membrane, were shown to modulate the inflammatory and migratory properties of SFs.

6.2 ARNO and sialic acid regulate SF migration

Cartilage invasiveness and migration are two unique features of SFs in RA. In RA, activated SFs, on the one hand, contribute to synovial membrane hyperplasia, leading to progressive destruction and degradation of the articular cartilage (Noss and Brenner, 2008). On the other hand, activated SFs promote the progression of disease by migrating to unaffected joints (Lefevre et al., 2009). The invasion and migration require dynamic interactions between cells and the surrounding matrix, and are dependent upon the transmission of signals from the extracellular environment and the reorganisation of actin cytoskeleton. However, the generation of pathogenic phenotypes is poorly understood in terms of molecular mechanisms.

6.2.1 Inhibition of ARNO reduces the migration of SFs

Before exploring the role of ARNO in SFs, we first confirmed that the protein is expressed in SFs and that its expression is regulated in response to the key pathogenic pro-inflammatory cytokine IL-1 β . Then, we confirmed that IL-1 β activated ARF6 in SFs as the ARNO-ARF6 axis has been implicated in cell

migration and barrier integrity in a variety of cell types (Brown, 2001). ARF6 is located at the plasma membrane and coordinates membrane traffic and cytoskeleton remodelling (Chavrier and Goud, 1999, D'Souza-Schorey et al., 1995), which distinguishes ARF6 from other members of ARF family. The classical role of ARNO as a guanine nucleotide exchange factor is to activate ARFs by replacing GDP with GTP. To study the impact of ARNO in SF migration, the expression of ARNO was silenced with siRNA. Downregulation of ARNO greatly reduced the movement of SFs without inhibiting the proliferation of SFs. Cell migration requires the reorganisation of the actin cytoskeleton on ECM, where the focal adhesion complex serves as a scaffold to physically link the cytoskeleton to ECM. Therefore, the observation of reduced formation of focal adhesions in ARNO-silenced SFs is of interest in explaining the effect of ARNO on cell migration. The data presented in chapter 4 also demonstrated a link between ARNO and STAT3 and PI3K/AKT signaling, pathways both implicated in cell motility (Lao et al., 2016, Liu et al., 2018). To determine which signalling pathways drive ARNO-mediated migration of SFs, we pharmacologically blocked each pathway, and this suggested that STAT3 was more involved. It has been shown that activated STAT3 regulates migration and invasion of RASFs by modulating the activation of Rac1 and its downstream regulators (Lao et al., 2016). Rac1 is a member of the Rho GTPase family, which also includes RhoA and Cdc42. Interestingly, cell migration requires the formation of lamellipodia, and the recruitment of ARNO to the plasma membrane by ARF6 can promote the activation of Rho GTPase, leading to the formation of lamellipodia (Humphreys et al., 2013, Singh et al., 2019, Boshans et al., 2000). Thus, it might be worthwhile to investigate the link between ARNO-regulated cell migration and ARF6-Rho GTPase signaling.

6.2.2 Sialic acid modulates cell migration

Sialic acid, which is located at the end of sugar chains, masks galactose residues and regulates various biological processes, including cell migration, inflammation and cancer genesis (Schauer, 2009). SFs deprived of sialic acid exhibited enhanced cell migration and presumably reflecting this, multiple adhesion molecules were upregulated in SFs upon removal of sialic acid from the cell surface (Figure 5-19B). Among these adhesion molecules, the expression of Icam1 and Vcam1 is elevated in RA and has been implicated in the pathogenesis

of RA (Wang et al., 2015, Szekanecz et al., 1994). In RA, the elevated expression of VCAM-1 and ICAM-1 enables leukocytes to leave the bloodstream and migrate to inflamed synovial tissues, hence initiating and/or exacerbating joint inflammatory responses. During the spreading and crawling of leukocytes, the interaction of adhesion molecules, such as VCAM-1 and ICAM-1, with integrins ensures the firm adhesion of leukocytes to the vascular endothelium (Simon and Green, 2005). Besides, integrins control cell motility by regulating cell-cell and cell-ECM contracts. Desialylation of SFs enhances cell migration and, interestingly, B1 integrin lacking $\alpha 2-6$ sialic acid exhibited enhanced cell adhesion to fibronectin (Semel et al., 2002), with specifically the binding of $\alpha 5\beta 1$ integrin to fibronectin being enhanced when treated with sialidase (Semel et al., 2002). The enhanced binding following loss of sialic acid may be associated with galectin3 (Gal-3). Gal-3 is highly expressed in fibroblasts, and RASFs release Gal-3 when cultured *in vitro* (Ohshima et al., 2003). Gal-3 mediates cell functions, such as cell adhesion, migration and cell-matrix adhesion, and it has been identified as a pro-inflammatory factor in RA and arthritis model. Gal-3 binds to galactose-containing glycoproteins in the plasma membrane, with its binding blocked by sialylation and enabled by desialylation (Zhuo and Bellis, 2011, Nomura et al., 2017). Studies have shown that integrins are also involved in Gal-3 mediated cell-matrix adhesion (Hughes, 2001, Zhao et al., 2010) and indeed, integrins also regulate Gal-3 binding to cell surface as the adhesion of Gal-3 to colonocytes was blocked by incubating cells with an integrin $\beta 1$ blocking antibody (Zhuo et al., 2008). Besides, the binding of Gal-3 to colonocytes was attenuated by St6gal1 activity (Zhuo et al., 2008), supporting the idea of sialic acid being key for facilitating Gal-3-integrin complexes in cell migration.

Cell adhesion regulated by integrin and Gal-3 might activate downstream regulators Rho GTPases such as Cdc42, Rac1 and Rho. Integrin-mediated cell migration requires Rho GTPases (Lawson and Burridge, 2014), and these factors regulate lamellipodia formation, membrane ruffling, cell polarity and stress fiber formation that contributes to cytoskeleton reorganisation and migration of SFs in RA (Chan et al., 2007, Liang et al., 2013, Peng et al., 2017). Thus, sialic acid-mediated SF migration on ECM may activate downstream Rho GTPases by regulating the binding of integrin to Gal-3 (Figure 6-1). Further studies will be

required to clarify the molecular mechanisms underpinning sialic acid-dependent cell migration.

6.3 ARNO and sialic acid regulate the inflammatory response of SFs

SFs are not just passively involved in rheumatoid joint destruction but actively contribute to synovial inflammation. RASFs contribute to the initiation and perpetuation of chronic inflammation by secreting a wide range of mediators, such as pro-inflammatory cytokines, chemokines and growth factors. Many mechanisms contribute to SF activation, and the data in Chapter 4 and Chapter 5 have demonstrated that ARNO and sialic acid modulate the expression of pro-inflammatory regulators in SFs, findings which may have potential clinical implications.

6.3.1 Inhibition of ARNO suppresses SF inflammation

To investigate the role of ARNO in SF inflammation, ARNO was downregulated in SFs from naïve mice as well as mice undergoing collagen-induced arthritis. Expression of pro-inflammatory cytokines, proteases that disrupt ECM and factors contributing to osteoclastogenesis were reduced in response to IL-1 β stimulation when ARNO was silenced. Furthermore, in conjunction with the previously discussed role of ARNO in cell migration, we conclude that inhibition of ARNO may be a potential target to inactivate aggressive SFs.

Cytokine regulation in the progression of RA has been shown related to TLR4 signaling. Activation of TLR4 induces two pathways, Myd88-dependent and Myd88-independent (Akira and Takeda, 2004). Myd88 and TIRAP are required for the Myd88-dependent pathway to activate NF- κ B and to increase the production of pro-inflammatory cytokines (Horng et al., 2002). Interestingly, ARNO has previously been shown to regulate endothelial barrier permeability via Myd88-ARNO-ARF6 signaling, although the role of this pathway in cytokine production was not investigated in that study (Zhu et al., 2012). Another study showed that ARF6 colocalises with TIRAP and ARF6 regulating TIRAP transportation (Kagan and Medzhitov, 2006). In this study, mouse embryonic fibroblasts transfected with ARF6 inhibitory peptide exhibited blocked production of LPS-induced

chemokine KC (Kagan and Medzhitov, 2006). PIP2 is required for TIRAP localization to the plasma membrane (Kagan and Medzhitov, 2006), suggesting that ARF6 might regulate TLR4 signaling by inducing PIP2 production and TIRAP localization. Besides, ARF6 has been observed to bind with vacuolar-type H⁺ adenosine triphosphatase (V-ATPase) which promotes TLR4 internalisation (Murase et al., 2018). Certainly, ARF6-regulated LPS uptake was impaired by ATP6V0D2 (one component of V-ATPase) deficiency and ARF6 deficiency reduced LPS-induced NF- κ B activation and cytokine expression (Murase et al., 2018). Although this research did not investigate the role of ARNO in LPS-induced NF- κ B activation, it is confirmed that both ARNO and ARF6 are bound to V-ATPase. Thus, as the investigation of the role of PI3K-AKT and STAT3 signaling pathways showed that inhibition of either pathway failed to reproduce the effects of ARNO downregulation on inflammatory factors, we propose that the regulation of pro-inflammatory cytokine production in SFs by ARNO may be achieved through TLR4 signalling. The downstream adaptor Myd88 is required for TLR4 to contribute to the inflammatory and destructive processes of RA (Sacre et al., 2007). The Myd88-ARNO-ARF6 signaling pathway appears to be an important factor contributing to the disruption of vascular stability (Zhu et al., 2012). This is reminiscent of the ES-62, an excretory-secretory (ES) protein secreted by filarial nematodes, which has previously been demonstrated to target TLR4 signaling via the adaptor protein Myd88 (Goodridge et al., 2007, Goodridge et al., 2005). Besides, it has been demonstrated that ES-62 has protective effects in mouse models of inflammatory diseases (Pineda et al., 2012, Pineda et al., 2014b). In addition, it has been observed that ES-62 inhibits PLD signaling in T cells and mast cells (Pineda et al., 2014a), which is associated with ARNO-ARF6, suggesting an ES-62/TLR4/ARNO/PLD signaling in SF inflammation.

6.3.2 Loss of sialic acid induces the production of pro-inflammatory mediators in SFs

After confirming the role of ARNO in the aggressive phenotype of SFs, it was shown here that sialic acid protects SFs from converting into a pathogenic phenotype and that loss of sialic acid significantly increased their expression of proinflammatory modulators. Altered glycosylation regulates inflammation and metastasis in cancer, pathways also associated with immune disorders. Arthritic SFs exhibited reduced St6gal1 expression, suggesting a special role of α 2-6 sialic

acid in SF biology under a proinflammatory milieu. Besides, *in vitro* culture of CIA SFs preserved their hyposialylated status and pathogenic characteristics. Strikingly, proinflammatory modulators triggered by removing sialic acid from SFs using exogenous sialidase partly overlap with those triggered by IL-1 β . Investigation of the molecular mechanisms underlying the activation of SF by sialic acid is required.

One possible mechanism for sialic acid-dependent SF activation is the absence of regulatory Siglec (sialic-acid-binding immunoglobulin-like lectin) signaling. Siglecs are mostly suppressive immunoreceptors. Expression of Siglecs has been proposed to facilitate oncogenesis, where cancer progression relies on escape from immune surveillance. Indeed, Hypersialylation is a common phenomenon in cancer cells and the sialidase-treated tumour transplantation study establishes a link between sialic acid and cancer pathology (Sedlacek et al., 1975). Thus, the binding of sialic acid and Siglecs inhibits T cell, B cell, NK cell and dendritic cell regulated immune responses (Takagi et al., 2011, Bednar et al., 2017, Jandus et al., 2014a). For example, B cell inactivation was observed in a human CD22 (Siglec-2) expressing transgenic mouse model, whilst hyper-responsiveness was observed in CD22^{-/-} B cells (Bednar et al., 2017). Moreover, enhanced cytotoxicity of human NK cells against myeloid leukaemia cells was observed upon blockade of Siglec-7 or Siglec-9 (Jandus et al., 2014b). Thus, as loss of sialic acid in SFs triggered the synthesis of cytokines and other immunoregulators, this was perhaps due to the lack of Siglec binding. Another possible mechanism for sialic acid-dependent SF activation could be increased binding of galectins. Galectins modulate immune system homeostasis, shaping physiological and pathological inflammatory processes. For example, inhibiting Gal-3 expression reduces TLR-2, -3, -4 mediated IL-6 production upon LPS stimulation (Arad et al., 2015) whilst Gal-3 induces IL-6, MMP3 and TNF α expression in SFs via PI3K/AKT and ERK signaling (Filer et al., 2009).

Alternatively, autoimmune responses in RA could be triggered by incorporation of nonhuman sialic acid (Neu5Gc) into human tissue. Humans have evolved to be deficient in CMAH gene expression and are not able to produce Neu5Gc as it is the only gene regulating the synthesis of Neu5Gc, and there is no known alternative pathway for Neu5Gc biosynthesis in humans. Consistent with this, CMAH^{-/-} mice display a complete absence of Neu5Gc (Hedlund et al., 2008).

Interestingly, Neu5Gc has been detected on gangliosides and glycoproteins from some human tumours (Hirabayashi et al., 1987b, Miyoshi et al., 1986, Kawachi et al., 1988). One possible explanation for this presence of Neu5Gc in human tissue is dietary incorporation, an idea that was validated by animal research in which Neu5Gc was detected in endothelial and epithelial cells of CMAH^{-/-} mice fed with Neu5Gc-glycoproteins (Banda et al., 2012). Neu5Gc is abundant in red meat and is common in cow's milk (Tangvoranuntakul et al.), both common in human diet. Although increases in anti-Neu5Gc antibodies are uncommon among autoimmune diseases (Eleftheriou et al., 2014), their presence has been shown to induce the development of systemic inflammation (Samraj et al., 2015).

Consumption of red meat increases the risk of multiple chronic diseases including cancers, diabetes and cardiovascular disease (Pan et al., 2011, Micha et al., 2010, Pan et al., 2012). Although disease induction from its high-fat content cannot be ruled out, or the polycyclic aromatic hydrocarbons and N-nitroso compounds produced during the processing of red meat such as grilling and curing, this may suggest that Neu5Gc may be responsible for the increased disease risk associated with red meat. The metabolic incorporation of Neu5Gc into human cells could be via pinocytosis and subsequent access to the sialic acid synthesis system and expression of conjugates at cell surface (Bardor et al., 2005), as Neu5Ac and Neu5Gc share the same synthesis route (Figure 1-3). Interestingly, this incorporation of free Neu5Gc is rare in normal tissue compared to tumours (Banda et al., 2012), suggesting differential mechanisms in normal and tumour tissues allowing accumulation of Neu5Gc in human tumours (Higashi et al., 1984, Hirabayashi et al., 1987a, Nakarai et al., 1987, Tangvoranuntakul et al.). The accumulation of Neu5Gc in tumour cells has been hypothesized to promote tumour progression by triggering lower-level chronic inflammatory responses that are not sufficient to kill tumour cells (Hedlund et al., 2008). For example, subcutaneously injected Neu5Gc-expressing B16 melanoma cells into CMAH^{-/-} mice (Human-like Neu5Gc deficiency mice) resulted in enhanced tumour growth relative to those injected into wild-type mice. The CMAH^{-/-} mice injected with tumour cells developed anti-Neu5Gc antibodies, and these anti-Neu5Gc antibodies enhanced the tumour growth (Hedlund et al., 2008). Such anti-Neu5Gc antibodies resulting in lower-level chronic inflammatory responses could contribute to the initiation of arthritis, suggesting a potential

link among red meat consumption, Neu5Gc incorporation and immune response initiation. This is consistent with epidemiological studies that red meat intake is associated with the onset of inflammatory arthritis (Jin et al., 2021, Pattison et al., 2004, Grant, 2000).

6.4 ARNO and Sialylation: walk the same way?

Enhanced migratory capacity and cytokine production are hallmarks of activated SFs, promoting research into SF as a therapeutic target for rheumatoid arthritis. Both ARNO and sialic acid regulate SF migration and inflammation, suggesting that these genes controlling ARF activation and cell sialylation are potential targets for controlling SF activation. Interestingly, the potential molecular mechanisms by which ARNO and sialic acid regulate the biology of SFs share some similarities (Figure 6-2). For example, PI3K/AKT signaling is a potential candidate regulating both sialic acid and ARNO-mediated SF inflammation. Thus, exposure of terminal galactose upon removal of sialic acid could increase the binding of Gal-3 and result in the production of cytokines by activation of PI3K/AKT pathway (Filer et al., 2009). Our results showed that inhibition of ARNO with siRNA greatly blocked AKT phosphorylation (Figure 4-13) and proinflammatory cytokine production (Figure 4-9). Besides, ARNO-ARF6 axis initiates the formation of autophagosome (Moreau et al., 2012) and AKT signaling (Carnero and Paramio, 2014, Bruntz et al., 2014) by inducing the production of PIP2 (Honda et al., 1999). Similarly, TLR4/NF- κ B signaling might be involved in ARNO and sialic acid regulation of SF inflammation as inhibition of Gal-3 expression reduces TLR-4 mediated IL-6 production upon LPS stimulation (Arad et al., 2015) and similar results were observed in cells transfected with ARF6-T27N (ARF6 inactivate mutant) (Murase et al., 2018). Alternatively, ARNO and sialic acid regulated cell migration might be through activation of Rho GTPases as both ARNO and sialic acid can regulate integrin-dependent cell migration (Oh and Santy, 2010, Salem et al., 2015, Yuan et al., 2016).

Overall, in this thesis, we identified two post-translational modulators which control the migration and inflammatory response of SFs, ARNO and sialic acid. Thus, it was discovered that ARNO is required for SF migration and actin cytoskeleton reorganisation. Specifically, ARNO is involved in the IL-1 β -mediated inflammatory responses in SFs and downregulation of ARNO reduces IL-1 β

induced production of proinflammatory modulators. In addition, it was established that sialic acid is reduced in CIA SFs, and this loss induces potent inflammatory responses and enhanced cell motility in SFs. Unfortunately, the molecule mechanisms driving ARNO and sialic acid regulated migration and inflammation could not be fully explored. Further studies of ARNO and sialic acid in co-culture systems with different type of cells will provide a deeper understanding of the role of these molecules in tissue immunoregulation and ultimately may even lead to the development of ARNO and sialic acid-based therapies for RA.

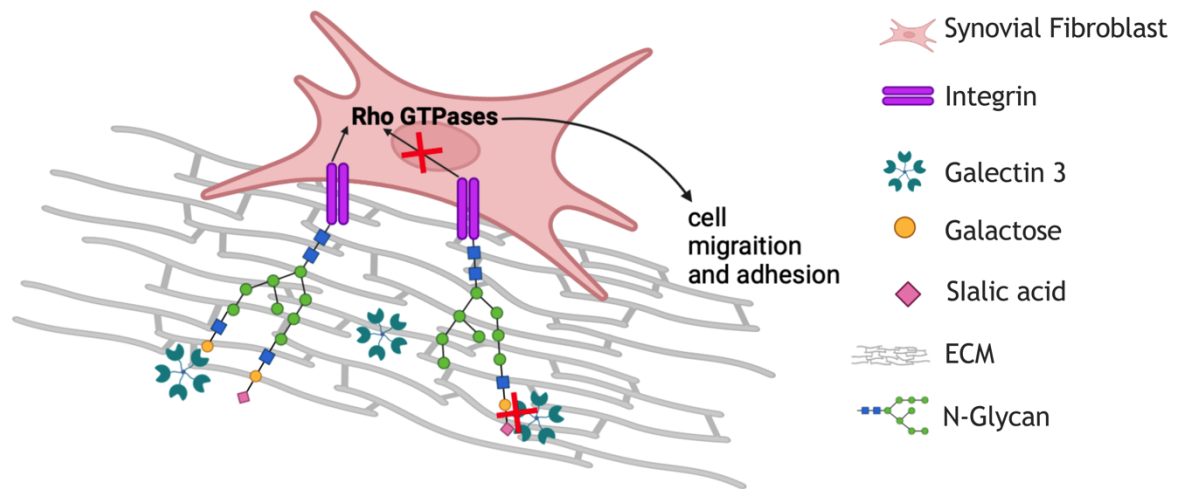


Figure 6-1 Illustration of Gal-3 binding to galactose in SFs.

Gal-3 binds to desialylated integrin which activates Rho GTPases and hence promotes cell migration and adhesion. Figure created with BioRender.com.

Chapter 7 Reference

NHS Photodynamic therapy (PDT) [Online]. Available:

<https://www.nhs.uk/conditions/photodynamic-therapy/> [Accessed].

- ADACHI, M., OKAMOTO, S., CHUJYO, S., ARAKAWA, T., YOKOYAMA, M., YAMADA, K., HAYASHI, A., AKITA, K., TAKENO, M., ITOH, S., TAKII, T., WAGURI-NAGAYA, Y., OTSUKA, T., HAYAKAWA, K., MIYAZAWA, K. & ONOZAKI, K. 2013. Cigarette smoke condensate extracts induce IL-1-beta production from rheumatoid arthritis patient-derived synoviocytes, but not osteoarthritis patient-derived synoviocytes, through aryl hydrocarbon receptor-dependent NF-kappa-B activation and novel NF-kappa-B sites. *J Interferon Cytokine Res*, 33, 297-307.
- ADAMS, O. J., STANCZAK, M. A., VON GUNTEN, S. & LÄUBLI, H. 2018. Targeting sialic acid-Siglec interactions to reverse immune suppression in cancer. *Glycobiology*, 28, 640-647.
- AI, R., HAMMAKER, D., BOYLE, D. L., MORGAN, R., WALSH, A. M., FAN, S., FIRESTEIN, G. S. & WANG, W. 2016. Joint-specific DNA methylation and transcriptome signatures in rheumatoid arthritis identify distinct pathogenic processes. *Nat Commun*, 7, 11849.
- AKIRA, S. & TAKEDA, K. 2004. Toll-like receptor signalling. *Nature Reviews Immunology*, 4, 499-511.
- ALIVERNINI, S., MACDONALD, L., ELMESMARI, A., FINLAY, S., TOLUSSO, B., GIGANTE, M. R., PETRICCA, L., DI MARIO, C., BUI, L., PERNIOLA, S., ATTAR, M., GESSI, M., FEDELE, A. L., CHILAKA, S., SOMMA, D., SANSOM, S. N., FILER, A., MCSHARRY, C., MILLAR, N. L., KIRSCHNER, K., NERVIANI, A., LEWIS, M. J., PITZALIS, C., CLARK, A. R., FERRACCIOLI, G., UDALOVA, I., BUCKLEY, C. D., GREMESE, E., MCINNES, I. B., OTTO, T. D. & KUROWSKA-STOLARSKA, M. 2020. Distinct synovial tissue macrophage subsets regulate inflammation and remission in rheumatoid arthritis. *Nat Med*, 26, 1295-1306.
- ALVARO-GRACIA, J. M., ZVAIFLER, N. J. & FIRESTEIN, G. S. 1990. Cytokines in chronic inflammatory arthritis. V. Mutual antagonism between interferon-gamma and tumor necrosis factor-alpha on HLA-DR expression, proliferation, collagenase production, and granulocyte macrophage colony-stimulating factor production by rheumatoid arthritis synoviocytes. *J Clin Invest*, 86, 1790-8.
- ARAD, U., MADAR-BALAKIRSKI, N., ANGEL-KORMAN, A., AMIR, S., TZADOK, S., SEGAL, O., MENACHEM, A., GOLD, A., ELKAYAM, O. & CASPI, D. 2015. Galectin-3 is a sensor-regulator of toll-like receptor pathways in synovial fibroblasts. *Cytokine*, 73, 30-5.
- ARMAKA, M., GKRETSI, V., KONTOYIANNIS, D. & KOLLIAS, G. 2009. A standardized protocol for the isolation and culture of normal and arthritogenic murine synovial fibroblasts. *Protocol Exchange*.
- AVRIL, T., ATTRILL, H., ZHANG, J., RAPER, A. & CROCKER, P. R. 2006. Negative regulation of leucocyte functions by CD33-related siglecs. *Biochem Soc Trans*, 34, 1024-7.
- BAI, S., LIU, H., CHEN, K. H., EKSARKO, P., PERLMAN, H., MOORE, T. L. & POPE, R. M. 2004. NF-kappaB-regulated expression of cellular FLIP protects rheumatoid arthritis synovial fibroblasts from tumor necrosis factor alpha-mediated apoptosis. *Arthritis Rheum*, 50, 3844-55.

- BANDA, K., GREGG, C. J., CHOW, R., VARKI, N. M. & VARKI, A. 2012. Metabolism of vertebrate amino sugars with N-glycolyl groups: mechanisms underlying gastrointestinal incorporation of the non-human sialic acid xeno-autoantigen N-glycolylneuraminic acid. *J Biol Chem*, 287, 28852-64.
- BARDOR, M., NGUYEN, D. H., DIAZ, S. & VARKI, A. 2005. Mechanism of uptake and incorporation of the non-human sialic acid N-glycolylneuraminic acid into human cells. *J Biol Chem*, 280, 4228-37.
- BARTOK, B. & FIRESTEIN, G. S. 2010. Fibroblast-like synoviocytes: key effector cells in rheumatoid arthritis. *Immunol Rev*, 233, 233-55.
- BASSAGAÑAS, S., PÉREZ-GARAY, M. & PERACAUOLA, R. 2014. Cell surface sialic acid modulates extracellular matrix adhesion and migration in pancreatic adenocarcinoma cells. *Pancreas*, 43, 109-17.
- BATEMAN, A. C., KARAMANSKA, R., BUSCH, M. G., DELL, A., OLSEN, C. W. & HASLAM, S. M. 2010. Glycan analysis and influenza A virus infection of primary swine respiratory epithelial cells: the importance of NeuAc{alpha}2-6 glycans. *J Biol Chem*, 285, 34016-26.
- BAYS, J. L., PENG, X., TOLBERT, C. E., GUILLUY, C., ANGELL, A. E., PAN, Y., SUPERFINE, R., BURRIDGE, K. & DEMALI, K. A. 2014. Vinculin phosphorylation differentially regulates mechanotransduction at cell-cell and cell-matrix adhesions. *J Cell Biol*, 205, 251-63.
- BEDNAR, K. J., SHANINA, E., BALLEST, R., CONNORS, E. P., DUAN, S., JUAN, J., ARLIAN, B. M., KULIS, M. D., BUTCHER, E. C., FUNG-LEUNG, W. P., RAO, T. S., PAULSON, J. C. & MACAULEY, M. S. 2017. Human CD22 Inhibits Murine B Cell Receptor Activation in a Human CD22 Transgenic Mouse Model. *J Immunol*, 199, 3116-3128.
- BETTERIDGE, K. B., ARKILL, K. P., NEAL, C. R., HARPER, S. J., FOSTER, R. R., SATCHELL, S. C., BATES, D. O. & SALMON, A. H. J. 2017. Sialic acids regulate microvessel permeability, revealed by novel in vivo studies of endothelial glycocalyx structure and function. *J Physiol*, 595, 5015-5035.
- BÖHMER, F. D. & FRIEDRICH, K. 2014. Protein tyrosine phosphatases as wardens of STAT signaling. *Jakstat*, 3, e28087.
- BOMBARDIERI, M., KAM, N. W., BRENTANO, F., CHOI, K., FILER, A., KYBURZ, D., MCINNES, I. B., GAY, S., BUCKLEY, C. & PITZALIS, C. 2011. A BAFF/APRIL-dependent TLR3-stimulated pathway enhances the capacity of rheumatoid synovial fibroblasts to induce AID expression and Ig class-switching in B cells. *Ann Rheum Dis*, 70, 1857-65.
- BONDESON, J., BLOM, A. B., WAINWRIGHT, S., HUGHES, C., CATERSON, B. & VAN DEN BERG, W. B. 2010. The role of synovial macrophages and macrophage-produced mediators in driving inflammatory and destructive responses in osteoarthritis. *Arthritis Rheum*, 62, 647-57.
- BOSHANS, R. L., SZANTO, S., VAN AELST, L. & D'SOUZA-SCHOREY, C. 2000. ADP-ribosylation factor 6 regulates actin cytoskeleton remodeling in coordination with Rac1 and RhoA. *Mol Cell Biol*, 20, 3685-94.
- BOTTINI, N. & FIRESTEIN, G. S. 2013. Duality of fibroblast-like synoviocytes in RA: passive responders and imprinted aggressors. *Nat Rev Rheumatol*, 9, 24-33.
- BOULAY, P. L., SCHLIENGER, S., LEWIS-SARAVALLI, S., VITALE, N., FERBEYRE, G. & CLAING, A. 2011. ARF1 controls proliferation of breast cancer cells by regulating the retinoblastoma protein. *Oncogene*, 30, 3846-61.
- BOYER, R. 2006. Posttranslational modification of proteins: Expanding nature's inventory. Christopher T. Walsh, Roberts & Company Publishers,

- Greenwood Village, CO, 2005, 576 pp., ISBN 0 - 9747077 - 3 - 2, \$98.00.
USA: John Wiley & Sons Inc.
- BRAND, D. D., LATHAM, K. A. & ROSLONIEC, E. F. 2007. Collagen-induced arthritis. *Nat Protoc*, 2, 1269-75.
- BRENNAN-OLSEN, S. L., COOK, S., LEECH, M. T., BOWE, S. J., KOWAL, P., NAIDOO, N., ACKERMAN, I. N., PAGE, R. S., HOSKING, S. M., PASCO, J. A. & MOHEBBI, M. 2017. Prevalence of arthritis according to age, sex and socioeconomic status in six low and middle income countries: analysis of data from the World Health Organization study on global AGEing and adult health (SAGE) Wave 1. *BMC Musculoskelet Disord*, 18, 271.
- BROWN, C. E. T. M. C. 2001. Cell motility: ARNO and ARF6 at the cutting edge. *Current Biology*, 11:R875-R877.
- BROWN, F. D., ROZELLE, A. L., YIN, H. L., BALLA, T. & DONALDSON, J. G. 2001. Phosphatidylinositol 4,5-bisphosphate and Arf6-regulated membrane traffic. *J Cell Biol*, 154, 1007-17.
- BRUNMARK, A. & O'ROURKE, A. M. 1997. Augmentation of mature CD4+ T cell responses to isolated antigenic class II proteins by fibronectin and intercellular adhesion molecule-1. *J Immunol*, 159, 1676-85.
- BRUNTZ, R. C., TAYLOR, H. E., LINDSLEY, C. W. & BROWN, H. A. 2014. Phospholipase D2 mediates survival signaling through direct regulation of Akt in glioblastoma cells. *J Biol Chem*, 289, 600-16.
- BUCKLEY, C. D., PILLING, D., LORD, J. M., AKBAR, A. N., SCHEEL-TOELLNER, D. & SALMON, M. 2001. Fibroblasts regulate the switch from acute resolving to chronic persistent inflammation. *Trends Immunol*, 22, 199-204.
- BULL, C., BOLTJE, T. J., WASSINK, M., DE GRAAF, A. M., VAN DELFT, F. L., DEN BROK, M. H. & ADEMA, G. J. 2013. Targeting aberrant sialylation in cancer cells using a fluorinated sialic acid analog impairs adhesion, migration, and in vivo tumor growth. *Mol Cancer Ther*, 12, 1935-46.
- BULL, C., COLLADO-CAMPS, E., KERS-REBEL, E. D., HEISE, T., SONDERGAARD, J. N., DEN BROK, M. H., SCHULTE, B. M., BOLTJE, T. J. & ADEMA, G. J. 2017. Metabolic sialic acid blockade lowers the activation threshold of moDCs for TLR stimulation. *Immunol Cell Biol*, 95, 408-415.
- BURGER, J. A., ZVAIFLER, N. J., TSUKADA, N., FIRESTEIN, G. S. & KIPPS, T. J. 2001. Fibroblast-like synoviocytes support B-cell pseudoemperipolesis via a stromal cell-derived factor-1- and CD106 (VCAM-1)-dependent mechanism. *J Clin Invest*, 107, 305-15.
- BUSCHIAZZO, A. & ALZARI, P. M. 2008. Structural insights into sialic acid enzymology. *Curr Opin Chem Biol*, 12, 565-72.
- CABRAL, M. G., SILVA, Z., LIGEIRO, D., SEIXAS, E., CRESPO, H., CARRASCAL, M. A., SILVA, M., PITEIRA, A. R., PAIXÃO, P., LAU, J. T. & VIDEIRA, P. A. 2013. The phagocytic capacity and immunological potency of human dendritic cells is improved by α 2,6-sialic acid deficiency. *Immunology*, 138, 235-45.
- CAO, H., WELLER, S., ORTH, J. D., CHEN, J., HUANG, B., CHEN, J. L., STAMNES, M. & MCNIVEN, M. A. 2005. Actin and Arf1-dependent recruitment of a cortactin-dynamin complex to the Golgi regulates post-Golgi transport. *Nat Cell Biol*, 7, 483-92.
- CARLSON, R. P., DATKO, L. J., O'NEILL-DAVIS, L., BLAZEK, E. M., DELUSTRO, F., BEIDEMAN, R. & LEWIS, A. J. 1985. Comparison of inflammatory changes in established type II collagen- and adjuvant-induced arthritis using outbred wistar rats. *International Journal of Immunopharmacology*, 7, 811-826.

- CARNERO, A. & PARAMIO, J. M. 2014. The PTEN/PI3K/AKT Pathway in vivo, Cancer Mouse Models. *Frontiers in Oncology*, 4.
- CASALOU, C., FAUSTINO, A. & BARRAL, D. C. 2016. Arf proteins in cancer cell migration. *Small GTPases*, 7, 270-282.
- CERONI, A., MAASS, K., GEYER, H., GEYER, R., DELL, A. & HASLAM, S. M. 2008. GlycoWorkbench: A Tool for the Computer-Assisted Annotation of Mass Spectra of Glycans. *Journal of Proteome Research*, 7, 1650-1659.
- CHAN, A., AKHTAR, M., BRENNER, M., ZHENG, Y., GULKO, P. S. & SYMONS, M. 2007. The GTPase Rac regulates the proliferation and invasion of fibroblast-like synoviocytes from rheumatoid arthritis patients. *Mol Med*, 13, 297-304.
- CHANG, S. K., NOSS, E. H., CHEN, M., GU, Z., TOWNSEND, K., GREHA, R., LEON, L., LEE, S. Y., LEE, D. M. & BRENNER, M. B. 2011a. Cadherin-11 regulates fibroblast inflammation. *Proceedings of the National Academy of Sciences*, 108, 8402-8407.
- CHANG, S. K., NOSS, E. H., CHEN, M., GU, Z., TOWNSEND, K., GREHA, R., LEON, L., LEE, S. Y., LEE, D. M. & BRENNER, M. B. 2011b. Cadherin-11 regulates fibroblast inflammation. *Proc Natl Acad Sci U S A*, 108, 8402-7.
- CHAVRIER, P. & GOUD, B. 1999. The role of ARF and Rab GTPases in membrane transport. *Curr Opin Cell Biol*, 11, 466-75.
- CHEN, X. & VARKI, A. 2010. Advances in the biology and chemistry of sialic acids. *ACS Chem Biol*, 5, 163-76.
- CHENG, F., SHEN, Y., MOHANASUNDARAM, P., LINDSTRÖM, M., IVASKA, J., NY, T. & ERIKSSON, J. E. 2016. Vimentin coordinates fibroblast proliferation and keratinocyte differentiation in wound healing via TGF- β -Slug signaling. *Proc Natl Acad Sci U S A*, 113, E4320-7.
- CHIN, Y. R. & TOKER, A. 2009. Function of Akt/PKB signaling to cell motility, invasion and the tumor stroma in cancer. *Cell Signal*, 21, 470-6.
- CHOY, E. H., KAVANAUGH, A. F. & JONES, S. A. 2013. The problem of choice: current biologic agents and future prospects in RA. *Nat Rev Rheumatol*, 9, 154-63.
- CHRISTENSEN, A. D., HAASE, C., COOK, A. D. & HAMILTON, J. A. 2016. K/BxN Serum-Transfer Arthritis as a Model for Human Inflammatory Arthritis. *Front Immunol*, 7, 213.
- CLAING, A., CHEN, W., MILLER, W. E., VITALE, N., MOSS, J., PREMONT, R. T. & LEFKOWITZ, R. J. 2001. beta-Arrestin-mediated ADP-ribosylation factor 6 activation and beta 2-adrenergic receptor endocytosis. *J Biol Chem*, 276, 42509-13.
- CLARK, R. A., AN, J. Q., GREILING, D., KHAN, A. & SCHWARZBAUER, J. E. 2003. Fibroblast migration on fibronectin requires three distinct functional domains. *J Invest Dermatol*, 121, 695-705.
- COHEN, L. A., HONDA, A., VARNAI, P., BROWN, F. D., BALLA, T. & DONALDSON, J. G. 2007. Active Arf6 recruits ARNO/cytohesin GEFs to the PM by binding their PH domains. *Molecular biology of the cell*, 18, 2244-2253.
- COLLINS, B. E., SMITH, B. A., BENGTSON, P. & PAULSON, J. C. 2006. Ablation of CD22 in ligand-deficient mice restores B cell receptor signaling. *Nat Immunol*, 7, 199-206.
- CORBET, M., PINEDA, M. A., YANG, K., TARAFDAR, A., MCGRATH, S., NAKAGAWA, R., LUMB, F. E., SUCKLING, C. J., HARNETT, W. & HARNETT, M. M. 2021. Suppression of inflammatory arthritis by the parasitic worm product ES-62 is associated with epigenetic changes in synovial fibroblasts. *PLoS Pathog*, 17, e1010069.

- CORNALL, R. J., CYSTER, J. G., HIBBS, M. L., DUNN, A. R., OTIPOBY, K. L., CLARK, E. A. & GOODNOW, C. C. 1998. Polygenic autoimmune traits: Lyn, CD22, and SHP-1 are limiting elements of a biochemical pathway regulating BCR signaling and selection. *Immunity*, 8, 497-508.
- COURTENAY, J. S., DALLMAN, M. J., DAYAN, A. D., MARTIN, A. & MOSEDALE, B. 1980. Immunisation against heterologous type II collagen induces arthritis in mice. *Nature*, 283, 666-668.
- CROCKER, P. R., PAULSON, J. C. & VARKI, A. 2007. Siglecs and their roles in the immune system. *Nat Rev Immunol*, 7, 255-66.
- CROFT, A. P., CAMPOS, J., JANSEN, K., TURNER, J. D., MARSHALL, J., ATTAR, M., SAVARY, L., WEHMEYER, C., NAYLOR, A. J., KEMBLE, S., BEGUM, J., DURHOLZ, K., PERLMAN, H., BARONE, F., MCGETTRICK, H. M., FEARON, D. T., WEI, K., RAYCHAUDHURI, S., KORSUNSKY, I., BRENNER, M. B., COLES, M., SANSOM, S. N., FILER, A. & BUCKLEY, C. D. 2019. Distinct fibroblast subsets drive inflammation and damage in arthritis. *Nature*, 570, 246-251.
- CROFT, A. P., NAYLOR, A. J., MARSHALL, J. L., HARDIE, D. L., ZIMMERMANN, B., TURNER, J., DESANTI, G., ADAMS, H., YEMM, A. I., MULLER-LADNER, U., DAYER, J. M., NEUMANN, E., FILER, A. & BUCKLEY, C. D. 2016. Rheumatoid synovial fibroblasts differentiate into distinct subsets in the presence of cytokines and cartilage. *Arthritis Res Ther*, 18, 270.
- CROSS, A. S. & WRIGHT, D. G. 1991. Mobilization of sialidase from intracellular stores to the surface of human neutrophils and its role in stimulated adhesion responses of these cells. *J Clin Invest*, 88, 2067-76.
- CULEMANN, S., GRUNEBOOM, A., NICOLAS-AVILA, J. A., WEIDNER, D., LAMMLE, K. F., ROTHE, T., QUINTANA, J. A., KIRCHNER, P., KRLJANAC, B., EBERHARDT, M., FERRAZZI, F., KRETZSCHMAR, E., SCHICHT, M., FISCHER, K., GELSE, K., FAAS, M., PFEIFLE, R., ACKERMANN, J. A., PACHOWSKY, M., RENNER, N., SIMON, D., HASELOFF, R. F., EKICI, A. B., BAUERLE, T., BLASIG, I. E., VERA, J., VOEHRINGER, D., KLEYER, A., PAULSEN, F., SCHETT, G., HIDALGO, A. & KRONKE, G. 2019. Locally renewing resident synovial macrophages provide a protective barrier for the joint. *Nature*, 572, 670-675.
- CURTIS, J. R. & SINGH, J. A. 2011. Use of biologics in rheumatoid arthritis: current and emerging paradigms of care. *Clin Ther*, 33, 679-707.
- D'SOUZA-SCHOREY, C., LI, G., COLOMBO, M. I. & STAHL, P. D. 1995. A regulatory role for ARF6 in receptor-mediated endocytosis. *Science*, 267, 1175-8.
- DAGIA, N. M., GADHOUM, S. Z., KNOBLAUCH, C. A., SPENCER, J. A., ZAMIRI, P., LIN, C. P. & SACKSTEIN, R. 2006. G-CSF induces E-selectin ligand expression on human myeloid cells. *Nature Medicine*, 12, 1185-1190.
- DALL'OLIO, F. & CHIRICOLO, M. 2001. Sialyltransferases in cancer. *Glycoconj J*, 18, 841-50.
- DALL'OLIO, F., CHIRICOLO, M., D'ERRICO, A., GRUPPIONI, E., ALTIMARI, A., FIORENTINO, M. & GRIGIONI, W. F. 2004. Expression of beta-galactoside alpha2,6 sialyltransferase and of alpha2,6-sialylated glycoconjugates in normal human liver, hepatocarcinoma, and cirrhosis. *Glycobiology*, 14, 39-49.
- DANKBAR, B., FENNEN, M., BRUNERT, D., HAYER, S., FRANK, S., WEHMEYER, C., BECKMANN, D., PARUZEL, P., BERTRAND, J., REDLICH, K., KOERS-WUNRAU, C., STRATIS, A., KORB-PAP, A. & PAP, T. 2015. Myostatin is a direct regulator of osteoclast differentiation and its inhibition reduces inflammatory joint destruction in mice. *Nat Med*, 21, 1085-90.
- DAVIS, C. T., ZHU, W., GIBSON, C. C., BOWMAN-KIRIGIN, J. A., SORENSEN, L., LING, J., SUN, H., NAVANKASATTUSAS, S. & LI, D. Y. 2014. ARF6 inhibition

- stabilizes the vasculature and enhances survival during endotoxic shock. *J Immunol*, 192, 6045-52.
- DE FRANCESCHI, N., HAMIDI, H., ALANKO, J., SAHGAL, P. & IVASKA, J. 2015. Integrin traffic - the update. *J Cell Sci*, 128, 839-52.
- DEDOVA, T., BRAICU, E. I., SEHOULI, J. & BLANCHARD, V. 2019. Sialic Acid Linkage Analysis Refines the Diagnosis of Ovarian Cancer. *Front Oncol*, 9, 261.
- DEKKERS, G., RISPENS, T. & VIDARSSON, G. 2018. Novel Concepts of Altered Immunoglobulin G Galactosylation in Autoimmune Diseases. *Front Immunol*, 9, 553.
- DEL RE, D. P., MIYAMOTO, S. & BROWN, J. H. 2008. Focal adhesion kinase as a RhoA-activable signaling scaffold mediating Akt activation and cardiomyocyte protection. *J Biol Chem*, 283, 35622-9.
- DEL REY, M. J., IZQUIERDO, E., CAJA, S., USATEGUI, A., SANTIAGO, B., GALINDO, M. & PABLOS, J. L. 2009. Human inflammatory synovial fibroblasts induce enhanced myeloid cell recruitment and angiogenesis through a hypoxia-inducible transcription factor 1 α /vascular endothelial growth factor-mediated pathway in immunodeficient mice. *Arthritis Rheum*, 60, 2926-34.
- DENG, X., ZHANG, J., LIU, Y., CHEN, L. & YU, C. 2017. TNF- α regulates the proteolytic degradation of ST6Gal-1 and endothelial cell-cell junctions through upregulating expression of BACE1. *Sci Rep*, 7, 40256.
- DENNIS, G., JR., HOLWEG, C. T., KUMMERFELD, S. K., CHOY, D. F., SETIADI, A. F., HACKNEY, J. A., HAVERTY, P. M., GILBERT, H., LIN, W. Y., DIEHL, L., FISCHER, S., SONG, A., MUSSELMAN, D., KLEARMAN, M., GABAY, C., KAVANAUGH, A., ENDRES, J., FOX, D. A., MARTIN, F. & TOWNSEND, M. J. 2014. Synovial phenotypes in rheumatoid arthritis correlate with response to biologic therapeutics. *Arthritis Res Ther*, 16, R90.
- DEON, D., AHMED, S., TAI, K., SCALETTA, N., HERRERO, C., LEE, I. H., KRAUSE, A. & IVASHKIV, L. B. 2001. Cross-talk between IL-1 and IL-6 signaling pathways in rheumatoid arthritis synovial fibroblasts. *J Immunol*, 167, 5395-403.
- DIMBERG, A. 2010. Chemokines in angiogenesis. *Curr Top Microbiol Immunol*, 341, 59-80.
- DINITTO, J. P., CRONIN, T. C. & LAMBRIGHT, D. G. 2003. Membrane recognition and targeting by lipid-binding domains. *Sci STKE*, 2003, re16.
- DINITTO, J. P., DELPRATO, A., GABE LEE, M. T., CRONIN, T. C., HUANG, S., GUILHERME, A., CZECH, M. P. & LAMBRIGHT, D. G. 2007. Structural basis and mechanism of autoregulation in 3-phosphoinositide-dependent Grp1 family Arf GTPase exchange factors. *Mol Cell*, 28, 569-83.
- DONLIN, L. T., JAYATILLEKE, A., GIANOPOULOU, E. G., KALLIOLIAS, G. D. & IVASHKIV, L. B. 2014. Modulation of TNF-induced macrophage polarization by synovial fibroblasts. *J Immunol*, 193, 2373-83.
- DOODY, K. M., STANFORD, S. M., SACCHETTI, C., SVENSSON, M. N., COLES, C. H., MITAKIDIS, N., KIOSSES, W. B., BARTOK, B., FOS, C., CORY, E., SAH, R. L., LIU-BRYAN, R., BOYLE, D. L., ARNETT, H. A., MUSTELIN, T., CORR, M., ESKO, J. D., TREMBLAY, M. L., FIRESTEIN, G. S., ARICESCU, A. R. & BOTTINI, N. 2015. Targeting phosphatase-dependent proteoglycan switch for rheumatoid arthritis therapy. *Sci Transl Med*, 7, 288ra76.
- DORST, D. N., RIJPKEMA, M., BOSS, M., WALGREEN, B., HELSEN, M. M. A., BOS, D. L., BROM, M., KLEIN, C., LAVERMAN, P., VAN DER KRAAN, P. M., GOTTHARDT, M., KOENDERS, M. I. & BUITINGA, M. 2020. Targeted

- photodynamic therapy selectively kills activated fibroblasts in experimental arthritis. *Rheumatology*, 59, 3952-3960.
- DUAN, S., KOZIOL-WHITE, C. J., JESTER, W. F., JR., SMITH, S. A., NYCHOLAT, C. M., MACAULEY, M. S., PANETTIERI, R. A., JR. & PAULSON, J. C. 2019. CD33 recruitment inhibits IgE-mediated anaphylaxis and desensitizes mast cells to allergen. *J Clin Invest*, 129, 1387-1401.
- DUNPHY, J. L., MORAVEC, R., LY, K., LASELL, T. K., MELANCON, P. & CASANOVA, J. E. 2006. The Arf6 GEF GEP100/BRAG2 regulates cell adhesion by controlling endocytosis of beta1 integrins. *Curr Biol*, 16, 315-20.
- ELEFTHERIOU, P., KYNIGOPOULOS, S., GIOVOU, A., MAZMANIDI, A., YOVOS, J., SKEPASTIANOS, P., VAGDATLI, E., PETROU, C., PAPARA, D. & EFTERPIOU, M. 2014. Prevalence of anti-Neu5Gc antibodies in patients with hypothyroidism. *Biomed Res Int*, 2014, 963230.
- ELLIES, L. G., SPERANDIO, M., UNDERHILL, G. H., YOUSIF, J., SMITH, M., PRIATEL, J. J., KANSAS, G. S., LEY, K. & MARTH, J. D. 2002. Sialyltransferase specificity in selectin ligand formation. *Blood*, 100, 3618-25.
- ELLIS, I. R., JONES, S. J., LINDSAY, Y., OHE, G., SCHOR, A. M., SCHOR, S. L. & LESLIE, N. R. 2010. Migration Stimulating Factor (MSF) promotes fibroblast migration by inhibiting AKT. *Cell Signal*, 22, 1655-9.
- EWERT, P., AGUILERA, S., ALLIENDE, C., KWON, Y. J., ALBORNOZ, A., MOLINA, C., URZÚA, U., QUEST, A. F., OLEA, N., PÉREZ, P., CASTRO, I., BARRERA, M. J., ROMO, R., HERMOSO, M., LEYTON, C. & GONZÁLEZ, M. J. 2010. Disruption of tight junction structure in salivary glands from Sjögren's syndrome patients is linked to proinflammatory cytokine exposure. *Arthritis Rheum*, 62, 1280-9.
- FANG, X. Q., LIU, X. F., YAO, L., CHEN, C. Q., LIN, J. F., GU, Z. D., NI, P. H., ZHENG, X. M. & FAN, Q. S. 2015. Focal adhesion kinase regulates the phosphorylation protein tyrosine phosphatase- α at Tyr789 in breast cancer cells. *Mol Med Rep*, 11, 4303-4308.
- FERRO, F., ELEFANTE, E., LUCIANO, N., TALARICO, R. & TODOERTI, M. 2017. One year in review 2017: novelties in the treatment of rheumatoid arthritis. *Clin Exp Rheumatol*, 35, 721-734.
- FESSLER, M. B., ARNDT, P. G., JUST, I., NICK, J. A., MALCOLM, K. C. & SCOTT WORTHEN, G. 2006. Dual role for RhoA in suppression and induction of cytokines in the human neutrophil. *Blood*, 109, 1248-1256.
- FILER, A. 2013. The fibroblast as a therapeutic target in rheumatoid arthritis. *Curr Opin Pharmacol*, 13, 413-9.
- FILER, A., BIK, M., PARSONAGE, G. N., FITTON, J., TREBILCOCK, E., HOWLETT, K., COOK, M., RAZA, K., SIMMONS, D. L., THOMAS, A. M., SALMON, M., SCHEEL-TOELLNER, D., LORD, J. M., RABINOVICH, G. A. & BUCKLEY, C. D. 2009. Galectin 3 induces a distinctive pattern of cytokine and chemokine production in rheumatoid synovial fibroblasts via selective signaling pathways. *Arthritis Rheum*, 60, 1604-14.
- FINCH, R., SOSTELLY, A., SUE-LING, K., BLAEUER, A., DUCHATEAU-NGUYEN, G., UKARMA, L., PETRY, C., RAVVA, P., VILLIGER, P. & JUNKER, U. 2019. OP0224 RESULTS OF A PHASE 2 STUDY OF RG6125, AN ANTI-CADHERIN-11 MONOCLONAL ANTIBODY, IN RHEUMATOID ARTHRITIS PATIENTS WITH AN INADEQUATE RESPONSE TO ANTI-TNFA THERAPY. *Annals of the Rheumatic Diseases*, 78, 189.
- FIRESTEIN, G. S. 1996. Invasive fibroblast-like synoviocytes in rheumatoid arthritis. Passive responders or transformed aggressors? *Arthritis Rheum*, 39, 1781-90.

- FIRESTEIN, G. S. 2003. Evolving concepts of rheumatoid arthritis. *Nature*, 423, 356-61.
- FIRESTEIN, G. S. 2017. Chapter 69 - Etiology and Pathogenesis of Rheumatoid Arthritis. In: FIRESTEIN, G. S., BUDD, R. C., GABRIEL, S. E., MCINNES, I. B. & O'DELL, J. R. (eds.) *Kelley and Firestein's Textbook of Rheumatology (Tenth Edition)*. Elsevier.
- FOSTER, S. L. & MEDZHITOV, R. 2009. Gene-specific control of the TLR-induced inflammatory response. *Clin Immunol*, 130, 7-15.
- FRANK, S. R., HATFIELD, J. C. & CASANOVA, J. E. 1998. Remodeling of the actin cytoskeleton is coordinately regulated by protein kinase C and the ADP-ribosylation factor nucleotide exchange factor ARNO. *Mol Biol Cell*, 9, 3133-46.
- FRANK-BERTONCELJ, M., TRENMANN, M., KLEIN, K., KAROUZAKIS, E., REHRAUER, H., BRATUS, A., KOLLING, C., ARMAKA, M., FILER, A., MICHEL, B. A., GAY, R. E., BUCKLEY, C. D., KOLLIAS, G., GAY, S. & OSPELT, C. 2017. Epigenetically-driven anatomical diversity of synovial fibroblasts guides joint-specific fibroblast functions. *Nat Commun*, 8, 14852.
- FREUNDLICH, B., BOMALASKI, J. S., NEILSON, E. & JIMENEZ, S. A. 1986. Regulation of fibroblast proliferation and collagen synthesis by cytokines. *Immunol Today*, 7, 303-7.
- FUKUI, Y., HASHIMOTO, O., SANUI, T., OONO, T., KOGA, H., ABE, M., INAYOSHI, A., NODA, M., OIKE, M., SHIRAI, T. & SASAZUKI, T. 2001. Haematopoietic cell-specific CDM family protein DOCK2 is essential for lymphocyte migration. *Nature*, 412, 826-31.
- GEE, K., KOZLOWSKI, M. & KUMAR, A. 2003. Tumor necrosis factor-alpha induces functionally active hyaluronan-adhesive CD44 by activating sialidase through p38 mitogen-activated protein kinase in lipopolysaccharide-stimulated human monocytic cells. *J Biol Chem*, 278, 37275-87.
- GENTILINI, D., BUSACCA, M., DI FRANCESCO, S., VIGNALI, M., VIGANO, P. & DI BLASIO, A. M. 2007. PI3K/Akt and ERK1/2 signalling pathways are involved in endometrial cell migration induced by 17beta-estradiol and growth factors. *Mol Hum Reprod*, 13, 317-22.
- GOLDFINGER, L. E., HAN, J., KIOSSES, W. B., HOWE, A. K. & GINSBERG, M. H. 2003. Spatial restriction of alpha4 integrin phosphorylation regulates lamellipodial stability and alpha4beta1-dependent cell migration. *J Cell Biol*, 162, 731-41.
- GOODRIDGE, H. S., MARSHALL, F. A., ELSE, K. J., HOUSTON, K. M., EGAN, C., AL-RIYAMI, L., LIEW, F. Y., HARNETT, W. & HARNETT, M. M. 2005. Immunomodulation via novel use of TLR4 by the filarial nematode phosphorylcholine-containing secreted product, ES-62. *J Immunol*, 174, 284-93.
- GOODRIDGE, H. S., MCGUINNESS, S., HOUSTON, K. M., EGAN, C. A., AL-RIYAMI, L., ALCOCER, M. J., HARNETT, M. M. & HARNETT, W. 2007. Phosphorylcholine mimics the effects of ES-62 on macrophages and dendritic cells. *Parasite Immunol*, 29, 127-37.
- GRANT, W. B. 2000. The role of meat in the expression of rheumatoid arthritis. *Br J Nutr*, 84, 589-95.
- GRAVALLESE, E. M. 2002. Bone destruction in arthritis. *Annals of the Rheumatic Diseases*, 61, ii84.
- GU, G., CHEN, Y., DUAN, C., ZHOU, L., CHEN, C., CHEN, J., CHENG, J., SHI, N., JIN, Y., XI, Q. & ZHONG, J. 2017. Overexpression of ARF1 is associated with cell proliferation and migration through PI3K signal pathway in ovarian cancer. *Oncol Rep*, 37, 1511-1520.

- GUERRERO, P. E., MIRO, L., WONG, B. S., MASSAGUER, A., MARTINEZ-BOSCH, N., LLORENS, R., NAVARRO, P., KONSTANTOPOULOS, K., LLOP, E. & PERACAUOLA, R. 2020a. Knockdown of alpha2,3-Sialyltransferases Impairs Pancreatic Cancer Cell Migration, Invasion and E-selectin-Dependent Adhesion. *Int J Mol Sci*, 21.
- GUERRERO, P. E., MIRÓ, L., WONG, B. S., MASSAGUER, A., MARTÍNEZ-BOSCH, N., LLORENS, R., NAVARRO, P., KONSTANTOPOULOS, K., LLOP, E. & PERACAUOLA, R. 2020b. Knockdown of α 2,3-Sialyltransferases Impairs Pancreatic Cancer Cell Migration, Invasion and E-selectin-Dependent Adhesion. *Int J Mol Sci*, 21.
- GUMBINER, B. M. 1996. Cell adhesion: the molecular basis of tissue architecture and morphogenesis. *Cell*, 84, 345-57.
- HANASAKI, K., VARKI, A. & POWELL, L. D. 1995. CD22-mediated cell adhesion to cytokine-activated human endothelial cells. Positive and negative regulation by alpha 2-6-sialylation of cellular glycoproteins. *J Biol Chem*, 270, 7533-42.
- HANASAKI, K., VARKI, A., STAMENKOVIC, I. & BEVILACQUA, M. P. 1994. Cytokine-induced beta-galactoside alpha-2,6-sialyltransferase in human endothelial cells mediates alpha 2,6-sialylation of adhesion molecules and CD22 ligands. *J Biol Chem*, 269, 10637-43.
- HANKITTICHAJ, P., LOU, H. J., WIKAN, N., SMITH, D. R., POTIKANOND, S. & NIMLAMOOL, W. 2020. Oxyresveratrol Inhibits IL-1beta-Induced Inflammation via Suppressing AKT and ERK1/2 Activation in Human Microglia, HMC3. *Int J Mol Sci*, 21.
- HARDUIN-LEPERS, A., MOLLICONE, R., DELANNOY, P. & ORIOL, R. 2005. The animal sialyltransferases and sialyltransferase-related genes: a phylogenetic approach. *Glycobiology*, 15, 805-817.
- HARDY, R. S., HÜLSO, C., LIU, Y., GASPARINI, S. J., FONG-YEE, C., TU, J., STONER, S., STEWART, P. M., RAZA, K., COOPER, M. S., SEIBEL, M. J. & ZHOU, H. 2013. Characterisation of fibroblast-like synoviocytes from a murine model of joint inflammation. *Arthritis Res Ther*, 15, R24.
- HARRISON, M. J., KIM, C. A., SILVERBERG, M. & PAGET, S. A. 2005. Does age bias the aggressive treatment of elderly patients with rheumatoid arthritis? *J Rheumatol*, 32, 1243-8.
- HASHIMOTO, S., ONODERA, Y., HASHIMOTO, A., TANAKA, M., HAMAGUCHI, M., YAMADA, A. & SABE, H. 2004. Requirement for Arf6 in breast cancer invasive activities. *Proc Natl Acad Sci U S A*, 101, 6647-52.
- HASSA, P. O., HAENNI, S. S., ELSER, M. & HOTTIGER, M. O. 2006. Nuclear ADP-ribosylation reactions in mammalian cells: where are we today and where are we going? *Microbiol Mol Biol Rev*, 70, 789-829.
- HASTINGS, J. F., SKHINAS, J. N., FEY, D., CROUCHER, D. R. & COX, T. R. 2019. The extracellular matrix as a key regulator of intracellular signalling networks. *Br J Pharmacol*, 176, 82-92.
- HAUSELMANN, I. & BORSIG, L. 2014. Altered tumor-cell glycosylation promotes metastasis. *Front Oncol*, 4, 28.
- HEDLUND, M., PADLER-KARAVANI, V., VARKI, N. M. & VARKI, A. 2008. Evidence for a human-specific mechanism for diet and antibody-mediated inflammation in carcinoma progression. *Proc Natl Acad Sci U S A*, 105, 18936-41.
- HEDSTRÖM, A. K., STAWIARZ, L., KLARESKOG, L. & ALFREDSSON, L. 2018. Smoking and susceptibility to rheumatoid arthritis in a Swedish population-based case-control study. *Eur J Epidemiol*, 33, 415-423.

- HERNÁNDEZ-ALCOCEBA, R., DEL PESO, L. & LACAL, J. C. 2000. The Ras family of GTPases in cancer cell invasion. *Cell Mol Life Sci*, 57, 65-76.
- HEUN, Y., GRÖFF, P., LAGARA, A., SCHELHORN, R., METTLER, R., POHL, U. D. I. & MANNELL, H. 2020. The GEF Cytohesin-2/ARNO Mediates Resistin induced Phenotypic Switching in Vascular Smooth Muscle Cells. *Scientific Reports*, 10.
- HIGASHI, H., NISHI, Y., FUKUI, Y., IKUTA, K., UEDA, S., KATO, S., FUJITA, M., NAKANO, Y., TAGUCHI, T., SAKAI, S. & ET AL. 1984. Tumor-associated expression of glycosphingolipid Hanganutziu-Deicher antigen in human cancers. *Gan*, 75, 1025-9.
- HIGUCHI, M., KIHARA, R., OKAZAKI, T., AOKI, I., SUETSUGU, S. & GOTOH, Y. 2013. Akt1 promotes focal adhesion disassembly and cell motility through phosphorylation of FAK in growth factor-stimulated cells. *J Cell Sci*, 126, 745-55.
- HILLEN, J., GEYER, C., HEITZMANN, M., BECKMANN, D., KRAUSE, A., WINKLER, I., PAVENSTÄDT, H., BREMER, C., PAP, T. & KORB-PAP, A. 2017. Structural cartilage damage attracts circulating rheumatoid arthritis synovial fibroblasts into affected joints. *Arthritis Research & Therapy*, 19, 40.
- HIRABAYASHI, Y., HIGASHI, H., KATO, S., TANIGUCHI, M. & MATSUMOTO, M. 1987a. Occurrence of tumor-associated ganglioside antigens with Hanganutziu-Deicher antigenic activity on human melanomas. *Jpn J Cancer Res*, 78, 614-20.
- HIRABAYASHI, Y., KASAKURA, H., MATSUMOTO, M., HIGASHI, H., KATO, S., KASAI, N. & NAIKI, M. 1987b. Specific expression of unusual GM2 ganglioside with Hanganutziu-Deicher antigen activity on human colon cancers. *Jpn J Cancer Res*, 78, 251-60.
- HOFFMANN, M. & SCHWARZ, U. S. 2013. A kinetic model for RNA-interference of focal adhesions. *BMC Systems Biology*, 7, 2.
- HOLDBROOKS, A. T., ANKENBAUER, K. E., HWANG, J. & BELLIS, S. L. 2020. Regulation of inflammatory signaling by the ST6Gal-I sialyltransferase. *PLoS One*, 15, e0241850.
- HOLMDAHL, R., ANDERSSON, M. E., GOLDSCHMIDT, T. J., JANSSON, L., KARLSSON, M., MALMSTRÖM, V. & MO, J. 1989. Collagen induced arthritis as an experimental model for rheumatoid arthritis. Immunogenetics, pathogenesis and autoimmunity. *Apmis*, 97, 575-84.
- HONDA, A., NOGAMI, M., YOKOZEKI, T., YAMAZAKI, M., NAKAMURA, H., WATANABE, H., KAWAMOTO, K., NAKAYAMA, K., MORRIS, A. J., FROHMAN, M. A. & KANAHO, Y. 1999. Phosphatidylinositol 4-phosphate 5-kinase alpha is a downstream effector of the small G protein ARF6 in membrane ruffle formation. *Cell*, 99, 521-32.
- HONDA, A., NOGAMI, M., YOKOZEKI, T., YAMAZAKI, M., NAKAMURA, H., WATANABE, H., KAWAMOTO, K., NAKAYAMA, K., MORRIS, A.J., FROHMAN, M.A. & KANAHO 1999. Phosphatidylinositol 4-Phosphate 5-Kinase a Is a Downstream Effector of the Small G Protein ARF6 in Membrane Ruffle Formation. *cell*, 99, 521-532.
- HORNG, T., BARTON, G. M., FLAVELL, R. A. & MEDZHITOV, R. 2002. The adaptor molecule TIRAP provides signalling specificity for Toll-like receptors. *Nature*, 420, 329-33.
- HORZUM, U., OZDIL, B. & PESEN-OKVUR, D. 2014. Step-by-step quantitative analysis of focal adhesions. *MethodsX*, 1, 56-9.
- HSU, C. C., LIN, T. W., CHANG, W. W., WU, C. Y., LO, W. H., WANG, P. H. & TSAI, Y. C. 2005. Soyasaponin-I-modified invasive behavior of cancer by changing cell surface sialic acids. *Gynecol Oncol*, 96, 415-22.

- HUBER, L. C., DISTLER, O., TARNER, I., GAY, R. E., GAY, S. & PAP, T. 2006. Synovial fibroblasts: key players in rheumatoid arthritis. *Rheumatology (Oxford)*, 45, 669-75.
- HUGHES, R. C. 2001. Galectins as modulators of cell adhesion. *Biochimie*, 83, 667-76.
- HUMPHREYS, D., DAVIDSON, A. C., HUME, P. J., MAKIN, L. E. & KORONAKIS, V. 2013. Arf6 coordinates actin assembly through the WAVE complex, a mechanism usurped by Salmonella to invade host cells. *Proc Natl Acad Sci U S A*, 110, 16880-5.
- ISHCHENKO, A. & LORIES, R. J. 2016. Safety and Efficacy of Biological Disease-Modifying Antirheumatic Drugs in Older Rheumatoid Arthritis Patients: Staying the Distance. *Drugs Aging*, 33, 387-98.
- ISHIBE, S., JOLY, D., LIU, Z. X. & CANTLEY, L. G. 2004. Paxillin serves as an ERK-regulated scaffold for coordinating FAK and Rac activation in epithelial morphogenesis. *Mol Cell*, 16, 257-67.
- ITO, A., FUKAYA, M., SAEGUSA, S., KOBAYASHI, E., SUGAWARA, T., HARA, Y., YAMAUCHI, J., OKAMOTO, H. & SAKAGAMI, H. 2018. Pallidin is a novel interacting protein for cytohesin-2 and regulates the early endosomal pathway and dendritic formation in neurons. *J Neurochem*, 147, 153-177.
- IVETIC, A., HOSKINS GREEN, H. L. & HART, S. J. 2019. L-selectin: A Major Regulator of Leukocyte Adhesion, Migration and Signaling. *Front Immunol*, 10, 1068.
- IZQUIERDO, E., CANETE, J. D., CELIS, R., DEL REY, M. J., USATEGUI, A., MARSAL, S., SANMARTI, R., CRIADO, G. & PABLOS, J. L. 2011. Synovial fibroblast hyperplasia in rheumatoid arthritis: clinicopathologic correlations and partial reversal by anti-tumor necrosis factor therapy. *Arthritis Rheum*, 63, 2575-83.
- J J MURTAGH, JR., MOWATT, M. R., LEE, C. M., LEE, F. J., MISHIMA, K., NASH, T. E., MOSS, J. & VAUGHAN, M. 1992. Guanine nucleotide-binding proteins in the intestinal parasite *Giardia lamblia*. Isolation of a gene encoding an approximately 20-kDa ADP-ribosylation factor. *The Journal of biological chemistry*, 267, 9654-9662.
- JACKSON, C. L. & CASANOVA, J. E. 2000. Turning on ARF: the Sec7 family of guanine-nucleotide-exchange factors. *Trends Cell Biol*, 10, 60-7.
- JACKSON, J. R., MINTON, J. A., HO, M. L., WEI, N. & WINKLER, J. D. 1997. Expression of vascular endothelial growth factor in synovial fibroblasts is induced by hypoxia and interleukin 1beta. *J Rheumatol*, 24, 1253-9.
- JANDUS, C., BOLIGAN, K. F., CHIJIJOKE, O., LIU, H., DAHLHAUS, M., DÉMOULINS, T., SCHNEIDER, C., WEHRLI, M., HUNGER, R. E., BAERLOCHER, G. M., SIMON, H.-U., ROMERO, P., MÜNZ, C. & VON GUNTEN, S. 2014a. Interactions between Siglec-7/9 receptors and ligands influence NK cell-dependent tumor immunosurveillance. *The Journal of Clinical Investigation*, 124, 1810-1820.
- JANDUS, C., BOLIGAN, K. F., CHIJIJOKE, O., LIU, H., DAHLHAUS, M., DÉMOULINS, T., SCHNEIDER, C., WEHRLI, M., HUNGER, R. E., BAERLOCHER, G. M., SIMON, H. U., ROMERO, P., MÜNZ, C. & VON GUNTEN, S. 2014b. Interactions between Siglec-7/9 receptors and ligands influence NK cell-dependent tumor immunosurveillance. *J Clin Invest*, 124, 1810-20.
- JAY, G. D., BRITT, D. E. & CHA, C. J. 2000. Lubricin is a product of megakaryocyte stimulating factor gene expression by human synovial fibroblasts. *J Rheumatol*, 27, 594-600.
- JIN, J., LI, J., GAN, Y., LIU, J., ZHAO, X., CHEN, J., ZHANG, R., ZHONG, Y., CHEN, X., WU, L., XIANG, X., ZHOU, Y., HE, J., GUO, J., LIU, X. & LI, Z.

2021. Red meat intake is associated with early onset of rheumatoid arthritis: a cross-sectional study. *Scientific Reports*, 11, 5681.
- JONES, C., VIRJI, M. & CROCKER, P. R. 2003. Recognition of sialylated meningococcal lipopolysaccharide by siglecs expressed on myeloid cells leads to enhanced bacterial uptake. *Mol Microbiol*, 49, 1213-25.
- JOOSTEN, L. A., HELSEN, M. M., VAN DE LOO, F. A. & VAN DEN BERG, W. B. 1996. Anticytokine treatment of established type II collagen-induced arthritis in DBA/1 mice. A comparative study using anti-TNF alpha, anti-IL-1 alpha/beta, and IL-1Ra. *Arthritis Rheum*, 39, 797-809.
- KAGAN, J. C. & MEDZHITOV, R. 2006. Phosphoinositide-mediated adaptor recruitment controls Toll-like receptor signaling. *Cell*, 125, 943-55.
- KAHN, R. A., CHERFILS, J., ELIAS, M., LOVERING, R. C., MUNRO, S. & SCHURMANN, A. 2006. Nomenclature for the human Arf family of GTP-binding proteins: ARF, ARL, and SAR proteins. *J Cell Biol*, 172, 645-50.
- KAROUZAKIS, E., GAY, R. E., MICHEL, B. A., GAY, S. & NEIDHART, M. 2009. DNA hypomethylation in rheumatoid arthritis synovial fibroblasts. *Arthritis Rheum*, 60, 3613-22.
- KAWACHI, S., SAIDA, T., UHARA, H., UEMURA, K. I., TAKETOMI, T. & KANO, K. 1988. Heterophile Hanganutziu-Deicher Antigen in Ganglioside Fractions of Human Melanoma Tissues. *International Archives of Allergy and Immunology*, 85, 381-383.
- KAWASHIMA, H., PETRYNIAK, B., HIRAOKA, N., MITOMA, J., HUCKABY, V., NAKAYAMA, J., UCHIMURA, K., KADOMATSU, K., MURAMATSU, T., LOWE, J. B. & FUKUDA, M. 2005. N-acetylglucosamine-6-O-sulfotransferases 1 and 2 cooperatively control lymphocyte homing through L-selectin ligand biosynthesis in high endothelial venules. *Nature Immunology*, 6, 1096-1104.
- KAY, J. & CALABRESE, L. 2004. The role of interleukin-1 in the pathogenesis of rheumatoid arthritis. *Rheumatology (Oxford)*, 43 Suppl 3, iii2-iii9.
- KEELY, P. J., WESTWICK, J. K., WHITEHEAD, I. P., DER, C. J. & PARISE, L. V. 1997. Cdc42 and Rac1 induce integrin-mediated cell motility and invasiveness through PI(3)K. *Nature (London)*, 390, 632-636.
- KELM, S., PELZ, A., SCHAUER, R., FILBIN, M. T., TANG, S., DE BELLARD, M. E., SCHNAAR, R. L., MAHONEY, J. A., HARTNELL, A., BRADFIELD, P. & ET AL. 1994. Sialoadhesin, myelin-associated glycoprotein and CD22 define a new family of sialic acid-dependent adhesion molecules of the immunoglobulin superfamily. *Curr Biol*, 4, 965-72.
- KEMMNER, W., MORGENTHALER, J. & BROSSMER, R. 1992. Alterations in cell surface carbohydrate composition of a human colon carcinoma cell line affect adhesion to extracellular matrix components. *Biochimie*, 74, 117-22.
- KHATUA, B., GHOSHAL, A., BHATTACHARYA, K., MANDAL, C., SAHA, B., CROCKER, P. R. & MANDAL, C. 2010. Sialic acids acquired by *Pseudomonas aeruginosa* are involved in reduced complement deposition and siglec mediated host-cell recognition. *FEBS Lett*, 584, 555-61.
- KHERADMAND, F., WERNER, E., TREMBLE, P., SYMONS, M. & WERB, Z. 1998. Role of Rac1 and oxygen radicals in collagenase-1 expression induced by cell shape change. *Science*, 280, 898-902.
- KIM, M. J., KIM, H., LEE, S. H., GU, D. R., LEE, S. Y., LEE, K. & JEONG, D. 2015. ADP-Ribosylation Factor 1 Regulates Proliferation, Migration, and Fusion in Early Stage of Osteoclast Differentiation. *Int J Mol Sci*, 16, 29305-14.
- KIM, Y. H., CHOI, K. H., PARK, J. W. & KWON, T. K. 2005. LY294002 inhibits LPS-induced NO production through a inhibition of NF-kappaB activation:

- independent mechanism of phosphatidylinositol 3-kinase. *Immunol Lett*, 99, 45-50.
- KLARLUND, J. K., TSIARAS, W., HOLIK, J. J., CHAWLA, A. & CZECH, M. P. 2000. Distinct polyphosphoinositide binding selectivities for pleckstrin homology domains of GRP1-like proteins based on diglycine versus triglycine motifs. *J Biol Chem*, 275, 32816-21.
- KLEIN, K., FRANK-BERTONCELJ, M., KAROUZAKIS, E., GAY, R. E., KOLLING, C., CIUREA, A., BOSTANCI, N., BELIBASAKIS, G. N., LIN, L. L., DISTLER, O., GAY, S. & OSPELT, C. 2017. The epigenetic architecture at gene promoters determines cell type-specific LPS tolerance. *J Autoimmun*, 83, 122-133.
- KLEIN, K., GAY, R. E., KOLLING, C., LIN, L. L., BOSTANCI, N., BELIBASAKIS, G., MICHEL, B. A., GAY, S. & OSPELT, C. 2016. SAT0024 Epigenetic Analysis of Lps-Induced Tolerance in Rheumatoid Arthritis Synovial Fibroblasts and Macrophages. *Annals of the Rheumatic Diseases*, 75, 672.
- KLEMKE, R. L., CAI, S., GIANNINI, A. L., GALLAGHER, P. J., DE LANEROLLE, P. & CHERESH, D. A. 1997. Regulation of cell motility by mitogen-activated protein kinase. *J Cell Biol*, 137, 481-92.
- KOBSAR, I., OETKE, C., KRONER, A., WESSIG, C., CROCKER, P. & MARTINI, R. 2006. Attenuated demyelination in the absence of the macrophage-restricted adhesion molecule sialoadhesin (Siglec-1) in mice heterozygously deficient in P0. *Molecular and Cellular Neuroscience*, 31, 685-691.
- KONDO, Y., HANAI, A., NAKAI, W., KATOH, Y., NAKAYAMA, K. & SHIN, H. W. 2012. ARF1 and ARF3 are required for the integrity of recycling endosomes and the recycling pathway. *Cell Struct Funct*, 37, 141-54.
- KOORELLA, C., NAIR, J. R., MURRAY, M. E., CARLSON, L. M., WATKINS, S. K. & LEE, K. P. 2014. Novel regulation of CD80/CD86-induced phosphatidylinositol 3-kinase signaling by NOTCH1 protein in interleukin-6 and indoleamine 2,3-dioxygenase production by dendritic cells. *J Biol Chem*, 289, 7747-62.
- KREMER, J. M., WESTHOVENS, R., LEON, M., DI GIORGIO, E., ALTEN, R., STEINFELD, S., RUSSELL, A., DOUGADOS, M., EMERY, P., NUAMAH, I. F., WILLIAMS, G. R., BECKER, J. C., HAGERTY, D. T. & MORELAND, L. W. 2003. Treatment of rheumatoid arthritis by selective inhibition of T-cell activation with fusion protein CTLA4Ig. *N Engl J Med*, 349, 1907-15.
- KRICK, S., HELTON, E. S., EASTER, M., BOLLENBECKER, S., DENSON, R., ZAHARIAS, R., COCHRAN, P., VANG, S., HARRIS, E., WELLS, J. M. & BARNES, J. W. 2021. ST6GAL1 and alpha2-6 Sialylation Regulates IL-6 Expression and Secretion in Chronic Obstructive Pulmonary Disease. *Front Immunol*, 12, 693149.
- KROCK, B. L., SKULI, N. & SIMON, M. C. 2011. Hypoxia-induced angiogenesis: good and evil. *Genes Cancer*, 2, 1117-33.
- KUCUKURAL, A., YUKSELEN, O., OZATA, D. M., MOORE, M. J. & GARBER, M. 2019. DEBrowser: interactive differential expression analysis and visualization tool for count data. *BMC Genomics*, 20, 6.
- KULKA, J. P., BOCKING, D., ROPES, M. W. & BAUER, W. 1955. Early joint lesions of rheumatoid arthritis; report of eight cases, with knee biopsies of lesions of less than one year's duration. *AMA Arch Pathol*, 59, 129-50.
- KWAN TAT, S., AMIABLE, N., PELLETIER, J. P., BOILEAU, C., LAJEUNESSE, D., DUVAL, N. & MARTEL-PELLETIER, J. 2009. Modulation of OPG, RANK and RANKL by human chondrocytes and their implication during osteoarthritis. *Rheumatology (Oxford)*, 48, 1482-90.

- KWIATKOWSKA, A., KIJEWSKA, M., LIPKO, M., HIBNER, U. & KAMINSKA, B. 2011. Downregulation of Akt and FAK phosphorylation reduces invasion of glioblastoma cells by impairment of MT1-MMP shuttling to lamellipodia and downregulates MMPs expression. *Biochimica et Biophysica Acta (BBA) - Molecular Cell Research*, 1813, 655-667.
- LAFYATIS, R., REMMERS, E. F., ROBERTS, A. B., YOCUM, D. E., SPORN, M. B. & WILDER, R. L. 1989. Anchorage-independent growth of synoviocytes from arthritic and normal joints. Stimulation by exogenous platelet-derived growth factor and inhibition by transforming growth factor-beta and retinoids. *J Clin Invest*, 83, 1267-76.
- LANDOLFI, N. F., LEONE, J. W., WOMACK, J. E. & COOK, R. G. 2004. Activation of T lymphocytes results in an increase in H-2-encoded neuraminidase. *Immunogenetics*, 22, 159-167.
- LAO, M., SHI, M., ZOU, Y., HUANG, M., YE, Y., QIU, Q., XIAO, Y., ZENG, S., LIANG, L., YANG, X. & XU, H. 2016. Protein Inhibitor of Activated STAT3 Regulates Migration, Invasion, and Activation of Fibroblast-like Synoviocytes in Rheumatoid Arthritis. *J Immunol*, 196, 596-606.
- LAUBLI, H. & BORSIG, L. 2019. Altered Cell Adhesion and Glycosylation Promote Cancer Immune Suppression and Metastasis. *Front Immunol*, 10, 2120.
- LAWSON, C. D. & BURRIDGE, K. 2014. The on-off relationship of Rho and Rac during integrin-mediated adhesion and cell migration. *Small GTPases*, 5, e27958.
- LEE, D. M., KIENER, H. P., AGARWAL, S. K., NOSS, E. H., WATTS, G. F., CHISAKA, O., TAKEICHI, M. & BRENNER, M. B. 2007. Cadherin-11 in synovial lining formation and pathology in arthritis. *Science*, 315, 1006-10.
- LEE, D. M. & WEINBLATT, M. E. 2001. Rheumatoid arthritis. *The Lancet (British edition)*, 358, 903.
- LEE, J. W., PAN, T., SUN, J., HU, J., HU, Y., ZHOU, J., CHEN, Z., XU, D., XU, W., ZHENG, S. & ZHANG, S. 2014. Cytohesins/ARNO: The Function in Colorectal Cancer Cells. *PLoS ONE*, 9.
- LEE, S., ISHITSUKA, A., KUROKI, T., LIN, Y. H., SHIBUYA, A., HONGU, T., FUNAKOSHI, Y., KANAHO, Y., NAGATA, K. & KAWAGUCHI, A. 2021. Arf6 exacerbates allergic asthma through cell-to-cell transmission of ASC inflammasomes. *JCI Insight*, 6.
- LEFEVRE, S., KNEDLA, A., TENNIE, C., KAMPMANN, A., WUNRAU, C., DINSER, R., KORB, A., SCHNAKER, E. M., TARNER, I. H., ROBBINS, P. D., EVANS, C. H., STURZ, H., STEINMEYER, J., GAY, S., SCHOLMERICH, J., PAP, T., MULLER-LADNER, U. & NEUMANN, E. 2009. Synovial fibroblasts spread rheumatoid arthritis to unaffected joints. *Nat Med*, 15, 1414-20.
- LEHMANN, F., TIRALONGO, E. & TIRALONGO, J. 2006. Sialic acid-specific lectins: occurrence, specificity and function. *Cell Mol Life Sci*, 63, 1331-54.
- LERNER, A., NEIDHÖFER, S., REUTER, S. & MATTHIAS, T. 2018. MMP3 is a reliable marker for disease activity, radiological monitoring, disease outcome predictability, and therapeutic response in rheumatoid arthritis. *Best Pract Res Clin Rheumatol*, 32, 550-562.
- LEY, K. 2003. The role of selectins in inflammation and disease. *Trends in Molecular Medicine*, 9, 263-268.
- LI, C. C., CHIANG, T. C., WU, T. S., PACHECO-RODRIGUEZ, G., MOSS, J. & LEE, F. J. 2007. ARL4D recruits cytohesin-2/ARNO to modulate actin remodeling. *Mol Biol Cell*, 18, 4420-37.
- LI, J., BALLIF, B. A., POWELKA, A. M., DAI, J., GYGI, S. P. & HSU, V. W. 2005. Phosphorylation of ACAP1 by Akt regulates the stimulation-dependent recycling of integrin beta1 to control cell migration. *Dev Cell*, 9, 663-73.

- LI, Y. & CHEN, X. 2012. Sialic acid metabolism and sialyltransferases: natural functions and applications. *Appl Microbiol Biotechnol*, 94, 887-905.
- LIANG, F., SEYRANTEPE, V., LANDRY, K., AHMAD, R., AHMAD, A., STAMATOS, N. M. & PSHEZHETSKY, A. V. 2006. Monocyte differentiation up-regulates the expression of the lysosomal sialidase, Neu1, and triggers its targeting to the plasma membrane via major histocompatibility complex class II-positive compartments. *J Biol Chem*, 281, 27526-38.
- LIANG, L. Q., HUANG, M. C., QIU, Q., XIAO, Y. J., SUN, M. Y., ZHAN, Z. P., YE, Y. J., FAN, J. J., YANG, X. Y. & XU, H. S. 2013. [Modulation of RhoA/Rho kinase on migration, invasion and proliferation of fibroblast like synoviocytes from patients with rheumatoid arthritis]. *Zhonghua Yi Xue Za Zhi*, 93, 1345-8.
- LIN, N. Y., BEYER, C., GIESSL, A., KIREVA, T., SCHOLTYSEK, C., UDERHARDT, S., MUNOZ, L. E., DEES, C., DISTLER, A., WIRTZ, S., KRÖNKE, G., SPENCER, B., DISTLER, O., SCHETT, G. & DISTLER, J. H. 2013. Autophagy regulates TNF α -mediated joint destruction in experimental arthritis. *Ann Rheum Dis*, 72, 761-8.
- LINOS, A., WORTHINGTON, J. W., O'FALLON, W. M. & KURLAND, L. T. 1980. The epidemiology of rheumatoid arthritis in Rochester, Minnesota: a study of incidence, prevalence, and mortality. *Am J Epidemiol*, 111, 87-98.
- LITHERLAND, G. J., DIXON, C., LAKEY, R. L., ROBSON, T., JONES, D., YOUNG, D. A., CAWSTON, T. E. & ROWAN, A. D. 2008. Synergistic collagenase expression and cartilage collagenolysis are phosphatidylinositol 3-kinase/Akt signaling-dependent. *J Biol Chem*, 283, 14221-9.
- LIU, S., CAO, C., ZHANG, Y., LIU, G., REN, W., YE, Y. & SUN, T. 2019. PI3K/Akt inhibitor partly decreases TNF- α -induced activation of fibroblast-like synoviocytes in osteoarthritis. *J Orthop Surg Res*, 14, 425.
- LIU, Y., PAN, Y. F., XUE, Y. Q., FANG, L. K., GUO, X. H., GUO, X., LIU, M., MO, B. Y., YANG, M. R., LIU, F., WU, Y. T., OLSEN, N. & ZHENG, S. G. 2018. uPAR promotes tumor-like biologic behaviors of fibroblast-like synoviocytes through PI3K/Akt signaling pathway in patients with rheumatoid arthritis. *Cell Mol Immunol*, 15, 171-181.
- LONDON, N. R., JR., THARAKAN, A., SMITH, A., THOMAS, K. R., ZHU, W., ODELBERG, S. J., RAMANATHAN, M., JR. & LANE, A. P. 2021. Deletion of Arno Reduces Eosinophilic Inflammation and Interleukin-5 Expression in a Murine Model of Rhinitis. *Ear Nose Throat J*, 145561320986055.
- LOWIN, T., STRAUB, R. H., NEUMANN, E., BOSSERHOFF, A., VOGEL, C., MOISSL, C., ANDERS, S., MÜLLER-LADNER, U. & SCHEDEL, J. 2009. Glucocorticoids increase α 5 integrin expression and adhesion of synovial fibroblasts but inhibit ERK signaling, migration, and cartilage invasion. *Arthritis Rheum*, 60, 3623-32.
- LUCHSINGER, C., AGUILAR, M., BURGOS, P. V., EHRENFELD, P. & MARDONES, G. A. 2018. Functional disruption of the Golgi apparatus protein ARF1 sensitizes MDA-MB-231 breast cancer cells to the antitumor drugs Actinomycin D and Vinblastine through ERK and AKT signaling. *PLoS One*, 13, e0195401.
- LUONG, P., HEDL, M., YAN, J., ZUO, T., FU, T. M., JIANG, X., THIAGARAJAH, J. R., HANSEN, S. H., LESSER, C. F., WU, H., ABRAHAM, C. & LENCER, W. I. 2018. INAVA-ARNO complexes bridge mucosal barrier function with inflammatory signaling. *Elife*, 7.
- LV, Q., ZHU, X.-Y., XIA, Y.-F., DAI, Y. & WEI, Z.-F. 2015. Tetrandrine inhibits migration and invasion of rheumatoid arthritis fibroblast-like synoviocytes through down-regulating the expressions of Rac1, Cdc42, and RhoA

- GTPases and activation of the PI3K/Akt and JNK signaling pathways. *Chinese Journal of Natural Medicines*, 13, 831-841.
- MACAULEY, M. S., CROCKER, P. R. & PAULSON, J. C. 2014. Siglec-mediated regulation of immune cell function in disease. *Nature Reviews Immunology*, 14, 653-666.
- MACGREGOR, A. J., SNIEDER, H., RIGBY, A. S., KOSKENVUO, M., KAPRIO, J., AHO, K. & SILMAN, A. J. 2000. Characterizing the quantitative genetic contribution to rheumatoid arthritis using data from twins. *Arthritis & Rheumatism: Official Journal of the American College of Rheumatology*, 43, 30-37.
- MACIA, E., PARTISANI, M., PALEOTTI, O., LUTON, F. & FRANCO, M. 2012. Arf6 negatively controls the rapid recycling of the β_2 adrenergic receptor. *J Cell Sci*, 125, 4026-35.
- MAIA, M., DE VRIESE, A., JANSSENS, T., MOONS, M., VAN LANDUYT, K., TAVERNIER, J., LORIES, R. J. & CONWAY, E. M. 2010. CD248 and its cytoplasmic domain: a therapeutic target for arthritis. *Arthritis Rheum*, 62, 3595-606.
- MAIRA, S. M., STAUFFER, F., SCHNELL, C. & GARCÍA-ECHEVERRÍA, C. 2009. PI3K inhibitors for cancer treatment: where do we stand? *Biochem Soc Trans*, 37, 265-72.
- MANNELL, H. K., PIRCHER, J., CHAUDHRY, D. I., ALIG, S. K., KOCH, E. G., METTLER, R., POHL, U. & KROTZ, F. 2012. ARNO regulates VEGF-dependent tissue responses by stabilizing endothelial VEGFR-2 surface expression. *Cardiovasc Res*, 93, 111-9.
- MARINOVA - MUTAFCHIEVA, L., WILLIAMS, R. O., MASON, L. J., MAURI, C., FELDMANN, M. & MAINI, R. N. 1997. Dynamics of proinflammatory cytokine expression in the joints of mice with collagen - induced arthritis (CIA). *Clinical and experimental immunology*, 107, 507-512.
- MATSUMOTO, A., SHIKATA, K., TAKEUCHI, F., KOJIMA, N. & MIZUOCHI, T. 2000. Autoantibody activity of IgG rheumatoid factor increases with decreasing levels of galactosylation and sialylation. *J Biochem*, 128, 621-8.
- MCEVER, R. P. 2002. Selectins: lectins that initiate cell adhesion under flow. *Curr Opin Cell Biol*, 14, 581-6.
- MCEVER, R. P. 2015. Selectins: initiators of leucocyte adhesion and signalling at the vascular wall. *Cardiovascular Research*, 107, 331-339.
- MCGETTRICK, H. M., SMITH, E., FILER, A., KISSANE, S., SALMON, M., BUCKLEY, C. D., RAINGER, G. E. & NASH, G. B. 2009. Fibroblasts from different sites may promote or inhibit recruitment of flowing lymphocytes by endothelial cells. *Eur J Immunol*, 39, 113-25.
- MCINNES, I. B., BUCKLEY, C. D. & ISAACS, J. D. 2016. Cytokines in rheumatoid arthritis - shaping the immunological landscape. *Nat Rev Rheumatol*, 12, 63-8.
- MEINECKE, I., CINSKI, A., BAIER, A., PETERS, M. A., DANKBAR, B., WILLE, A., DRYNDA, A., MENDOZA, H., GAY, R. E., HAY, R. T., INK, B., GAY, S. & PAP, T. 2007. Modification of nuclear PML protein by SUMO-1 regulates Fas-induced apoptosis in rheumatoid arthritis synovial fibroblasts. *Proc Natl Acad Sci U S A*, 104, 5073-8.
- MÉNÉTREY, J., MACIA, E., PASQUALATO, S., FRANCO, M. & CHERFILS, J. 2000. Structure of Arf6-GDP suggests a basis for guanine nucleotide exchange factors specificity. *Nature Structural Biology*, 7, 466-469.
- MICHA, R., WALLACE, S. K. & MOZAFFARIAN, D. 2010. Red and processed meat consumption and risk of incident coronary heart disease, stroke, and

- diabetes mellitus: a systematic review and meta-analysis. *Circulation*, 121, 2271-83.
- MITCHELL, M. D., LAIRD, R. E., BROWN, R. D. & LONG, C. S. 2007. IL-1beta stimulates rat cardiac fibroblast migration via MAP kinase pathways. *Am J Physiol Heart Circ Physiol*, 292, H1139-47.
- MIYOSHI, I., HIGASHI, H., HIRABAYASHI, Y., KATO, S. & NAIKI, M. 1986. Detection of 4-O-acetyl-N-glycolylneuraminyl lactosylceramide as one of tumor-associated antigens in human colon cancer tissues by specific antibody. *Mol Immunol*, 23, 631-8.
- MIZOGUCHI, F., SLOWIKOWSKI, K., WEI, K., MARSHALL, J. L., RAO, D. A., CHANG, S. K., NGUYEN, H. N., NOSS, E. H., TURNER, J. D., EARP, B. E., BLAZAR, P. E., WRIGHT, J., SIMMONS, B. P., DONLIN, L. T., KALLIOLIAS, G. D., GOODMAN, S. M., BYKERK, V. P., IVASHKIV, L. B., LEDERER, J. A., HACOHN, N., NIGROVIC, P. A., FILER, A., BUCKLEY, C. D., RAYCHAUDHURI, S. & BRENNER, M. B. 2018. Functionally distinct disease-associated fibroblast subsets in rheumatoid arthritis. *Nat Commun*, 9, 789.
- MON, N. N., SENGA, T. & ITO, S. 2017. Interleukin-1beta activates focal adhesion kinase and Src to induce matrix metalloproteinase-9 production and invasion of MCF-7 breast cancer cells. *Oncol Lett*, 13, 955-960.
- MONTEIRO, V. G., SOARES, C. P. & DE SOUZA, W. 1998. Host cell surface sialic acid residues are involved on the process of penetration of *Toxoplasma gondii* into mammalian cells. *FEMS Microbiol Lett*, 164, 323-7.
- MOREAU, K., RAVIKUMAR, B., PURI, C. & RUBINSZTEIN, D. C. 2012. Arf6 promotes autophagosome formation via effects on phosphatidylinositol 4,5-bisphosphate and phospholipase D. *J Cell Biol*, 196, 483-96.
- MORI, T., MIYAMOTO, T., YOSHIDA, H., ASAKAWA, M., KAWASUMI, M., KOBAYASHI, T., MORIOKA, H., CHIBA, K., TOYAMA, Y. & YOSHIMURA, A. 2011. IL-1B and TNF α -initiated IL-6-STAT3 pathway is critical in mediating inflammatory cytokines and RANKL expression in inflammatory arthritis. *Int Immunol*, 23, 701-12.
- MORISHIGE, M., HASHIMOTO, S., OGAWA, E., TODA, Y., KOTANI, H., HIROSE, M., WEI, S., HASHIMOTO, A., YAMADA, A., YANO, H., MAZAKI, Y., KODAMA, H., NIO, Y., MANABE, T., WADA, H., KOBAYASHI, H. & SABE, H. 2008. GEP100 links epidermal growth factor receptor signalling to Arf6 activation to induce breast cancer invasion. *Nat Cell Biol*, 10, 85-92.
- MOSTAFAVI-POUR, Z., ASKARI, J. A., PARKINSON, S. J., PARKER, P. J., NG, T. T. C. & HUMPHRIES, M. J. 2003. Integrin-specific signaling pathways controlling focal adhesion formation and cell migration. *Journal of Cell Biology*, 161, 155-167.
- MURASE, M., KAWASAKI, T., HAKOZAKI, R., SUEYOSHI, T., PUTRI, D. D. P., KITAI, Y., SATO, S., IKAWA, M. & KAWAI, T. 2018. Intravesicular Acidification Regulates Lipopolysaccharide Inflammation and Tolerance through TLR4 Trafficking. *The Journal of Immunology*, 200, 2798.
- NAKAHASHI, A., TANIGUCHI, T., MIURA, N. & MONDE, K. 2007. Stereochemical studies of sialic acid derivatives by vibrational circular dichroism. *Org Lett*, 9, 4741-4.
- NAKARAI, H., SAIDA, T., SHIBATA, Y., IRIE, R. F. & KANO, K. 1987. Expression of heterophile, Paul-Bunnell and Hanganutziu-Deicher antigens on human melanoma cell lines. *Int Arch Allergy Appl Immunol*, 83, 160-6.
- NAN, X., CARUBELLI, I. & STAMATOS, N. M. 2007. Sialidase expression in activated human T lymphocytes influences production of IFN-gamma. *J Leukoc Biol*, 81, 284-96.

- NAYLOR, A. J., FILER, A. & BUCKLEY, C. D. 2013. The role of stromal cells in the persistence of chronic inflammation. *Clin Exp Immunol*, 171, 30-5.
- NEUMANN, E., RIEPL, B., KNEDLA, A., LEFÈVRE, S., TARNER, I. H., GRIFKA, J., STEINMEYER, J., SCHÖLMERICH, J., GAY, S. & MÜLLER-LADNER, U. 2010. Cell culture and passaging alters gene expression pattern and proliferation rate in rheumatoid arthritis synovial fibroblasts. *Arthritis Research & Therapy*, 12, R83.
- NGUYEN, L., MCCORD, K. A., BUI, D. T., BOUWMAN, K. M., KITOVA, E. N., ELAISH, M., KUMAWAT, D., DASKHAN, G. C., TOMRIS, I., HAN, L., CHOPRA, P., YANG, T. J., WILLOWS, S. D., MASON, A. L., MAHAL, L. K., LOWARY, T. L., WEST, L. J., HSU, S. D., HOBMAN, T., TOMPKINS, S. M., BOONS, G. J., DE VRIES, R. P., MACAULEY, M. S. & KLASSEN, J. S. 2021. Sialic acid-containing glycolipids mediate binding and viral entry of SARS-CoV-2. *Nat Chem Biol*.
- NOMURA, K., VILALTA, A., ALLENDORF, D. H., HORNIK, T. C. & BROWN, G. C. 2017. Activated Microglia Desialylate and Phagocytose Cells via Neuraminidase, Galectin-3, and Mer Tyrosine Kinase. *J Immunol*, 198, 4792-4801.
- NORMAN, J. C., JONES, D., BARRY, S. T., HOLT, M. R., COCKCROFT, S. & CRITCHLEY, D. R. 1998. ARF1 Mediates Paxillin Recruitment to Focal Adhesions and Potentiates Rho-stimulated Stress Fiber Formation in Intact and Permeabilized Swiss 3T3 Fibroblasts. *Journal of Cell Biology*, 143, 1981-1995.
- NOSS, E. H. & BRENNER, M. B. 2008. The role and therapeutic implications of fibroblast-like synoviocytes in inflammation and cartilage erosion in rheumatoid arthritis. *Immunol Rev*, 223, 252-70.
- NUMAHATA, K., SATOH, M., HANDA, K., SAITO, S., OHYAMA, C., ITO, A., TAKAHASHI, T., HOSHI, S., ORIKASA, S. & HAKOMORI, S. I. 2002. Sialosyl-Le(x) expression defines invasive and metastatic properties of bladder carcinoma. *Cancer*, 94, 673-85.
- NYGAARD, G. & FIRESTEIN, G. S. 2020. Restoring synovial homeostasis in rheumatoid arthritis by targeting fibroblast-like synoviocytes. *Nat Rev Rheumatol*, 16, 316-333.
- OGURA, H., MURAKAMI, M., OKUYAMA, Y., TSURUOKA, M., KITABAYASHI, C., KANAMOTO, M., NISHIHARA, M., IWAKURA, Y. & HIRANO, T. 2008. Interleukin-17 promotes autoimmunity by triggering a positive-feedback loop via interleukin-6 induction. *Immunity*, 29, 628-36.
- OH, S. J. & SANTY, L. C. 2010. Differential effects of cytohesins 2 and 3 on beta1 integrin recycling. *J Biol Chem*, 285, 14610-6.
- OH, S. J. & SANTY, L. C. 2012. Phosphoinositide specificity determines which cytohesins regulate beta1 integrin recycling. *J Cell Sci*, 125, 3195-201.
- OHMI, Y., ISE, W., HARAZONO, A., TAKAKURA, D., FUKUYAMA, H., BABA, Y., NARAZAKI, M., SHODA, H., TAKAHASHI, N., OHKAWA, Y., JI, S., SUGIYAMA, F., FUJIO, K., KUMANOGOH, A., YAMAMOTO, K., KAWASAKI, N., KUROSAKI, T., TAKAHASHI, Y. & FURUKAWA, K. 2016. Sialylation converts arthritogenic IgG into inhibitors of collagen-induced arthritis. *Nat Commun*, 7, 11205.
- OHSHIMA, S., KUCHEN, S., SEEMAYER, C. A., KYBURZ, D., HIRT, A., KLINZING, S., MICHEL, B. A., GAY, R. E., LIU, F. T., GAY, S. & NEIDHART, M. 2003. Galectin 3 and its binding protein in rheumatoid arthritis. *Arthritis Rheum*, 48, 2788-95.

- OKABE, Y. & MEDZHITOV, R. 2014. Tissue-specific signals control reversible program of localization and functional polarization of macrophages. *Cell*, 157, 832-44.
- OPDENAKKER, G., RUDD, P. M., WORMALD, M., DWEK, R. A. & VAN DAMME, J. 1995. Cells regulate the activities of cytokines by glycosylation. *The FASEB journal*, 9, 453-457.
- ORIA, R., WIEGAND, T., ESCRIBANO, J., ELOSEGUI-ARTOLA, A., URIARTE, J. J., MORENO-PULIDO, C., PLATZMAN, I., DELCANALE, P., ALBERTAZZI, L., NAVAJAS, D., TREPAT, X., GARCIA-AZNAR, J. M., CAVALCANTI-ADAM, E. A. & ROCA-CUSACHS, P. 2017. Force loading explains spatial sensing of ligands by cells. *Nature*, 552, 219-224.
- ORR, S. J., MORGAN, N. M., ELLIOTT, J., BURROWS, J. F., SCOTT, C. J., MCVICAR, D. W. & JOHNSTON, J. A. 2007. CD33 responses are blocked by SOCS3 through accelerated proteasomal-mediated turnover. *Blood*, 109, 1061-8.
- PALACIOS, F., PRICE, L., SCHWEITZER, J., COLLARD, J. G. & D'SOUZA-SCHOREY, C. 2001. An essential role for ARF6-regulated membrane traffic in adherens junction turnover and epithelial cell migration. *The EMBO journal*, 20, 4973-4986.
- PALEOLOG, E. M. 2002. Angiogenesis in rheumatoid arthritis. *Arthritis Res*, 4 Suppl 3, S81-90.
- PALLY, D., PRAMANIK, D., HUSSAIN, S., VERMA, S., SRINIVAS, A., KUMAR, R. V., EVEREST-DASS, A. & BHAT, R. 2021. Heterogeneity in 2,6-Linked Sialic Acids Potentiates Invasion of Breast Cancer Epithelia. *ACS Cent Sci*, 7, 110-125.
- PAN, A., SUN, Q., BERNSTEIN, A. M., SCHULZE, M. B., MANSON, J. E., STAMPFER, M. J., WILLETT, W. C. & HU, F. B. 2012. Red meat consumption and mortality: results from 2 prospective cohort studies. *Arch Intern Med*, 172, 555-63.
- PAN, A., SUN, Q., BERNSTEIN, A. M., SCHULZE, M. B., MANSON, J. E., WILLETT, W. C. & HU, F. B. 2011. Red meat consumption and risk of type 2 diabetes: 3 cohorts of US adults and an updated meta-analysis. *Am J Clin Nutr*, 94, 1088-96.
- PAPPU, B. P. & SHRIKANT, P. A. 2004. Alteration of cell surface sialylation regulates antigen-induced naive CD8+ T cell responses. *J Immunol*, 173, 275-84.
- PARK, J. Y., KANG, S. E., AHN, K. S., UM, J. Y., YANG, W. M., YUN, M. & LEE, S. G. 2020. Inhibition of the PI3K-AKT-mTOR pathway suppresses the adipocyte-mediated proliferation and migration of breast cancer cells. *J Cancer*, 11, 2552-2559.
- PARK, Y. K., JUNG, S. & PARK, S. H. 2016. Induction of tolerance against the arthritogenic antigen with type-II collagen peptide-linked soluble MHC class II molecules. *BMB Rep*, 49, 331-6.
- PASI, S., KANT, R., GUPTA, S. & SUROLIA, A. 2015. Novel multimeric IL-1 receptor antagonist for the treatment of rheumatoid arthritis. *Biomaterials*, 42, 121-33.
- PASQUALATO, S., MÉNÉTREY, J., FRANCO, M. & CHERFILS, J. 2001. The structural GDP/GTP cycle of human Arf6. *EMBO Rep*, 2, 234-8.
- PASSANITI, A. & HART, G. W. 1988. Cell surface sialylation and tumor metastasis. Metastatic potential of B16 melanoma variants correlates with their relative numbers of specific penultimate oligosaccharide structures. *The Journal of biological chemistry*, 263, 7591-7603.

- PASZKOWSKA, A., BERBEĆ, H., SEMCZUK, A. & CYBULSKI, M. 1998. Sialic acid concentration in serum and tissue of endometrial cancer patients. *European Journal of Obstetrics & Gynecology and Reproductive Biology*, 76, 211-215.
- PATTISON, D. J., SYMMONS, D. P., LUNT, M., WELCH, A., LUBEN, R., BINGHAM, S. A., KHAW, K. T., DAY, N. E. & SILMAN, A. J. 2004. Dietary risk factors for the development of inflammatory polyarthritis: evidence for a role of high level of red meat consumption. *Arthritis Rheum*, 50, 3804-12.
- PENG, W.-X., ZHU, S.-L., ZHANG, B.-Y., SHI, Y.-M., FENG, X.-X., LIU, F., HUANG, J.-L. & ZHENG, S. G. 2017. Smoothed Regulates Migration of Fibroblast-Like Synoviocytes in Rheumatoid Arthritis via Activation of Rho GTPase Signaling. *Frontiers in Immunology*, 8.
- PETERS, M. A., WENDHOLT, D., STRIETHOLT, S., FRANK, S., PUNDT, N., KORB-PAP, A., JOOSTEN, L. A., VAN DEN BERG, W. B., KOLLIAS, G., ECKES, B. & PAP, T. 2012. The loss of α 2B1 integrin suppresses joint inflammation and cartilage destruction in mouse models of rheumatoid arthritis. *Arthritis Rheum*, 64, 1359-68.
- PETERS, P. J., HSU, V. W., OOI, C. E., FINAZZI, D., TEAL, S. B., OORSCHOT, V., DONALDSON, J. G. & KLAUSNER, R. D. 1995. Overexpression of wild-type and mutant ARF1 and ARF6: distinct perturbations of nonoverlapping membrane compartments. *J Cell Biol*, 128, 1003-17.
- PICCO, G., JULIEN, S., BROCKHAUSEN, I., BEATSON, R., ANTONOPOULOS, A., HASLAM, S., MANDEL, U., DELL, A., PINDER, S., TAYLOR-PAPADIMITRIOU, J. & BURCHELL, J. 2010. Over-expression of ST3Gal-I promotes mammary tumorigenesis. *Glycobiology*, 20, 1241-50.
- PIGUET, P. F., GRAU, G. E., VESIN, C., LOETSCHER, H., GENTZ, R. & LESSLAUER, W. 1992. Evolution of collagen arthritis in mice is arrested by treatment with anti-tumour necrosis factor (TNF) antibody or a recombinant soluble TNF receptor. *Immunology*, 77, 510-4.
- PINCUS, T., FERRACCIOLI, G., SOKKA, T., LARSEN, A., RAU, R., KUSHNER, I. & WOLFE, F. 2002. Evidence from clinical trials and long-term observational studies that disease-modifying anti-rheumatic drugs slow radiographic progression in rheumatoid arthritis: updating a 1983 review. *Rheumatology (Oxford)*, 41, 1346-56.
- PINEDA, M. A., AL-RIYAMI, L., HARNETT, W. & HARNETT, M. M. 2014a. Lessons from helminth infections: ES-62 highlights new interventional approaches in rheumatoid arthritis. *Clin Exp Immunol*, 177, 13-23.
- PINEDA, M. A., MCGRATH, M. A., SMITH, P. C., AL-RIYAMI, L., RZEPECKA, J., GRACIE, J. A., HARNETT, W. & HARNETT, M. M. 2012. The parasitic helminth product ES-62 suppresses pathogenesis in collagen-induced arthritis by targeting the interleukin-17-producing cellular network at multiple sites. *Arthritis Rheum*, 64, 3168-78.
- PINEDA, M. A., RODGERS, D. T., AL-RIYAMI, L., HARNETT, W. & HARNETT, M. M. 2014b. ES-62 protects against collagen-induced arthritis by resetting interleukin-22 toward resolution of inflammation in the joints. *Arthritis Rheumatol*, 66, 1492-503.
- POBER, J. S. & SESSA, W. C. 2007. Evolving functions of endothelial cells in inflammation. *Nature Reviews Immunology*, 7, 803-815.
- POWELKA, A. M., SUN, J., LI, J., GAO, M., SHAW, L. M., SONNENBERG, A. & HSU, V. W. 2004. Stimulation-dependent recycling of integrin beta1 regulated by ARF6 and Rab11. *Traffic*, 5, 20-36.
- POWELL, L. D., JAIN, R. K., MATTA, K. L., SABESAN, S. & VARKI, A. 1995. Characterization of sialyloligosaccharide binding by recombinant soluble

- and native cell-associated CD22. Evidence for a minimal structural recognition motif and the potential importance of multisite binding. *J Biol Chem*, 270, 7523-32.
- POWELL, L. D., SGROI, D., SJOBERG, E. R., STAMENKOVIC, I. & VARKI, A. 1993. Natural ligands of the B cell adhesion molecule CD22 beta carry N-linked oligosaccharides with alpha-2,6-linked sialic acids that are required for recognition. *J Biol Chem*, 268, 7019-27.
- PRIATEL, J. J., CHUI, D., HIRAOKA, N., SIMMONS, C. J., RICHARDSON, K. B., PAGE, D. M., FUKUDA, M., VARKI, N. M. & MARTH, J. D. 2000. The ST3Gal-I sialyltransferase controls CD8+ T lymphocyte homeostasis by modulating O-glycan biosynthesis. *Immunity*, 12, 273-83.
- QWARNSTRÖM, E. E., MACFARLANE, S. A., PAGE, R. C. & DOWER, S. K. 1991. Interleukin 1 beta induces rapid phosphorylation and redistribution of talin: a possible mechanism for modulation of fibroblast focal adhesion. *Proceedings of the National Academy of Sciences*, 88, 1232-1236.
- RAJU, T. S., BRIGGS, J. B., CHAMOW, S. M., WINKLER, M. E. & JONES, A. J. S. 2001. Glycoengineering of Therapeutic Glycoproteins: In Vitro Galactosylation and Sialylation of Glycoproteins with Terminal N-Acetylglucosamine and Galactose Residues. *Biochemistry*, 40, 8868-8876.
- RAVETCH, J. V. & LANIER, L. L. 2000. Immune inhibitory receptors. *Science*, 290, 84-9.
- RECCHI, M. A., HEBBAR, M., HORNEZ, L., HARDUIN-LEPERS, A., PEYRAT, J. P. & DELANNOY, P. 1998. Multiplex reverse transcription polymerase chain reaction assessment of sialyltransferase expression in human breast cancer. *Cancer Res*, 58, 4066-70.
- REPARON-SCHUIJT, C. C., VAN ESCH, W. J., VAN KOOTEN, C., ROZIER, B. C., LEVARHT, E. W., BREEDVELD, F. C. & VERWEIJ, C. L. 2000. Regulation of synovial B cell survival in rheumatoid arthritis by vascular cell adhesion molecule 1 (CD106) expressed on fibroblast-like synoviocytes. *Arthritis Rheum*, 43, 1115-21.
- ROBBINS, S. L., KUMAR, V. & COTRAN, R. S. 2010. *Robbins and Cotran pathologic basis of disease*, Philadelphia, Pa, Saunders/Elsevier.
- ROBERTS, E. W., DEONARINE, A., JONES, J. O., DENTON, A. E., FEIG, C., LYONS, S. K., ESPELI, M., KRAMAN, M., MCKENNA, B., WELLS, R. J., ZHAO, Q., CABALLERO, O. L., LARDER, R., COLL, A. P., O'RAHILLY, S., BRINDLE, K. M., TEICHMANN, S. A., TUVESON, D. A. & FEARON, D. T. 2013. Depletion of stromal cells expressing fibroblast activation protein- α from skeletal muscle and bone marrow results in cachexia and anemia. *J Exp Med*, 210, 1137-51.
- ROBERTSON, K. D. 2005. DNA methylation and human disease. *Nature Reviews Genetics*, 6, 597-610.
- ROBINSON, S. D., FRENETTE, P. S., RAYBURN, H., CUMMISKEY, M., ULLMAN-CULLERE, M., WAGNER, D. D. & HYNES, R. O. 1999. Multiple, Targeted Deficiencies in Selectins Reveal a Predominant Role for P-Selectin in Leukocyte Recruitment. *Proceedings of the National Academy of Sciences - PNAS*, 96, 11452-11457.
- RODRIGUES, E. & MACAULEY, M. S. 2018. Hypersialylation in Cancer: Modulation of Inflammation and Therapeutic Opportunities. *Cancers (Basel)*, 10.
- RODRIGUES, J. G., BALMANA, M., MACEDO, J. A., POCAS, J., FERNANDES, A., DEFREITAS-JUNIOR, J. C. M., PINHO, S. S., GOMES, J., MAGALHAES, A., GOMES, C., MEREITER, S. & REIS, C. A. 2018. Glycosylation in cancer: Selected roles in tumour progression, immune modulation and metastasis. *Cell Immunol*, 333, 46-57.

- ROSAS, M., DAVIES, L. C., GILES, P. J., LIAO, C. T., KHARFAN, B., STONE, T. C., O'DONNELL, V. B., FRASER, D. J., JONES, S. A. & TAYLOR, P. R. 2014. The transcription factor Gata6 links tissue macrophage phenotype and proliferative renewal. *Science*, 344, 645-648.
- ROSEN, S. D., SINGER, M. S., YEDNOCK, T. A. & STOOLMAN, L. M. 1985. Involvement of sialic acid on endothelial cells in organ-specific lymphocyte recirculation. *Science*, 228, 1005-7.
- ROSENGREN, S., BOYLE, D. L. & FIRESTEIN, G. S. 2007. Acquisition, culture, and phenotyping of synovial fibroblasts. *Methods Mol Med*, 135, 365-75.
- ROTHSCHILD, B. M. & WOODS, R. J. 1990. Symmetrical erosive disease in Archaic Indians: the origin of rheumatoid arthritis in the New World? *Semin Arthritis Rheum*, 19, 278-84.
- ROTHSCHILD, B. M., WOODS, R. J., ROTHSCCHILD, C. & SEBES, J. I. 1992. Geographic distribution of rheumatoid arthritis in ancient North America: implications for pathogenesis. *Semin Arthritis Rheum*, 22, 181-7.
- RZEPECKA, J., PINEDA, M. A., AL-RIYAMI, L., RODGERS, D. T., HUGGAN, J. K., LUMB, F. E., KHALAF, A. I., MEAKIN, P. J., CORBET, M., ASHFORD, M. L., SUCKLING, C. J., HARNETT, M. M. & HARNETT, W. 2015. Prophylactic and therapeutic treatment with a synthetic analogue of a parasitic worm product prevents experimental arthritis and inhibits IL-1beta production via NRF2-mediated counter-regulation of the inflammasome. *J Autoimmun*, 60, 59-73.
- SABEH, F., FOX, D. & WEISS, S. J. 2010. Membrane-type I matrix metalloproteinase-dependent regulation of rheumatoid arthritis synoviocyte function. *J Immunol*, 184, 6396-406.
- SACRE, S. M., ANDREAKOS, E., KIRIAKIDIS, S., AMJADI, P., LUNDBERG, A., GIDDINS, G., FELDMANN, M., BRENNAN, F. & FOXWELL, B. M. 2007. The Toll-like receptor adaptor proteins MyD88 and Mal/TIRAP contribute to the inflammatory and destructive processes in a human model of rheumatoid arthritis. *Am J Pathol*, 170, 518-25.
- SADAKATA, T., SHINODA, Y., SEKINE, Y., SARUTA, C., ITAKURA, M., TAKAHASHI, M. & FURUICHI, T. 2010. Interaction of calcium-dependent activator protein for secretion 1 (CAPS1) with the class II ADP-ribosylation factor small GTPases is required for dense-core vesicle trafficking in the trans-Golgi network. *J Biol Chem*, 285, 38710-9.
- SALEM, J. C., REVIRIEGO-MENDOZA, M. M. & SANTY, L. C. 2015. ARF-GEF cytohesin-2/ARNO regulates R-Ras and alpha5-integrin recycling through an EHD1-positive compartment. *Mol Biol Cell*, 26, 4265-79.
- SALMON, M., SCHEEL-TOELLNER, D., HUISSOON, A. P., PILLING, D., SHAMSADEEN, N., HYDE, H., D'ANGEAC, A. D., BACON, P. A., EMERY, P. & AKBAR, A. N. 1997. Inhibition of T cell apoptosis in the rheumatoid synovium. *J Clin Invest*, 99, 439-46.
- SAMRAJ, A. N., PEARCE, O. M. T., LÄUBLI, H., CRITTENDEN, A. N., BERGFELD, A. K., BANDA, K., GREGG, C. J., BINGMAN, A. E., SECREST, P., DIAZ, S. L., VARKI, N. M. & VARKI, A. 2015. A red meat-derived glycan promotes inflammation and cancer progression. *Proceedings of the National Academy of Sciences*, 112, 542-547.
- SANDYA, S., ACHAN, M. A. & SUDHAKARAN, P. R. 2009. Multiple matrix metalloproteinases in type II collagen induced arthritis. *Indian Journal of Clinical Biochemistry*, 24, 42-48.
- SANTY, L. C. & CASANOVA, J. E. 2001. Activation of ARF6 by ARNO stimulates epithelial cell migration through downstream activation of both Rac1 and phospholipase D. *J Cell Biol*, 154, 599-610.

- SANTY, L. C., RAVICHANDRAN, K. S. & CASANOVA, J. E. 2005. The DOCK180/Elmo complex couples ARNO-mediated Arf6 activation to the downstream activation of Rac1. *Curr Biol*, 15, 1749-54.
- SATO, T., TAKAHASHI, M., KAWADO, T., TAKAYAMA, E. & FURUKAWA, K. 2005. Effect of staurosporine on N-glycosylation and cell adhesion to fibronectin of SW480 human colorectal adenocarcinoma cells. *Eur J Pharm Sci*, 25, 221-7.
- SAWAI, H., OKADA, Y., FUNAHASHI, H., MATSUO, Y., TAKAHASHI, H., TAKEYAMA, H. & MANABE, T. 2005. Activation of focal adhesion kinase enhances the adhesion and invasion of pancreatic cancer cells via extracellular signal-regulated kinase-1/2 signaling pathway activation. *Molecular Cancer*, 4, 37.
- SCHAUER, R. 2000. Achievements and challenges of sialic acid research. *Glycoconj J*, 17, 485-99.
- SCHAUER, R. 2009. Sialic acids as regulators of molecular and cellular interactions. *Curr Opin Struct Biol*, 19, 507-14.
- SCHAUER, R. & KAMERLING, J. P. 1997. Chapter 11 - Chemistry, biochemistry and biology of sialic acids. In: MONTREUIL, J., VLIAGENTHART, J. F. G. & SCHACHTER, H. (eds.) *New Comprehensive Biochemistry*. Elsevier.
- SCHAUER, R. & KAMERLING, J. P. 2018. Chapter One - Exploration of the Sialic Acid World. In: BAKER, D. C. (ed.) *Advances in Carbohydrate Chemistry and Biochemistry*. Academic Press.
- SCHRAEN-MASCHKE, S. & ZANETTA, J. P. 2003. Role of oligomannosidic N-glycans in the proliferation, adhesion and signalling of C6 glioblastoma cells. *Biochimie*, 85, 219-29.
- SCHULTZ, M. J., SWINDALL, A. F., WRIGHT, J. W., SZTUL, E. S., LANDEN, C. N. & BELLIS, S. L. 2013. ST6Gal-I sialyltransferase confers cisplatin resistance in ovarian tumor cells. *J Ovarian Res*, 6, 25.
- SCHUMACHER, B. L., BLOCK, J. A., SCHMID, T. M., AYDELOTTE, M. B. & KUETTNER, K. E. 1994. A novel proteoglycan synthesized and secreted by chondrocytes of the superficial zone of articular cartilage. *Arch Biochem Biophys*, 311, 144-52.
- SCHWARZKOPF, M., KNOBELOCH, K.-P., ROHDE, E., HINDERLICH, S., WIECHENS, N., LUCKA, L., HORAK, I., REUTTER, W. & HORSTKORTE, R. 2002. Sialylation is essential for early development in mice. *Proceedings of the National Academy of Sciences*, 99, 5267-5270.
- SCOTT, S., PANDOLFI, F. & KURNICK, J. T. 1990. Fibroblasts mediate T cell survival: a proposed mechanism for retention of primed T cells. *J Exp Med*, 172, 1873-6.
- SEDLACEK, H. H., MEESMANN, H. & SEILER, F. R. 1975. Regression of spontaneous mammary tumors in dogs after injection of neuraminidase-treated tumor cells. *Int J Cancer*, 15, 409-16.
- SEMEL, A. C., SEALES, E. C., SINGHAL, A., EKLUND, E. A., COLLEY, K. J. & BELLIS, S. L. 2002. Hyposialylation of integrins stimulates the activity of myeloid fibronectin receptors. *J Biol Chem*, 277, 32830-6.
- SEVERI, E., HOOD, D. W. & THOMAS, G. H. 2007. Sialic acid utilization by bacterial pathogens. *Microbiology (Reading)*, 153, 2817-2822.
- SHAIKH, F. M., SEALES, E. C., CLEM, W. C., HENNESSY, K. M., ZHUO, Y. & BELLIS, S. L. 2008. Tumor cell migration and invasion are regulated by expression of variant integrin glycoforms. *Exp Cell Res*, 314, 2941-50.
- SHARON, N. & LIS, H. 1981. Glycoproteins: research booming on long-ignored, ubiquitous compounds. *Chemical & Engineering News Archive*, 59, 21-44.

- SHELEF, M. A., BENNIN, D. A., YASMIN, N., WARNER, T. F., LUDWIG, T., BEGGS, H. E. & HUTTENLOCHER, A. 2014. Focal adhesion kinase is required for synovial fibroblast invasion, but not murine inflammatory arthritis. *Arthritis Research & Therapy*, 16, 464.
- SIMON, A. R., VIKIS, H. G., STEWART, S., FANBURG, B. L., COCHRAN, B. H. & GUAN, K.-L. 2000. Regulation of STAT3 by Direct Binding to the Rac1 GTPase. *Science (American Association for the Advancement of Science)*, 290, 144-147.
- SIMON, S. I. & GREEN, C. E. 2005. Molecular mechanics and dynamics of leukocyte recruitment during inflammation. *Annu Rev Biomed Eng*, 7, 151-85.
- SIMONET, W. S., LACEY, D. L., DUNSTAN, C. R., KELLEY, M., CHANG, M. S., LÜTHY, R., NGUYEN, H. Q., WOODEN, S., BENNETT, L., BOONE, T., SHIMAMOTO, G., DEROSE, M., ELLIOTT, R., COLOMBERO, A., TAN, H. L., TRAIL, G., SULLIVAN, J., DAVY, E., BUCAY, N., RENSHAW-GEGG, L., HUGHES, T. M., HILL, D., PATTISON, W., CAMPBELL, P., SANDER, S., VAN, G., TARPLEY, J., DERBY, P., LEE, R. & BOYLE, W. J. 1997. Osteoprotegerin: a novel secreted protein involved in the regulation of bone density. *Cell*, 89, 309-19.
- SINGH, J. A., ARAYSSI, T., DURAY, P. & SCHUMACHER, H. R. 2004. Immunohistochemistry of normal human knee synovium: a quantitative study. *Ann Rheum Dis*, 63, 785-90.
- SINGH, V., DAVIDSON, A. C., HUME, P. J., HUMPHREYS, D. & KORONAKIS, V. 2019. Arf GTPase interplay with Rho GTPases in regulation of the actin cytoskeleton. *Small GTPases*, 10, 411-418.
- SLOWIKOWSKI, K., NGUYEN, H. N., NOSS, E. H., SIMMONS, D. P., MIZOGUCHI, F., WATTS, G. F. M., GURISH, M. F., BRENNER, M. B. & RAYCHAUDHURI, S. 2019.
- SMITH, D. W., GARDINER, B. S., ZHANG, L. & GRODZINSKY, A. J. 2019. Lubrication, Friction, and Wear in Diarthrodial Joints. In: SMITH, D. W., GARDINER, B. S., ZHANG, L. & GRODZINSKY, A. J. (eds.) *Articular Cartilage Dynamics*. Singapore: Springer Singapore.
- SMITH, M. D. 2011. The normal synovium. *Open Rheumatol J*, 5, 100-6.
- SMITH, M. D., BARG, E., WEEDON, H., PAPENGELIS, V., SMEETS, T., TAK, P. P., KRAAN, M., COLEMAN, M. & AHERN, M. J. 2003. Microarchitecture and protective mechanisms in synovial tissue from clinically and arthroscopically normal knee joints. *Annals of the rheumatic diseases*, 62, 303-307.
- SPERANDIO, M., FROMMHOLD, D., BABUSHKINA, I., ELLIES, L. G., OLSON, T. S., SMITH, M. L., FRITZSCHING, B., PAULY, E., SMITH, D. F., NOBILING, R., LINDERKAMP, O., MARTH, J. D. & LEY, K. 2006. α 2,3 - Sialyltransferase - IV is essential for L - selectin ligand function in inflammation. *European journal of immunology*, 36, 3207-3215.
- STAMATOS, N. M., CURRELI, S., ZELLA, D. & CROSS, A. S. 2004. Desialylation of glycoconjugates on the surface of monocytes activates the extracellular signal-related kinases ERK 1/2 and results in enhanced production of specific cytokines. *J Leukoc Biol*, 75, 307-13.
- STANFORD, S. M., ALEMAN MUENCH, G. R., BARTOK, B., SACCHETTI, C., KIOSSES, W. B., SHARMA, J., MAESTRE, M. F., BOTTINI, M., MUSTELIN, T., BOYLE, D. L., FIRESTEIN, G. S. & BOTTINI, N. 2016a. TGF β responsive tyrosine phosphatase promotes rheumatoid synovial fibroblast invasiveness. *Ann Rheum Dis*, 75, 295-302.

- STANFORD, S. M., SVENSSON, M. N., SACCHETTI, C., PILO, C. A., WU, D. J., KIOSSES, W. B., HELLVARD, A., BERGUM, B., MUENCH, G. R., ELLY, C., LIU, Y. C., DEN HERTOOG, J., ELSON, A., SAP, J., MYDEL, P., BOYLE, D. L., CORR, M., FIRESTEIN, G. S. & BOTTINI, N. 2016b. Receptor Protein Tyrosine Phosphatase α -Mediated Enhancement of Rheumatoid Synovial Fibroblast Signaling and Promotion of Arthritis in Mice. *Arthritis Rheumatol*, 68, 359-69.
- STEARNS, T., WILLINGHAM, M. C., BOTSTEIN, D. & KAHN, R. A. 1990. ADP-ribosylation factor is functionally and physically associated with the Golgi complex. *Proc Natl Acad Sci U S A*, 87, 1238-42.
- STENCEL-BAERENWALD, J. E., REISS, K., REITER, D. M., STEHLE, T. & DERMODY, T. S. 2014. The sweet spot: defining virus-sialic acid interactions. *Nat Rev Microbiol*, 12, 739-49.
- SYVERSEN, S. W., GOLL, G. L., VAN DER HEIJDE, D., LANDEWÉ, R., LIE, B. A., ØDEGÅRD, S., UHLIG, T., GAARDER, P. I. & KVIEN, T. K. 2010. Prediction of radiographic progression in rheumatoid arthritis and the role of antibodies against mutated citrullinated vimentin: results from a 10-year prospective study. *Annals of the Rheumatic Diseases*, 69, 345.
- SZEKANECZ, Z., HAINES, G. K., LIN, T. R., HARLOW, L. A., GOERDT, S., RAYAN, G. & KOCH, A. E. 1994. Differential distribution of intercellular adhesion molecules (ICAM-1, ICAM-2, and ICAM-3) and the MS-1 antigen in normal and diseased human synovia. Their possible pathogenetic and clinical significance in rheumatoid arthritis. *Arthritis Rheum*, 37, 221-31.
- SZEKANECZ, Z. & KOCH, A. E. 2000. Cell-cell interactions in synovitis. Endothelial cells and immune cell migration. *Arthritis Res*, 2, 368-73.
- SZKLARCZYK, D., GABLE, A. L., LYON, D., JUNGE, A., WYDER, S., HUERTA-CEPAS, J., SIMONOVIC, M., DONCHEVA, N. T., MORRIS, J. H., BORK, P., JENSEN, L. J. & MERING, C. V. 2019. STRING v11: protein-protein association networks with increased coverage, supporting functional discovery in genome-wide experimental datasets. *Nucleic Acids Res*, 47, D607-D613.
- SZTUL, E., CHEN, P. W., CASANOVA, J. E., CHERFILS, J., DACKS, J. B., LAMBRIGHT, D. G., LEE, F. S., RANDAZZO, P. A., SANTY, L. C., SCHURMANN, A., WILHELMI, I., YOHE, M. E. & KAHN, R. A. 2019. ARF GTPases and their GEFs and GAPs: concepts and challenges. *Mol Biol Cell*, 30, 1249-1271.
- SZYF, M. 2001. The role of DNA methyltransferase 1 in growth control. *Front Biosci*, 6, D599-609.
- TAGUE, S. E., MURALIDHARAN, V. & D'SOUZA-SCHOREY, C. 2004. ADP-ribosylation factor 6 regulates tumor cell invasion through the activation of the MEK/ERK signaling pathway. *Proceedings of the National Academy of Sciences of the United States of America*, 101, 9671-9676.
- TAKAGI, H., FUKAYA, T., EIZUMI, K., SATO, Y., SATO, K., SHIBAZAKI, A., OTSUKA, H., HIJIKATA, A., WATANABE, T., OHARA, O., KAISHO, T., MALISSEN, B. & SATO, K. 2011. Plasmacytoid dendritic cells are crucial for the initiation of inflammation and T cell immunity in vivo. *Immunity*, 35, 958-71.
- TAKEMURA, S., BRAUN, A., CROWSON, C., KURTIN, P. J., COFIELD, R. H., O'FALLON, W. M., GORONZY, J. J. & WEYAND, C. M. 2001. Lymphoid neogenesis in rheumatoid synovitis. *J Immunol*, 167, 1072-80.
- TANG, M., TIAN, L., LUO, G. & YU, X. 2018. Interferon-Gamma-Mediated Osteoimmunology. *Frontiers in Immunology*, 9.

- TANGVORANUNTAKUL, P., GAGNEUX P FAU - DIAZ, S., DIAZ S FAU - BARDOR, M., BARDOR M FAU - VARKI, N., VARKI N FAU - VARKI, A., VARKI A FAU - MUCHMORE, E. & MUCHMORE, E. Human uptake and incorporation of an immunogenic nonhuman dietary sialic acid.
- TAYEB, M. A., SKALSKI, M., CHA, M. C., KEAN, M. J., SCAIFE, M. & COPPOLINO, M. G. 2005. Inhibition of SNARE-mediated membrane traffic impairs cell migration. *Exp Cell Res*, 305, 63-73.
- THORBECKE, G. J., SHAH, R., LEU, C. H., KURUVILLA, A. P., HARDISON, A. M. & PALLADINO, M. A. 1992. Involvement of endogenous tumor necrosis factor alpha and transforming growth factor beta during induction of collagen type II arthritis in mice. *Proc Natl Acad Sci U S A*, 89, 7375-9.
- TIAN, B., LESSAN, K., KAHM, J., KLEIDON, J. & HENKE, C. 2002. beta 1 integrin regulates fibroblast viability during collagen matrix contraction through a phosphatidylinositol 3-kinase/Akt/protein kinase B signaling pathway. *J Biol Chem*, 277, 24667-75.
- TIAN, J., CHEN, J. W., GAO, J. S., LI, L. & XIE, X. 2013. Resveratrol inhibits TNF-alpha-induced IL-1beta, MMP-3 production in human rheumatoid arthritis fibroblast-like synoviocytes via modulation of PI3kinase/Akt pathway. *Rheumatol Int*, 33, 1829-35.
- TOLEDO, L. M., LYDON, N. B. & ELBAUM, D. 1999. The structure-based design of ATP-site directed protein kinase inhibitors. *Curr Med Chem*, 6, 775-805.
- TOLLOCZKO, B., TURKEWITSCH, P., AL-CHALABI, M. & MARTIN, J. G. 2004. LY-294002 [2-(4-morpholinyl)-8-phenyl-4H-1-benzopyran-4-one] affects calcium signaling in airway smooth muscle cells independently of phosphoinositide 3-kinase inhibition. *J Pharmacol Exp Ther*, 311, 787-93.
- TORII, T., MIYAMOTO, Y., SANBE, A., NISHIMURA, K., YAMAUCHI, J. & TANOUE, A. 2010. Cytohesin-2/ARNO, through its interaction with focal adhesion adaptor protein paxillin, regulates preadipocyte migration via the downstream activation of Arf6. *J Biol Chem*, 285, 24270-81.
- TRENTHAM, D. E. 1982. Collagen arthritis as a relevant model for rheumatoid arthritis. evidence pro and con. *Arthritis and rheumatism*, 25, 911-916.
- TUREK-PLEWA, J. & JAGODZIŃSKI, P. P. 2005. The role of mammalian DNA methyltransferases in the regulation of gene expression. *Cell Mol Biol Lett*, 10, 631-47.
- TURNER, J. D. & FILER, A. 2015. The role of the synovial fibroblast in rheumatoid arthritis pathogenesis. *Curr Opin Rheumatol*, 27, 175-82.
- TYRRELL, D., JAMES, P., RAO, N., FOXALL, C., ABBAS, S., DASGUPTA, F., NASHED, M., HASEGAWA, A., KISO, M., ASA, D. & ET AL. 1991. Structural requirements for the carbohydrate ligand of E-selectin. *Proc Natl Acad Sci U S A*, 88, 10372-6.
- ULGEN, E., OZISIK, O. & SEZERMAN, O. U. 2019. pathfindR: An R Package for Comprehensive Identification of Enriched Pathways in Omics Data Through Active Subnetworks. *Front Genet*, 10, 858.
- VAN ACKER, T., EYCKERMAN, S., VANDE WALLE, L., GERLO, S., GOETHALS, M., LAMKANFI, M., BOVIJN, C., TAVERNIER, J. & PEELMAN, F. 2014. The small GTPase Arf6 is essential for the Tram/Trif pathway in TLR4 signaling. *J Biol Chem*, 289, 1364-76.
- VAN DINTHER-JANSSEN, A. C., HORST, E., KOOPMAN, G., NEWMANN, W., SCHEPER, R. J., MEIJER, C. J. & PALS, S. T. 1991. The VLA-4/VCAM-1 pathway is involved in lymphocyte adhesion to endothelium in rheumatoid synovium. *The Journal of Immunology*, 147, 4207.

- VAN RINSUM, J., SMETS, L. A., VAN ROOY, H. & VAN DEN EIJNDEN, D. H. 1986. Specific inhibition of human natural killer cell - mediated cytotoxicity by sialic acid and sialo - oligosaccharides. *International journal of cancer*, 38, 915-922.
- VARKI, A. 2007. Glycan-based interactions involving vertebrate sialic-acid-recognizing proteins. *Nature*, 446, 1023-9.
- VARKI, A. 2008. Sialic acids in human health and disease. *Trends Mol Med*, 14, 351-60.
- VARKI, A. 2010. Uniquely human evolution of sialic acid genetics and biology. *Proceedings of the National Academy of Sciences*, 107, 8939-8946.
- VASKO, R., STREICH, J. H., BLASCHKE, S., MÜLLER, G. A., MAI, B., KOSTRZEWA, M., SPARBIER, K., KORSTEN, P., BOHR, S. & DIHAZI, H. 2016. Vimentin fragments are potential markers of rheumatoid synovial fibroblasts. *Clin Exp Rheumatol*, 34, 513-20.
- VENKATESWARLU, K., GUNN-MOORE, F., OATEY, P. B., TAVARÉ, J. M. & CULLEN, P. J. 1998a. Nerve growth factor- and epidermal growth factor-stimulated translocation of the ADP-ribosylation factor-exchange factor GRP1 to the plasma membrane of PC12 cells requires activation of phosphatidylinositol 3-kinase and the GRP1 pleckstrin homology domain. *The Biochemical journal*, 335 (Pt 1), 139-46.
- VENKATESWARLU, K., OATEY, P. B., TAVARÉ, J. M. & CULLEN, P. J. 1998b. Insulin-dependent translocation of ARNO to the plasma membrane of adipocytes requires phosphatidylinositol 3-kinase. *Curr Biol*, 8, 463-6.
- VERHEIJEN, F. W., VERBEEK, E., AULA, N., BEERENS, C. E., HAVELAAR, A. C., JOOSSE, M., PELTONEN, L., AULA, P., GALJAARD, H., VAN DER SPEK, P. J. & MANCINI, G. M. 1999. A new gene, encoding an anion transporter, is mutated in sialic acid storage diseases. *Nat Genet*, 23, 462-5.
- WANG, L., DING, Y., GUO, X. & ZHAO, Q. 2015. Role and mechanism of vascular cell adhesion molecule-1 in the development of rheumatoid arthritis. *Exp Ther Med*, 10, 1229-1233.
- WANG, L., LI, S., YU, X., HAN, Y., WU, Y., WANG, S., CHEN, X., ZHANG, J. & WANG, S. 2019. alpha2,6-Sialylation promotes immune escape in hepatocarcinoma cells by regulating T cell functions and CD147/MMP signaling. *J Physiol Biochem*, 75, 199-207.
- WANG, Y., KURAMITSU, Y., BARON, B., KITAGAWA, T., TOKUDA, K., AKADA, J., MAEHARA, S. I., MAEHARA, Y. & NAKAMURA, K. 2017. PI3K inhibitor LY294002, as opposed to wortmannin, enhances AKT phosphorylation in gemcitabine-resistant pancreatic cancer cells. *Int J Oncol*, 50, 606-612.
- WEI, A., FAN, B., ZHAO, Y., ZHANG, H., WANG, L., YU, X., YUAN, Q., YANG, D. & WANG, S. 2016. ST6Gal-I overexpression facilitates prostate cancer progression via the PI3K/Akt/GSK-3 β / β -catenin signaling pathway. *Oncotarget*, 7, 65374-65388.
- WILLIAMS, L. M., LALI, F., WILLETTS, K., BALAGUE, C., GODESSART, N., BRENNAN, F., FELDMANN, M. & FOXWELL, B. M. 2008. Rac mediates TNF-induced cytokine production via modulation of NF-kappaB. *Mol Immunol*, 45, 2446-54.
- WILLIAMS, R. 1998. Rodent models of arthritis: relevance for human disease. *Clinical & Experimental Immunology*, 114, 330-332.
- WILLIAMS, R. O. 2004. Collagen-induced arthritis as a model for rheumatoid arthritis. *Methods Mol Med*, 98, 207-16.

- WILLIAMS, R. O., FELDMANN, M. & MAINI, R. N. 1992. Anti-tumor necrosis factor ameliorates joint disease in murine collagen-induced arthritis. *Proc Natl Acad Sci U S A*, 89, 9784-8.
- WILLIAMS, R. O., GHRAYEB, J., FELDMANN, M. & MAINI, R. N. 1995. Successful therapy of collagen-induced arthritis with TNF receptor-IgG fusion protein and combination with anti-CD4. *Immunology*, 84, 433-9.
- WILSON, I. B. 2002. Glycosylation of proteins in plants and invertebrates. *Curr Opin Struct Biol*, 12, 569-77.
- WU, J. Y. & KUO, C. C. 2012a. Pivotal role of ADP-ribosylation factor 6 in Toll-like receptor 9-mediated immune signaling. *J Biol Chem*, 287, 4323-34.
- WU, J. Y. & KUO, C. C. 2012b. TLR9-mediated ARF6 activation is involved in advancing CpG ODN cellular uptake. *Commun Integr Biol*, 5, 316-8.
- WUENSCH, S. A., HUANG, R. Y., EWING, J., LIANG, X. & LAU, J. T. Y. 2000. Murine B cell differentiation is accompanied by programmed expression of multiple novel β -galactoside α 2,6-sialyltransferase mRNA forms. *Glycobiology*, 10, 67-75.
- WURTZEL, J. G., LEE, S., SINGHAL, S. S., AWASTHI, S., GINSBERG, M. H. & GOLDFINGER, L. E. 2015. RLIP76 regulates Arf6-dependent cell spreading and migration by linking ARNO with activated R-Ras at recycling endosomes. *Biochem Biophys Res Commun*, 467, 785-91.
- XU, D. & QU, C. K. 2008. Protein tyrosine phosphatases in the JAK/STAT pathway. *Front Biosci*, 13, 4925-32.
- XU, X., WANG, Q., HE, Y., DING, L., ZHONG, F., OU, Y., SHEN, Y., LIU, H. & HE, S. 2017. ADP-ribosylation factor 1 (ARF1) takes part in cell proliferation and cell adhesion-mediated drug resistance (CAM-DR). *Ann Hematol*, 96, 847-858.
- XUE, C., TAKAHASHI, M., HASUNUMA, T., AONO, H., YAMAMOTO, K., YOSHINO, S., SUMIDA, T. & NISHIOKA, K. 1997. Characterisation of fibroblast-like cells in pannus lesions of patients with rheumatoid arthritis sharing properties of fibroblasts and chondrocytes. *Annals of the Rheumatic Diseases*, 56, 262.
- XUE, G. & HEMMINGS, B. A. 2013. PKB/Akt-Dependent Regulation of Cell Motility. *JNCI: Journal of the National Cancer Institute*, 105, 393-404.
- YANG, C. M., LUO, S. F., HSIEH, H. L., CHI, P. L., LIN, C. C., WU, C. C. & HSIAO, L. D. 2010. Interleukin-1 β induces ICAM-1 expression enhancing leukocyte adhesion in human rheumatoid arthritis synovial fibroblasts: involvement of ERK, JNK, AP-1, and NF- κ B. *J Cell Physiol*, 224, 516-26.
- YANG, L., TANG, L., DAI, F., MENG, G., YIN, R., XU, X. & YAO, W. 2017. Raf-1/CK2 and RhoA/ROCK signaling promote TNF- α -mediated endothelial apoptosis via regulating vimentin cytoskeleton. *Toxicology*, 389, 74-84.
- YEE, K. L., WEAVER, V. M. & HAMMER, D. A. 2008. Integrin-mediated signalling through the MAP-kinase pathway. *IET Syst Biol*, 2, 8-15.
- YU, S., FAN, J., LIU, L., ZHANG, L., WANG, S. & ZHANG, J. 2013. Caveolin-1 up-regulates integrin α 2,6-sialylation to promote integrin α 5 β 1-dependent hepatocarcinoma cell adhesion. *FEBS Lett*, 587, 782-7.
- YUAN, Y., WU, L., SHEN, S., WU, S. & BURDICK, M. M. 2016. Effect of alpha 2,6 sialylation on integrin-mediated adhesion of breast cancer cells to fibronectin and collagen IV. *Life Sci*, 149, 138-45.
- ZEGEYE, M. M., LINDKVIST, M., FALKER, K., KUMAWAT, A. K., PARAMEL, G., GRENEGARD, M., SIRSSJO, A. & LJUNGBERG, L. U. 2018. Activation of the JAK/STAT3 and PI3K/AKT pathways are crucial for IL-6 trans-signaling-

- mediated pro-inflammatory response in human vascular endothelial cells. *Cell Commun Signal*, 16, 55.
- ZHAI, Y., WU, B., LI, J., YAO, X. Y., ZHU, P. & CHEN, Z. N. 2016. CD147 promotes IKK/I κ B/NF- κ B pathway to resist TNF-induced apoptosis in rheumatoid arthritis synovial fibroblasts. *J Mol Med (Berl)*, 94, 71-82.
- ZHANG, F., WEI, K., SLOWIKOWSKI, K., FONSEKA, C. Y., RAO, D. A., KELLY, S., GOODMAN, S. M., TABECHIAN, D., HUGHES, L. B., SALOMON-ESCOTO, K., WATTS, G. F. M., JONSSON, A. H., RANGEL-MORENO, J., MEEDNU, N., ROZO, C., APRUZZESE, W., EISENHAURE, T. M., LIEB, D. J., BOYLE, D. L., MANDELIN, A. M., 2ND, ACCELERATING MEDICINES PARTNERSHIP RHEUMATOID, A., SYSTEMIC LUPUS ERYTHEMATOSUS, C., BOYCE, B. F., DICARLO, E., GRAVALLESE, E. M., GREGERSEN, P. K., MORELAND, L., FIRESTEIN, G. S., HACOEN, N., NUSBAUM, C., LEDERER, J. A., PERLMAN, H., PITZALIS, C., FILER, A., HOLERS, V. M., BYKERK, V. P., DONLIN, L. T., ANOLIK, J. H., BRENNER, M. B. & RAYCHAUDHURI, S. 2019. Defining inflammatory cell states in rheumatoid arthritis joint synovial tissues by integrating single-cell transcriptomics and mass cytometry. *Nat Immunol*, 20, 928-942.
- ZHANG, Z., WUHRER, M. & HOLST, S. 2018. Serum sialylation changes in cancer. *Glycoconj J*, 35, 139-160.
- ZHAO, Q., BARCLAY, M., HILKENS, J., GUO, X., BARROW, H., RHODES, J. M. & YU, L.-G. 2010. Interaction between circulating galectin-3 and cancer-associated MUC1 enhances tumour cell homotypic aggregation and prevents anoikis. *Molecular Cancer*, 9, 154.
- ZHENG, D. Q., WOODARD, A. S., TALLINI, G. & LANGUINO, L. R. 2000. Substrate specificity of alpha(v)beta(3) integrin-mediated cell migration and phosphatidylinositol 3-kinase/AKT pathway activation. *J Biol Chem*, 275, 24565-74.
- ZHENG, K., BANTOG, C. & BAYER, R. 2011. The impact of glycosylation on monoclonal antibody conformation and stability. *MAbs*, 3, 568-76.
- ZHOU, Y., ZHOU, B., PACHE, L., CHANG, M., KHODABAKHSHI, A. H., TANASEICHUK, O., BENNER, C. & CHANDA, S. K. 2019. Metascape provides a biologist-oriented resource for the analysis of systems-level datasets. *Nat Commun*, 10, 1523.
- ZHU, W., LONDON, N. R., GIBSON, C. C., DAVIS, C. T., TONG, Z., SORENSEN, L. K., SHI, D. S., GUO, J., SMITH, M. C., GROSSMANN, A. H., THOMAS, K. R. & LI, D. Y. 2012. Interleukin receptor activates a MYD88-ARNO-ARF6 cascade to disrupt vascular stability. *Nature*, 492, 252-5.
- ZHUO, Y. & BELLIS, S. L. 2011. Emerging role of alpha2,6-sialic acid as a negative regulator of galectin binding and function. *J Biol Chem*, 286, 5935-41.
- ZHUO, Y., CHAMMAS, R. & BELLIS, S. L. 2008. Sialylation of beta1 integrins blocks cell adhesion to galectin-3 and protects cells against galectin-3-induced apoptosis. *J Biol Chem*, 283, 22177-85.
- ZIMMERMANN, T., KUNISCH, E., PFEIFFER, R., HIRTH, A., STAHL, H.-D., SACK, U., LAUBE, A., LIESAUS, E., ROTH, A., PALOMBO-KINNE, E., EMMRICH, F. & KINNE, R. W. 2000. Isolation and characterization of rheumatoid arthritis synovial fibroblasts from primary culture – primary culture cells markedly differ from fourth-passage cells. *Arthritis Research & Therapy*, 3, 72.